

**LATE CRETACEOUS (MAESTRICHTIAN)
CALCAREOUS NANNOPLANKTON BIOGEOGRAPHY
With Emphasis on Events Immediately Preceding the
Cretaceous/Paleocene Boundary**

by

Thomas Wolfgang Ehrendorfer

Magister rer. nat., University of Vienna, Austria
(1987)

SUBMITTED IN PARTIAL FULFILLMENT OF THE
REQUIREMENTS FOR THE DEGREE OF

DOCTOR OF PHILOSOPHY

at the

MASSACHUSETTS INSTITUTE OF TECHNOLOGY

and the

WOODS HOLE OCEANOGRAPHIC INSTITUTION

February 1993

© Copyright Thomas W. Ehrendorfer, 1993. All rights reserved.

The author hereby grants to MIT and WHOI permission to reproduce
and distribute copies of this thesis document in whole or in part.

Signature of Author _____
Joint Program in Oceanography,
Massachusetts Institute of Technology/Woods Hole
Oceanographic Institution

Certified by _____
William A. Berggren
Thesis Supervisor

Accepted by _____
Marcia McNutt
Chairman, Joint Committee for Marine Geology and Geophysics
Massachusetts Institute of Technology/Woods Hole
Oceanographic Institution

MASSACHUSETTS INSTITUTE
OF TECHNOLOGY
WITHDRAWN
FROM 1993
LIBRARIES

This work is dedicated to my parents.

LATE CRETACEOUS (MAESTRICHTIAN)
CALCAREOUS NANNOPLANKTON BIOGEOGRAPHY
With Emphasis on Events Immediately Preceding the
Cretaceous/Paleocene Boundary

by Thomas Wolfgang EHRENDORFER

Submitted to the
Department of Earth, Atmospheric, and Planetary Sciences,
Massachusetts Institute of Technology
and the
Department of Marine Geology and Geophysics,
Woods Hole Oceanographic Institution

on February 8, 1993
in partial fulfillment of the requirements
for the Degree of Doctor of Philosophy

ABSTRACT

The Maestrichtian biogeography of calcareous nannoplankton is investigated in order to characterize paleoenvironmental conditions in the marine photic zone during the latest Cretaceous. Different theories explaining the biospheric turnover at the Cretaceous/Paleocene (K/P) boundary have alternatively suggested or denied substantial environmental perturbations during the last ~500 ky of the Cretaceous. The purpose of this study is to determine whether evidence from calcareous nannoplankton supports a gradual (or stepwise) decline of the photic zone environment presaging the K/P boundary.

In order to achieve this goal a detailed quantitative study of the biogeography of calcareous nannoplankton was carried out in three time slices from early and late Maestrichtian. Well preserved material was investigated from five sections: Ocean Drilling Program Site 690 in the Atlantic sector of the Southern Ocean represents the Maestrichtian high southern nannoplankton province. Indian Ocean Sites 217 and 761, South Atlantic Site 528 and the land based, epicontinental section from Millers Ferry, Alabama, represent the Maestrichtian mid-/low latitudinal bioprovince. Quantitative counts were performed on settling slides under the light microscope. Occasionally scanning electron microscopy was employed to resolve taxonomic uncertainties.

A pronounced turnover from early to late Maestrichtian occurred in the nannoplankton in high southern latitudes. Numerous taxa (*Biscutum boletum*, *B. coronum*, *B. dissimilis*, *B. magnum*, *Misceomarginatus* spp., *Monomarginatus* spp., *Neocrepidolithus watkinsii*, *Nephrolithus corystus*, *Octocyclus magnus*, *Phanulithus obscurus*, *Psyktosphaera firthii*, and *Reinhardtites* spp.) that are restricted to (or most abundant in) high southern latitudes became extinct in the latest early and earliest late Maestrichtian (between ~72.4 and 70.4 Ma), resulting in a loss of about one third of the early Maestrichtian

nannoplankton (corresponding to ~20-25% of the assemblage). It is argued that the extinctions are not a consequence of temperature changes alone. Instead they may be a consequence of increased surface water fertility (and only secondarily due to a temperature decrease).

In addition to the extinctions, about another third of all taxa present (Biscutum constans, B. notaculum, Biscutum sp. 1, Chiastozygus garrisonii, C. amphipons, Discorhabdus ignotus, Rhombolithion rhombicum, Scapholithus fossilis, Staurolithites laffittei, Watznaueria barnesae, Zygodiscus compactus, and Z. diplogrammus) disappeared from high southern latitudes during the same time interval (~72.4 and 70.4 Ma) but persisted until the end of the Maestrichtian in lower latitudes. These geographic restrictions are interpreted as a consequence of global cooling. No comparable changes were recorded in mid- and low latitudes in the early Maestrichtian, but this may represent an artifact of sampling.

While previous speculations on the paleoenvironmental preferences of some nannofossil taxa have been confirmed, several commonly accepted interpretations of the biogeographic significance of other taxa are contradicted. Micula staurophora seems to be a warm water indicator and abundance peaks of this species cannot be attributed exclusively to diagenetic effects. The biogeographic evolution of the high latitude taxon Ahmullerella octoradiata does not correlate with temperature trends suggested from stable isotope studies implying that this taxon is not a cold water indicator. Abundance changes of other high latitude taxa (e.g. Nephrolithus frequens, Cribrosphaerella? daniae, Kampnerius magnificus, and Gartnerago spp.) correlate roughly with temperature changes, but seem to respond only beyond a certain threshold.

No gradual or stepwise extinctions were observed during the last 500 ky of the Maestrichtian. Environmental perturbations as indicated by stable isotope studies (e.g. warming pulse, circulation changes) led to abundance fluctuations of a few taxa, but did not result in any extinctions. This supports previous observations that the extinctions of the calcareous nannoplankton at the K/P boundary were not presaged during the Maestrichtian.

Thesis Supervisor: Dr. William A. Berggren, Senior Scientist

ACKNOWLEDGEMENTS

My thanks go first and foremost to my parents for their love and support during my studies here in the United States.

Special thanks go to the members of my thesis committee, particularly to my supervisors Marie-Pierre Aubry and Bill Berggren for their inexhaustible support during all parts of my graduate studies. This thesis would have never been written without their constant scientific and personal advice, encouragement, and help. I am grateful to Dick Norris for all our discussions on scientific as well as personal matters. I am also thankful for the advice and support from my other committee members, Ed Boyle, Lloyd Keigwin, and Pat Lohmann.

Discussions with Tim Bralower and Steve D'Hondt have helped me focus on specific research questions; their advice is gratefully acknowledged. Special thanks are due to Rindy Ostermann for helping me with the carbonate content analyses. Colleen Hurter and the library staff must be commended for their invaluable help in tracking down hard-to-find literature. I want to thank the staff at the Center for Data Processing of the University of Agriculture in Vienna, Austria, for their help with various statistical questions. My acknowledgements also go to the staff of the Core Repositories of the Ocean Drilling Program at Lamont, College Station, and La Jolla for their friendly support during my sampling trips.

I thank El Uchupi for serving on a moment's notice as chairman at my General Examination, and for his continual help and support as student advisor. I am grateful to Jake Peirson, Abbie Jackson, and Stella Callagee in the Education Office for their help in all matters ranging from registration and exhausted student accounts to technical details regarding the preparation of this document. Thanks are also due to Pam Foster, Roy Smith and Janet Johnson for their friendly help.

I was fortunate to have met friends like Mike and Danusia Kaminski, Peter Schweitzer, Luc Beaufort, Bernward and Felicita Hay, Niall Slowey, JoAnn Muramoto, Carol Arnosti, and Rick Krishfield. Special thanks go to my office mate of the last two years, Javier Escartin, not only for his help in programming, but, more importantly, for his companionship and cheerfulness.

Special thanks are due to my fiancée, Lee Goodell, for her love, patience and understanding during periods when my work absorbed me completely. I also want to thank her parents and her uncle's family for their warm hospitality.

I gratefully acknowledge receiving a Graduate Research Assistantship from the Woods Hole Oceanographic Institution during most of my tenure in the Joint Program. Additional funding from the following sources is also appreciated: a travel grant from the Austrian-American Educational Commission (Fulbright Commission); a Grant-in-Aid from the American Association of Petroleum Geologists (1990); a grant from the Ocean Ventures Fund at W.H.O.I. (1991); a Research Grant-in-Assistance from the Paleontological Society/Margaret C. Wray Trust (1991); a Grant-in-Aid of Research from the Sigma Xi Society (1992).

TABLE OF CONTENTS

Abstract	4
Acknowledgements	6
Table of Contents	7
Introduction	10
Chapter 1. Maestrichtian Climate and Oceanography	12
1) Global Temperature Gradients.....	12
2) Biospheric Changes at the Cretaceous/Paleocene Boundary and Extinction Hypotheses.....	14
3) Calcareous Nannoplankton.....	16
Chapter 2. Samples and Methods	19
1) Samples.....	19
(A) Sections Investigated in This Study.....	19
(B) Sampling Strategy and Sample Intervals.....	21
2) Methods.....	23
(A) Sample Preparation.....	23
(B) Counting Procedure.....	23
(C) Data Processing.....	25
Chapter 3. Chronology	30
1) Biohorizons.....	30
2) ODP Hole 690C.....	36
3) ODP Hole 761B.....	46
4) ODP Hole 761C.....	52
5) DSDP Hole 217.....	56
6) DSDP Hole 528	62
7) Millers Ferry Section.....	67
Chapter 4. Results of Nannofossil Counts	69
1) ODP Hole 690C.....	69
2) ODP Holes 761B and 761C.....	89
3) DSDP Hole 217.....	102
4) DSDP Hole 528.....	120

5) Millers Ferry Section.....	141
Chapter 5. Discussion.....	145
1) Maestrichtian Evolutionary and Biogeographic Events	
at High Latitudes.....	145
(A) Evolutionary Changes.....	145
(a) Extinctions.....	145
(b) Originations.....	145
(B) Biogeographic Changes.....	149
(a) Emigrations.....	149
(b) Abundance Changes.....	149
2) Maestrichtian Evolutionary and Biogeographic Events	
in Mid/Low Latitudes.....	154
(A) Evolutionary Changes.....	154
(a) Extinctions.....	154
(b) Originations.....	155
(B) Biogeographic Changes and Abundance Changes.....	155
3) Maestrichtian Nannoplankton Evolution.....	159
(A) Austral Taxa.....	159
(a) Which are the "austral" taxa?.....	159
(b) Paleogeographic distribution of austral taxa.....	160
(c) Why did austral calcareous nannoplankton species become extinct?.....	163
(B) Nannoplankton Response to Environmental Perturbations	
During the Last 500 ky of the Cretaceous (66.9 to 66.4 Ma).....	171
(a) High latitude evidence.....	171
(b) Mid-latitude trends.....	177
(C) Paleoenvironmental Significance of Selected Nannoplankton Species.....	181
(a) Previous studies.....	181
(b) <u>Biscutum constans</u>	183
(c) <u>Discorhabdus ignotus</u>	186
(d) <u>Nephrolithus frequens</u> and other high latitude taxa.....	186
(e) <u>Ahmuellerella octoradiata</u>	190
4) Implications of High Resolution Biogeographic Studies	190
5) Implications for the Extinctions at the K/P Boundary.....	192

6) Summary.....	193
Chapter 6. Synopsis.....	196
Literature.....	205
Appendix I: Taxonomy.....	219
Appendix II: Data.....	230
Curriculum Vitae.....	288

INTRODUCTION

The Maestrichtian represents the last 8.1 m.y. of the Cretaceous (74.5 Ma - 66.4 Ma; Kent and Gradstein, 1985; Berggren et al., 1985). Its end (at 66.4 Ma; Berggren et al., 1985) corresponds to the Cretaceous/Paleocene (K/P) boundary, when one of the most severe extinctions of life on Earth occurred (e.g. Russell, 1977; Raup and Sepkoski, 1984). Pronounced changes of the climate, surface water circulation, and stratification of the photic zone during the Maestrichtian have been proposed (e.g. Douglas and Savin, 1975; Huber and Watkins, 1992). Little micropaleontologic evidence is available to assess how these changes affected the marine micro- and nannoplankton. Some authors have concluded that stable ecological conditions prevailed in the photic zone during the last 15 m.y of the Cretaceous (e.g. Thierstein, 1981). Others have argued that environmental perturbations and long term climate shifts were responsible for gradual extinctions in some groups of organisms (inoceramids, dinosaurs; see Kauffman, 1984, for a review) during the Maestrichtian.

The extinction event at the end of the Cretaceous is one of the most severe of the Phanerozoic (Raup and Sepkoski, 1984) but the mechanisms causing the extinctions are still vehemently debated. The impact of an asteroid (Alvarez et al., 1980) or of a comet (Hsü, 1980) has been proposed to explain the abruptness of the K/P extinctions in numerous groups of organisms. Progressive cooling (Stanley, 1984), possibly linked to massive volcanic eruptions (Courtillot et al., 1986), and changes in the ocean circulation (deep water formation) as a consequence of sea level fall (Brinkhuis and Zachariasse, 1988) have been proposed as alternative mechanisms. Paleontologic evidence in support of either mechanism has been presented (e.g. Thierstein, 1982; Kauffman, 1984).

In this study I investigate the Maestrichtian biogeographic evolution of the calcareous nannoplankton in order to determine how the changes in the oceanic surface water habitat affected them. Biogeographic changes, migrations, and extinctions of calcareous nannoplankton species are documented and their causal relation to environmental perturbations are explored. The biogeographic patterns observed in the early and mid-Maestrichtian are compared to those of the last ~500 ky of the Maestrichtian in order to assess whether increased environmental stress could be documented.

Calcareous nanoplankton are well suited to study the effect of proposed oceanic environmental perturbations on the marine plankton for several reasons. 1) The ubiquitous presence of fossil remains of calcareous nanoplankton in calcareous marine sediments allows worldwide sample coverage and comparisons between different paleoenvironments. 2) Due to the small size and abundance of calcareous nanofossils, samples can be very closely spaced, allowing high temporal resolution; only very little material is necessary to conduct quantitative studies. 3) In contrast to previous synoptic studies (Thierstein, 1981), material from high southern latitudes recovered by the Ocean Drilling Project during the past few years is included in this investigation. It is essential to include high and low latitudes sites in a biogeographic study of Maestrichtian calcareous nanoplankton, because of the pronounced bioprovincialism that has been documented (e.g Wind, 1979a, b; Wise, 1988).

CHAPTER 1

MAESTRICHTIAN CLIMATE AND OCEANOGRAPHY

1) Global Temperature Gradients

Geological and paleontological evidence indicate that the Cretaceous period was considerably warmer than today, with strongly reduced latitudinal and vertical temperature gradients in the oceans (reviewed by Savin, 1977; compare also Barron et al., 1981). Polar ice caps did not exist (Miller and Fairbanks, 1987) and ocean surface temperatures in low latitudes were between 17°-20°C (similar to today), while bottom water temperatures ranged from 5°-8°C (Douglas and Savin, 1971, 1973, 1975; Saito and Van Donk, 1974; Savin, 1977; Saltzman and Barron, 1982) or 6.5°-10°C according to Shackleton and Boersma (1984), which is much warmer than today's 1-3°C.

Latitudinal temperature gradients were lower than today: high southern latitude surface water temperatures were ~4.5°-10.5°C (Barrera et al., 1987). Studies of plant fossils from the North Slope of Alaska led Parrish and Spicer (1988) to estimate that mean annual Arctic temperatures were 2°-8°C.

Cooling Trend

Oxygen isotope analyses of planktonic and benthic foraminifera, of fine fraction carbonate (primarily calcareous nannofossils), and of well preserved macrofossils (inoceramids) imply a general cooling trend during the Late Cretaceous (Albian to Maestrichtian, Douglas and Savin, 1975).

A temperature decrease in the early Maestrichtian of bottom and surface waters was reported by Douglas and Savin (1975), Margolis et al. (1977), and Boersma (1984b) in low and mid-latitudes. Clauser (1987) reported a cooling peak straddling the late Campanian/early Maestrichtian boundary from a section near Bidart (southwest France). No temperature changes are reported during the middle Maestrichtian (Boersma, 1984b). While Margolis et al. (1977) reported a slight decline of surface- and bottom water temperatures during the late Maestrichtian, Douglas and Savin (1975) reported a temperature increase in the early Danian. Shackleton and Boersma (1984) indicated "somewhat higher mean surface temperatures" in the Paleocene than in the Maestrichtian in the South Atlantic (Walvis Ridge, paleolatitude of about 40°S). Zachos et al. (1989) reported cooling beginning in the latest Cretaceous (about 200 ky before the K/P boundary) and a warming peak in the

early Paleocene (~600 ky after the K/P boundary). Barrera and Huber (1990) presented stable isotope evidence from the high southern Atlantic Ocean (Maud Rise) indicating that surface and deep waters cooled throughout the Maestrichtian.

Latest Maestrichtian Warming Pulse

Stott and Kennett (1990b) reported a brief warming pulse (~2°C) in the latest Maestrichtian (between ~66.9 and 66.6 Ma; i.e. this pulse did not straddle the K/P boundary). Land plant evidence from the western interior of North America (Wyoming and North Dakota) also suggest a brief warming trend during the last 350 ky (from early Subchron C29R) of the Maestrichtian (Johnson, 1992).

Deep Water Formation

Ocean bottom waters were much warmer than they are today (see above). Two hypotheses exist for deep water formation in the Cretaceous oceans: 1) formation of dense, saline waters on subtropical shelves where evaporation exceeded precipitation (Brass et al., 1982); and 2) deep water formation due to cooling in high latitudes (e.g. Barrera et al., 1987). Brinkhuis and Zachariasse (1988) speculated that the regression at the K/P boundary led to the cessation of deep water formation; the resulting interruption of deep ocean circulation and upwelling of nutrients from the deep ocean caused the collapse of the marine ecosystem at the K/P boundary. This hypothesis, however, does not explain the extinctions of terrestrial organisms.

Maestrichtian Sedimentary Cycles

Cyclic variations of carbonate content (expressed visually as red and white color cycles) occur in Upper Cretaceous - lower Cenozoic sediments in the South-Atlantic. Herbert and D'Hondt (1990) interpreted these variations as resulting from precessional climate cycles. It has been shown that certain calcareous nannofossil species fluctuate in response to orbital forcing (e.g. Chepstow-Lusty et al., 1989; Beaufort and Aubry, 1990; Erba et al., 1992). This has not yet been demonstrated for the Maestrichtian. The identification of such taxa would be very valuable for paleoclimatic as well as stratigraphic investigations (see discussion in Herbert and D'Hondt, 1990).

Sea level changes

Haq et al. (1987) have reported a sea level fall at the early/late Maestrichtian boundary as well as at the K/P boundary. Huber (1992a) speculated that the mid-Maestrichtian sea level fall led to significant changes in the ocean circulation and ended the isolation of the austral planktonic foraminiferal province. Brinkhuis and Zachariasse (1988) speculated about the consequences of the sea level fall at the K/P boundary (see above).

2) Biospheric Changes at the Cretaceous/Paleocene boundary and Extinction Hypotheses

Biospheric Changes at the K/P boundary

Extinction or significant reduction of species diversity at the K/P boundary are documented for groups as diverse as marine calcareous plankton (foraminifera: Loeblich and Tappan, 1957; Luterbacher and Premoli-Silva, 1964; coccolithophorids: Bramlette and Martini, 1964), marine macrobenthos (bivalves, brachiopods, bryozoans, echinoderms; see review by Hallam and Perch-Nielsen, 1990) and marine nekton (belemnites: Christensen, 1976; ammonites: Cobban and Scott, 1972, Wiedmann, 1964), as well as land vertebrates (dinosaurs: Van Valen and Sloan, 1977; for an overview see Kauffman, 1984). A major extinction event was also documented for land plants (Johnson and Hickey, 1990). Some of these groups disappeared rather abruptly (most calcareous marine plankton), others had already been on the decline prior to the end of the Cretaceous (inoceramids, and dinosaurs; see Kauffman, 1984, for a review). Theoretical considerations by Signor and Lipps (1982) and findings of recent fieldwork (summarized by Kerr, 1991) challenge this view of gradual attrition and claim that the apparently gradual extinctions may be sampling artifacts resulting from the increasing scarcity of macrofossils in the strata below the boundary.

In contrast to the extinctions, some groups of organisms were little affected by the K/P boundary event(s). These included some phytoplankton groups, such as organic walled dinoflagellates (Brinkhuis and Zachariasse, 1988) and siliceous diatoms (Kitchell et al., 1986) as well as some macroinvertebrates (nautiloids: Kauffman, 1984), and vertebrates (turtles: Hutchison and Archibald, 1986; snakes, crocodilians: Kauffman, 1984) and mammals.

Cretaceous/Paleocene Boundary Hypotheses

In addition to the biological changes, chemical and mineralogical anomalies in sediments on both sides of the K/P boundary are well known. Assuming a causal connection between the chemical and mineralogical anomalies on one hand, and the extinctions on the other hand, Alvarez et al. (1980) proposed the impact of a 10-km-diameter asteroid at the K/P boundary (for a review see Alvarez, 1986). Other workers suggested the impact of a comet (Hsü, 1980) or several simultaneous impacts (Smit, 1990). Among others, a circular subsurface structure near Chicxulub on the Yucatán Peninsula (Mexico) was proposed as the site of the K/P boundary impact (Hildebrand et al., 1991).

In contrast to extraterrestrial causes of the K/P extinctions, Courtillot et al. (1986) claimed that extended intense volcanism associated with the formation of the Deccan Traps could explain the biospheric changes and the mineralogical/chemical signatures more readily (see also Officer et al., 1987). Other researchers have claimed that earthbound, environmental changes (e.g. global cooling; Stanley, 1984) during the Late Cretaceous were sufficient to explain the K/P extinctions.

The basic differences between the extraterrestrial and the earthbound extinction hypotheses are the timing and duration of their respective influences on the biosphere. The flood basalt volcanism of the Deccan Traps straddled the K/P boundary and lasted about 0.5 to 1 m.y. (paleomagnetic and paleontologic data indicate that the bulk of the Deccan Traps were extruded during Chron 29R, the oldest and the youngest flood basalts were extruded during times of normal polarity; Courtillot et al., 1986; Courtillot, 1990). In contrast, the impact of an extraterrestrial body is an instantaneous event. Paleontologists have pointed out that a discrepancy exists between the instantaneous, severe, and non-selective extinctions expected by the impact-hypothesis, and the actual changes in fossil assemblages occurring prior to and extending across the K/P boundary, as pointed out above (Clemens et al., 1981).

3) Calcareous Nannoplankton

Remains of calcareous nannoplankton are ubiquitous in marine calcareous sediments. Their small size and great abundance in the sediments permit quantitative investigations of abundance changes of individual taxa. Cores drilled by the Deep Sea Drilling Project (DSDP) and the Ocean Drilling Program (ODP) in the world's oceans provide an unprecedented opportunity to study these changes at very high resolution at almost all latitudes.

Previous Studies: Paleoprovincialism and Biogeographic Changes

Only few studies have investigated biogeographic changes of calcareous nannofossils during the Maestrichtian. Yet several observations are well documented.

Provincialism: Maestrichtian provincialism of calcareous nannoplankton was first pointed out by Worsley and Martini (1970) who showed that the late Maestrichtian marker species Micula murus and Nephrolithus frequens were largely restricted to low and high latitudes, respectively. Worsley (1974), Thierstein (1976, 1981) and Wind (1979a, b) conducted superregional studies and confirmed that numerous species had pronounced latitudinal abundance gradients in the Maestrichtian. This latitudinally-defined provincialism was in contrast to the conditions in the mid-Cretaceous (Barremian to Cenomanian; Roth and Bowdler, 1981) when latitudinal provincialism was weak, but oceanic versus neritic provincialism well developed (Roth and Bowdler, 1981). Wise (1988) argued that the increase of latitudinal provincialism of calcareous nannofossils during the Late Cretaceous reflected the global cooling that progressed during the same time (compare e.g. Douglas and Savin, 1975). Similarly, Wind (1979a) speculated that some high latitude taxa (B. magnum and B. coronum) were indicative of cool surface water temperatures, whereas others (such as e.g. B. constans) were characteristic of warmer water temperatures.

Biostratigraphy: The latitudinal provincialism during the Late Cretaceous is also reflected in the fact that nannofossil taxa that have been used for stratigraphic purposes in low latitudes (e.g. Bukry, 1973) were absent from mid- and high latitudes. For this reason, different zonations have been developed for different latitudinal zones.

Geographic and Temporal Changes: Thierstein (1981) performed semiquantitative analyses of late Campanian to early Paleocene calcareous

nannoplankton associations. His study includes sections from all ocean basins and from high as well as from low latitudes. Only one site was from very high southern latitudes (DSDP Hole 327A) and its stratigraphic range was misinterpreted¹. In addition to latitudinal bioprovincialism (see above) Thierstein (1981) concluded in particular that (i) nannofossil abundances did not change significantly during late Campanian through Maestrichtian, indicating stable oceanic surface environments, (ii) that no gradual or stepwise extinctions of Cretaceous taxa occurred prior to the K/P boundary and (iii) that the persistent taxa (i.e. those that "survive" the K/P extinctions; Percival and Fischer, 1977) occurred mainly at high latitude sites possibly indicative of their adaptation to higher seasonality of temperature, salinity or light.

Doeven (1983) investigated abundance changes of calcareous nannoplankton taxa from Campanian to Maestrichtian in the northwest Atlantic Ocean (Canadian Atlantic Margin). He interpreted the abundance increase of some taxa (e.g. A. cymbiformis, K. magnificus and M. staurophora) and the decrease of W. barnesae as indicative of cooling of surface waters in the early Maestrichtian, possibly as a consequence of circulation changes caused by early seafloor spreading in the Labrador Sea.

The resolution in both of these studies was very low: Thierstein's (1981) sample spacing throughout most of the late Campanian and Maestrichtian was ~1-5m (~100-200 ky), but increased significantly (sample spacing <10cm: ~5-10 ky) immediately below (~1m) the K/P boundary. Doeven (1983) investigated one (or two) samples in each of the five Campanian to Maestrichtian nannofossil zones in nine drillholes (29 samples total).

In addition, both studies only reported on the abundance trends of the most abundant taxa present (>2% of the assemblage), since the authors believed that abundance changes of rarer taxa were unreliable.

¹Thierstein (1981) thought that the age of Cores 327A-10 to 327A-12 was late Maestrichtian (while in fact it was early Maestrichtian), most likely because he mistook the early Maestrichtian species Nephrolithus corystus for the late Maestrichtian marker species N. frequens. The same mistake was made in the original core descriptions (Shipboard Scientific Party, 1977; Wise and Wind, 1977). It was only in 1979 that Wind (1979a) had recognized the taxonomic and stratigraphic differences between N. corystus and N. frequens.

K/P Boundary Studies of Calcareous Nannoplankton Associations

Calcareous nannoplankton associations have been studied extensively in K/P boundary sections all over the world (e.g Percival and Fischer, 1977; papers in Christensen and Birkelund, 1979; Perch-Nielsen et al., 1982; Thierstein, 1981; Jiang and Gartner, 1986). Most studies concentrated on the abrupt extinctions at the K/P boundary and the recovery of the calcareous nannoplankton in the early Paleocene. No quantitative, high resolution studies exist that documented abundance changes of all calcareous nannofossil taxa during the last 500 ky of the Cretaceous.

CHAPTER 2

SAMPLES AND METHODS

1) Samples

(A) SECTIONS INVESTIGATED IN THIS STUDY

Three sites (ODP Holes 690C, 761B and DSDP Hole 217) were selected for detailed study based on 1) their latitude during the Maestrichtian (high southern and mid-latitudes; Figure 1; see also site descriptions in Chapter 3), 2) the completeness of their Maestrichtian sedimentary record, and 3) the high quality of calcareous nannofossil preservation. In addition, three sections were selected (ODP Hole 761C, DSDP Hole 528, and Millers Ferry Section) to study calcareous nannoplankton biogeographic evolution in detail during the last several 100 ky prior to the K/P boundary (Figure 1).

Hole 690C (~65°S) is one of the few Maestrichtian sections in calcareous facies recovered in high southern latitudes to date. Its Maestrichtian latitude was very similar to its present latitude (see Chapter 3). This hole represents southern high latitudes and the austral province in this study.

Hole 761B is located at 16°S on the northwestern Australian margin (Wombat Plateau, Indian Ocean); its Maestrichtian location was in (high) mid latitudes (~40°S; see Chapter 3). Hole 761C was included in this study because the K/P boundary section in this hole appears to be continuous, whereas an unconformity occurred in Hole 761B (see Chapter 3).

Hole 217 is presently located at 8°N (Ninetyeast Ridge, Bay of Bengal, Indian Ocean). This site was originally included in this study to represent tropical latitudes, but results from recent ODP Legs in the Indian Ocean indicate that the Maestrichtian latitude of this site was ~>30°S (see Chapter 3).

DSDP Hole 528 is located on Walvis Ridge in the South Atlantic Ocean (28°S). Its Maestrichtian latitude was ~35°S (Chave, 1984). This site was included in order to investigate nannofossil changes associated with the pronounced sediment color variation at this site.

The section at Millers Ferry (Alabama) represents the only section from the northern hemisphere investigated in this study. It was located in (low) mid-latitudes during the Maestrichtian (~30-35°N). It also represents the only epicontinental section studied herein.

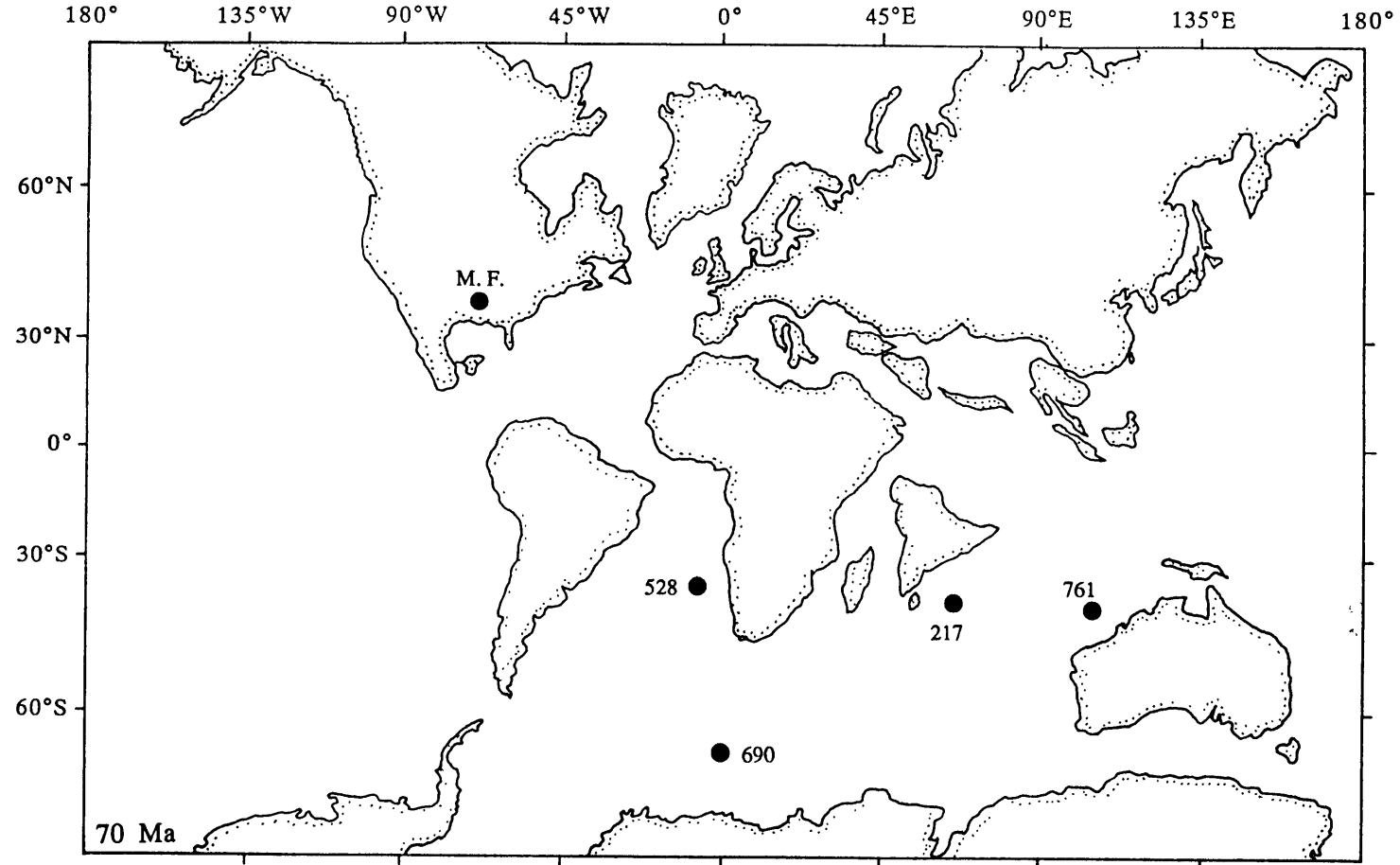


Figure 1: Maestrichtian locations of the sections investigated in this study. Numbers indicate DSDP and ODP Sites, M. F. indicates the Millers Ferry Section. Paleogeontinal reconstruction of the mid-Maestrichtian (70 Ma) after Coffin et al. (1992).

(B) SAMPLING STRATEGY AND SAMPLE INTERVALS

In order to investigate the response of calcareous nanoplankton to short term environmental perturbations as well as their biogeographic evolution through the Maestrichtian, different degrees of temporal resolution (through different sampling density) were used in different parts of the sections studied (see Figure 2).

Herbert and D'Hondt (1990) showed that the carbonate content varied cyclically in Upper Cretaceous-lower Cenozoic marine sediments over ~20 m.y. in the South Atlantic. They interpreted this carbonate content cyclicity as a response to precessional climatic cycles and calculated a mean absolute period of 23.5 ± 4.4 ky. To avoid the problem of aliasing, a minimum of two samples per cycle is required (Blackman and Tukey, 1958) but Ledbetter and Ellwood (1976) suggested that at least four samples per cycle should be analyzed in order to increase the reliability of the results. Following Ledbetter and Ellwood (1976) I attempted to obtain a chronologic resolution of ~5 ky in order to investigate whether calcareous nanofossil fluctuations occur in cycles of ~20 ky: very closely spaced samples (every ~3 cm) were taken in the uppermost 2.7 m of the Cretaceous in Hole 690C (representing the last ~60 ky of the Maestrichtian) and every ~5 cm in the uppermost 7.5 m in Hole 528 (representing the last ~75 ky; stippled intervals in Figure 2). A temporal resolution of ~3 ky was thus achieved in both holes.

The remainder of the "latest Maestrichtian interval" (cross hatched interval prior to the K/P boundary in Figure 2) represented in Holes 690C and 528 was investigated at slightly lower temporal resolution (only ~10 ky in Hole 690C, corresponding to sample intervals of ~10 cm; ~20 ky in Hole 528, corresponding to sample intervals of ~20 cm). Similar resolution (between ~10-20 ky) was also achieved for the latest Maestrichtian interval represented in Holes 761B, 761C, and 217.

In order to assess whether nanoplankton changes during the last ~500 ky of the Maestrichtian were inherently different from those earlier in the Maestrichtian, control intervals with a temporal resolution of ~10-20 ky were selected (cross hatched intervals in the early and mid-Maestrichtian in Figure 2).

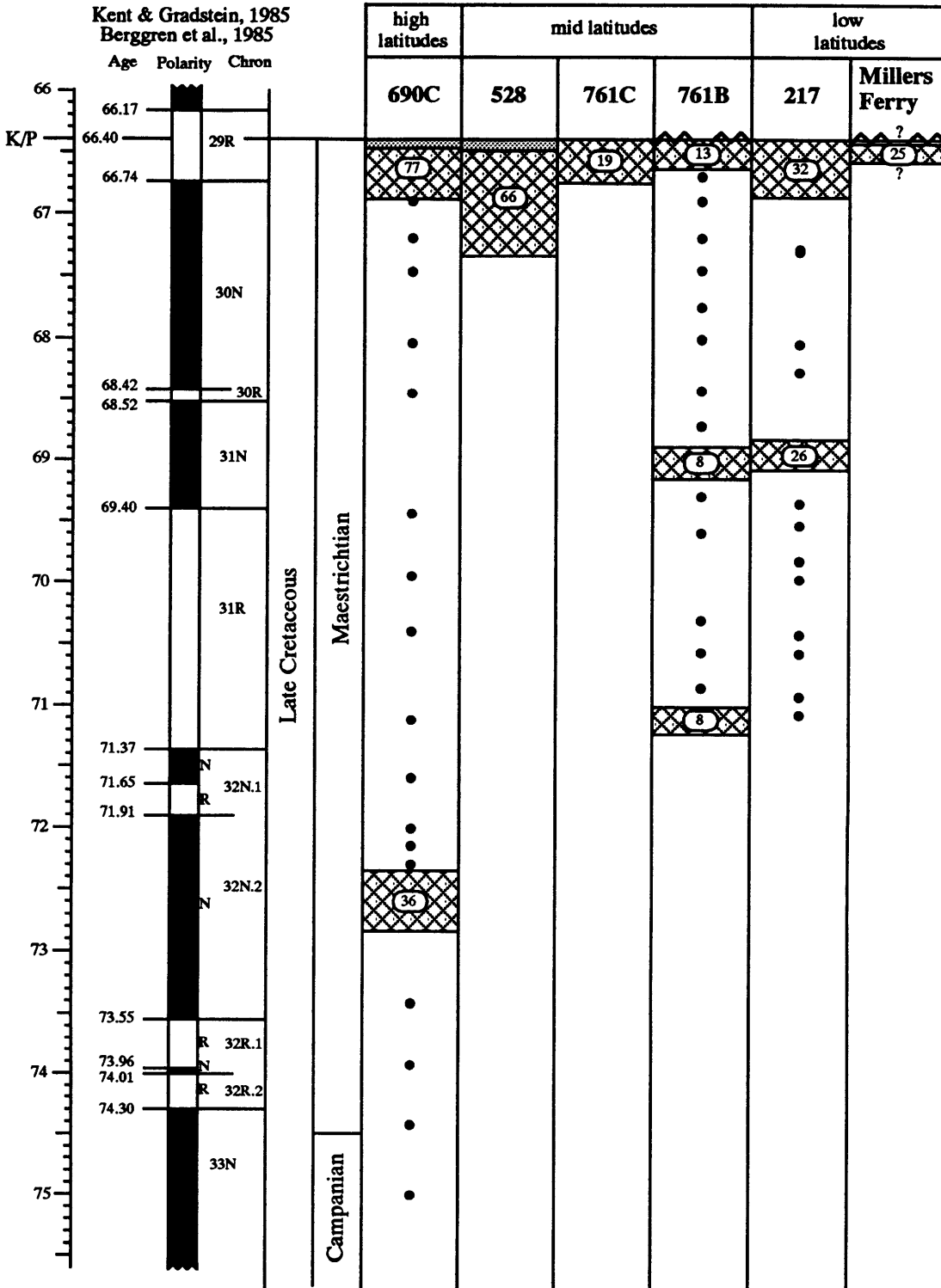


Figure 2: Schematic representation of the samples investigated in this study. The cross hatched and stippled patterns indicate intervals of high sample resolution. The numbers in each interval are the number of samples studied. The black dots represent the widely spaced samples between the intervals of high temporal resolution.

The portions between the intervals of very high resolution (cross hatched intervals in Figure 2) were investigated at much lower resolution (about one sample every 500 ky; black dots in Figure 2).

2) Methods

(A) SAMPLE PREPARATION

Counts were performed on settling slides for DSDP Holes 217 and 528, ODP Holes 690C, 761B and 761C. Smear slides were used for the section at Millers Ferry. The settling slides were prepared following Beaufort (1991) with slight modifications. Tap water was used to disaggregate the sediment and to prepare the nannofossil suspension. As tap water was slightly acidic having very noticeable etching effects on the calcareous nannofossils, the water was alkalinized by adding Ammoniumhydroxide (NH_4OH) which has the advantage of dissociating and evaporating in the heater oven without leaving a precipitate on the nannofossils. The largest problem encountered during sample preparation was that as the water degassed in the drying oven tiny gas bubbles accumulated under the cover slips and frequently lifted them from the platforms on which they were resting. It was not unusual to lose a quarter of the samples in a batch during the last step of sample preparation because of this phenomenon. This problem was avoided by weighing down the cover slip with a small amount of plasticine held above the suspension by four tooth-picks (Figure 3).

(B) COUNTING PROCEDURE

All counts for this study were performed using a Zeiss Axiophot light microscope. Three hundred specimens were selected as the minimum number to be counted because with this sum there is a 95% probability of encountering at least one specimen of a taxon whose true abundance in the assemblage is 1%. Because of the predominance of one species in most samples (*P. stoveri* in Hole 690C, *M. staurophora* in Holes 217, 528, 761B, 761C, and at Millers Ferry), counting was usually performed in two steps: first, all specimens were counted until a sum of ~300 was reached. Then, all taxa were counted except the single most abundant one until the sum of these (rarer) taxa was at least 300. In most samples the sum of all taxa exclusive of the dominant one was >500. Only when preservation was poor were fewer than 300 specimens counted. In samples

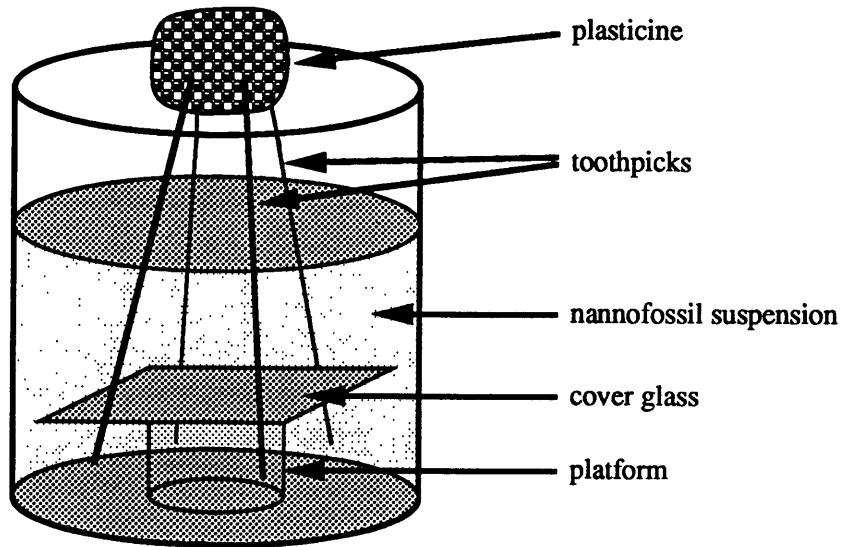


Figure 3: Toothpicks were used to hold a piece of plasticine (modelling compound) above the nanofossil suspension in order to hold the cover glass in place during the evaporation period in the heater oven.

with a preponderance of P. stoveri or M. staurophora all taxa were counted in at least 20 viewfields. If the sum of all taxa exclusive of the dominant one was <300 after examination of 20 viewfields, counting was continued.

Samples located near zonal boundaries or samples with very good preservation were scanned in addition to the counts. Any taxa that were observed during this additional scanning and had not been recorded previously are noted in the data tables (Appendix II) with an asterisk (*) or a 'P'. For calculation purposes an abundance of 0.5 "specimens" was assigned to these rare taxa.

(C) DATA PROCESSING

Percent of nannofossil taxa were calculated exclusive of the most abundant taxon because the dominance of one species (P. stoveri or M. staurophora) would have suppressed the percentages of all other taxa to such a degree that genuine abundance variations would have been obscured.

Absolute abundances: By counting on settling slides it is possible to estimate the number of specimens per gram sediment using the following equation (Beaufort, 1991):

$$X_{sed} = \frac{A}{G \times N} \times \frac{V_d \times r^2 \pi}{S \times (V_b + V_p - r^2 \pi \times H)}$$

where

X_{sed} = number of specimens per gram sediment

A = number of specimens counted

G = weight of sediment used to prepare the slide (in gram)

N = number of viewfields counted

V_d = volume of dilution = 1000 ml

r = radius of beaker..... = 2.65 cm for 150 ml beaker

..... = 2.32 cm for 100 ml beaker

S = area of one viewfield = 1.65×10^{-4} cm² (at 1250x mag.)

V_b = volume of suspension..... = 100 ml for 150 ml beaker

poured in beaker..... = 80 ml for 100 ml beaker

V_p = volume of platform..... = 3.4 cm³

H = height of platform..... = 2.69 cm

Two different kinds of beakers were used to prepare the settling slides of the uppermost Maestrichtian samples in Hole 690C: the different radii of the beakers and the different volumes of suspension used in the sample preparations for Hole 690C were taken into account in the calculations. The constants that were used to calculate the numbers of specimens per gram sediment in each of the two cases are given below (they are listed as "Beaker Constant" for all samples of Hole 690C in the data tables, Appendix II):

$$X_{\text{sed}} = \frac{A}{G \times N} \times 3.0 \times 10^6 \quad \text{for 150 ml beakers and}$$

$$X_{\text{sed}} = \frac{A}{G \times N} \times 2.7 \times 10^6 \quad \text{for 100 ml beakers.}$$

Only the smaller beakers were used for the preparations of samples from all other sites.

In order to take the changing carbonate content into consideration the number of specimens per gram carbonate, rather than per gram sediment have to be compared. They are calculated using the following equation:

$$X_{\text{CO}_3} = \frac{X_{\text{sed}}}{[\text{CO}_3]/100} = \frac{A}{G \times ([\text{CO}_3]/100) \times N} \times \text{const.}$$

Fluxes: The flux of coccoliths and nannoliths (number of specimens per cm² per kiloyear) was calculated using the following formula:

$$\text{Flux} = (X_{\text{CO}_3}) \times (W - (P/100) \cdot 1.01) \times \text{SR}$$

where

X_{CO_3} = number of nannofossil specimens per gram carbonate

W = wet bulk density (g/cm³)

P = porosity (%)

SR = sedimentation rate (cm/ky)

The values for wet bulk density and for porosity were taken from DSDP and ODP Initial Reports and the sedimentation rates used are given in Chapter 3 "Chronology".

Accumulation rates of carbonate and of insolubles: The carbonate accumulation rate (CAR) was calculated using the following formula:

$$\text{CAR} = ([\text{CO}_3]/100) \times (W - (P/100) \times 1.01) \times \text{SR}$$

where $[\text{CO}_3]$ = carbonate content in %, W = wet bulk density, P = porosity, and SR = sedimentation rate. The accumulation rate of insolubles was calculated in a similar way, but the first term in the equation above was replaced by $(1 - [\text{CO}_3]/100)$.

Reproducibility: On several slides multiple counts were performed to test whether the results were reproducible. Multiple counts of four samples were tested for homogeneity at the Center for Data Processing, University of Agriculture, Vienna, Austria, and the results are given in Table 1. Only the more abundant taxa in the samples were tested. Each field in Table 1 contains the numbers of specimens counted in the top row. In the lower row of each field the calculated χ^2 value as well as an indication of its significance are given (n.s. = not significant; (*) = significant at the 99% level; * = significant at the 95% level). Generally, these results imply homogeneity among different counts on the same slide, since one or two significant values among 60 are expected at a 0.05 probability level (i.e. one significant value out of 20).

Reliability: In the graphs in Chapter 4 ("Results of Nannofossil Counts") the data are plotted without further statistical treatment. These 1) reveal an apparent short term variability and 2) show the distribution of very rare taxa. These raw data may contain valuable information. However, when statistical treatments as described below are applied, some of the changes are not significant at the 95% confidence level. Thus, only major long term trends should be deduced from the raw data. In order to assess the significance of relatively small abundance changes (<~5%) and short term trends (i.e. ~100-500 ky) the following calculations were performed on data included in the discussion in Chapter 5: in order to reduce the short term variability of the

Hole	690C		690C		690C		690C		
Core-Section	16-1		15-CC		15-6		15-5		
cm-interval	21-22		19-20		40-41		79-80		
	count 1	count 2	count 1	count 2	count 1	count 2	count1	count 2	count 3
Number of Fields counted	30	37	30	11	30	26	30	34	33
	0.012	n.s.	0.006	n.s.	0.145	n.s.	2.61	n.s.	
<i>L. cayeuxii</i>	18	23	5	0	2	2	24	33	50
	0.005	n.s.	0.603	n.s.	0.248	n.s.	0.914	n.s.	
<i>A. octoradiata</i>	2	3	5	3	13	10	0	2	3
	0.094	n.s.	0.172	n.s.	0.191	n.s.	0.572	n.s.	
<i>Arkhangelskiella</i> spp.	14	14	24	5	12	12	5	3	13
	0.3	n.s.	0.586	n.s.	0.04	n.s.	2.524	n.s.	
<i>C. ? daniae</i>	22	35	46	8	21	11	10	9	17
	0.365	n.s.	2.709	n.s.	2.742	(*)	0.192	n.s.	
<i>C. ehrenbergii</i>	6	4	11	2	3	4	1	4	6
	0.576	n.s.	0.233	n.s.	0	n.s.	0.833	n.s.	
<i>Cretarhabdus</i> spp.	11	13	12	4	10	1	6	3	10
	0.003	n.s.	0.083	n.s.	5.982	*	1.073	n.s.	
<i>E. turriseiffeli</i>	9	8	9	2	5	0	2	2	1
	0.328	n.s.	0.03	n.s.	3.248	(*)	0.235	n.s.	
<i>Gartnerago</i> spp.	6	4	4	4	4	1	1	2	3
	0.576	n.s.	1.531	n.s.	0.816	n.s.	0.058	n.s.	
<i>G. fessus</i>	3	12	6	4	15	20	5	5	3
	2.486	n.s.	0.549	n.s.	0.474	n.s.	1.268	n.s.	
<i>K. magnificus</i>	20	41	74	20	40	36	17	10	18
	2.588	n.s.	0.597	n.s.	0.154	n.s.	2.576	n.s.	
<i>N. frequens</i>	42	42	87	24	30	51	48	55	64
(multiperforate)	1.546	n.s.	0.614	n.s.	5.796	*	2.215	n.s.	
<i>N. frequens</i>	24	22	20	6	12	14	8	7	8
(biperforate)	1.266	n.s.	0	n.s.	0.036	n.s.	0.578	n.s.	
<i>P. fibuliformis</i>	1	3	12	4	13	17	0	1	1
	0.054	n.s.	0.083	n.s.	0.306	n.s.	0.176	n.s.	
<i>P. cretacea</i>	26	39	43	20	28	29	19	22	31
	0.181	n.s.	1.363	n.s.	0	n.s.	0.007	n.s.	
<i>P. spinosa</i>	11	8	9	3	9	9	5	11	11
	1.163	n.s.	0.111	n.s.	0.054	n.s.	1.213	n.s.	
Total	236	310	421	140	250	251	162	181	265

Table 1: Results of test of homogeneity between different counts on the same slide.

data and to recognize underlying trends a five-point running average was calculated after the following method:

$$P_i = \frac{\sum_{i=-2}^2 x_i}{\sum_{i=-2}^2 \text{sum}_i}$$

where x_i is the number of specimens of a particular species counted in sample i and sum_i is the sum of all species in this sample (exclusive of the most abundant species). The age assigned to the five-point average was the mean of all five sample ages. In order to assess the reliability of the abundance variations observed in the curves of the five-point running average, approximate 95% confidence intervals were calculated following the method described by Mosimann (1965: p. 643).

$$P_L = \frac{p + [3.84/(2n)] \pm 1.96 \sqrt{[p(1-p)/n] + [3.84/(4n^2)]}}{1 + (3.84/n)}$$

where the larger value obtained is the upper limit and the smaller value is the lower limit.

CHAPTER 3 CHRONOLOGY

1) Biohorizons

In this chapter I present a discussion of the Maestrichtian biohorizons (calcareous nannofossils and planktonic foraminifera) used to construct the sedimentation rate curves. Age estimates of these biohorizons are based on calibration against magnetostratigraphy in sections with a reliable paleomagnetic record, using the magnetostratigraphy of Berggren et al. (1985). The depth-levels of the biohorizons in each section were compiled from the literature and were calculated as the average between the highest/lowest sample in which the taxon was present, and the subsequent higher/lower sample where it was absent. In all cases several different age estimates of the same biohorizon were obtained from different sections (Figure 4). For some biohorizons the age estimates cluster fairly tightly, whereas for others they show considerable spread. The reliability of the different estimates is discussed as well as the age (and error) ultimately assigned to a particular biohorizon. Generally, the age assigned to any biohorizon is the average of all the ages listed here, the error assigned to each age estimate is the difference to the extreme values listed.

First Appearance Datum (FAD) of *Micula prinsii*: 66.63 Ma (+0.38; -0.17)

Hole	Age (Ma)
527	66.46
525A	66.47
577	66.57
577A	66.63
524	67.01

Except for Hole 524 the lowest occurrence of *M. prinsii* lies in the Maestrichtian portion of Chron C29R. Thus the level of the K/P boundary and the Chron C29R/30N reversal boundary were used as tiepoints to estimate the age of this biohorizon. Because the Maestrichtian portion of Chron C29R is quite short (only about 0.34 m.y.; Berggren et al., 1985) even a short hiatus at the K/P boundary could lead to a significant underestimate of the sedimentation rate. A complete sequence of biozones in the early Paleocene

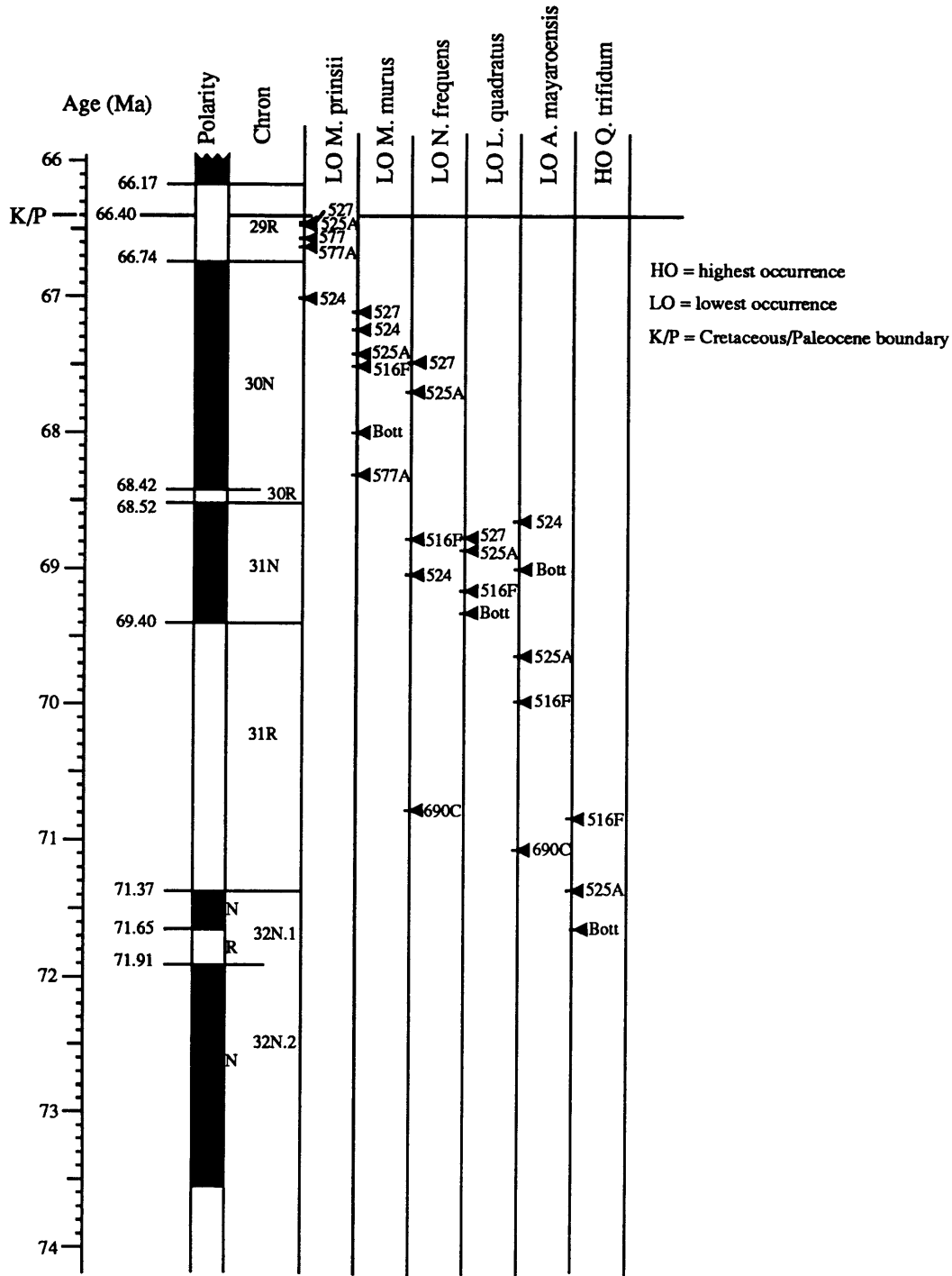


Figure 4: For each species the highest/lowest occurrences in different DSDP- and ODP Holes, and in the Bottaccione Section (Bott), Italy, are plotted against magnetostratigraphy (after Berggren et al., 1985). For literature used to compile this chart see text.

and the presence of an iridium enrichment in Hole 524 (Percival, 1984; Hsü et al., 1982) and in Hole 577B (iridium was not measured in Holes 577 and 577A; Michel et al., 1985) suggest that these sections are indeed complete. In Holes 525A and 527 no iridium enrichment was reported, but based on biostratigraphy the K/P boundary sequences (calcareous nannofossils: Manivit, 1984; planktonic foraminifera: Boersma, 1984a) in these holes appear to be continuous.

The lowest occurrence of M. prinsii is most precisely delineated in Holes 577 and 577A (within 30 and 50 cm, respectively; Monechi, 1985).

In Holes 525A and 527 the lowest occurrence of M. prinsii is not very well constrained: Micula prinsii was reported only from one sample in each hole (Manivit, 1984).

The lowest occurrence of M. prinsii in Hole 524 is an exception insofar as it occurs in Chron C30N (Percival, 1984). Percival does not discuss his species concept of M. prinsii, and he does not report any peculiarities associated with it.

The age assigned to the FAD of M. prinsii is 66.63 Ma (+0.38; -0.17 m.y.) when all available sections are included. If the outlier of Hole 524 is disregarded the FAD of M. prinsii is at 66.53 Ma (+0.1; -0.07).

First Appearance Datum of Micula murus: 67.60 Ma (+0.71; -0.49)

Hole/Section	Age (Ma)
527	67.11
524	67.24 (68.39?)
525A	67.42
516F	67.51
Bottacione Section	68.00
577A	68.31

The calcareous nannofossils in Hole 524 were studied by Percival (1984) who presented a range chart in which M. murus occurred continuously from the K/P boundary to 524-22-CC (228.0 mbsf; corresponding to 67.24 Ma). Below this sample no specimen of M. murus was recorded until sample 524-26-5, 39-40 cm (262.89 mbsf; corresponding to 68.39 Ma) where M. murus was observed again very rarely. Percival (1984) used this isolated, lowermost occurrence of M. murus to delineate the lowest occurrence of M. murus. I believe that it is more appropriate to use the base of the continuous occurrence of M. murus as

the level of its lowest occurrence; therefore the age estimate of 67.24 Ma is preferred for the lowest occurrence of M. murus in Hole 524.

It appears that the six ages estimated for the lowest occurrence of M. murus fall into two groups: the South-Atlantic Holes (516F, 524, 525A, 527: Shipboard Scientific Party, 1983; Percival, 1984; Manivit, 1984) have values between 67.11 and 67.51 Ma, whereas the tropical hole 577A (Monechi, 1985) and the Tethys-section (Bottacione Section: Monechi and Thierstein, 1985) have values of 68.31 and 68.00, respectively. Micula murus is the low latitude marker species of the late Maestrichtian, and it is possible that this form occurs earlier in tropical latitudes than at middle latitudes.

The average of all values listed for the lowest occurrence of M. murus is 67.60 Ma (+0.71; -0.49). If the paleolatitude of a section is very well known, it may be permissible to use a value of 67.32 Ma \pm 0.2 for mid latitude sites, or of 68.15 Ma \pm 0.15 for tropical/tethyan sections.

First Appearance Datum of Nephrolithus frequens

Hole	Age (Ma)
527	67.48
525A	67.70
516F	68.78
524	69.04
690C	70.78

The diachrony of this biohorizon is very apparent in Figure 4 (compare also Pospichal and Wise, 1990a: fig. 6). Whereas the lowest occurrence of N. frequens in Hole 690C lies in the lower half of Chron C31R (Pospichal and Wise, 1990a; Hamilton, 1990), it lies within C31N in Holes 524 (Percival, 1984; Tauxe et al., 1984) and 516F (Shipboard Scientific Party, 1983; Hamilton et al., 1983), and in Chron C30N in Holes 525A and 527 (Manivit, 1984; Chave, 1984). It is not strictly correlated with latitude, or else the lowest occurrences of this species in the Walvis Ridge Sites (latitude and paleolatitude within five degrees of each other: 524, 525A, 527) should be clustered more tightly, which is not the case. In fact, the temporal difference in the lowest occurrence between Hole 524 and 527 (1.56 m.y.) is almost as large as the difference between Hole 524 and 690C (1.74 m.y.)! Still, it is intriguing that the lowest occurrences of N. frequens in the Walvis Ridge sites occurs progressively from the more southern to the northern sites (i.e. earliest first occurrence in Hole 524, then

in 525A, then in 527). It has been suggested (Pospichal and Wise, 1990) that the diachronous lowest occurrences of N. frequens in different sections reflects the equatorward spreading of high latitude water mass properties (e.g. cooler temperatures) throughout the Maestrichtian. If this is correct, then this spreading did not proceed at a constant pace from high latitude Site 690 to the equator. It took N. frequens roughly the same amount of time to conquer all the Atlantic Ocean between Antarctica (Hole 690C) and the Walvis Ridge (Hole 524) as it needed to cross the Walvis Ridge itself (from Hole 524 to Hole 527).

As a consequence of the highly diachronous first occurrences of N. frequens no average age is assigned to this biohorizon. The list given above may help, though, to estimate an approximate age of the lowest occurrence of N. frequens in a sections of which the paleolatitude is known.

First Appearance Datum of *Abathomphalus mayaroensis*: 69.67 Ma (+1.4; -1.02)

Hole/Section	Age (Ma)
524	68.65
Bottacione Section	69.00
525A	69.64
516F	69.98
690C	71.07

The lowest occurrence of this planktonic foraminifer varies considerably between the sections included in this compilation, occurring in different magnetochrons in different sections: in Hole 524 (Smith and Poore, 1984) and in the Bottacione Section its lowest occurrence lies in Chron C31N (Luterbacher and Premoli Silva, 1964), whereas in Holes 516F (Weiss, 1983), 525A (Boersma, 1984a), and 690C (Huber, 1990) it lies in Chron C31R. No clear correlation of this diachrony of the lowest occurrence with paleolatitude is apparent, other than its earliest first occurrence in southern high latitude Site 690 (see also discussion in Huber and Watkins, 1992). The age estimate of this biohorizon is fairly poorly constrained: 69.67 Ma (+1.4; -1.02).

First Appearance Datum of *Lithraphidites quadratus*: 69.03 Ma (+0.29; -0.26)

Hole/Section	Age (Ma)
527	68.77
525A	68.86
516F	69.16
Bottacione Section	69.32

The ages estimates for this biohorizon in different sections cluster fairly tightly compared with other biohorizons. The lowest occurrence of *L. quadratus* in all sections lies in Chron C31N (calcareous nannofossil results from Shipboard Scientific Party, 1983; Manivit, 1984; Monechi and Thierstein, 1985; paleomagnetic results from Alvarez et al., 1977; Hamilton et al., 1983; Chave, 1984). The average age is 69.03 Ma (+ 0.29; -0.26).

Last Appearance Datum of *Quadrum trifidum*: 71.28 Ma (+0.34; -0.44)

516F	70.84
525A	71.36
Bottacione Section	71.65

Age estimates of this biohorizon cluster fairly tightly around the boundary between Chrons C31R and C32N (calcareous nannofossil results from Shipboard Scientific Party, 1983; Manivit, 1984; Monechi and Thierstein, 1985; paleomagnetic results from Alvarez et al., 1977; Hamilton et al., 1983; Chave, 1984). The average age assigned to this biohorizon is 71.28 Ma (+0.37; -0.44).

2) ODP Hole 690C

Location

ODP Hole 690C was drilled on the southwestern flank of Maud Rise in the Atlantic Sector of the Antarctic Ocean (Weddell Sea) at 65°9.621'S, 1°12.285'E in 2914 m waterdepth (Shipboard Scientific Party, 1988). This site was included in this study because it represents one of the southernmost Maestrichtian sections in calcareous facies drilled to date. It contains a biostratigraphically complete K/P boundary section with an iridium enrichment.

Lithology

About 70 m of Upper Cretaceous (upper Campanian/lower Maestrichtian to K/P boundary) sediment were penetrated (sediment/basement contact at 317.0 mbsf; K/P boundary at 247.79 mbsf). The sediment was divided into two lithologic units, based on the calcareous nannofossil content (Shipboard Scientific Party, 1988; Figure 5): in the lower unit (unit V: 317.0 to 281.1 mbsf) foraminifera and terrigenous quartz and clay constitute the dominant components of the sediment, in the upper unit (unit IV: 281.1 to 137.8 mbsf) calcareous nannofossils dominate; the boundary between these lithologic units coincides approximately with the boundary between the middle and upper Maestrichtian.

The relative abundances of different sedimentary components vary widely throughout the Maestrichtian (Figure 5). Calcareous nannofossils fluctuate considerably (10-40%) in the uppermost Campanian to middle Maestrichtian; they constitute about 50% of the upper Maestrichtian sediment. In the Paleocene they increase to values >80%. Foraminifera attain peak abundances of 30-35% in the uppermost Campanian/lowermost Maestrichtian. They fluctuate between 2-20% throughout the middle and upper Maestrichtian; in the uppermost Maestrichtian (about 4 m below the K/P boundary) foraminifera reach a peak of 25%. Quartz and clay constitute 10-20% of the sedimentary components in the uppermost Campanian/lowest Maestrichtian, reach peak abundances over 80% in the middle Maestrichtian, and decrease to very low values (<10%) in the lowest Paleocene. Mica content increases throughout the Maestrichtian from <10% in the uppermost Campanian/lower Maestrichtian to almost 20% in the upper Maestrichtian. About 4 m below the K/P boundary mica decreases to ca. 5% and remains at this level through the

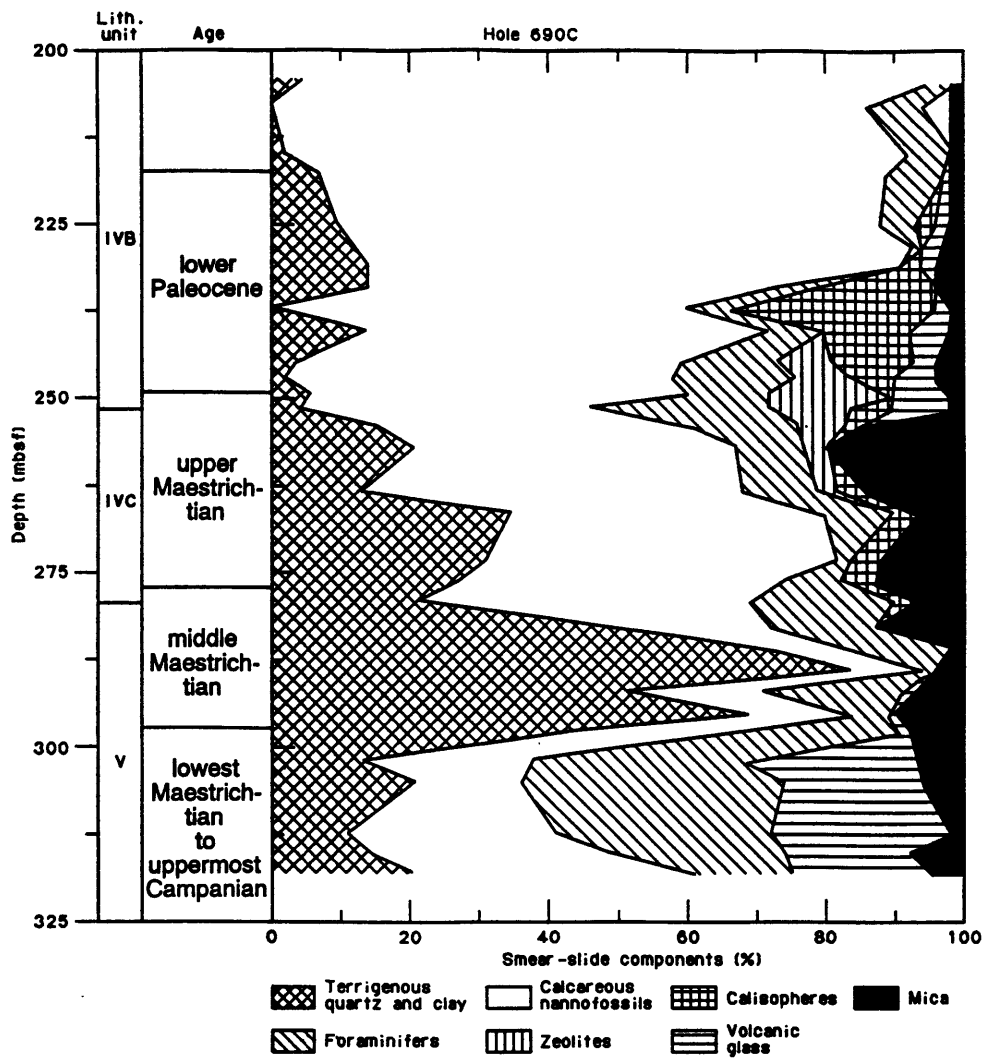


Figure 5: Lithologic composition of Maestrichtian and lower Paleocene sediments in Hole 690C (from Shipboard Scientific Party, 1988: p. 191).

lower Paleocene. Volcanic glass is an important sedimentary component (20-25%) below ca. 300 mbsf (uppermost Campanian to lowermost Maestrichtian). A light greenish ash-layer occurs at 314.38 mbsf. Volcanic glass is virtually absent in most of the middle and upper Maestrichtian sediments, but reoccurs towards the top of the Maestrichtian (ca. 4 m below the K/P boundary) where it reaches values of ca. 10% and declines to 0% during the lower Paleocene. Zeolites are present only in upper Maestrichtian and lower Paleocene sediments; they reach their peak abundance (almost 20%) in the immediate vicinity of the K/P boundary. Calcispheres occur as minor sediment components (<5%) in the upper part of the middle and in the upper Maestrichtian. In the lowermost Paleocene they reach peak abundances of almost 30%. Pale brown and yellowish brown chert fragments and layers occur sporadically in the lowermost sediments at this site.

Bioturbation is minor to strong throughout the Upper Cretaceous section, often obscured by drilling disturbance in the uppermost Campanian/lowest Maestrichtian sediments.

Cretaceous/Paleocene boundary:

The change of Cretaceous to Paleocene assemblages of planktonic foraminifera and of calcareous nannofossils occurs in section 690C-15-4, between about 50 and 30cm (Stott and Kennett, 1990a; Pospichal and Wise, 1990b; personal observation). Also in the immediate vicinity of the K/P boundary (Section 690C-15-4, between ca. 60 and 30 cm) occurs a very distinct, but heavily bioturbated lithology- and color-change from white nannofossil chalk below to pale-brown nannofossil mud above. The carbonate content of the sediment in this interval decreases from 80-90% in the white chalk to <50% in the pale-brown sediment (Figure 6). The peak abundance of zeolites (which are the product of diagenetic alteration of volcanogenic sediments) and the presence of moderate amounts (ca. 10%) of volcanic glass support the argument of Shipboard Scientific Party (1988) that the darker color of the sediment above the contact may be due to volcanic influence.

Pospichal and Wise (1990b) showed that the white nannofossil chalk contains typical Cretaceous nannofossil assemblages, whereas the pale-brown sediments contain approximately 20% persistent and incoming taxa. They argue therefore that the K/P-boundary should be drawn at the top of the highest autochthonous white chalk clast (690C-15-4, between 41.5 and 41.8 cm;

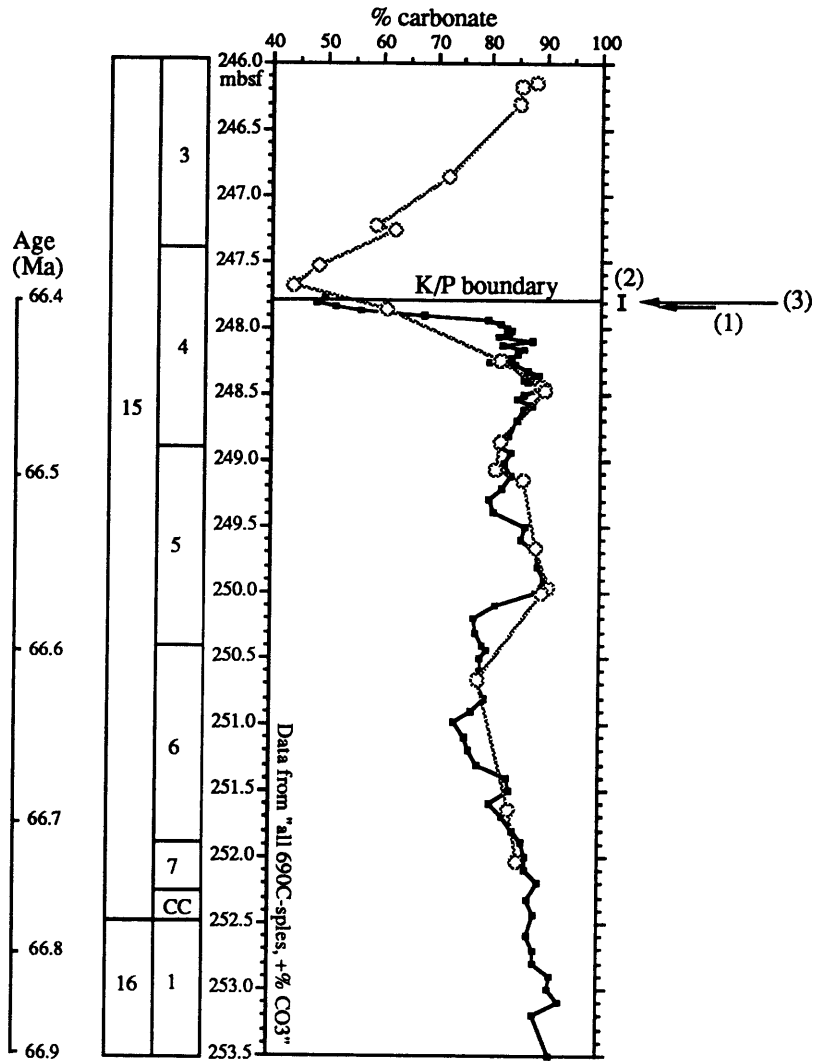


Figure 6: Decrease in carbonate content at the Cretaceous/Paleocene boundary (black squares: this study; open circles: Stott and Kennett, 1990b).
 (1) Level where Pospichal and Wise (1990b) place the K/P boundary (based on calcareous nannofossils).
 (2) Interval of planktonic foraminiferal turnover from Maestrichtian to Paleocene assemblages (Stott and Kennett, 1990b).
 (3) Peak of iridium enrichment (Michel et al., 1990).

247.815 and 247.817 mbsf; Pospichal and Wise, 1990b). This approach - which differs from the definition of the K/P boundary as the "level of extinction of most Upper Cretaceous species" (Cepek and Hay, 1969) - was justified by the fact that no extinction horizon is apparent in this section, due to reworking (or survival) of Cretaceous species into the Paleocene.

In the planktonic foraminifera there is no well defined extinction horizon at the K/P boundary. Cretaceous taxa are replaced by Cenozoic taxa over a 10-cm interval (between samples 690C, 15X-4, 45-47 cm and 15X-4, 35-37 cm, 247.85 and 247.75 cm, respectively; Stott and Kennett, 1990a). Stott and Kennett place the K/P boundary at the level where Paleogene species become dominant (>50%) over Cretaceous species. It must be stressed, that this is not the proper definition of the K/P boundary in planktonic foraminifera biostratigraphy (i.e. the extinction horizon of Cretaceous taxa) but rather an attempt to circumvent the problem of intensive reworking in this section.

An iridium-enrichment occurs in Core 690C-15X with a well-defined peak at 15X-4, 39-40cm (247.79 mbsf; Michel et al., 1990).

Benthic foraminifera show only minor changes at the K/P boundary (Thomas, 1990), whereas calcareous dinoflagellates show a dramatic turnover (Fütterer, 1990).

Because bioturbation makes it impossible to draw the K/P boundary unambiguously with nanno- and microfossils, the level of the Ir-enrichment is used as the level of the K/P boundary in this study.

Paleoenvironment during the Maestrichtian

The Maestrichtian latitude of Site 690 was about 70°S based on paleocontinental reconstructions of Firstbrook et al. (1979) and of Smith et al. (1977).

The Upper Cretaceous and Cenozoic sediments at Site 690 were laid down in a pelagic, open-ocean environment (Shipboard Scientific Party, 1988, p. 236). Paleontological (benthic foraminifera; Thomas, 1990) as well as geochemical evidence (Mn/Fe ratios; Robert and Maillot, 1990) suggest that bottom waters were well oxygenated. Water depth estimates were based on comparison of benthic foraminiferal assemblages at Site 690 (Thomas, 1990) with results from benthic foraminifera studies in the South Atlantic (Katz and Miller, 1990). Estimates of water depth are tenuous and indicate middle to lower bathyal depths (1000-2500m) during the Late Cretaceous and early Paleocene.

and subsequent deepening to upper abyssal depths (2500m or deeper) for the remainder of the Cenozoic (Shipboard Scientific Party, 1988, p. 213).

Paleoclimate

Smectite dominates the clay mineral fraction from the Upper Cretaceous through the upper Eocene in sediments of Sites 689 and 690 (65-100%; Robert and Maillot, 1990). This indicates warm climatic conditions with alternating periods of humidity and aridity in Antarctica, the source area of the clay minerals. Starting in the Paleocene kaolinite is present at Site 690 indicating increased humidity on Antarctica at this time (Robert and Maillot, 1990).

Stable isotope results ($\delta^{18}\text{O}$) from Maestrichtian planktonic and benthic foraminifera indicate long term cooling throughout the entire Maestrichtian with a short warming event during the last 0.5 m.y. before the K/P boundary (Barrera and Huber, 1990; Stott and Kennett, 1990b; see Chapter 5 for discussion).

Nannofossil Biostratigraphy

The initial sampling was based on the nannofossil biostratigraphy of Pospichal and Wise (1990a) which was subsequently refined in the course of this study. The following problems were encountered:

First occurrence of Nephrolithus frequens: This species evolves in the late Maestrichtian, possibly from Nephrolithus corystus (Pospichal and Wise, 1990a). Consequently there are many forms close to the first occurrence of N. frequens that are intermediate between a typical N. corystus and a typical N. frequens. Pospichal and Wise report that N. frequens is absent in sample 19X-1, 130-132 (282.41 mbsf), that it is questionably present at 18X, CC (281.10 mbsf) and that it occurs 'commonly' in sample 18X-5, 36-38 cm (277.76 mbsf). My own investigations showed that N. frequens occurs commonly in sample 18X-5, 54 cm (277.94 mbsf), where it constitutes about 22% of the assemblage. In sample 19X-1, 107cm intermediate forms between N. frequens and N. corystus occur infrequently. These forms do not bear a central stem, they have a comparatively narrow margin, they are smaller and have fewer perforations than the 'typical', stem-bearing specimens of N. corystus in this sample. In addition, these forms mostly have a distinct kidney-shaped outline, whereas N. corystus often has an almost elliptical outline. At this time it is impossible to assign these intermediate forms unambiguously to either species because the

structural differences of the central area - which are the only pertinent criteria to distinguish N. frequens from N. corystus - are not visible under the light microscope. Until these questions can be resolved in a subsequent study on the SEM the first (certain) occurrence of N. frequens is recorded in sample 690C-18-5, 54 cm (277.94 mbsf); N. frequens is (probably) absent in 690C-19-1, 107cm (282.17 mbsf).

Last occurrence of Nephrolithus corystus: The last occurrence of this species lies in an interval where preservation of calcareous nannofossils is very poor. Unquestionable specimens are present up to 690C-18-2, 60-61 cm (273.5 mbsf). In overlying samples from sections 18-2 and 18-1 no specimens of N. corystus were observed; only the most dissolution resistant taxa are present in this interval. In sample 690C-17-CC, 20-21 cm (271.4 mbsf) the preservation of calcareous nannofossils improves and one specimen was found after extremely careful search in a sample where large forms were enriched by centrifuging. Nephrolithus corystus is absent in the remainder of Core 690C-17. Due to the poor preservation of calcareous nannofossils in the interval where N. corystus disappears (between 690C-18-2, 60-61 cm and 690C-17-CC) it is not possible to establish whether N. corystus is present continuously through sections 690C-18-2 and -18-1, or whether the occurrence in 690C-17-CC should be discarded as an artifact of reworking.

Last occurrence of Biscutum magnum: This species disappears between samples 690C-18-CC, 15-16 cm (281.10 mbsf) and 690C-18-5, 54 cm (277.94 mbsf). No sediment was recovered between these sections. These observations agree with Pospichal and Wise's (1990a) practice of drawing the boundary between the B. magnum Zone and the N. corystus Subzone (i.e. LO of B. magnum, Pospichal and Wise, 1990a) at the same level, despite the observation of one specimen in sample 690C-18-5, 36-38 cm (277.76 mbsf; Pospichal and Wise, 1990a).

Last occurrence of Biscutum coronum: The last occurrence of this species was observed in sample 690C-20-1, 136 cm (292.16 mbsf), it is absent in sample 690C-20-1, 133 cm (292.13 mbsf). This level is a little higher than previously reported by Pospichal and Wise (1990a).

Last occurrence of R. levis: This species was observed in sample 690C-18-5, 54 cm, albeit very rarely. According to Pospichal and Wise (1990a) R. levis is absent in sample 690C-18-5, 36-38 cm (277.76 mbsf).

Magnetostratigraphy

High resolution paleomagnetic data of high quality were obtained from Upper Cretaceous sediments of Holes 690C and 689B (Hamilton, 1990). Hamilton (1990) indicated that the combined results from both holes yielded sufficient evidence to decipher the Upper Cretaceous magnetostratigraphy of Maud Rise. Due to the high latitude of Maud Rise in the Late Cretaceous (not significantly different from its present day location; Hamilton, 1990) it was acceptable to use the inclination of the remanent magnetization vector as a reliable index of magnetic polarity. Normal magnetization overprint of most samples could be satisfactorily removed through magnetic cleaning. The high rate of recovery allowed high resolution sampling and yielded a sharp definition of the polarity record in Hole 690C (Hamilton, 1990).

The polarity record as well as the magnetostratigraphic interpretation (after Hamilton, 1990) are shown in Figure 7.

All biostratigraphic zones around the K/P boundary which occurs in Chron C29R were identified (Pospichal and Wise, 1990b; Stott and Kennett, 1990a). Interestingly, in Hole 690C this boundary occurs closer to the top of 29R than in other pelagic sections (Herbert and D'Hondt, 1990). This may be due to a very low sedimentation rate in the earliest Paleocene, or may indicate the presence of a hiatus within CP1a or at the CP1a/CP1b zonal boundary (Pospichal and Wise, 1990b). The fact that Cruciplacolithus primus and C. tenuis appear at about the same level (Pospichal and Wise, 1990b) supports the possibility of a hiatus between these two subzones. Poor preservation of planktonic foraminifera (R. D. Norris, oral comm.) in the lowermost Paleocene may indicate partial carbonate dissolution; no similar preservational pattern is reported in the calcareous nannofossils (Pospichal and Wise, 1990b).

Sedimentation rates: Sedimentation rates in the Maestrichtian of Hole 690C are based on the paleomagnetic results of Hamilton (1990). Magnetochron boundaries are very well constrained (Figure 7) except for the C32R/33N boundary, which occurs between samples that are more than six meters apart. The sedimentation rate of the overlying interval (Chron C32N) is extended to the bottom of the section. The data used are tabulated in Table 2, the results included in Figure 7.

Table 2: The depth assignments of the magnetozone boundaries are taken from Hamilton (1990), the K/P boundary was placed at the level of the iridium-peak (Michel et al., 1990). Numerical ages were assigned to these boundaries according to Kent and Gradstein (1985) and Berggren et al. (1985).

Boundary	Depth (mbsf)	Age (Ma)	Sedimentation Rate (m/m.y.)
29N/29R	247.55	66.17	
K/P boundary	247.79	66.40	0.24m/0.23m.y. = 1.04
29R/30N	252.28	66.74	4.49m/0.34m.y. = 13.21
31N/31R	272.25	69.40	19.97m/2.66m.y. = 7.51
31R/32N	283.39	71.37	11.14m/1.97m.y. = 5.65
32N/32R	302.78	73.55	19.39m/2.18m.y. = 8.89

8.89

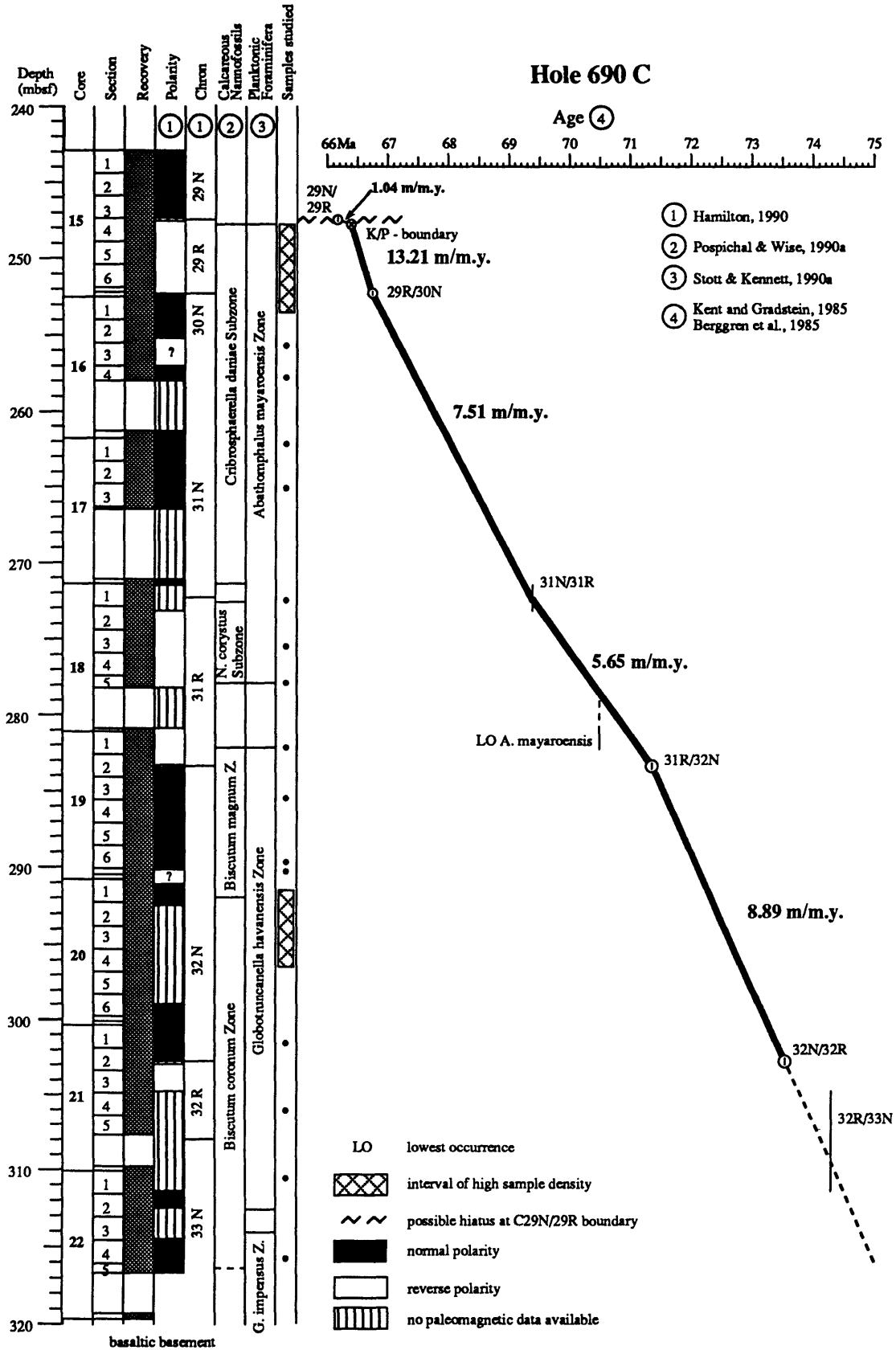


Figure 7: Sedimentation rate curve for the Maestrichtian section in Hole 690C.

3) ODP Hole 761B

Location

Hole 761B is located in the eastern Indian Ocean on the central part of Wombat Plateau (16°44.23'S, 115°32.10'E) about 400 km off the Australian coast in 2167.9 m waterdepth (Shipboard Scientific Party, 1990). The paleolatitude of this site during the Maestrichtian was about 40-45°S according to Firstbrook et al. (1979), and about 30-40°S according to the paleocontinental reconstructions of Smith and Briden (1977).

Lithology

The Maestrichtian sediments in this Hole are light-colored nannofossil chalks with foraminifera (lithologic unit II; Shipboard Scientific Party, 1990); this unit was divided into three subunits based on changing abundances of biogenic and lithologic components. Subunit IIA (175.9-198.7 mbsf) consists of fairly pure, extensively bioturbated nannofossil chalk, with <10% foraminifera and usually <2% detrital mica. Yellowish brown porcellanite chert nodules are present but rare. The top of this subunit coincides with the K/P boundary where a distinct color and lithologic change occurs.

In Subunit IIB (198.7-240.0 mbsf) foraminifera increase to 10-25% and zeolite constitutes up to 5 % of the sediment in core 761B-24X. Inoceramus shell fragments are common throughout this subunit, particularly abundant in core 761B-25X. Bioturbation is extensive throughout; sediment colors are very pale brown, light gray, and white. Brownish yellow chert nodules are present but rare. The base of this lithologic subunit is early to middle Albian.

The K/P boundary

Calcareous Nannofossils: The K/P boundary is a drilling contact and coincides with a conspicuous lithologic and colour change, from light-gray, clay-rich Paleocene chalk to white late Maestrichtian nannofossil chalk at 761B-21-4, 126 cm (175.96 mbsf; Shipboard Scientific Party, 1990). A hiatus is present at the K/P boundary as the lowermost Paleocene nannofossil zone (NP1) is missing. Cruciplacolithus primus and C. tenuis both are present together in 761-21-4, 125 cm (Shipboard Scientific Party, 1990). The uppermost Maestrichtian at 761B belongs to the M. murus Zone.

Planktonic Foraminifera: The hiatus at the K/P boundary is also recognized by planktonic foraminifera as the lowermost Paleocene assemblages indicate Zone P1C (Shipboard Scientific Party, 1990).

Biostratigraphy

Calcareous Nannofossils: The uppermost Maestrichtian marker fossil, M. prinsii, was not observed in this hole, nor in the more complete hole 761C (Bralower and Siesser, 1992). The reason for its absence may be a short hiatus in Hole 761B or paleoceanographic exclusion. The latter explanation is favored because M. prinsii is also absent in Hole 761C where an iridium enrichment at the K/P boundary (Rocchia et al., 1992) and a complete sequence of upper Maestrichtian and (condensed) Paleocene nannofossil zones indicate that the K/P transition is complete. On the other hand, the absence of M. prinsii at Site 761 cannot be strictly a function of paleolatitude, since this species is present in the Walvis Ridge sites (e.g. 528) which have a very similar paleolatitude to Site 761 in the Upper Cretaceous.

The upper Maestrichtian marker fossils M. murus and N. frequens are both present in this section. The lowest sample where unquestionable specimens of M. murus were observed is 761B-22-1, 80 cm (180.50 mbsf). Specimens very similar to M. murus but with slightly shorter arms were observed in sample 761 B, 22-2, 80 cm (182.0 mbsf). Micula murus is absent in sample 761 B, 22-3, 80 cm (183.50 mbsf) and below. Specimens intermediate between M. staurophora and M. murus were observed down to 761B-23-2, 81 cm (191.51 mbsf). These forms have a compact, square center with the extinction pattern of M. staurophora in cross polarized light, and elongate arms reminiscent of M. murus. The lowest occurrence of M. murus observed here is considerably higher in the section than reported by Bralower and Siesser (1992; 23-1, 81-83 cm; 190.01 mbsf). The reason for this discrepancy is unclear. Different taxonomic concepts of M. murus between this study and Bralower and Siesser's investigation cannot be invoked, since Bralower and Siesser (1992) were aware of the intermediate forms between M. staurophora and M. murus (compare their illustrations: plate 7, figures 1-6). It should be noted that the lowest occurrence of M. murus as reported by Bralower and Siesser (1992) is unusually low compared with the level of this biohorizon in other sections (see Chapter Biohorizons).

Nephrolithus frequens occurs continuously down to sample 761B-23-1, 81 cm (190.01 mbsf). This agrees well with Bralower and Siesser's (1992) observation of the lowest occurrence of N. frequens in 761B-23-1, 81-83 cm. The isolated occurrence in sample 761B-23-3, 90cm (193.10 mbsf; see data table for Hole 761B) is unexplained (bioturbation? truly discontinuous occurrence?). It is not taken as the level of the lowest occurrence of N. frequens since careful inspection of smear slides could not verify the presence of N. frequens in the samples between.

The lowest occurrence of L. quadratus was reported in 761B-23-3, 40-41 cm (192.60 mbsf; Bralower and Siesser, 1992) at which level this species occurs frequently (Bralower and Siesser, 1992). In my count data the lowest occurrence of L. quadratus is in sample 761B-23-3, 150 cm (193.70 mbsf; see data table for Hole 761B).

The highest occurrence of R. levis was found in 761B-24-1, 39-40 cm (199.09 mbsf; Bralower and Siesser, 1992).

A very low sedimentation rate or a hiatus in the lower Maestrichtian is indicated by the very close (or concomitant) occurrence of the following three nannofossil biohorizons. The highest occurrence of E. eximius lies in 761B-24-CC (208.2 mbsf, Bralower and Siesser, 1992). Bralower and Siesser (1992) report the highest occurrence of B. parca constricta from 761B-24-5, 34-35 cm and use this level as the highest occurrence of B. parca. This is not followed here, since the highest occurrence in 761B-24-5, 34-35 is discontinuous from the other levels where this species was observed; in addition, section 761B-24-5 does not exist in the barrel sheets of the core description (Shipboard Scientific Party, 1992; p. 506) and was not present in the ODP core repository in College Station, Texas, where I took my samples. Therefore the highest occurrence of B. parca is placed in 761B-25-1, 41-42 cm (208.61 mbsf), which is the highest level of continuous occurrence of B. parca parca and B. parca constricta in 761B (Bralower and Siesser, 1992). The highest occurrence of Q. trifidum was also reported from 761B, 25-1, 41-42 cm (208.61 mbsf). The presence of a hiatus in the lower Maestrichtian in 761B is indicated in the sedimentation rate curve supplied by Shipboard Scientific Party (1990). In contrast, Bralower and Siesser (1992) indicate that the Maestrichtian is complete (at least as far as nannofossil biostratigraphy indicates), but that the Campanian portion is condensed.

Cretaceous planktonic foraminifera indicate that only the upper to middle Maestrichtian are fully developed (Wonders, 1992), the remainder of the Upper Cretaceous (lower Maestrichtian to Coniacian/upper Turonian) is condensed. The lowest occurrence of A. mayaroensis was reported in 761B-24-1, 56-58 cm (199.28 mbsf; absent in 761B-24-2, 63-65cm; 200.85 mbsf; Wonders, 1992) and defines the bottom of the A. mayaroensis Zone.

The middle Maestrichtian C. contusa Zone was recognized between 761B-24-2, 63-65 cm (200.85mbsf) and 761B-24-4,61-63 cm (203.83 mbsf; Wonders, 1992), underlain by the H. rajagopalani Zone: 761B-25-1, 59-62 cm (208.82 mbsf) to 761B-25-5, 59-62 cm (214.82 mbsf; Wonders, 1992). The bottom of this zone (lowest occurrence of H. rajagopalani) is of late Campanian age (within the G. calcarata Zone, according to Nederbragt, 1990; Wonders, 1992).

Magnetostratigraphy

Paleomagnetic data are available from Upper Cretaceous sediments of Hole 761B (Galbrun, 1992; Table 3). Thermal cleaning, alternating field demagnetization, or both, revealed a stable remanent component of normal or reverse polarity in most samples (Galbrun, 1992). The magnetic polarity sequences were correlated with the standard magnetic polarity time scale with the aid of calcareous nannofossil biostratigraphy (Galbrun, 1992). Above the K/P boundary where sedimentation rates are low, some polarity zones were indicated by single samples only (e.g. C29N, C28). For this reason these chrons were not included in Figure 8. It is a striking, but unexplained feature of the NRM intensity curve that the intensities show a minimum in the upper Maestrichtian and lower Paleocene (Galbrun, 1992: figure 4). No correlation between variation of NRM intensity and of lithology was noted (Galbrun, 1992).

Table 3: Fixpoints used to calculate sedimentation rates in the Maestrichtian of Hole 761B.

Boundary	Depth (mbsf)	Age (Ma)	Sed. Rate (m/m.y.)
K/P boundary	175.96	66.40	
29R/30N	181.17	66.74	5.21m/0.34m.y. = 15.32
31N/31R	194.94	69.40	13.77m/2.66m.y. = 5.18

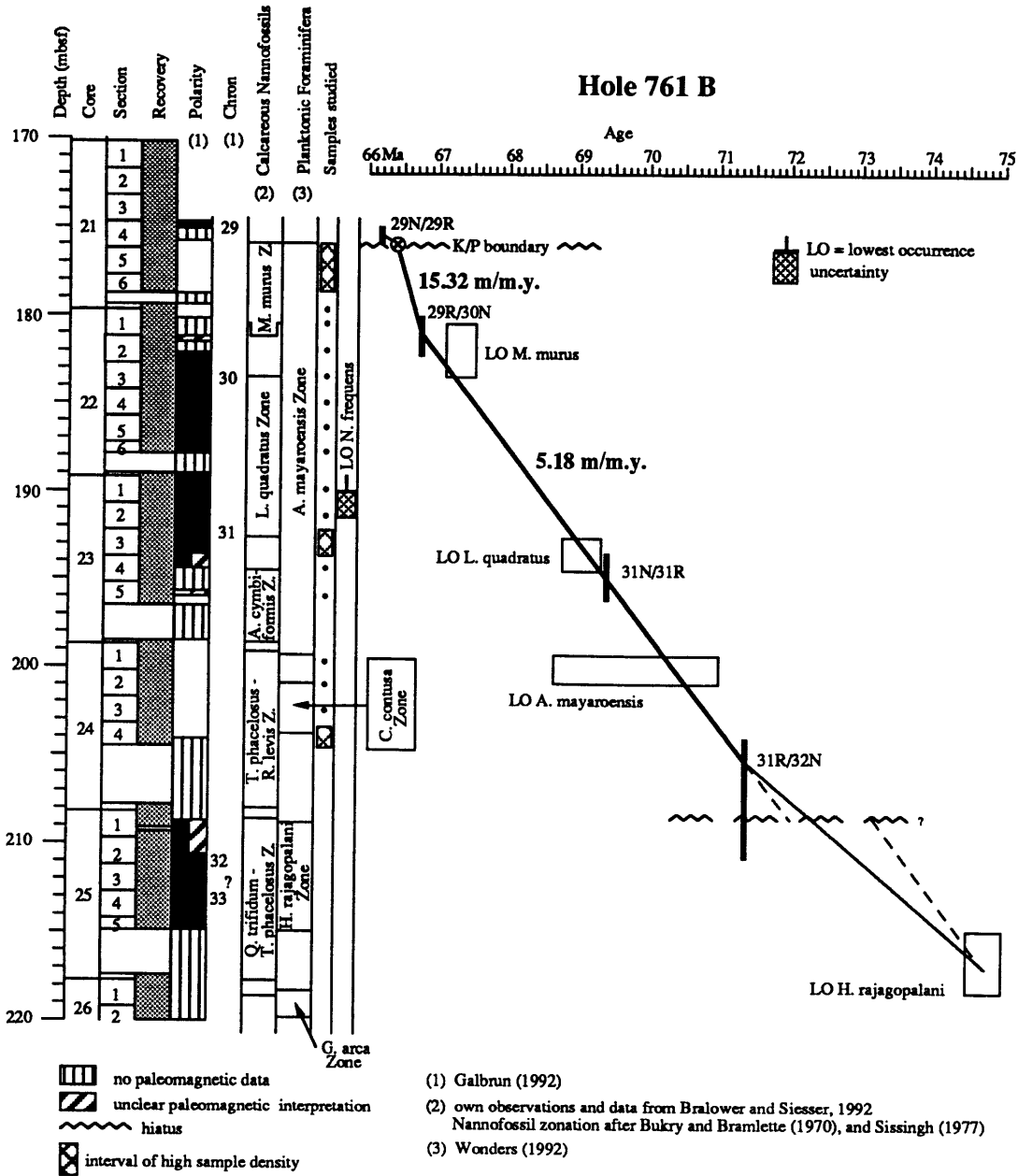


Figure 8: Sedimentation rate curve for the Maestrichtian section in Hole 761B.

4) ODP Hole 761C

This hole was drilled 20 m north of Hole 761B and contains a more complete K/P sequence than Hole 761B.

A gap in recovery of about 1 m was reported in section 761C-3R-2 (Shipboard Scientific Party, 1990). However, for calculation of the sample depths by ODP and in papers included in ODP Volume 122, Scientific Reports, this gap was ignored (i.e. section 761C-3R-2 was considered to be only 0.5 m long). Sample depths included in the following discussion were calculated in the same manner (i.e. the gap in section 761C-3R-2 is ignored) in order to facilitate comparison between this study and previous publications.

The K/P boundary

A distinct lithologic and color change occurs in core 761C-3R-3, between 75 and 77 cm. The contact is sharp and inclined (Figure 9), with white nannofossil chalk below and greenish-grey nannofossil chalk above. Bioturbation is common in both lithologies, but is more conspicuous in the darker, overlying sediment. The carbonate content decreases from about 85-90% in the white sediment to about 70% in the greyish chalk (Figure 10a). Two pieces of chert are present about 1 cm below the sharp color contact; another piece of chert lies about 12 cm higher in the section (at 761C-3-3, 66-67 cm; Figure 9). At both chert layers the section is apparently drilling disturbed.

The lowest occurrence of B. sparsus was observed in sample 761C-3-3, 70 cm (Figure 10b). The next lower sample available to me is from the white chalk at 761C-3-3, 75 cm and contains a typical upper Maestrichtian nannofossil assemblage (without B. sparsus) indicating that the K/P boundary should be placed between these two samples.

An iridium enrichment with a well defined peak was reported by Rocchia et al. (1992; Figure 10c). It coincides with the sharp color contact at 761C-3R-3, 75 cm (Figure 9).

Based on nannofossil, sedimentological and geochemical evidence the K/P boundary is thus placed between 761C-3R-3, 75 and 77 cm (172.45-172.47 mbsf).

In contrast, Pospichal and Bralower (1992) placed the K/P boundary about 9 cm higher in this section (between samples 761C-3-3, 66-68 cm, 172.36-

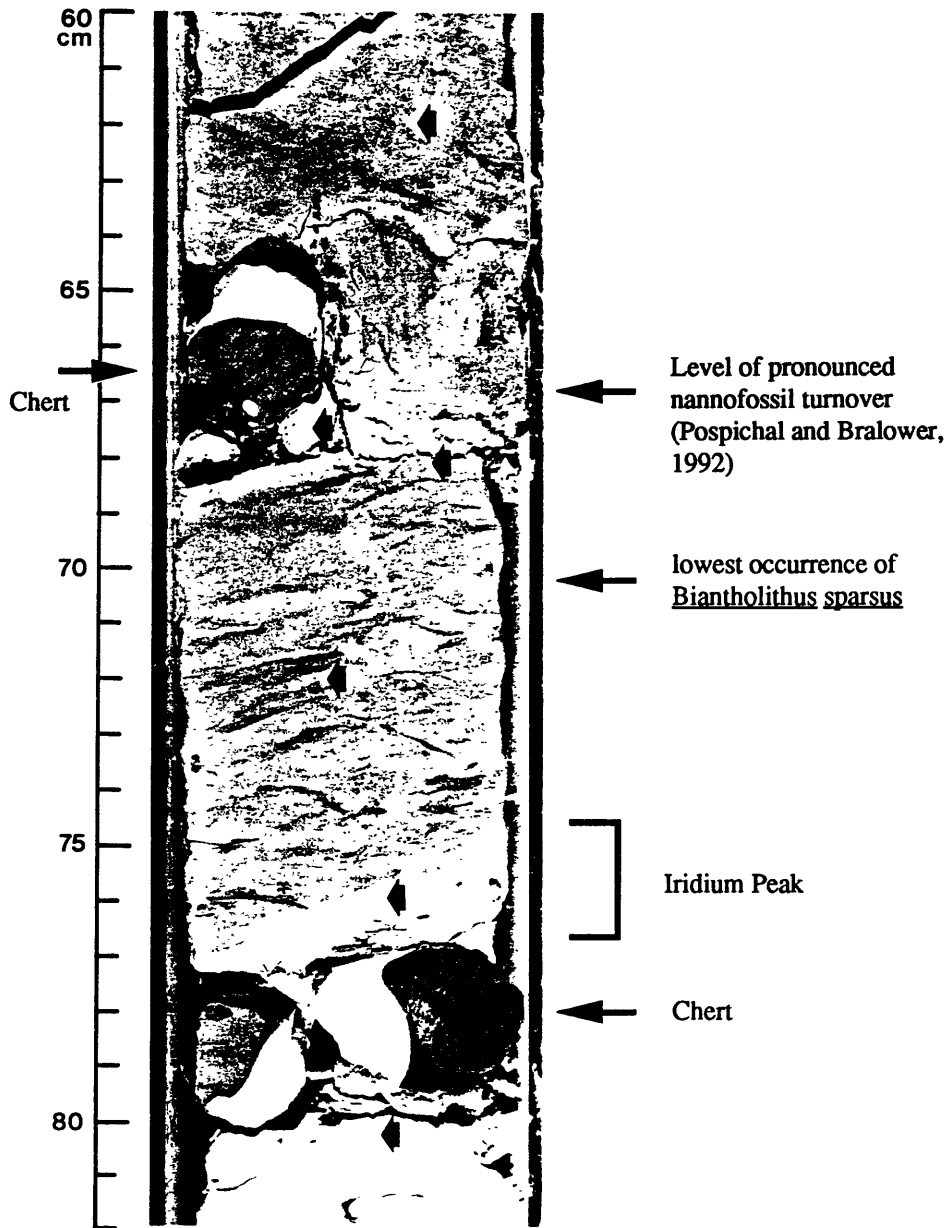


Figure 9: The lithology in the vicinity of the K/P boundary in Hole 761C (Section 761C-3R-3, 60-82 cm; from Pospichal and Bralower, 1992). The short fat arrows indicate levels where Pospichal and Bralower (1992) took samples.

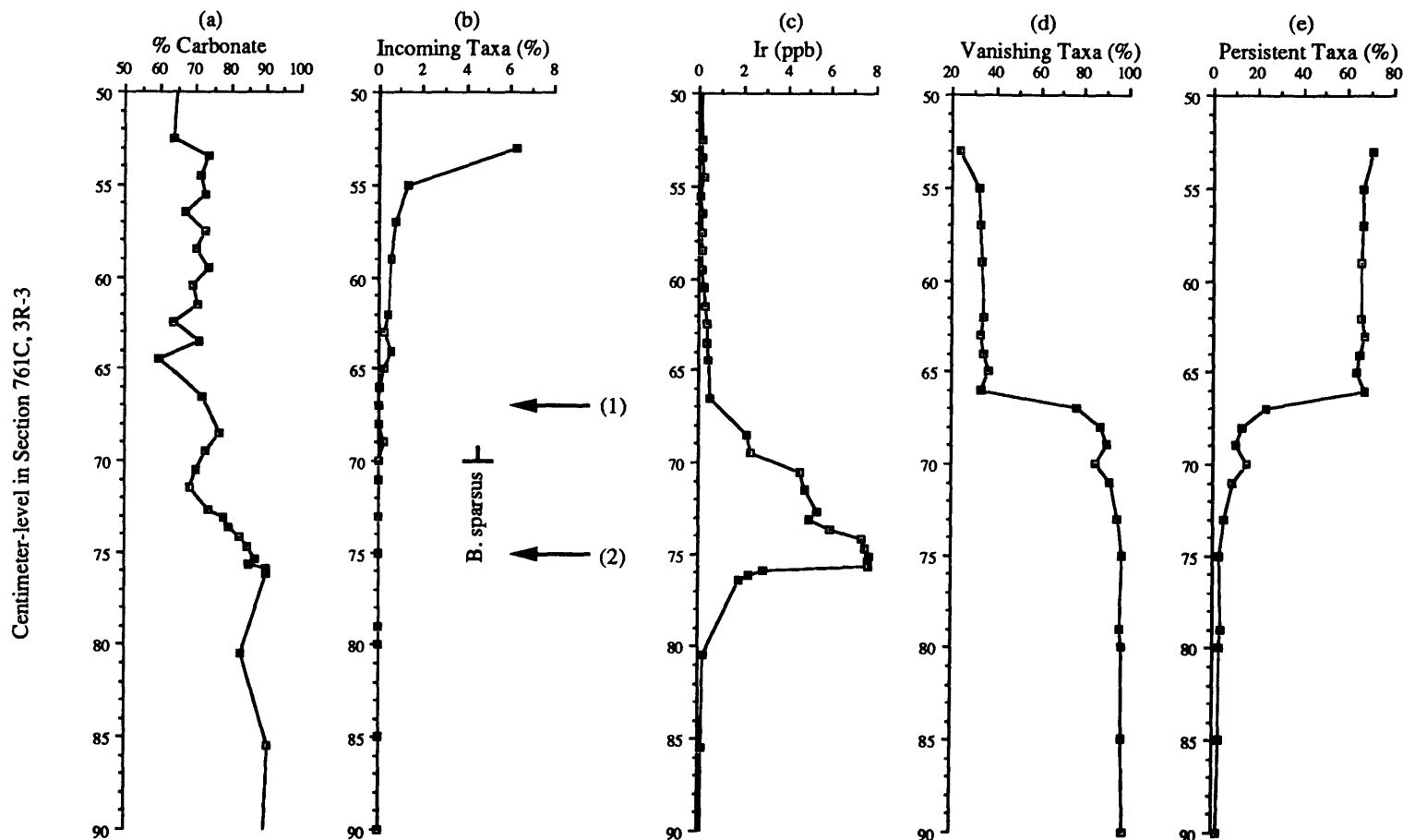


Figure 10: The K/P boundary interval in Hole 761C. (a) Carbonate content (Rocchia et al., 1992). (b) Abundance distribution of incoming calcareous nannofossil taxa (Pospichal and Bralower, 1992) and level of the first occurrence of *Biantholithus sparsus* (this study). (1) denotes the location of the K/P boundary after Pospichal and Bralower, 1992. (2) shows the level where the K/P boundary was placed in this study. (c) Iridium content in the sediment (Rocchia et al., 1992). (d) and (e) Abundance distribution of vanishing and incoming calcareous nannofossil taxa (Pospichal and Bralower, 1992).

172.38 mbsf), based on the pronounced change in the calcareous nannofossil assemblages at this level (compare Figure 10b, d, e); the vanishing taxa decrease from >80% to about 40% of the assemblage, whereas the persistent taxa (dominated by Cyclagelosphaera spp.) increase from <20% to about 60%. Pospichal and Bralower (1992) found one specimen of B. sparsus in sample 761C-3-3, 69 cm which they considered as reworked and disregarded it in their placement of the K/P boundary; this interpretation is not supported by my own observations (see above). The pronounced turnover of calcareous nannofossil assemblages at the level where Pospichal and Bralower place the boundary may be due to a hiatus: a lithologic discontinuity is indicated by subtle color differences of the sediment below and above this level. In addition, the sediment below this horizon is more conspicuously mottled and bioturbated than the sediment above. Unfortunately, the exact nature of the sediment contact is obliterated by the drilling disturbance caused by the chert pebble (Figure 9) at this level.

No data on planktonic foraminifera were available to delineate the level of the K/P boundary in this hole.

Magnetostratigraphy

Paleomagnetic data are available from Core 761C-3 (Rocchia et al, 1992) indicating that the K/P boundary occurs in a reverse polarity interval (C29R). The boundary between Chrons C29R and C30N was not encountered since the lowest sample analyzed (761C-3-6, 83 cm; 177.05 mbsf) was still of reversed polarity.

Sedimentation Rate

According to Berggren et al. (1985) the age of the K/P boundary is 66.40 Ma, the base of Chron C29R occurs at 66.74 Ma. With the K/P boundary at 761C-3-3, 75-77 cm (172.46 mbsf) the Maestrichtian portion of C29R is at least 4.59 m long. This corresponds to a sedimentation rate of at least 13.50 m/m.y. for the latest Cretaceous. The same sedimentation rate as calculated for the uppermost Maestrichtian in Hole 761B is also used in Hole 761C.

5) DSDP Hole 217

Location

Hole 217 is located at 8°55.57'N, 90°32.33'E on the northernmost portion of Ninetyeast Ridge in 3010 m waterdepth, just south of the flat turbidite sediments of the Bengal Fan (Shipboard Scientific Party, 1974). The paleolatitude of this site during the Maestrichtian was about >30°S according to the paleocontinental reconstructions of Smith and Briden (1977). A much lower paleolatitude during the Maestrichtian (~15°S) was indicated by Firstbrook et al. (1979; compare their reconstruction of the southern hemisphere at 70 Ma) apparently due to the fact that they did not place Hole 217 on the Indian Plate. Information obtained through recent ODP Legs (Leg 116 - 121) in the Indian Oceans (see detailed discussion in Royer et al., 1991) supports Smith and Briden's reconstruction which is also used in this study.

Lithology

The Maestrichtian sediments (421 to about 530 mbsf) were divided into two lithologic subunits, 2c and 2d (Shipboard Scientific Party, 1974). From the K/P boundary between cores 17 and 16 (421 mbsf) to about 480 mbsf the sediment consists of light grey to light brown nannofossil chalk with moderate to intense bioturbation (subunit 2c).

Lithologic subunit 2d (420-600 mbsf) ranges from middle Maestrichtian to Campanian. The Maestrichtian portion of this subunit consists of carbonate siltstone (480 to about 500 mbsf) and micarb chalk (about 510-555 mbsf); concurrent with the change to micarb chalk occurs a prominent increase in shell fragments of Inoceramus, oysters and other unidentified large molluscs (Shipboard Scientific Party, 1974). Foraminifera constitute about 3-5% of the sediment, clay minerals about 5-10%. Trace amounts of pyrite, glauconite, and volcanic glass are also present. The presence of oyster shells, glauconite, and of microfossils with shallow-water affinities led Shipboard Scientific Party (1974) to the conclusion that the paleo-waterdepth during the Late Cretaceous was less than about 500 m.

The K/P boundary

Calcareous nannofossils: Calcareous nannofossil assemblages in samples 217-16-6, 76-77 cm and 217-16-6, 128-129 cm are moderately to poorly

between cores 217-16 and 217-17 at 421.0 mbsf, on the tenuous evidence that the Maestrichtian foraminifera in 217-16-CC represent upward reworking rather than downhole contamination (McGowran, 1974).

Biostratigraphy

Calcareous Nannofossils: In agreement with Wind (1979a) but contrary to Shipboard Scientific Party (1974) the upper Maestrichtian marker species Micula murus and Nephrolithus frequens are both present in Hole 217. Bukry (1974) reported the presence of "Micula murus Zone assemblages" in cores 217-17 and 217-18 but does not indicate whether the marker species is present.

Forms very similar to Micula prinsii are present throughout core 217-17. They have elongate, curved arms, but do not have the bifurcation at the ends of their arms which is characteristic of M. prinsii. I consider these forms as intermediate between M. murus and M. prinsii, possibly representing early morphotypes of M. prinsii.

The lowest occurrence of Micula murus lies between 217-18-CC (M. murus still present) and 217-19-3, 100 cm (M. murus absent; Wind, 1979a), indicating the base of the M. murus Zone (Bukry and Bramlette, 1970).

The high-latitude marker species of the latest Maestrichtian, N. frequens, is also present in Hole 217. It is rare and was not observed in all samples; its lowest occurrence was observed in 217-24-CC, which is very close to the top of the Q. trifidum Zone. Because of its anomalous low occurrence, N. frequens is not used in the biostratigraphic zonation of this hole.

The lowest continuous occurrence of L. quadratus was observed in 217-20-CC, it was absent in 217-21-2, 101 cm (Wind, 1979a). An isolated occurrence of this species was reported in 217-21-5, 100 cm (Wind, 1979a; dotted square in Figure 11). The lowest occurrence of this species indicates the base of the L. quadratus Zone (Cepek and Hay, 1969) which corresponds to the base of Zone CC25c (highest part of the A. cymbiformis Zone, Sissingh, 1977).

The highest occurrences of R. levis, of T. phacelosus, and of B. parca were observed in 217-24-1, 49-50 cm (these forms were absent in 23-4, 53-54 cm). The highest occurrence of R. levis indicates the base of the A. cymbiformis Zone (CC 25, Sissingh, 1977); the other two species are used to delineate the base of the R. levis Zone (CC24) and to subdivide the T. phacelosus Zone (CC23), respectively. Further biostratigraphic refinement is required to distinguish these boundaries or to determine whether a hiatus is present. For

preserved and are dominated by fragments of Thoracosphaera spp. and by P. sigmoides; Cruciplacolithus primus and rare Biantholithus sparsus are present and indicate an age of early Paleocene (upper part of Biochron NP1). In addition, uppermost Maestrichtian calcareous nannofossils (e.g. M. murus) are present. Gartner (1974) reported that the nannofossils in 217-16-CC are "Maestrichtian in age, though admixed with some Danian forms". In the range chart he recorded an isolated occurrence of Cruciplacolithus tenuis in sample 217-16-CC (Gartner, 1974) which would indicate nannofossil Zone NP2 (Martini, 1971). My own observations do not corroborate the presence of C. tenuis in the lowermost samples of Core 217-16-6. Furthermore, the base of the continuous occurrence of C. tenuis lies only in 217-15-CC (Gartner, 1974). Consequently, the lowermost nannofossil zone identified in 217-16-6, 128-129 is (the upper part of) NP1. No samples of 217-16-CC are available to me. Based on my observations in section 217-16-6, and on the isolated occurrence of C. tenuis in 217-16-CC, Gartner's observation of mixed Danian and Maestrichtian nannofossils in 217-16-CC are interpreted here as constituting Danian assemblages with admixed Cretaceous taxa.

Sample 217-17-1, 18-19 cm contains a moderately to well preserved, typical upper Maestrichtian assemblage, including the marker species M. murus and N. frequens. Forms very close to M. prinsii (elongate, curved arms, but no distinct bifurcation) were also observed. Paleocene forms were not encountered. Based on own observations and on Gartner's (1974) results the K/P boundary is placed between cores 217-16 and 217-17. There may be a short hiatus at the K/P boundary since the lowermost Paleocene sediment is assigned to the upper part of NP1 (or, possibly, NP2).

Planktonic Foraminifera: Typical Danian forms (Eoglobigerina, Chiloguembelina) were observed in core 217-16 (McGowran, 1974). The lower Paleocene subzone P1b was identified tentatively in sample 217-16-6, 148-150 cm (McGowran, 1974); subzone P1a was indicated in 217-16-CC (on the barrel sheets of the core description; Shipboard Scientific Party, 1974). Accordingly, the Danian biostratigraphic record is almost complete (McGowran, 1974). In sections 217-16-6 and 217-16-CC large specimens of the Maestrichtian planktonic foraminifer Hedbergella monmouthensis occur abundantly (McGowran, 1974). A typically diverse, tropical Maestrichtian assemblage occurs in section 217-17-1 (McGowran, 1974). The K/P boundary is placed

this reason these biohorizons were not included in the construction of the sedimentation rate curve. Because of the absence of Reinhardtites anthophorus cores 217-24 to 217-26 were assigned to the lower part of the T. phacelosus Zone (CC23a, Sissingh, 1977).

The highest occurrence of Q. trifidum was observed in 217-25-CC, but could not be identified confidently in 217-24-CC. Wind (1979a) reported the highest occurrence of this form in 217-25-2, 76 cm (absent in 24-6, 125 cm). Thus the highest occurrence of Q. trifidum is placed between 217-25-2, 76 cm and 217-24-CC. This agrees with Bukry (1974), but is in contrast to Gartner (1974) who places this biohorizon about 10 m lower in Hole 217. According to Perch-Nielsen (1983) the highest occurrence of Q. trifidum should be above that of B. parca, which is not the case in this hole. The highest occurrence of Q. trifidum seems to be a temporally narrowly defined biohorizon (compare chapter "Biohorizons"; see also Monechi and Thierstein, 1985) and therefore it was used as the lowest point in the construction of the sedimentation rate curve for Hole 217.

Planktonic Foraminifera: The upper Maestrichtian A. mayaroensis Zone ranges from core 217-23 to the K/P boundary. The lowest occurrence of A. mayaroensis was reported in 217-23-CC (487.5 mbsf; McGowran, 1974); it is absent in sample 217-24-1, 80-82 cm (488.3 mbsf; Pessagno and Michael, 1974). In the top part of core 217-24 Abathomphalus intermedius is still present, possibly indicating the mid-Maestrichtian Gansserina gansseri Zone (Shipboard Scientific Party, 1974). The planktonic foraminiferal zonation of the remainder of the Upper Cretaceous is problematic because of the lack of zonal marker species. The presence of Bolivinooides draco miliaris in core 217-27 indicates upper Campanian to lower Maestrichtian, the presence of Globotruncana of the arca/rosetta group in core 217-36 suggests a Campanian age (Shipboard Scientific Party, 1974).

Age Model

Since no paleomagnetic data are available for DSDP Hole 217, the age model relies on nannofossil and planktonic foraminiferal biostratigraphy. The biohorizons available to construct the sedimentation rate curve are discussed in the previous chapter and are listed in Table 4. The results are plotted in Figure 11. The depth assigned to each biohorizon is the average between the

lowest/highest occurrence and the subsequent sample in which the species was not observed.

All five biohorizons can be connected with one straight line. Since the K/P boundary and the LO Q. trifidum are the best constrained datum points available, they were used to calculate the sedimentation rate (15.81 m/m.y.).

Table 4: Biohorizons used to construct the sedimentation rate curve of Hole 217 (HO = highest occurrence, LO = lowest occurrence). For age assignments see chapter "Biohorizons". The depth determination of each biohorizon is described in the previous chapter.

Boundary/ Biohorizon	Sample (mbsf)	average Depth	Age	Sed. rate (m/m.y.)
K/P boundary	16-CC (421.0) 17-1 (421.0)	421.00	66.40	
LO <u>M. murus</u>	18-CC (440.0) 19-3, 100 cm (444.0)	442.0	67.60	
LO <u>L. quadratus</u>	20-CC (459.0) 21-2, 101 cm (461.51)	460.26	69.03	
LO <u>A. mayaroensis</u>	23-CC (487.5) 24-1, 80-82 cm (488.3)	487.90	69.67	
LO <u>Q. trifidum</u>	24-CC (497.0) 25-2, 76 cm (499.26)	498.13	71.28	

77.13m/4.88 m. y.=

15.81

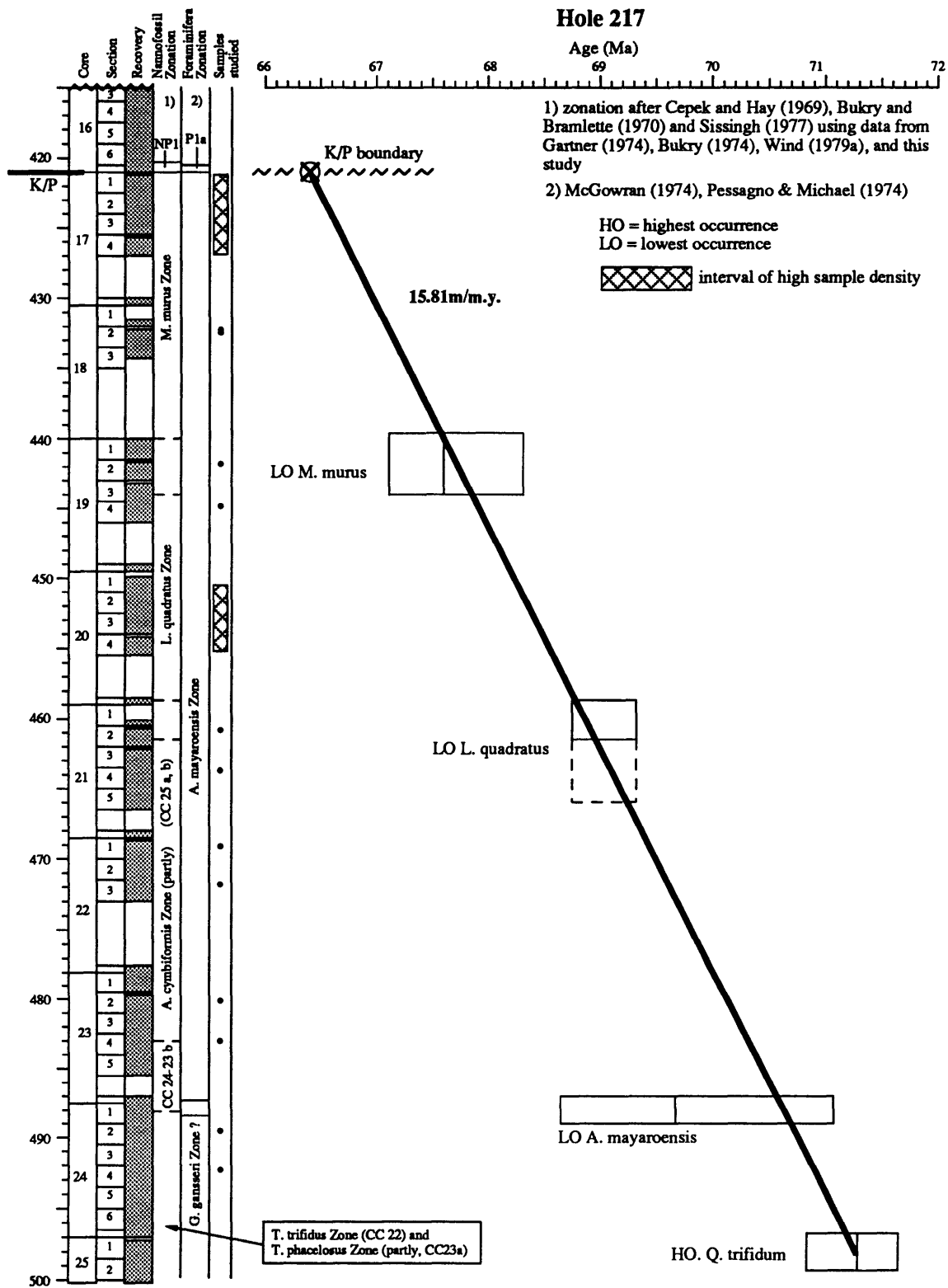


Figure 11: Sedimentation rate curve for the Maestrichtian section in Hole 217.

slumps occur in Core 528-31 corroborating geophysical evidence for reworking and erosion on the slope of Walvis Ridge. The lower slump (528-31-6, 90-150 cm) occurred within Chron C29R and had to be subtracted for the calculation of the lowest Paleocene sedimentation rate.

Cores 528-39 to 528-47 penetrated basaltic basement rocks with interbedded upper Maestrichtian sediment (lithologic unit IV; Shipboard Scientific Party, 1984).

The K/P boundary

In agreement with Manivit (1984) the K/P boundary occurs between Cores 528-31 and 528-32. The sediments at the very top of Core 528-32 (sample 528-32-1, 8 cm) contain a moderately well preserved uppermost Maestrichtian assemblage, including the markers M. prinsii, M. murus and N. frequens which indicate the upper part of the N. frequens Zone (Perch-Nielsen, 1979). In contrast, the nannofossil assemblages in 528-31-CC are poorly preserved and dominated by fragments of Thoracosphaera. Other persistent taxa (P. sigmoides, Neocrepidolithus spp., B. constans, M. inversus) are much more abundant than in the underlying core. Biantholithus sparsus, the first truly Cenozoic calcareous nannofossil taxon, was encountered in sample 528-31-7, 58-59 cm, 0.3 m above the boundary between Cores 528-32 and -31. Manivit (1984) reported B. sparsus from sample 528-31-CC, and the first occurrence of C. primus in 528-31-5, 150 cm (405.00m), indicating that the lower part of NP1 is present between 528-31-CC and -31-5, 150 cm (407.0-405.0 mbsf). Thus calcareous nannofossils indicate that the K/P boundary is complete in Hole 528 (i.e. all nannofossil zones are present).

Planktonic foraminifera indicate that the K/P boundary occurs between Cores 528-31 and -32 (Boersma, 1984) in agreement with the calcareous nannofossil boundary. A very thin (0.5-1cm), blue-tinged, fine-grained sediment layer occurs at the very top of the Maestrichtian at all Walvis Ridge Sites, containing a unique foraminiferal fauna (528-32-1, 1 cm; Boersma, 1984): small individuals, typical of the upper Maestrichtian A. mayaroensis Zone together with Hedbergella monmouthensis and heavily costate Pseudoguembelina excolata characterize this layer. Substantial amounts of pyrite were present in the foraminifera tests (Boersma, 1984). The P. eugubina Zone (lowermost Paleocene) occurs in Core 528-31-CC to -31-7, 24 cm (Boersma, 1984). The sediment contains volcanic glass and less pyrite than below the

6) DSDP Hole 528

Location

DSDP Hole 528 is located on the north western slope of Walvis Ridge in the South-Atlantic (28°31.49'S; 2°19.44'E) in 3800 m waterdepth (Shipboard Scientific Party, 1984). The latitude of Walvis Ridge during the late Maestrichtian was 36°S±1° (Chave, 1984). Because this hole reached basement in the A. cymbiformis Zone only the uppermost Maestrichtian interval was investigated in detail in this study.

A conspicuous cyclical alternation of reddish-brown and white sediment-layers occurs in the Maestrichtian in Hole 528 (Borella, 1984); the individual layers are about 0.3 to 0.5 m thick. It has been argued that these color cycles are a record of Late Cretaceous precessional climate cyclicity, because the mean absolute period of the color cycles (23.5±4.4 kyr) is similar to the predicted Late Cretaceous precessional period (20.8 kyr; Herbert and D'Hondt, 1990). One of the reasons that Hole 528 was included in this study was to ascertain whether and in which way calcareous nannofossil assemblages change in response to the proposed climatic cycles.

Four samples that were counted are assigned to the lowermost Paleocene because at the beginning of the study of this hole, the exact location of the K/P boundary (within 528-31-CC, or between Cores 528-31 and 528-32) was unclear.

Lithology

About 63 m (Cores 528-32 to 528-38) of upper Maestrichtian sediment were penetrated in DSDP Hole 528. The sediment consists of foraminiferal nannofossil chalk interbedded with volcanoclastic turbidite sandstone (lithologic unit III, Shipboard Scientific Party, 1984). Turbidite sediments occur most abundantly in Cores 528-37 and 528-38 (lithologic subunit IIIC). Fining upward volcanoclastic sequences with varying clay content (10-78%, Shipboard Scientific Party, 1984) alternate irregularly with nannofossil chinks. Parallel laminations, normal and reversed graded bedding, and flaser bedding are common in the sandstone layers. Scoured contacts between the volcanoclastic and the chalky layers resulted from turbidity currents. Volcanoclastic turbidites occur also in Cores 528-32 to 528-37, but they are much rarer and thinner. The turbidite beds as reported in the core description of Hole 528 (Shipboard Scientific Party, 1984) are shown in Figure 12. Two

boundary. Inverse to the trend in nannofossil preservation, foraminiferal preservation is better above the boundary than below (moderately well versus poor). Based on comparison of planktonic foraminiferal biohorizons (LADs, FADs) in this section with those in more expanded, epicontinental K/P sections (Brazos River and El Kef) MacLeod and Keller (1991) argue that a hiatus of 100 to 250 kyr exists at the K/P boundary in Hole 528; it is unclear if this hiatus occurs exclusively in the Paleocene or if it extends into the Maestrichtian.

Magnetostratigraphy

Paleomagnetic measurements were performed on samples taken at 30-60 cm intervals in undisturbed cores (Chave, 1984). Demagnetizing fields of 15-30 mT were sufficient in most cases to remove any magnetic overprint. All samples were measured, demagnetized, and measured again (Chave, 1984). The natural remanence of the sediments proved to be very strong and yielded essentially the same stratigraphic interpretation as the demagnetized results (Chave, 1984). Walvis Ridge Holes 525A and 527 have better recovery and therefore more complete paleomagnetic records than 528. Comparison of the paleomagnetic record of 528 with those of 525A and 527 and integration of micropaleontological data yielded consistent paleomagnetic interpretation of the four Walvis Ridge Sites.

The following magnetochrons were identified in Hole 528 (Figure 12): the K/P boundary occurs close to the top of a reverse interval (Chron C29R). The boundary to the underlying normal interval is very sharp (Chave, 1984); it occurs between Sections 528-32-4 and -5. Micula murus first occurs in the upper half of this long normal interval indicating Chron C30N (Monechi and Thierstein, 1985). The normal interval extends down to the base of Core 528-37. Very low values of inclination occurred in the top half of Core 528-33 (ca. 417-420.5 mbsf; Chave, 1984). Lithraphidites quadratus was observed to have its first occurrence very close to the base of the long normal interval (Manivit, 1984), indicating Chron C31N (Monechi and Thierstein, 1985). The short reverse Chron C30R was not identified in Hole 528. The boundary with the underlying reverse interval could not be established precisely, because of turbiditic sediments in the upper two sections of Core 528-38. The lowermost sediments above the uppermost basalts of Hole 528 (lower half of Core 528-38) are of reverse polarity, representing Chron C31R.

Age Model (Table 5 and Figure 12)

The sedimentation rate of the lowermost Paleocene was calculated using the K/P boundary and the 29N/29R boundary.

Two paleomagnetic boundaries (29R/30N and 31N/31R), the K/P boundary and two biohorizons (lowest occurrence of M. murus, LO L. quadratus) are available to construct the sedimentation rate curve for the upper Maestrichtian. The age estimate assigned to the lowest occurrence of M. murus is an average calculated from the four South Atlantic sites listed in chapter "Biohorizons" (see discussion there). The K/P boundary, the 29R/30N boundary and the lowest occurrence of M. murus can be connected with a straight line, corresponding to a sedimentation rate of 19.56 m/m.y. The age of the lowest occurrence of M. murus thus obtained (67.4 Ma) is used as the upper tie-point for the sedimentation rate in the lower portion of the section which is about 20 m/m.y.

Table 5: Sedimentation Rates in the lowermost Paleocene and Upper Cretaceous in Hole 528.

Boundary	Depth ¹⁾²⁾ (mbsf)	Age ³⁾ (Ma)	Sed. Rate (m/m.y.)
29N/29R	406.0	66.17	
K/P boundary	407.0	66.14	1.0-0.6m(slump)/0.23m.y. = 1.74
29R/30N	413.65	66.74	6.65m/0.34m.y. = 19.56
LO M. murus	424.47	67.40	19.56
31N/31R	465.0	69.40	40.53m/2.0m.y. = 20.27

1) magnetostratigraphy after Chave (1984)

2) biostratigraphy after Manivit (1984), Boersma (1984) and own observations

3) after Berggren et al. (1985) and Kent and Gradstein (1985)

Hole 528

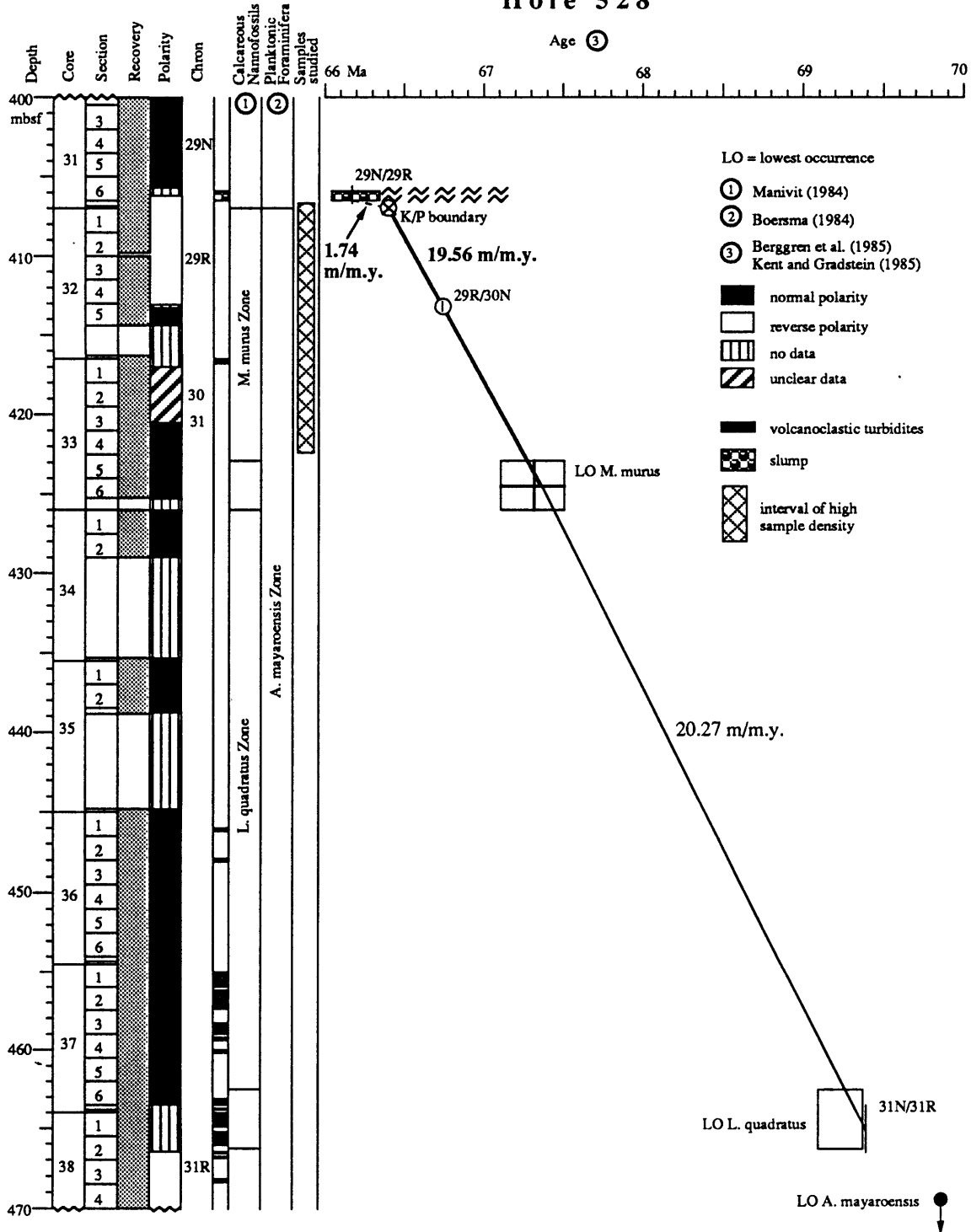


Figure 12: Sedimentation rate curve for the Maestrichtian section in Hole 528.

7) Miller's Ferry Section (Hole 226), Alabama

The Cretaceous/Paleocene sequence near Millers Ferry (Alabama) was cored by the U.S. Army Corps of Engineers during the construction of the Millers Ferry Dam on the Alabama River. The samples included in this study are from one of the boreholes drilled (Hole 226) and were supplied by R. K. Olsson (Rutgers University). This core represents a low latitude, epicontinental section. Its latitude in the latest Cretaceous was about 30°-35°N (paleocontinental reconstructions of Smith and Briden, 1977, and of Firstbrook et al., 1979). The sequence recovered in Millers Ferry Hole 226 consists of Upper Cretaceous chalk of the Prairie Bluff Formation and of lower Paleocene sandstone, siltstones, and marls of the Pine Barren Member (Clayton Formation). Planktonic foraminifera in this section were investigated by Liu (1992) who placed the K/P boundary at the top of the Prairie Bluff Chalk, a level where Guembelitra cretacea increases in relative abundance. The upper Maestrichtian marker species A. mayaroensis is absent in Millers Ferry (e.g. Mancini et al, 1989). Liu (1992) reports that the lowermost planktonic foraminiferal zone (P0) is missing in Hole 226, indicating a short hiatus at the K/P boundary.

Investigation of the calcareous nannofossils in Hole 226 showed that the uppermost Maestrichtian marker fossils of low latitudes, Micula murus and Micula prinsii, as well as the high latitude marker species Nephrolithus frequens are present (Olsson et al, 1992). Consequently, the absence of A. mayaroensis must be explained as environmental exclusion and not as the consequence of a hiatus. Immediately above the level where Liu (1992) placed the K/P boundary there is a conspicuous increase of Cyclagelosphaera spp., similar to ODP Hole 761C, but Cretaceous (vanishing) nannofossil taxa still dominate the assemblage in the lowermost Paleocene samples. The lowest occurrence of Biantholithus sparsus was observed in sample #5, 4 cm above the K/P boundary.

Age Model

Few constraints exist in the Maestrichtian portion of this section to estimate the sedimentation rate. Paleomagnetic data are not available; the zonal boundary between the M. prinsii Zone and the M. murus Zone is not present in the core, M. prinsii occurs throughout; a hiatus is present in this

hole in the lowermost Paleocene (planktonic foraminiferal zone PO is absent: Liu, 1992) and it is unclear whether this hiatus is restricted to the Paleocene or whether it extends down into the Maestrichtian. Because of these uncertainties only a minimum estimate of the sedimentation rate can be given based on the fact that M. prinsii is present throughout the section. The average duration of the M. prinsii Zone is 0.23 m.y.: (see chapter Biohorizons), leading to an estimated minimum sedimentation rate of 10.2 m/m.y. This figure is comparable to the sedimentation rates of upper Maestrichtian chalks in the other sites included in this study (12.7-19.6 m/m.y.; Holes 217 and 528, respectively).

In comparison, a sedimentation rate of 5.1 m/m.y. was reported for the upper Maestrichtian section near Braggs, Alabama (Channell and Dobson, 1989). But the presence of (at least) one hiatus of unknown duration (minimum 80 000 years, Channell and Dobson, 1989) in the Braggs section, as well as different lithology (predominantly clastic; Copeland and Mancini, 1986) make a direct comparison of sedimentation rates between the two sections difficult.

For this study a sedimentation rate of 10 m/m.y. is adopted to estimate sample ages in the Millers Ferry section and I assume that the hiatus in the lowest Paleocene does not extend into the Maestrichtian.

CHAPTER 4 RESULTS

1) ODP Hole 690C

(A) Differences between the early and the late Maestrichtian

The number of taxa recorded in each sample decreased from about 30-40 taxa per sample in the early Maestrichtian to less than 25 taxa per sample in the late Maestrichtian (Figure 13a). The anomalously low values at about 72.1 Ma and at about 75 Ma were recorded in poorly preserved samples and are not considered to reflect a genuine diversity decrease at these levels. The diversity decrease occurred rather abruptly between 71.1 and 70.4 Ma. There is a slight decrease in preservation between these two samples (from moderate preservation at 71.1 Ma to moderately poor preservation at 70.4 Ma) but I consider it too small to cause the diversity decrease from 34 to 19 taxa.

The species that shows the most pronounced abundance increase from the early to the late Maestrichtian is Prediscosphaera stoveri (Figure 13b). This species constituted <10% of the assemblage in most samples in the lower Maestrichtian. After ~70 Ma the abundance of this species increased rapidly; it constituted 40-60% of the entire assemblage during most of the latest Maestrichtian (67-66.4 Ma) with a peak value of >80%. The relative abundances given for P. stoveri are percentages of the entire nannofossil assemblage. In contrast, the abundances given for all other taxa were calculated exclusive of P. stoveri; otherwise the mass occurrence of P. stoveri during the late Maestrichtian would have largely obscured the abundance fluctuations of other taxa.

The majority of nannofossils that disappeared close to the early/late Maestrichtian boundary are representatives of typical austral taxa that were either unknown or extremely rare at middle and low latitudes. They include Biscutum magnum, Chiastozygus garrisonii, Monomarginatus spp., Misceomarginatus spp., Neocrepidolithus watkinsii, Nephrolithus corystus, Phanulithus obscurus, Psyktosphaera firthii and Reinhardtites spp. (Figure 14a - h). All of these taxa are common or abundant in the early Maestrichtian. The following taxa were present as minor components (less than about 2%) during the early Maestrichtian, but were absent during the late Maestrichtian: Biscutum boletum, Biscutum coronum, Biscutum dissimilis, Biscutum sp. 1, Biscutum sp. 2, Chiastozygus amphipons, Chiastozygus sp. 1, Octocyclus magnus,

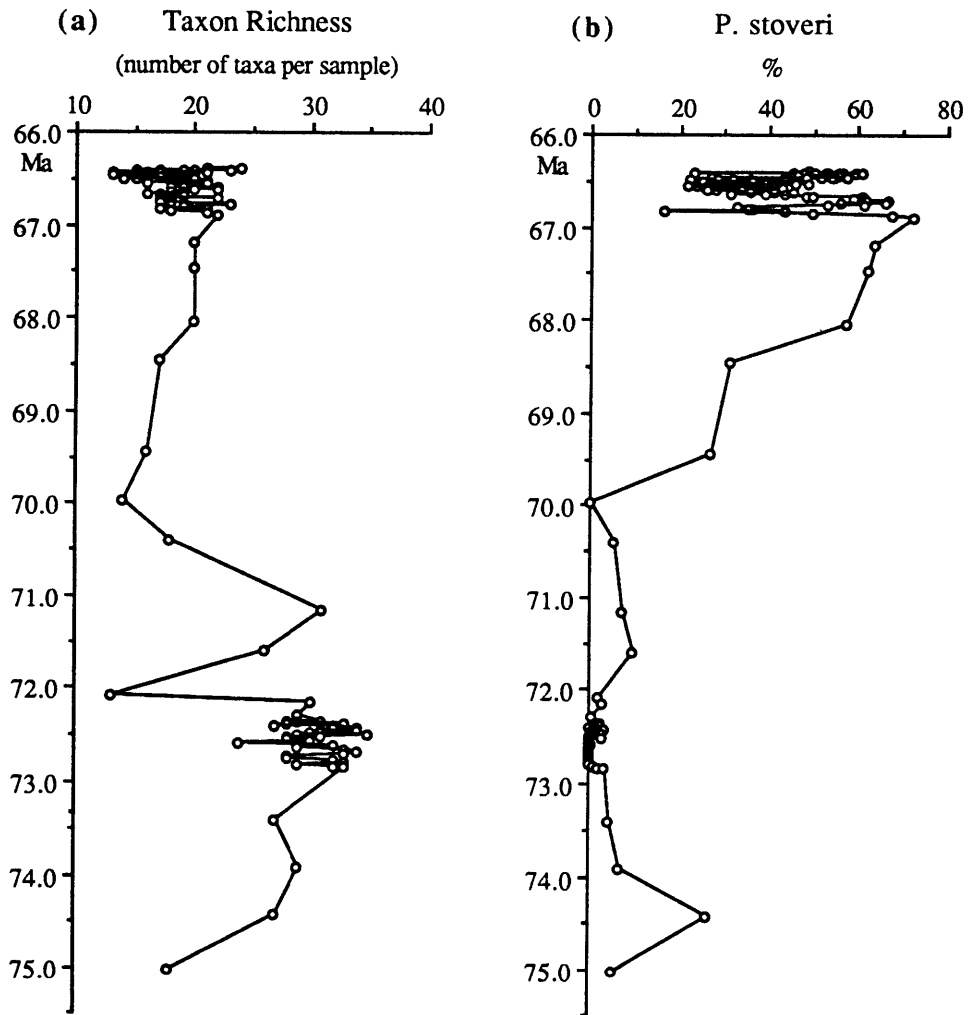


Figure 13: (a) Taxon richness in Hole 690C plotted against age. Note the pronounced abundance decrease between ~71 - 70 Ma. (see text for discussion). (b) Relative abundance of *Prediscosphaera stoveri* in Hole 690C. This species becomes very abundant in the late Maestrichtian.

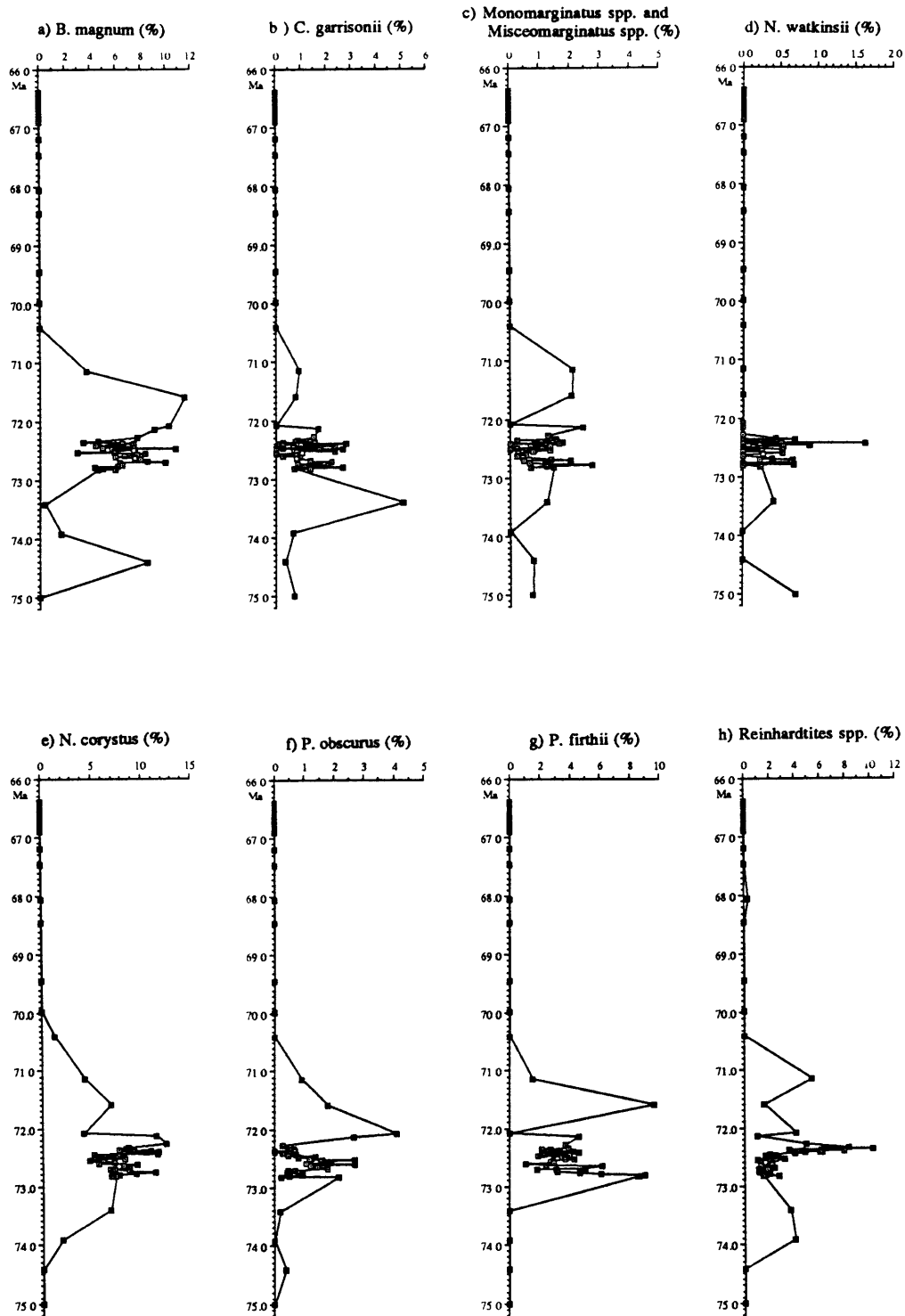


Figure 14: Relative abundances (%) of nannofossil taxa which decrease in abundance during the Maestrichtian in Hole 690C. (Percent were calculated exclusive of *P. stoveri*.)

Scapholithus fossilis, Staurolithites laffittei, Zygodiscus compactus, and Zygodiscus diplogrammus (Figure 15a - h; Figure 16a - d).

Several taxa displayed higher relative abundances in the early than in the late Maestrichtian assemblages. Biscutum notaculum (Figure 16e) shows this trend most pronouncedly: it reached peak values of almost 40% during the early Maestrichtian, drops to less than 5% between 71.1 Ma and 70.4 Ma (which is coeval with the diversity decrease) and was absent from the counts in almost the entire upper Maestrichtian interval (Figure 16e). A very similar trend was observed for the group A. octoradiata and P. regularis (Figure 16f): while common to abundant during the early Maestrichtian and up to 71.1 Ma (about 10-15%) this group drops to almost 0% at 70.4 Ma and remains at values below 5% during most of the late Maestrichtian. Other taxa that occurred commonly or rarely during the early Maestrichtian but were extremely rare or absent during the late Maestrichtian include Biscutum constans, Discorhabdus ignotus, Placozygus bussonii, Prediscosphaera arkhangel'skyi, Rhombolithion rhombicum, and Watznaueria barnesae (Figure 17a - f). Thoracosphaera spp. and Vagalapilla spp. decrease in abundance between the early and the late Maestrichtian, but are common to rare in both intervals (Figure 17g, h).

Nephrolithus frequens (Figure 18a) is the only taxon that evolved during the late Maestrichtian. This species was absent prior to ~71 Ma, but constituted over 20% of the assemblage where it was first observed (at about 70.4 Ma). During the late Maestrichtian this species constituted up to 40% of the entire assemblage. Two other taxa are almost completely absent during the early Maestrichtian, but are important assemblage elements during the late Maestrichtian: Cribrosphaerella(?) daniae (Figure 18b) increased from about 1% at 71.1 Ma to >15% at 70.4 Ma, dropped again to values <5% between about 69.5 Ma and 68.4 Ma, and reached abundances of up to >10% in the latest Maestrichtian (67-66.4 Ma). Similarly, G. fessus (Figure 18c) was absent in most samples prior to about 70 Ma, it was present in low abundances (<1%) between about 70 and 68 Ma, and reached values up to almost 8% in the latest Maestrichtian (about 67-66.4 Ma). Creterhabdus spp., C. ehrenbergii, K. magnificus, L. cayeuxii, P. fibuliformis, and P. cretacea (Figures 18d-h and 19a) were common to abundant during the entire Maestrichtian and showed a slight abundance increase from the early to the late Maestrichtian.

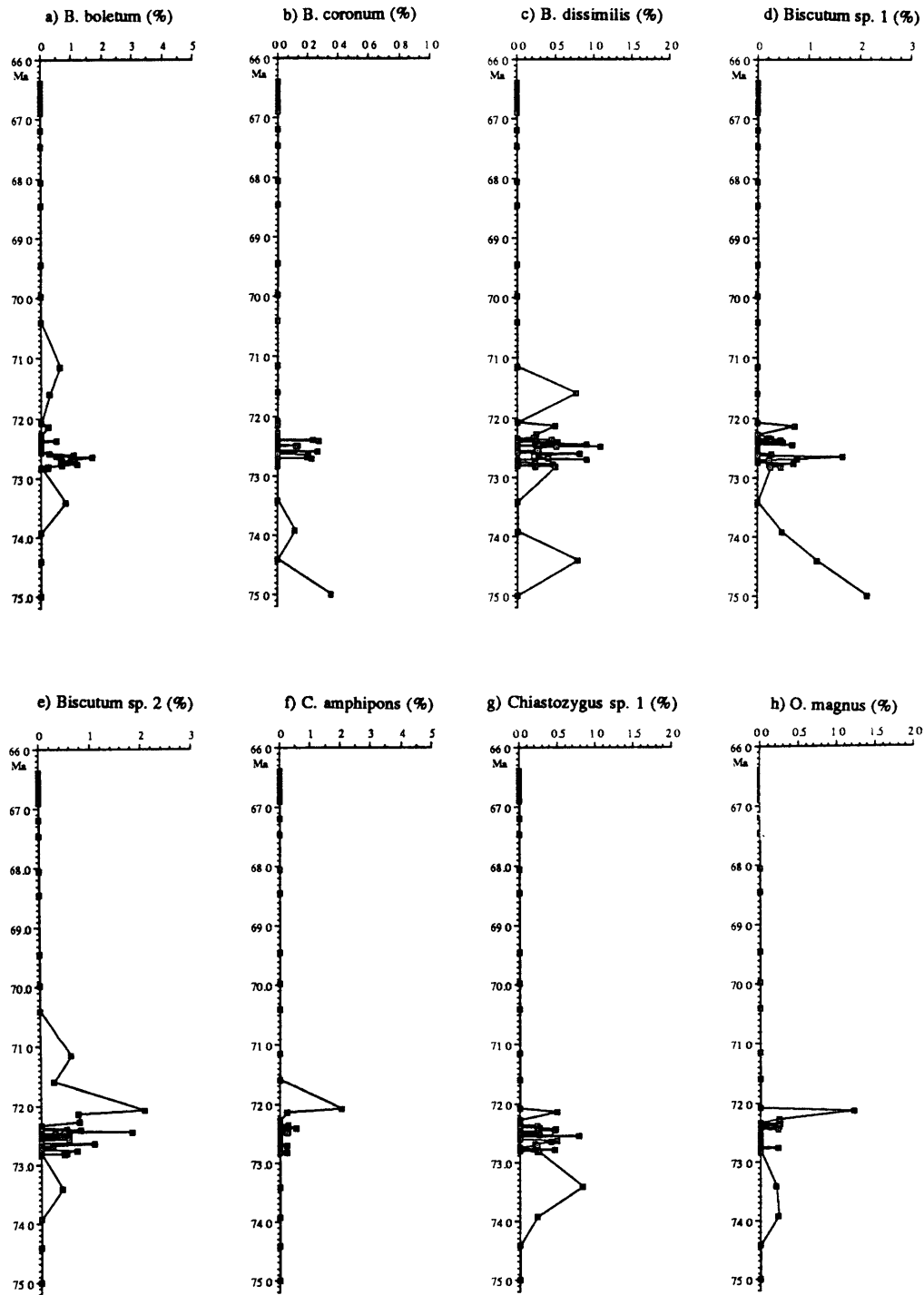


Figure 15: Relative abundances (%) of nannofossil taxa which decrease in abundance during the Maestrichtian in Hole 690C. (Percent were calculated exclusive of *P. stoveri*.)

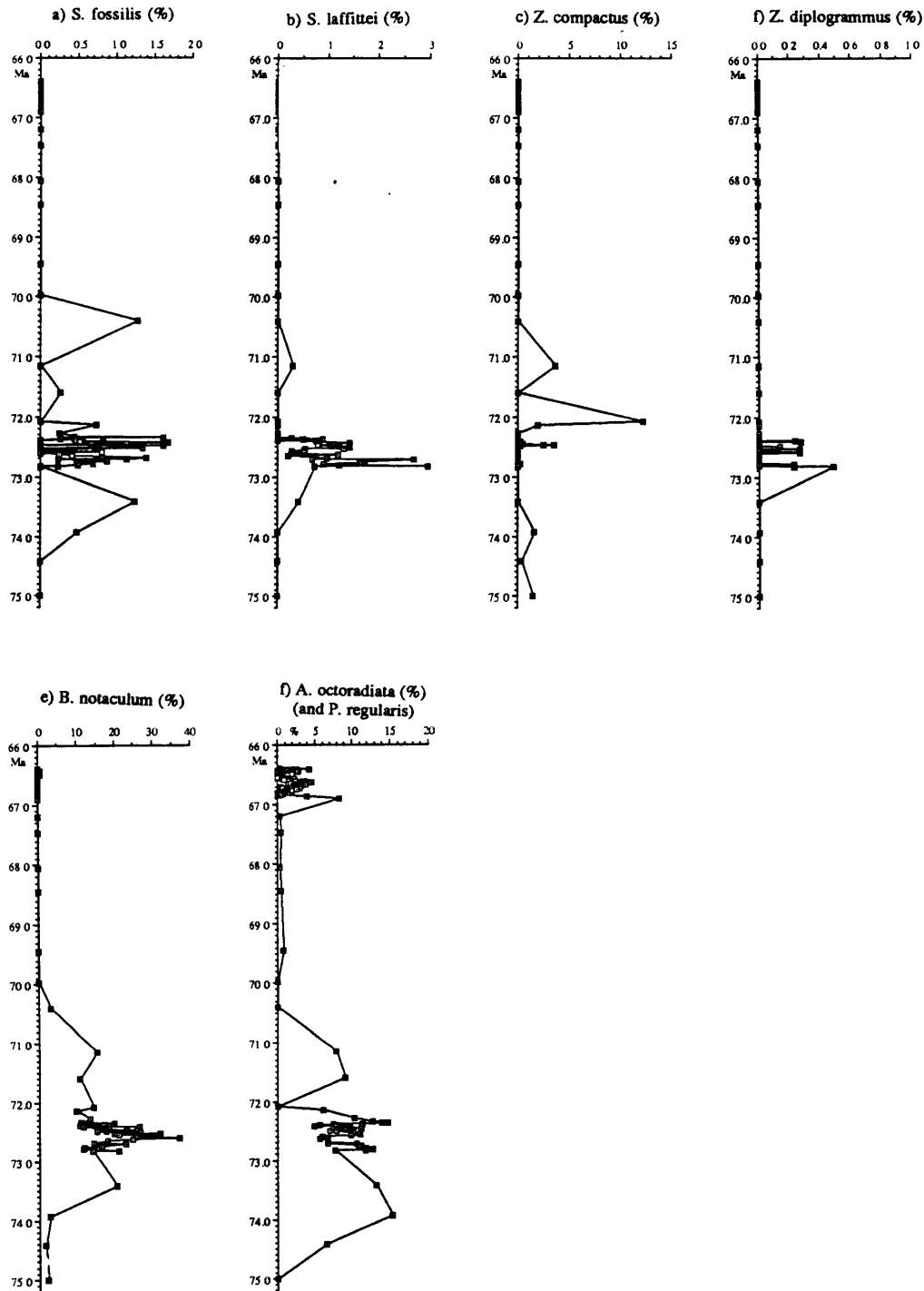


Figure 16: Relative abundances (%) of nannofossil taxa which decrease in abundance during the Maestrichtian in Hole 690C. (Percent were calculated exclusive of *P. stoveri*.)

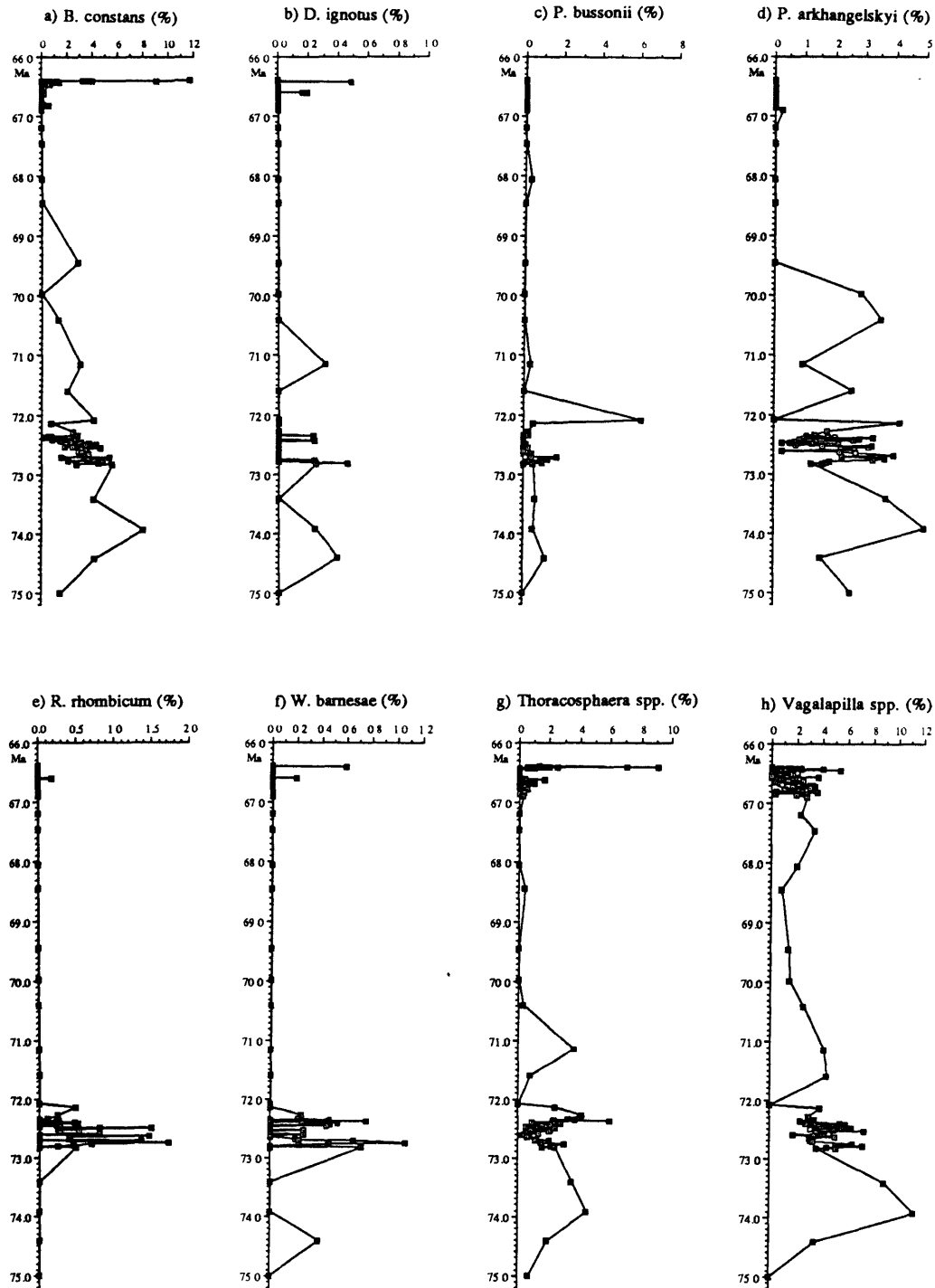


Figure 17: Relative abundances (%) of nannofossil taxa which decrease in abundance during the Maestrichtian in Hole 690C. (Percent were calculated exclusive of *P. stoveri*.)

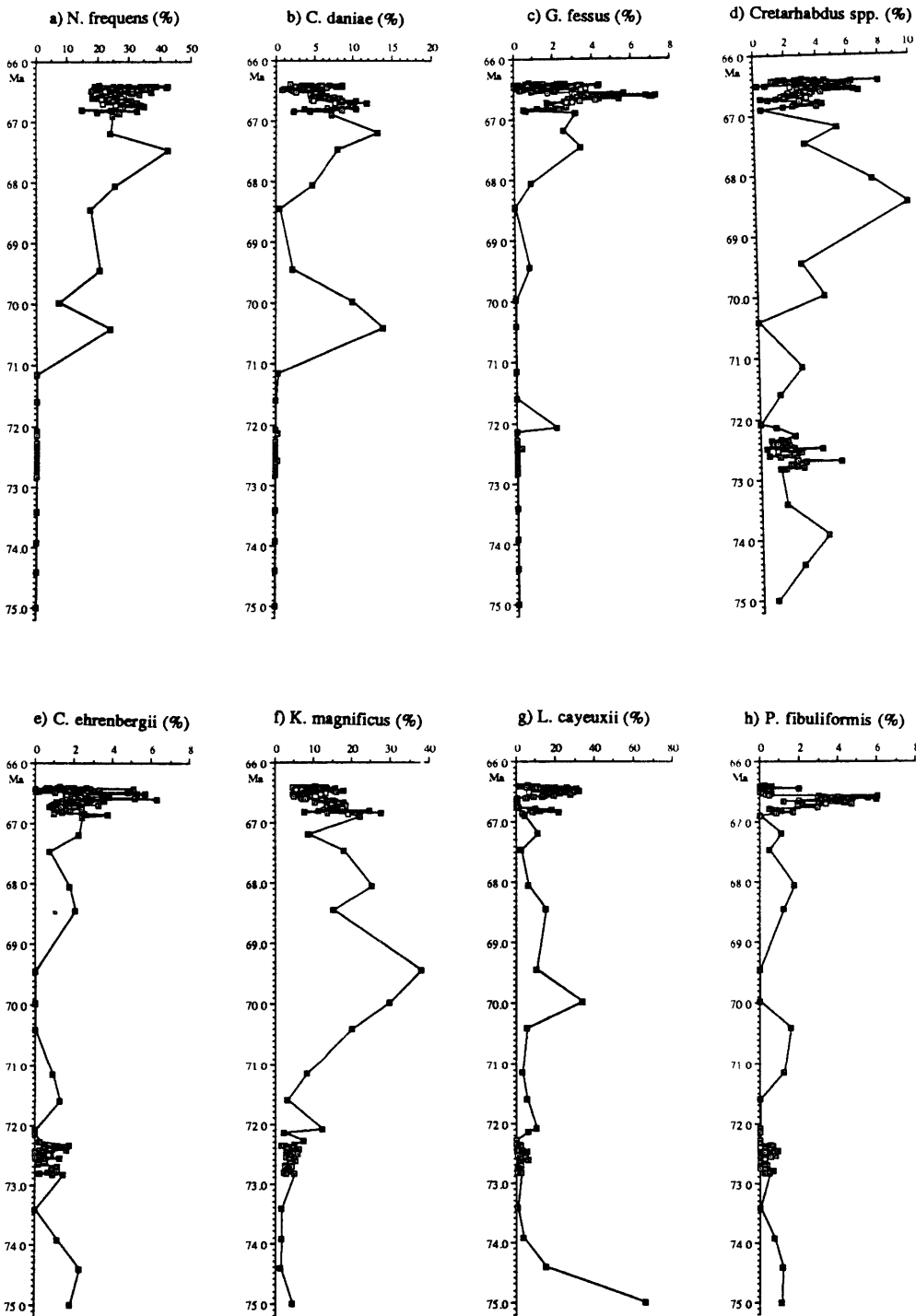


Figure 18: Relative abundances (%) of nannofossil taxa in Hole 690C. (Percent were calculated exclusive of *P. stoveri*.)

Hardly any changes between the abundances in the early and the late Maestrichtian are apparent in Arkhangelskiella spp. and Broinsonia spp. (possibly a slight increase?), E. turrisseiffeli (possibly slight decrease?), Gartnerago spp., M. staurophora (possibly slight increase?), and P. spinosa (possibly slight decrease; Figure 19b-f); all of these taxa are common to abundant throughout the Maestrichtian, except for M. staurophora which is rare (<3%, Figure 19e).

B) Abundance Changes of Calcareous Nannofossils Between 66.90 and 66.40 Ma

Taxon Richness: Taxon richness remained essentially constant during most of the latest Maestrichtian (16-21 taxa; Figure 20a). A slight diversity decrease is discernible around 66.45 Ma, possibly due to dissolution effects in several poorly preserved samples around this level. A diversity increase followed these low values and continued up to the K/P boundary; in two samples immediately preceding the K/P boundary the highest diversity values of the latest Maestrichtian interval were recorded (23 taxa, Figure 20a). These high values are due to increasing abundances of the persistent taxa (B. constans, M. inversus, Neocrepidolithus spp., P. sigmoides, Thoracosphaera spp.; Figure 20b-f) resulting in their constant recognition in the counts performed. In addition, typical incoming species (Hornibrookina, Cruciplacolithus) were encountered in several samples before the K/P boundary and artificially increased the diversity; their presence is interpreted as a consequence of heavy bioturbation of the K/P boundary interval (see also the discussion in Pospichal et al., 1990).

Relative abundance: Several taxa show very conspicuous abundance variations during the latest Maestrichtian. Lucianorhabdus cayeuxii displays the most pronounced abundance changes (Figure 20g): it is common to abundant between about 66.78 and 66.90 Ma, but is virtually absent between ~66.76 and 66.61 Ma; it increases in abundance again after 66.60 Ma and constitutes up to >30% of the assemblage during most of the last 200 ky of the Maestrichtian. However, a constant decline begins at about 66.44 Ma and continues until the K/P boundary; in the youngest samples investigated this species constitutes <5% of the entire assemblage.

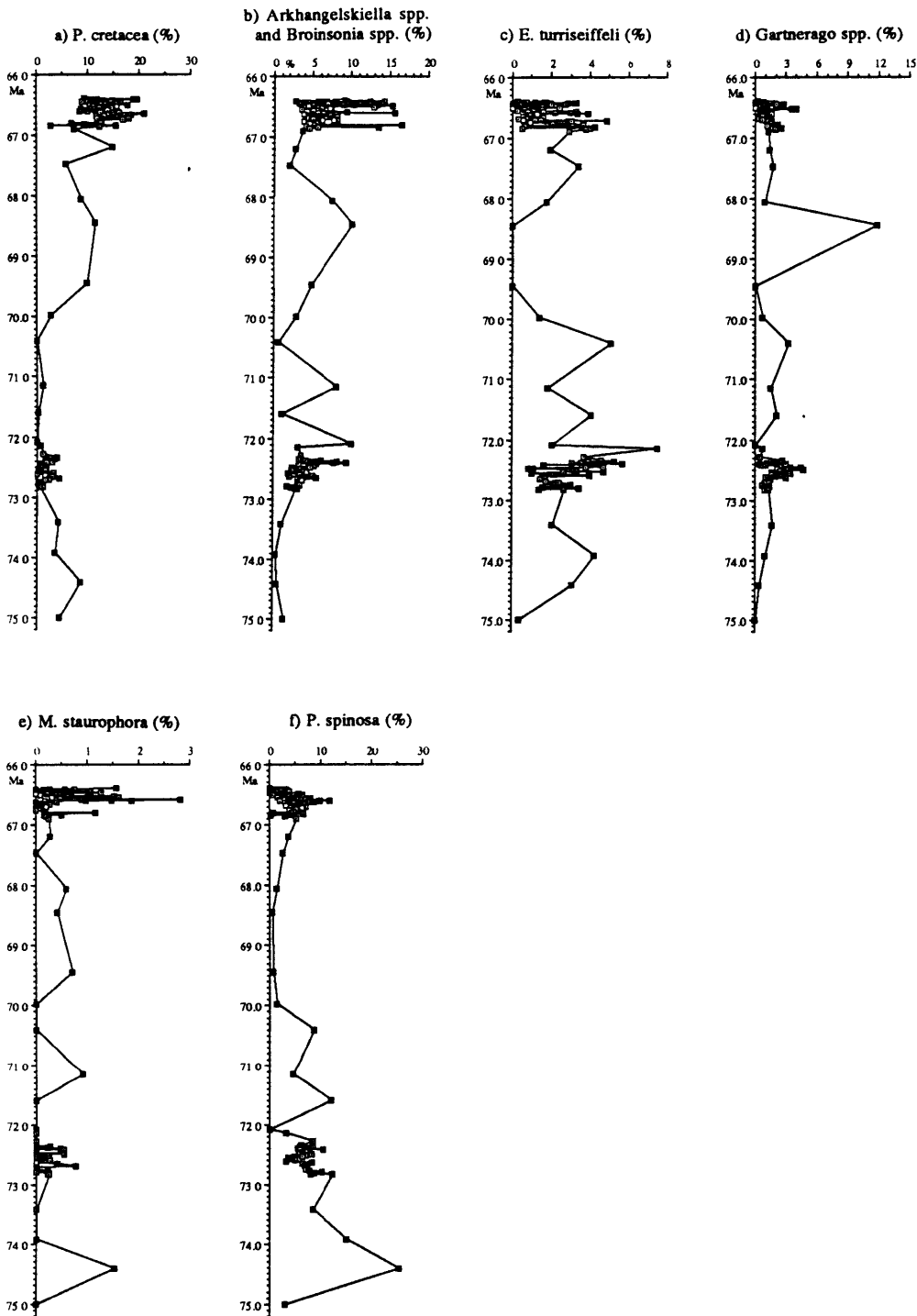


Figure 19: Relative abundances (%) of nannofossil taxa in Hole 690C. (Percent were calculated exclusive of *P. stoveri*.)

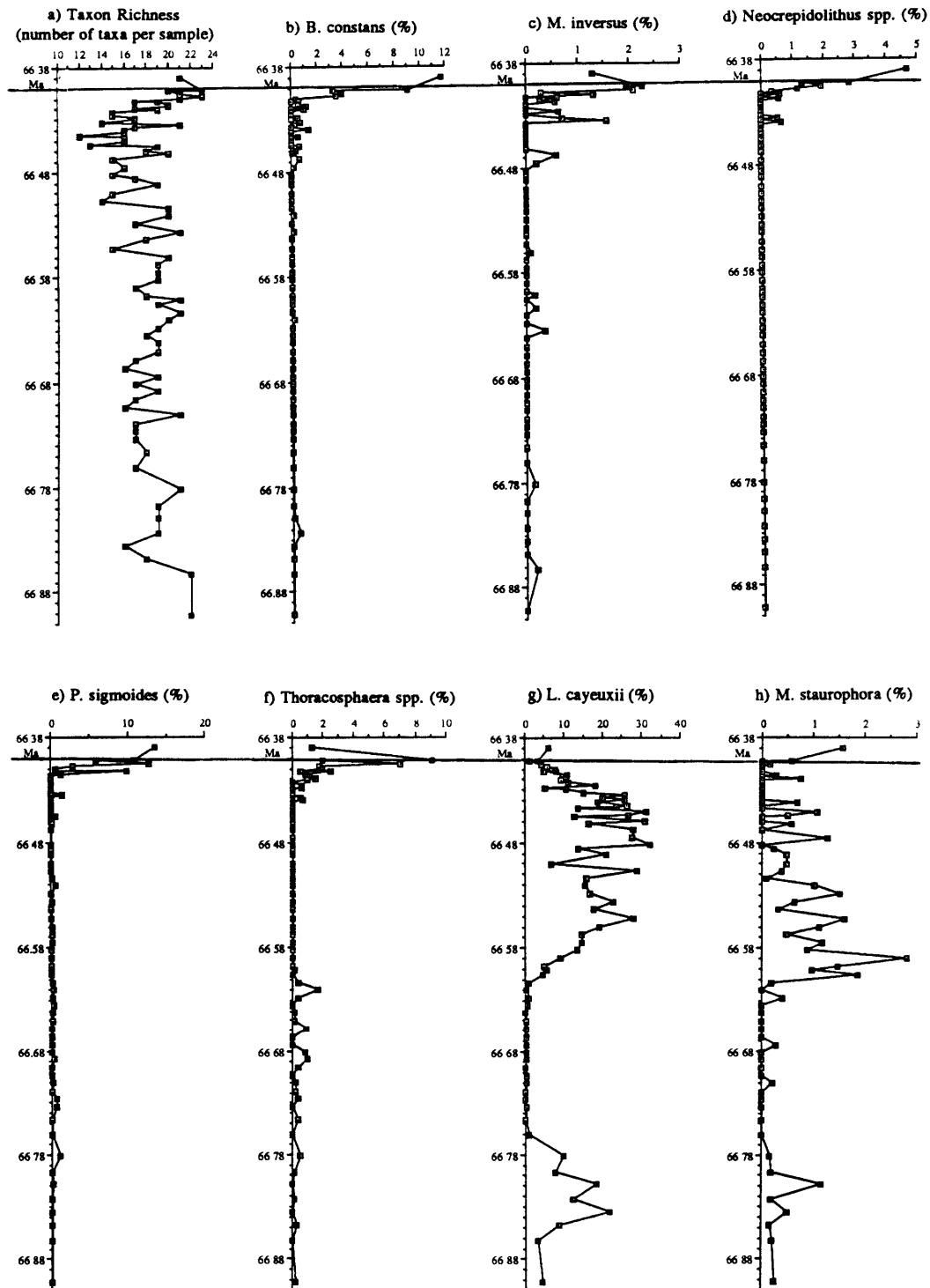


Figure 20: Relative abundances (%) of nannofossil taxa in the latest Maestrichtian (~66.4 - 66.9 Ma) in Hole 690C. The K/P boundary lies at 66.4 Ma. (Percent were calculated exclusive of *P. stoveri*.)

Micula staurophora is an order of magnitude rarer than L. cayeuxii but shows similar abundance variations (Figure 20h). It is rare (<1%) prior to about 66.78 Ma, virtually absent between about 66.78 and 66.62 Ma, and comparatively more abundant (up to 3%) between ~66.78 Ma and 66.52 Ma. After ~66.52 Ma it is very rare again (virtually always <1.5%) and was not encountered during the counts in many samples.

Placozygus fibuliformis (Figure 21a) displays abundance variations that are almost exactly opposite to those of L. cayeuxii: Placozygus fibuliformis increases in abundance from <2% to 2-6% between 66.78 and 66.76 Ma. At about 66.58 Ma it reaches its peak abundance (>6%), and then drops precipitously to very low values (<1%) at about 66.56 Ma; P. fibuliformis remained a minor component in the latest Maestrichtian assemblage.

Microrhabdulus decoratus, a very rare species (always <1%; Figure 21b) was more often encountered during the interval when P. fibuliformis showed increased abundance.

It must be pointed out that L. cayeuxii and M. staurophora on one hand, and P. fibuliformis (and M. decoratus) on the other, are not mutually exclusive; all four taxa occur together between about 66.60 and 66.57 Ma. This overlap cannot result from bioturbation since P. fibuliformis and M. staurophora show very sudden abundance changes, whereas bioturbation would tend to smear out abrupt changes.

Glaukolithus fessus increases in abundance from about 66.85 Ma (<2%) to about 66.63 Ma (almost 8%; Figure 21c). High, but strong fluctuations (4-8%) occur between ~66.63 and 66.58 Ma after which a fairly abrupt abundance decrease occurred (between 66.58 and 66.56 Ma) to values <1%. This decrease was coeval with the abundance decrease in P. fibuliformis. Strongly fluctuating abundance values (between 0 and >4%) occur in this species during the last 150 ky of the Maestrichtian (66.55 to 66.40 Ma).

Ahmuellerella octoradiata and P. regularis (Figure 21d) were grouped together at this site, because these species could not be differentiated consistently in all samples due to poor preservation in some samples. However, I believe that almost all specimens included in this group belong to A. octoradatia. During most of the latest Maestrichtian this group represents <5% of the assemblage. The abundance variations are similar to those of G. fessus: an abundance increase occurs between ~66.80 and 66.63 Ma where maximum

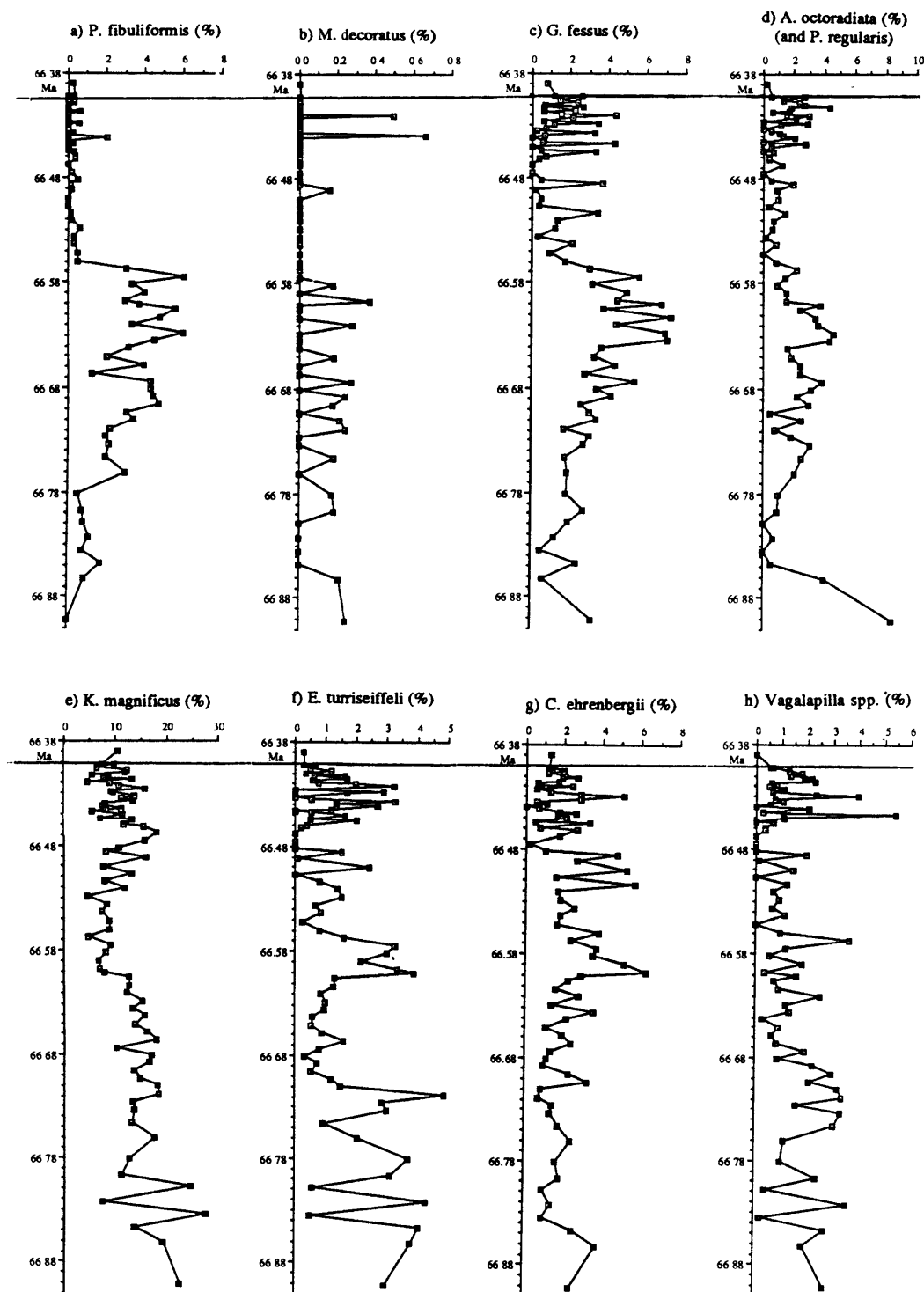


Figure 21: Relative abundances (%) of nannofossil taxa in the latest Maestrichtian (~66.4 - 66.9 Ma) in Hole 690C. The K/P boundary lies at 66.4 Ma. (Percent were calculated exclusive of *P. stoveri*.)

values of >4% were recorded. Subsequently values decreased again to about 1% or less at 66.55 Ma and remained low for the remainder of the Maestrichtian. During the very latest part of the Maestrichtian (66.40 to 66.46 Ma) high abundance fluctuations occurred (between 0 and 4%).

Kamptnerius magnificus reached two abundance maxima in the early part of the latest Maestrichtian (at ~66.84 and at 66.81 Ma) when this species constituted between 25 and 30% of the entire assemblage (Figure 21e). Apart from these isolated peak values, the abundance of K. magnificus changed only little during the last 0.5 m.y. of the Maestrichtian. A slight decrease in abundance occurred at ~66.60 Ma (from values around 13% to <10%). This is at the time when L. cayeuxii and M. staurophora increased in abundance; it is possible that this decrease of K. magnificus is only an effect of the closed sum of the calculation of percentages. At ~66.52 Ma abundance values increased again and between this time and the K/P boundary values fluctuated between 5 and 15%.

Eiffellithus turriseiffeli varied considerably in relative abundance during the latest Maestrichtian (Figure 21f): very low values (<1%) occur at ~66.84 and at 66.81 Ma. An abundance peak of about 5% occurred at ~66.72 Ma; after this maximum values decreased to about 1% and remained low until about 66.61 Ma. Eiffellithus turriseiffeli became more abundant (~2-4%) between about 66.60 and 66.57 Ma. This is also the time when P. fibuliformis and L. cayeuxii occurred together. Close to 66.57 Ma the abundance of E. turriseiffeli declined to low values (about 1%). As G. fessus, E. turriseiffeli displayed somewhat higher and highly variable abundance during the last 150 ky of the Maestrichtian (between about 66.55 and 66.40 Ma).

Cribrosphaerella ehrenbergii constituted about 2% of the assemblage during the early part of the latest Maestrichtian (between about 66.91 and 66.60 Ma; Figure 21g). It reached a peak abundance of >6% at ~66.595 Ma and decreased again to lower values ~2%. Fairly variable values were recorded between about 66.55 and 66.40 Ma.

Vagalapilla spp. displayed very low abundances at 66.835 and at 66.81 Ma (Figure 21h); between 66.75 and 66.69 Ma relative abundance values of this group of species lay between 2 and 3%; subsequently they decreased and fluctuated around 1% while isolated peaks occurred at 66.57 Ma (>3.5%), at 66.45 Ma (5.5%) and at 66.43 Ma (about 4%).

The abundance of Gartnerago spp. decreased gradually throughout most of the latest Maestrichtian (Figure 22a) from about 2.5% at 66.91 Ma to <1% at ~66.55 Ma. A peak abundance of 3.5-4% occurred between ~66.54 to 66.53 Ma. During the latest Maestrichtian (66.40 to 66.46 Ma) abundance values of species of this genus displayed considerable variability (0 - ~3%).

During most of the latest Maestrichtian the relative abundance of N. frequens (Figure 22b) remained constant around 25% (\pm ~5%). However, its abundance increased to values between 30-40% during the very latest Maestrichtian (between about 66.43 and 66.41 Ma).

Abundance values of P. spinosa fluctuated around 4% (\pm ~2%; Figure 22c) during most of the latest Maestrichtian (~66.91 - 66.48 Ma); after about 66.48 Ma its abundance decreased to values averaging 1% (0-4%).

The relative abundance of the group of Arkhangelskiella spp. and Broinsonia spp. remained fairly constant throughout the late Maestrichtian (Figure 22d). Abundance peaks were recorded at ~66.84 and at ~66.81 Ma, and at ~66.605 Ma. This group displayed conspicuous abundance variations during the latest Maestrichtian (between about 66.46 and 66.40 Ma).

Prediscosphaera cretacea was among the more abundant taxa (Figure 22e), constituting on average around 10% of the late Maestrichtian assemblage. Lower abundance values occurred at ~66.84 and at ~66.81 Ma, and an abundance peak of almost 10% above the longterm average (i.e. >20% vs. ~10%) occurred between ~66.67 and 66.63 Ma.

Prediscosphaera stoveri predominated in the latest Maestrichtian assemblage. This species constituted about 70% of all calcareous nannofossils prior to ~66.85 Ma (Figure 22f), its abundance decreased sharply at ~66.84 Ma, but recovered subsequently and reached an unprecedented peak of almost 80% at about 66.73 Ma. Afterwards the abundance of P. stoveri decreased to ~50% (at ~66.67 Ma) and remained close to this abundance during the remainder of the latest Maestrichtian (Figure 22f).

Abundance values of Cretarhabdus spp. changed little during the latest Maestrichtian (Figure 22g). Only around 66.50 Ma two very low values were recorded. During the very latest part of the late Maestrichtian (~66.48 to 66.40 Ma) the abundance values of the species of Cretarhabdus displayed a higher intersample variability than throughout the earlier part.

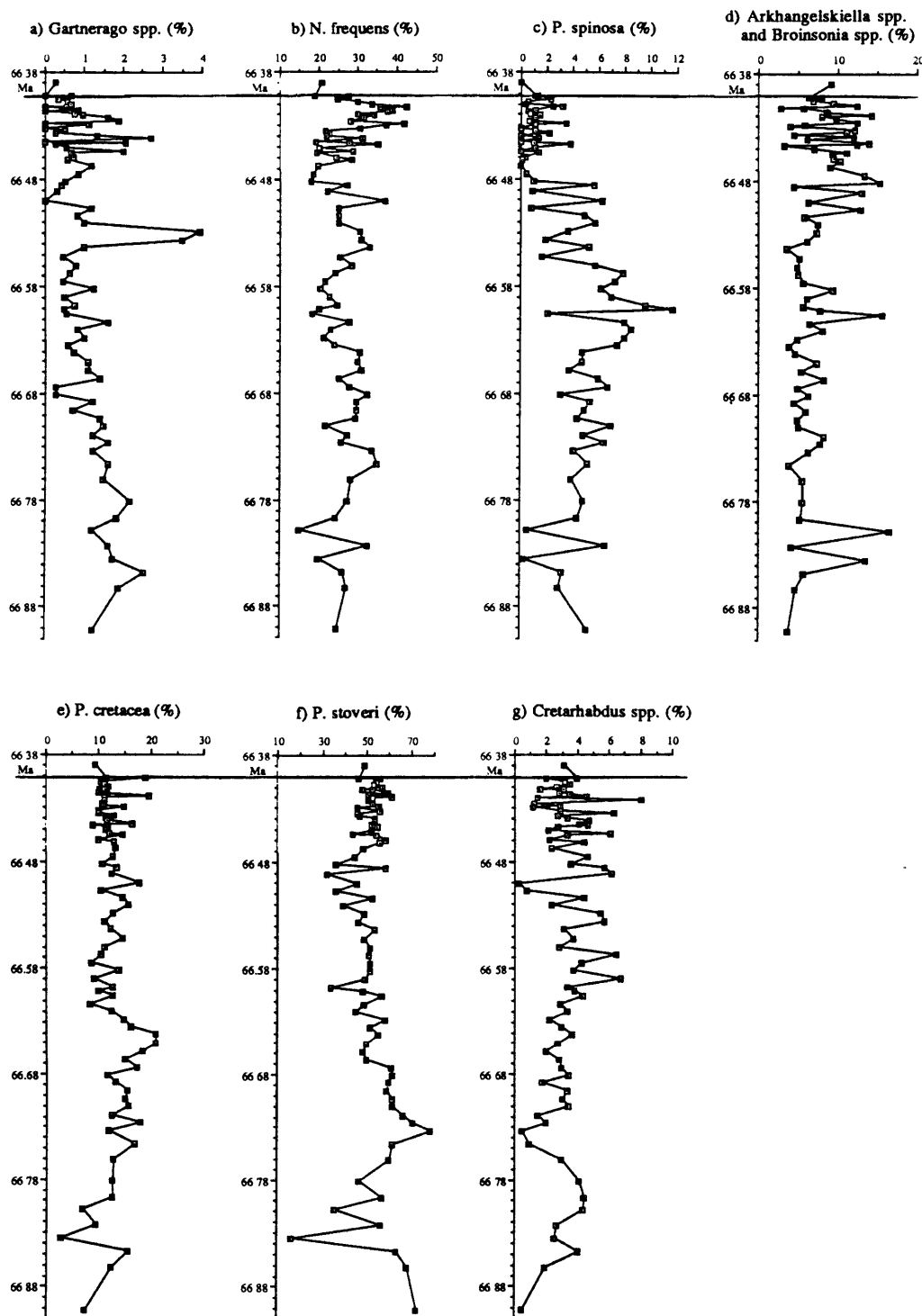


Figure 22: Relative abundances (%) of nannofossil taxa in the latest Maestrichtian (~66.4 - 66.9 Ma) in Hole 690C. The K/P boundary lies at 66.4 Ma. (a) to (e) and (g): Percent were calculated exclusive of *P. stoveri*.

Absolute abundance and fluxes: The number of coccoliths and nannoliths (exclusive of the placoliths P. stoveri) that were observed per viewfield are plotted in Figure 23a. High values prior to ~66.84 Ma are followed by a pronouncedly lower values between ~66.84 and 66.78 Ma. Subsequently, values increased again and reached maxima between ~66.75 - 66.66 Ma. Between ~66.66-66.55 Ma the numbers of placoliths per viewfield decreased steadily, and remained at a constant level between ~66.55 and 66.40 Ma. A similar trend was observed in the abundance variations of the number of placoliths of P. stoveri between 66.90 and 66.40 Ma (Figure 24a).

In the curve of coccoliths and nannoliths per viewfield (Figure 23a) low values occur at ~66.83 Ma, ~66.81 Ma and at ~66.74 Ma. These correspond to a reduction of nannofossil specimens of 80% and 70%, respectively. Micarb (microcrystalline carbonate) is much more abundant in these samples than in the adjacent ones. This, as well as the relative enrichment of dissolution resistant taxa (according to Thierstein, 1980) at these levels (L. cayeuxii, K. magnificus, Arkhangelskiella spp. and Broinsonia spp.; Figures 20g, 21e, 22d) and the massive reductions of dissolution susceptible taxa (e.g. G. fessus, E. turriseiffeli, Vagalapilla spp., P. spinosa; Figures 21c, f, h, 22c), suggest that the low values of calcareous nannofossils per viewfield do not correspond to a primary signal but reflect extensive dissolution. The older two outlier values are also apparent in the curve of P. stoveri (Figure 22f), but the value at 66.74 Ma is not unusually low.

The long term abundance reduction of P. stoveri as well as of the sum of all other coccoliths and nannoliths after ~66.70 Ma is considered to be a genuine signal rather than an artifact of deteriorating preservation: examination of the preparations did not reveal long term trends of changing preservation or increasing micarb content upsection; relative abundances of dissolution resistant taxa do not increase in concert with the falling "specimens-per-viewfield" curves (L. cayeuxii, Figure 20g; K. magnificus, Figure 21e; Arkhangelskiella and Broinsonia, Figure 22d), nor do dissolution susceptible taxa display systematic decreases (e.g. E. turriseiffeli, Figure 21f; Vagalapilla spp., Figure 21h; P. spinosa, Figure 22c).

The numbers of coccoliths and placoliths per gram sediment and per gram carbonate as well as the fluxes derived from these data are plotted in Figure 23b-e). The same calculations were performed for P. stoveri and the

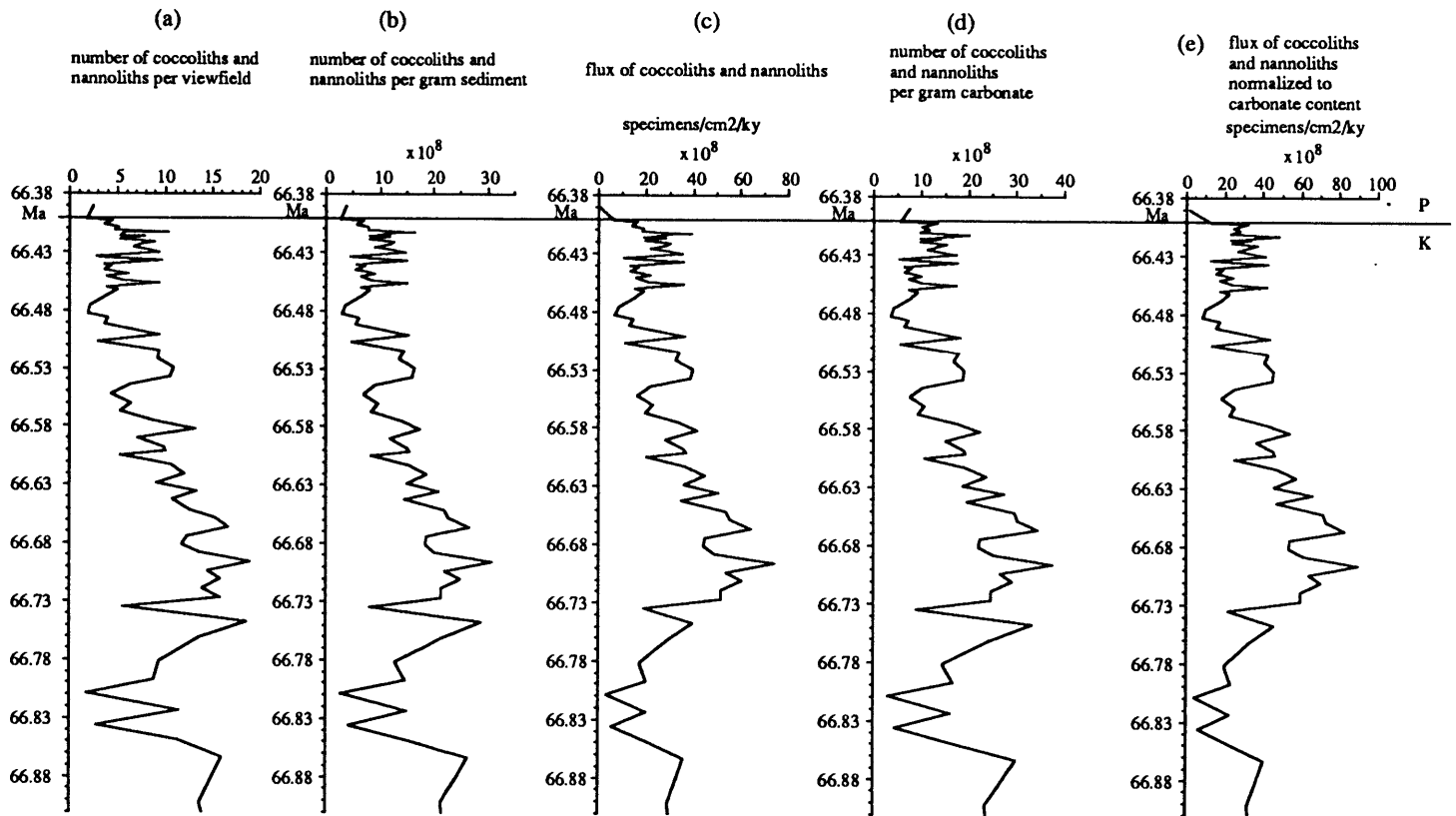


Figure 23: Abundance fluctuations of coccoliths and nannoliths during the latest Maestrichtian in Hole 690C. All data exclusive of P. stoveri.

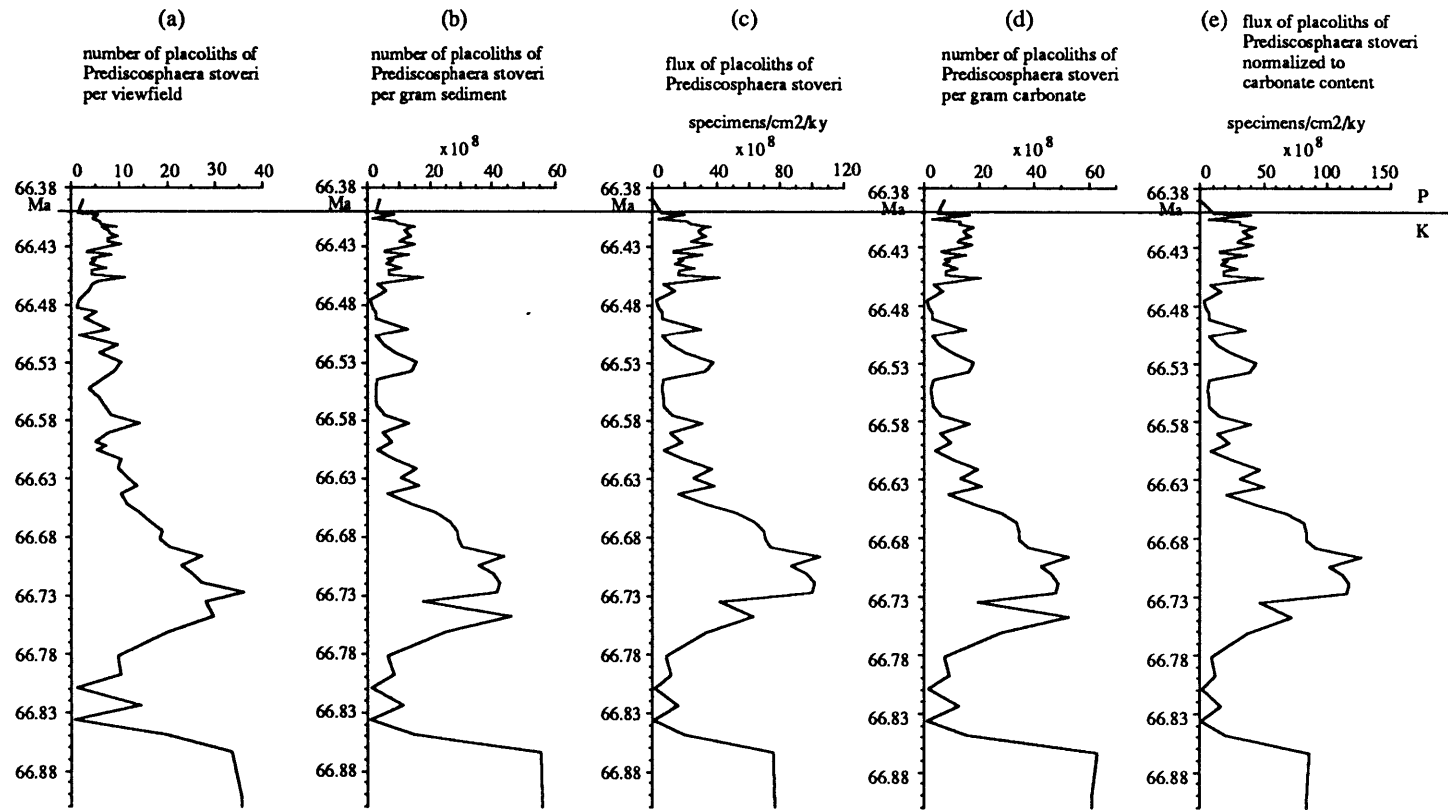


Figure 24: Absolute abundance fluctuations of *P. stoveri* during the latest Maestrichtian.

data plotted in Figure 24b-e. These plots reiterate the trends observed in the curves of specimens per viewfields as discussed above. The graphs of the fluxes of calcareous nannofossils (Figure 23c and e) indicate that the elevated values between about 66.72 and 66.60 Ma represent a brief excursion over lower background values ($60-80 \times 10^8$ versus $20-40 \times 10^8$ specimens/cm²/ky). Also the flux of P. stoveri shows a pronounced increase in about the same interval (Figure 24e).

The decrease of absolute abundances of calcareous nannofossils during the latest Maestrichtian is not reflected in a similar decrease of the carbonate content. The discrepancy between these two curves is most likely accounted for by the increase of foraminifera as a sedimentary component during this time interval (compare Figure 5 in Chapter 3 on page 37).

2) ODP Hole 761B and ODP Hole 761C

(A) Long term trends: Hole 761B

The taxon richness recorded in all samples in Hole 761B is plotted against age in Figure 25. An increase in species richness from about 30-35 taxa per sample to values between about 40-45 occurs throughout the entire section investigated. This increase is more pronounced between about 71-69 Ma than afterwards.

All relative abundances that are discussed below were calculated exclusive of M. staurophora.

Lithravidites quadratus and L. praequadratus both were beyond the detection limit prior to about 69.5 Ma. After that both taxa increased in abundance (Figure 26a, b); this increase was very abrupt and pronounced in L. praequadratus, which remained at about the same abundance level (~3%) for the remainder of the Maestrichtian. In contrast, L. quadratus was always rarer (hardly ever exceeding 1%), but increased steadily in relative abundance between 69 Ma and the K/P boundary. Tranolithus macloedae (Figure 26c) was absent prior to about 69.5 Ma. Subsequently it was encountered in most samples but remained a minor component of the nannofossil assemblages (<2%).

Biscutum constans (Figure 27a) is one of the taxa displaying more or less constant abundances (around 5%) throughout the late Maestrichtian, but displays an abrupt and drastic abundance decrease at about 67 Ma. During the late Maestrichtian this species constituted <1% of the nannofossil assemblage.

A pattern that is almost inverse to that of B. constans was recorded for Biscutum sp. 1 (Figure 27b): this species constituted <5% during most of the late Maestrichtian, but increased in abundance during between ~67.5 Ma and 66.4 Ma (to ~7%). A similar pattern was recorded for Corollithion exiguum: this species was so rare that it was beyond the detection limit prior to ~66.5 Ma: after ~66.5 Ma this species was still rare (<1%), but it was recorded almost consistently between 66.5 - 66.4 Ma (Figure 27c). The abundance distribution of Cribrosphaerella(?) daniae (Figure 27d) was very similar to that of C. exiguum: C. daniae was rare (<1.5%) but recorded almost consistently between ~66.5 - 66.4 Ma, whereas prior to ~ 66.5 Ma this species was almost always absent. Cylindralithus gallicus (Figure 27e) was rare during most of the late

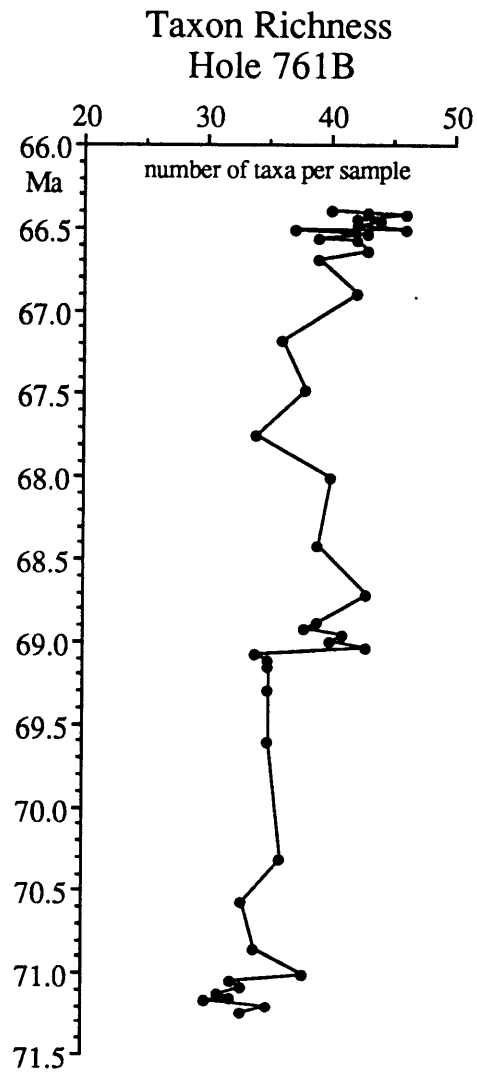


Figure 25: Plot of taxon richness (number of taxa per sample) versus age. The taxon richness increased slightly during the late Maestrichtian, no gradual or stepwise decline prior to the K/P boundary (at 66.40 Ma) is discernible.

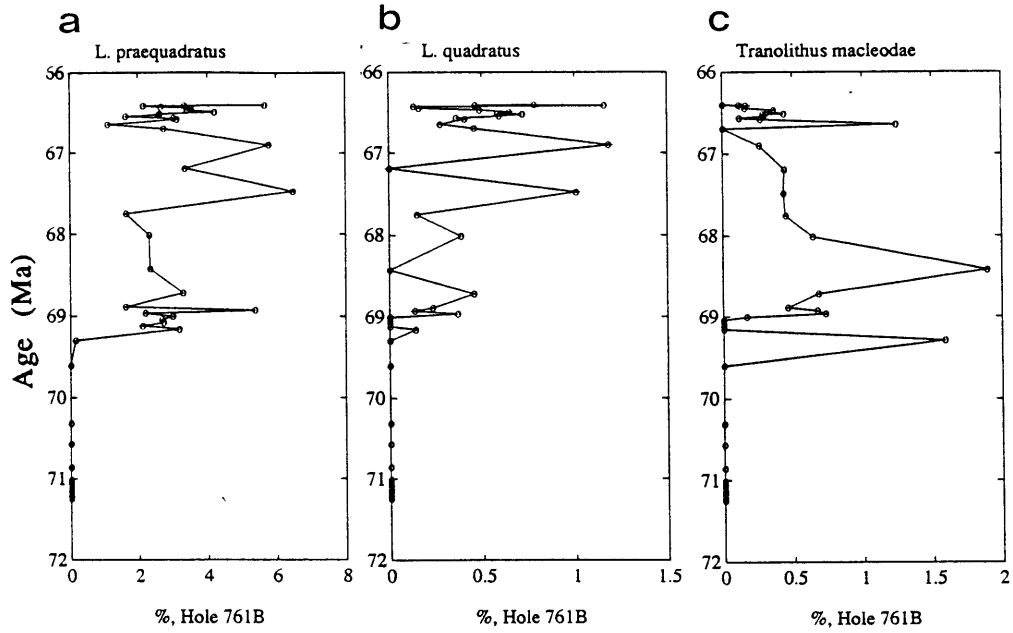


Figure 26: Relative abundance plots of selected taxa in Hole 761B during the late Maestrichtian. The data were calculated exclusive of M. staurophora.

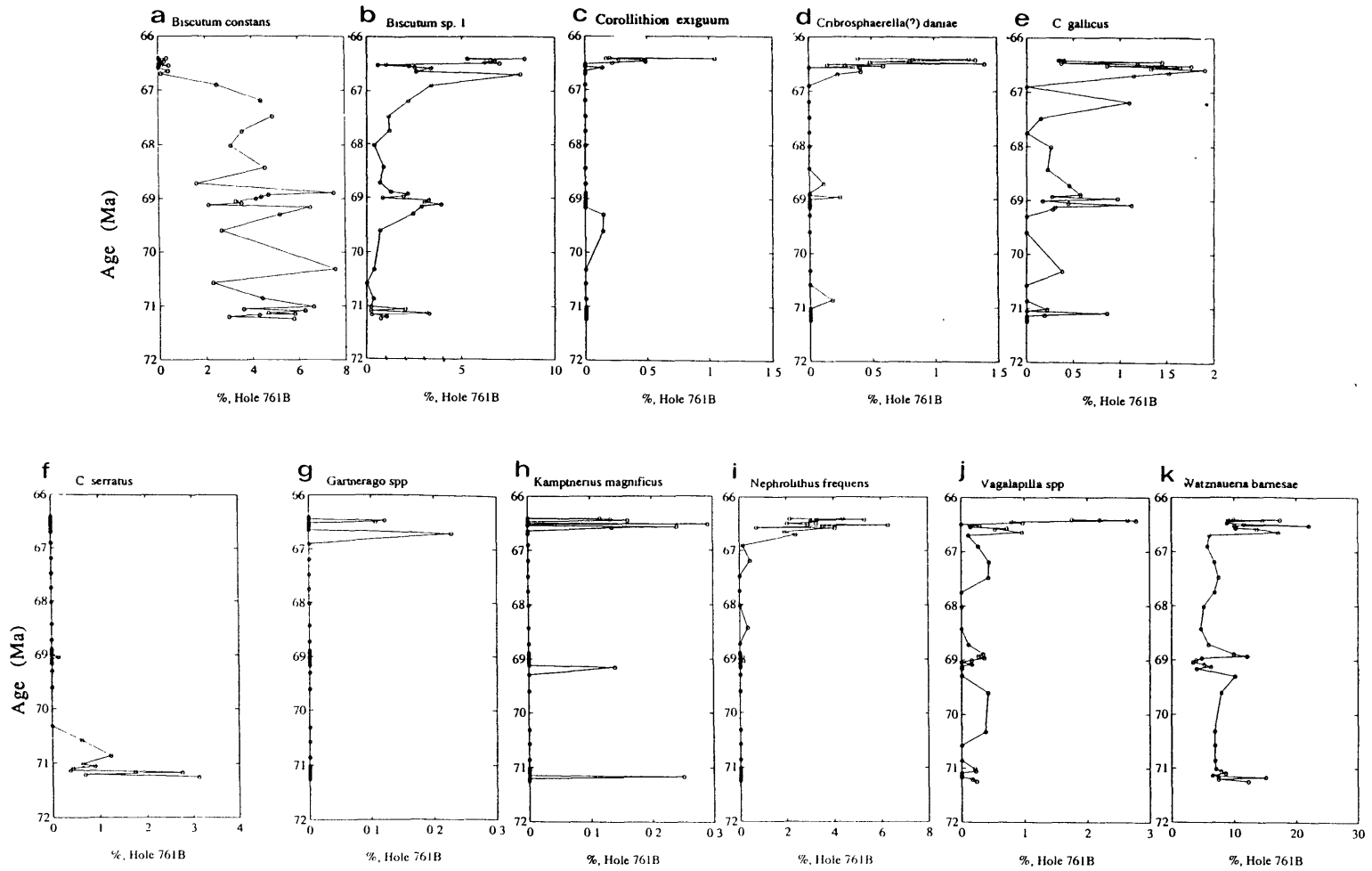


Figure 27: Relative abundance plots of selected taxa in Hole 761B during the late Maestrichtian. The data were calculated exclusive of *M. staurophora*.

Maestrichtian (<1%) but its abundance increased abruptly to values >1.5% after ~67 Ma. After peak values (~2%) had been reached at ~67 Ma, relative abundance of C. gallicus decreased again between ~67 Ma and 66.4 Ma.

Cylindralithus serratus was encountered commonly prior to ~70.5 Ma (Figure 27f) when it reached relative abundance peaks of >3%. Between ~70.5 Ma and 66.4 Ma this species was recorded only once. Zygodiscus sp. 1 was very rare (<1%) prior to about 68 Ma (Figure 28a). Between about 68 Ma and 66.7 Ma this species increased gradually in abundance (to ~1-2%). Between ~66.7 to 66.4 Ma this species first decreased in abundance (<0.5% between about 66.6 and 66.5 Ma), but then increased again to values between 1.5 and 3% during the last 50 ky of the Maestrichtian. Ceratolithoides sp. cf. C. aculeus was common (2-5% in most samples) prior to ~66.6 Ma; between ~66.6 and 66.4 Ma this taxon was always very rare (<1%; Figure 28b).

The relative abundance of G. fessus increased gradually throughout the late Maestrichtian (Figure 28c). It constituted between about 1-2% around 71 Ma and increased to values close to 5% after ~66.8 Ma. An unusually high value (>10%) was recorded around 69 Ma. Manivitella pemmatoidea was recorded consistently prior to about 69 Ma, although the relative abundances decreased between ~71.1 - 69 Ma from about 1% to <0.5% (Figure 28d). After about 69 Ma this species was very rare and recorded only intermittently. An almost reverse trend was recorded for M. belgicus, which was absent or very rare (<0.5%) prior to about 69 Ma, but subsequently increased in abundance and was recorded consistently between about 69 Ma and the K/P boundary (Figure 29e). The relative abundances of P. stoveri increased from ~2% to values >10% between about 71.2 and 68 Ma.

Watznaueria barnesae was one of the major constituents of the Maestrichtian nannofossil assemblages in Hole 761B (Figure 27k); in contrast to most other abundant taxa its relative abundances did not fluctuate very much but essentially remained between 5-10%. At about 66.65 Ma the relative abundances of W. barnesae increased fairly abruptly to values between ~10 and 15% at which level it remained until 66.4 Ma. The relative abundances of Arkhangelskiella spp. were <5% in most samples (Figure 28g); between about 71 and 70 Ma the abundances were higher, between 5 and 10%.

Cribrosphaerella ehrenbergii (Figure 28h) displayed abundance variations similar to Arkhangelskiella spp. in so far as this species was rarer around 69

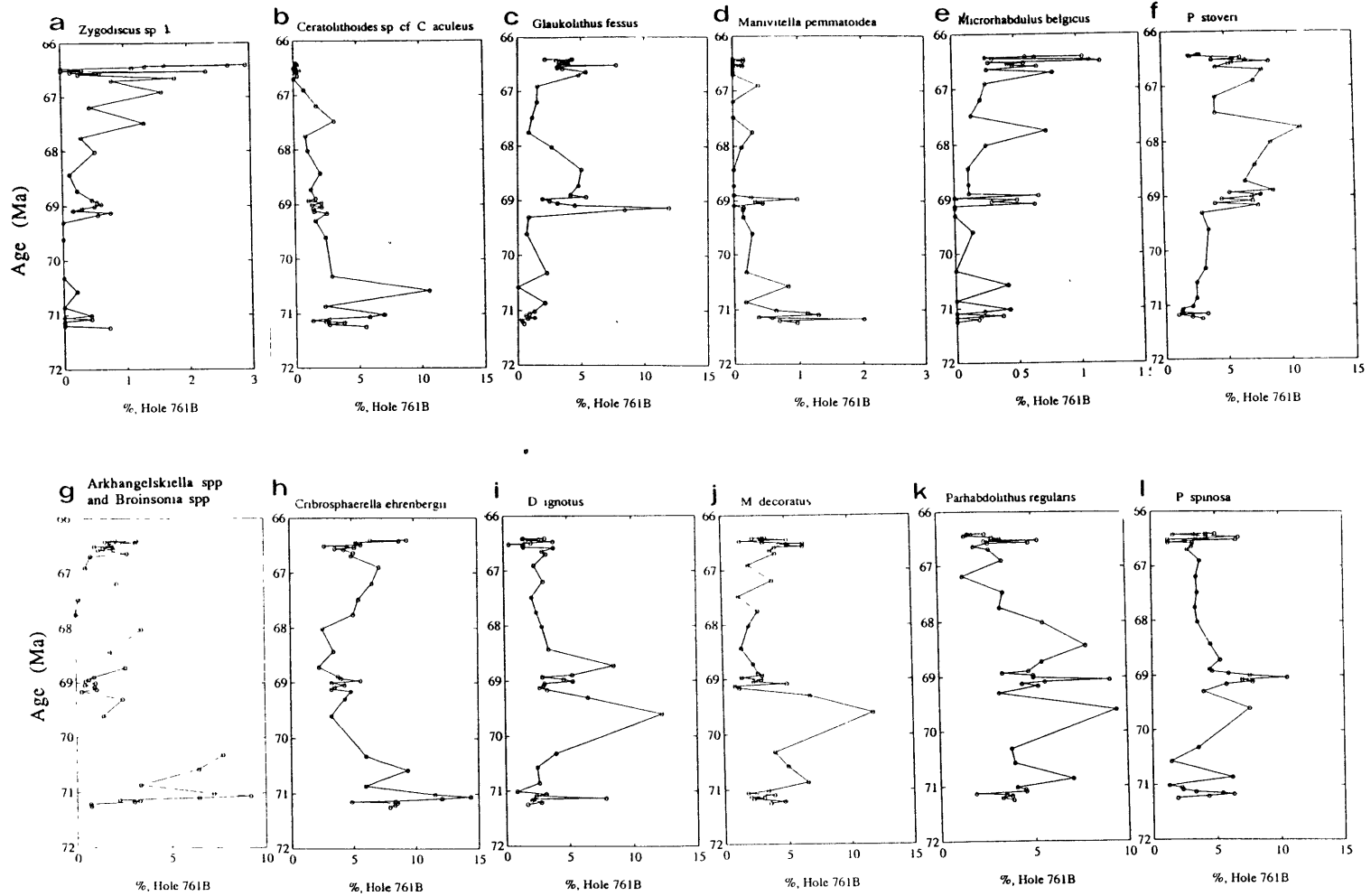


Figure 28: Relative abundance plots of selected taxa in Hole 761B during the late Maestrichtian. The data were calculated exclusive of M. staurophora.

Ma than either before or after this interval. Discorhabdus ignotus displayed only minor long term trends during the Maestrichtian (Figure 28i): its abundance was highest between ~ 70.3 and 68.5 Ma. The relative abundance of M. decoratus remained essentially unchanged during the late Maestrichtian (Figure 28j); an abundance peak of >10% was recorded at ~70 Ma. Parhabdolithus regularis constituted between 1-10% of the assemblage during the late Maestrichtian (Figure 28k); slightly higher values were recorded around 69 Ma than either before or after. The relative abundance of P. spinosa was highest (~5-10%) between ~69.5 - 68.5 Ma, whereas lower values (~3-5%) were recorded prior to and after this increase (Figure 28l).

Ahmullerella octoradiata was rare in Hole 761B (Figure 29a). Its abundance in most samples is <0.5%. Although rare, this species was recorded in most samples prior to ~68 Ma, but was not observed in any sample thereafter. Highly variable abundance data were recorded for P. fibuliformis (Figure 29b). In the earliest five samples recorded the data fluctuate from ~4-11% between adjacent samples, reminiscent of the abundance fluctuations of M. staurophora. Between about 71.1 and 69.3 Ma comparatively low values were recorded (around 2%). After that the relative abundances increased abruptly to values slightly >5% and remained at this level until about 66.8 Ma (with two lower values around 67 Ma). During the latest part of the Maestrichtian (66.7 Ma - 66.4 Ma) the relative abundances of P. fibuliformis decreased from ~8% to ~2% (Figure 29b). Placozygus sp. displayed low (between ~0.5 and 1%, Figure 29c) but fairly constant relative abundances during most of the late Maestrichtian: somewhat higher values (between 1 and 2%) were recorded prior to 71 Ma as well as during the last ~50 ky of the Maestrichtian. The relative abundances of P. cretacea varied widely during the Maestrichtian (Figure 29f). At about 71 Ma adjacent samples yielded values of 15% and almost 30%. The average relative abundances remained approximately constant between 20-25% between about 71.2 and 67 Ma. Between 67 Ma and the K/P boundary the relative abundances of P. cretacea were slightly lower and varied between ~15-20%. The abundance of Rhagodiscus splendens (Figure 29d) increased from values <0.5% around 71 Ma to ~1% at about 69 Ma; subsequently its abundance decreased again to low values (<0.5%) immediately preceding the K/P boundary. Stephanolithion spp. (Figure 29e) were very rare prior to 71 Ma and increased throughout the late Maestrichtian to values

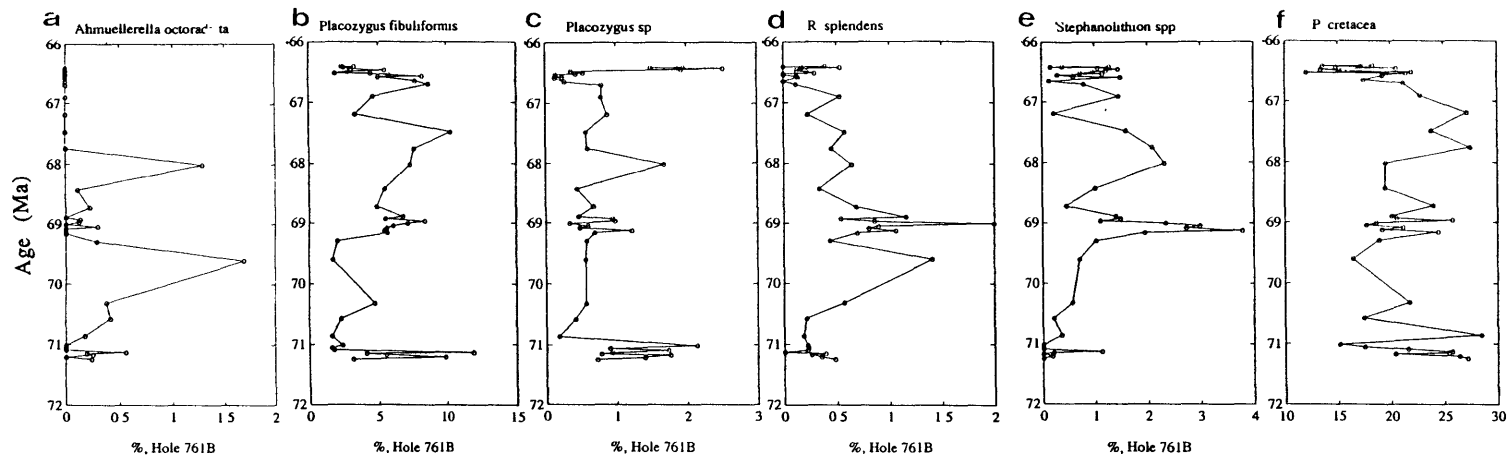


Figure 29: Relative abundance plots of selected taxa in Hole 761B during the late Maestrichtian. The data were calculated exclusive of M. staurophora.

around 1% at ~66.4 Ma. Comparatively very high values (between 2-3%) were recorded at about 69 Ma and 68 Ma.

B) The latest Maestrichtian: Holes 761B and 761C

Subtle changes in the calcareous nannofossil assemblages in Hole 761B occurred during the last 500 ky of the Maestrichtian. In both holes, 761B and 761C, the relative abundance of P. fibuliformis decreased between ~66.7 and 55.4 Ma (Figure 30j). The magnitude of the decrease was similar in both holes (around 8-9% at about 66.7 Ma; 2-3% at the K/P boundary). The decrease proceeded more or less gradually in both holes, except for isolated outlier values that seem to be associated with poorer preservation in some instances (e.g. unusually low values around 66.5 Ma in Hole 761B where M. staurophora showed increased abundance values).

Several taxa that were important components of the nannofossil assemblages in high southern latitude Hole 690C appeared or increased in abundance during the latest part of the Maestrichtian in Hole 761B. These taxa included C. daniae, Gartnerago spp., K. magnificus, N. frequens, and Vagalapilla spp (Figure 30c, i; 31c, d). Species of the genus Gartnerago were absent from most samples in Hole 761B, but were recorded in three samples between 66.7 and 66.4 Ma. Kamptnerius magnificus was always very rare (<0.5%). Prior to ~67 Ma it was recorded only in isolated samples. Between ~67 Ma and ~66.4 Ma its abundance increased slightly and it was encountered in several samples. Nephrolithus frequens displayed one of the most conspicuous abundance increases at about 67 Ma: this species was recorded as early as at ~69 Ma, but between about 69 and 67 Ma it was very rare. After ~67 Ma the relative frequency of N. frequens increased abruptly from values <0.5% to values between 2 and 4% (with a maximum value >6%). Species of Vagalapilla were rare (<0.5%) throughout most of the Maestrichtian studied in Hole 761B but increased in abundance ~50 ky before the K/P boundary and reached abundance values between 2-3%. All of these taxa are characteristic components of high latitude assemblages.

Also C. ehrenbergii (Figure 30d) which was present during the entire Maestrichtian in Hole 761B increased in relative abundance during the last 350 ky of the Maestrichtian.

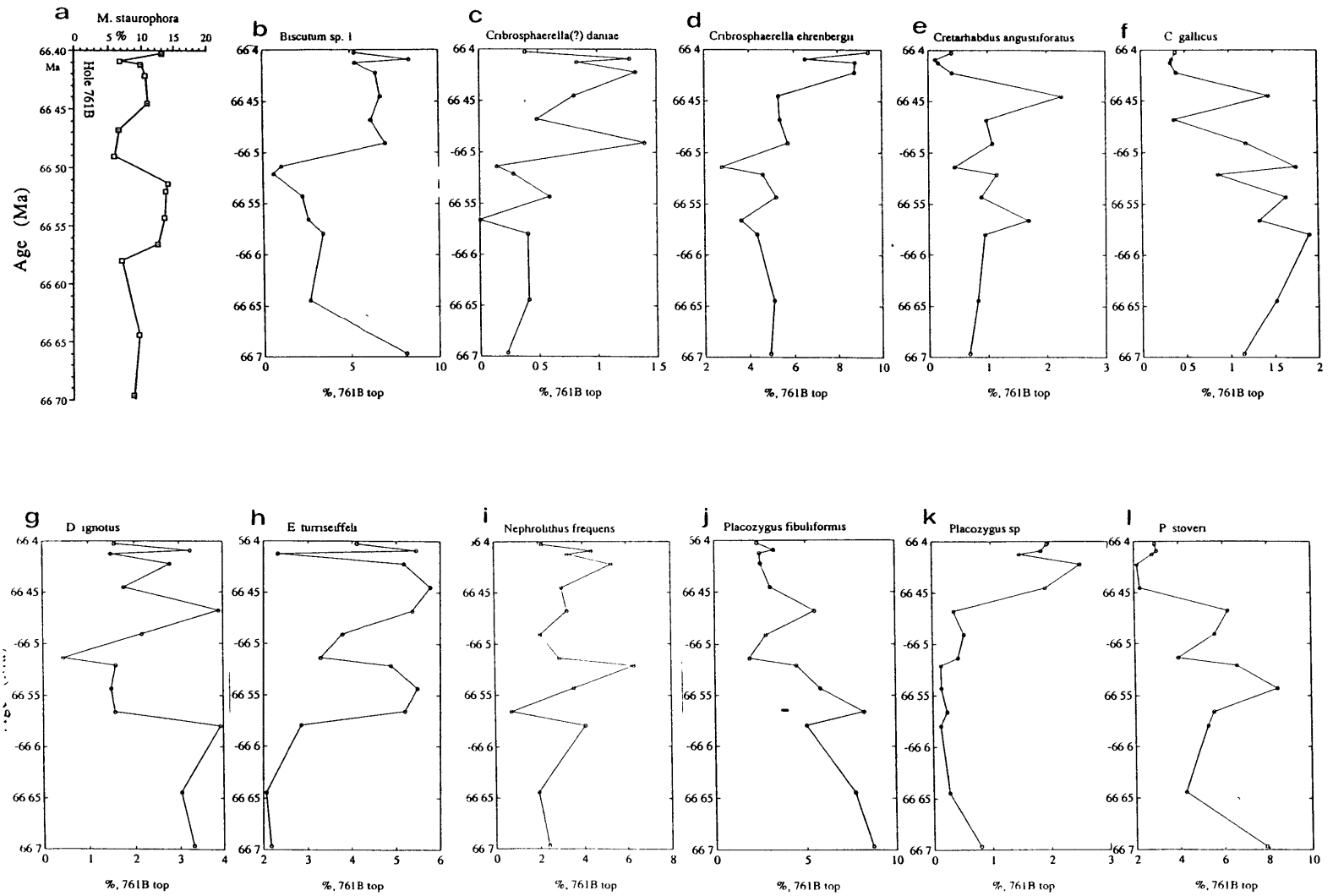


Figure 30: Relative abundance plots of selected taxa versus age (Hole 761B). Only the latest Maestrichtian is represented. (Abundances calculated excl. of *M. staurophora*).

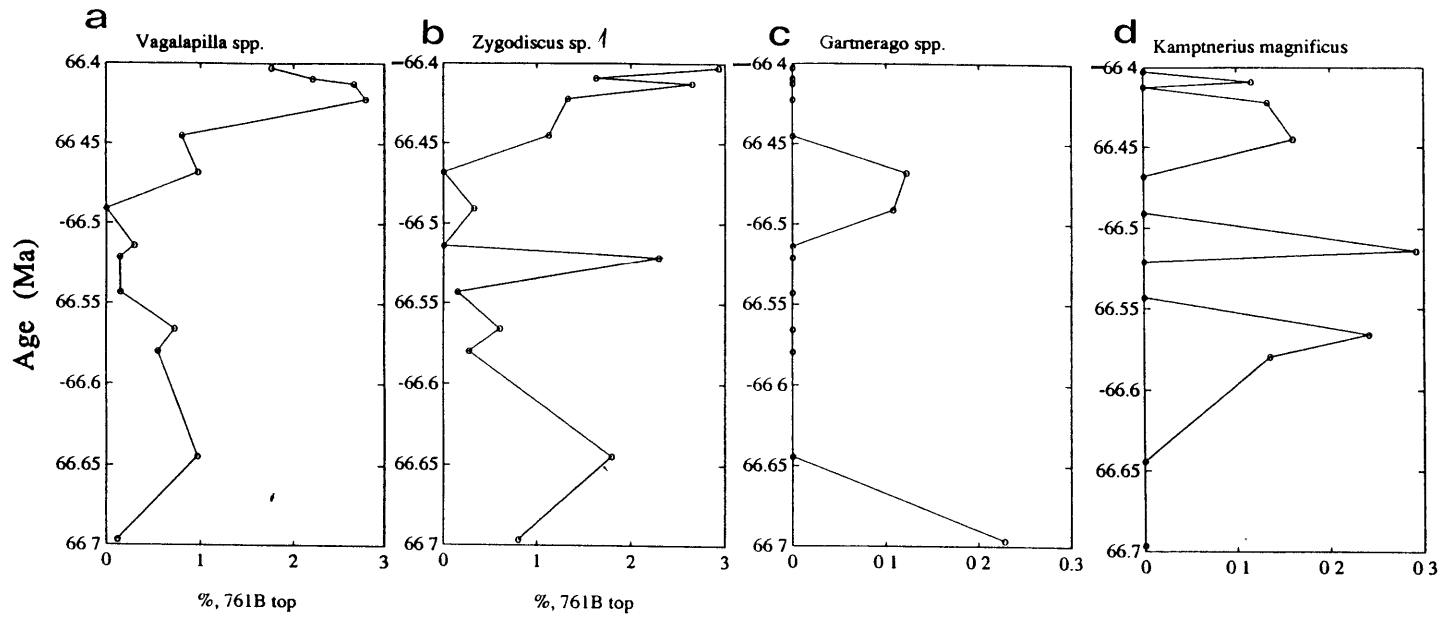


Figure 31:Relative abundance plots of selected taxa versus age (Hole 761B). Only the latest Maestrichtian is represented. (Abundances calculated excl. of M. staurophora).

C) Assessment of Preservation

The influence of dissolution on the nannofossil assemblages was investigated at Site 761 by comparing the abundance variations of dissolution resistant and dissolution susceptible taxa: nannofossil assemblages that were modified by increased dissolution should be enriched in the former group and depleted in the later group. Following Thierstein (1980) four taxa were included in the dissolution resistant group: Arkhangelskiella spp., Broinsonia spp., K. magnificus, and W. barnesae. The last taxon is by far the most abundant one and controls the pattern of the shape of the curve of the dissolution resistant group. Included in the dissolution susceptible group were B. constans, C. ehrenbergii, D. ignotus, E. turriseiffelii, N. frequens, P. regularis, P. fibuliformis, P. cretacea, and P. spinosa. In addition the relative abundances of M. staurophora was used as an additional very dissolution resistant indicator. The graphs are presented in Figure 32. One sample at around 66.51 was identified where all three 'dissolution indices' indicated increased dissolution (circled in Figure 32a, b, c). In all other samples there is no unambiguous signal indicating increased dissolution and consequently all other data points are considered to represent genuine abundance variations. In some of the older samples (prior to about 70.5 Ma) very high fluctuations in the relative abundances of the dissolution susceptible group as well as of M. staurophora were recorded. Since there were no corresponding abundance variations in the dissolution resistant group, these samples were not considered to be extensively modified by increased dissolution; however, this possibility could not be completely ruled out and the samples in question were marked with a circle and a question-mark (Figure 32d, e, f).

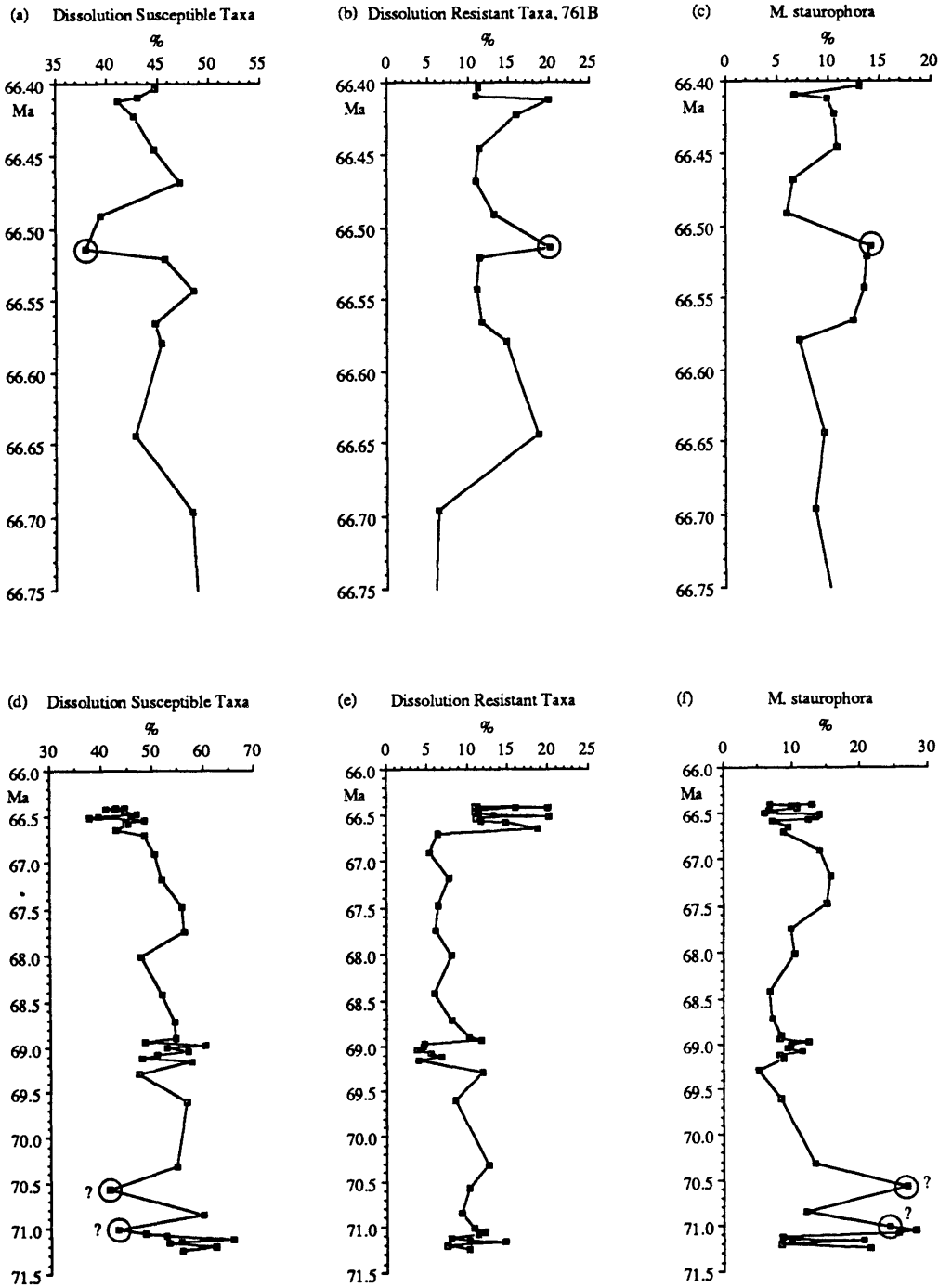


Figure 32: Plots of dissolution susceptible and dissolution resistant taxa, as well as of *M. staurophora* versus age. The graphs on top represent the latest Maestrichtian only, while those below represent the entire Maestrichtian section investigated. The data points that are circled are most likely modified due to increased dissolution. The K/P boundary lies at 66.40 Ma.

3) DSDP Hole 217

A) Nannofossil Abundance Patterns

The number of taxa per sample recorded in the upper Maestrichtian chalk in Hole 217 varies between 27 and 44 (Figure 33). Below 455.19 mbsf (~68.56 Ma) between 35 and 43 taxa per sample were recorded; in the interval of high sample resolution between 455.19 and 450.49 mbsf (~68.56 and 68.27 Ma) species richness was highly variable, with values on average lower than below, fluctuating around 35 taxa. The lowest species richness was recorded at 426.70 mbsf (~66.76 Ma; 27 taxa); above this level species richness increased again and values as high as in the lowest part of the section (between ~35-40 taxa per sample) were recorded immediately below the K/P boundary.

While the counts were made the preservation in each sample was noted, and there was no indication of systematic poorer preservation in the samples that displayed reduced species richness (compare "Preservation" among samples in Appendix II: Table 217). Therefore the trend of decreasing species richness between 492.32 and 426.70 mbsf (~71-66.76 Ma) and the ensuing increase in the uppermost 5.5 m of the Maestrichtian is considered to be a genuine signal rather than an artifact of preservation. Below I discuss the abundance patterns of selected taxa in order to examine which taxa disappear from the assemblages below 426.7 mbsf (~66.76 Ma), and which taxa first occurred at this level or became more abundant causing the increased species richness just below the K/P boundary.

Micula staurophora is among the most abundant taxa constituting ~10% to 25% (average 15%) of the entire Maestrichtian assemblage with peak abundances exceeding 30% (Figure 34). No long term trend of increasing or decreasing abundance was recorded. Because of the high abundance of M. staurophora the percentages of all other nannofossil taxa were calculated exclusive of M. staurophora. As in the other sections this procedure was chosen so that smaller abundance changes in comparatively rare taxa would not be suppressed.

a) Taxa decreasing in relative abundance:

Ahmuellerella octoradiata constitutes several percent of the assemblage in the lower part of the section (below 469.06 mbsf; ~69.4 Ma; Figure 35a), its

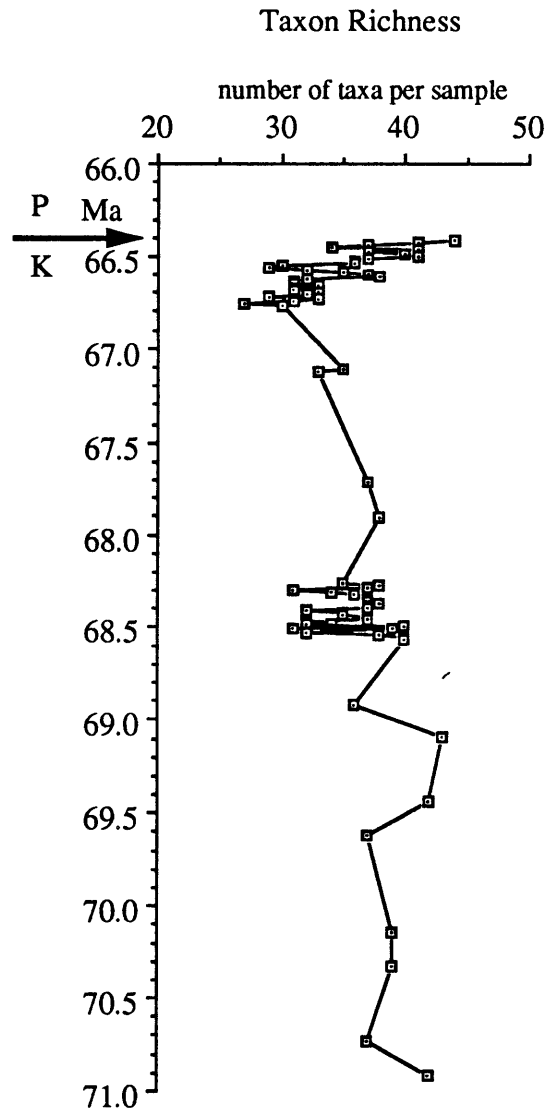


Figure 33: Species Richness (number of taxa per sample) plotted against age. The decrease between about 71 Ma and 67 Ma and the subsequent increase cannot be explained as dissolution artifacts.

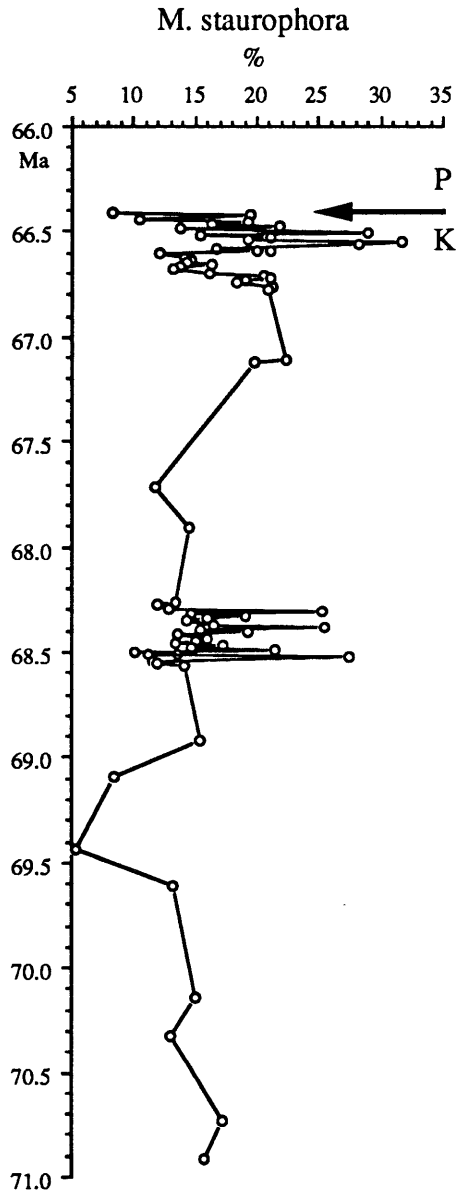


Figure 34: Relative abundance changes (%) of Micula staurophora during the late Maestrichtian in Hole 217.

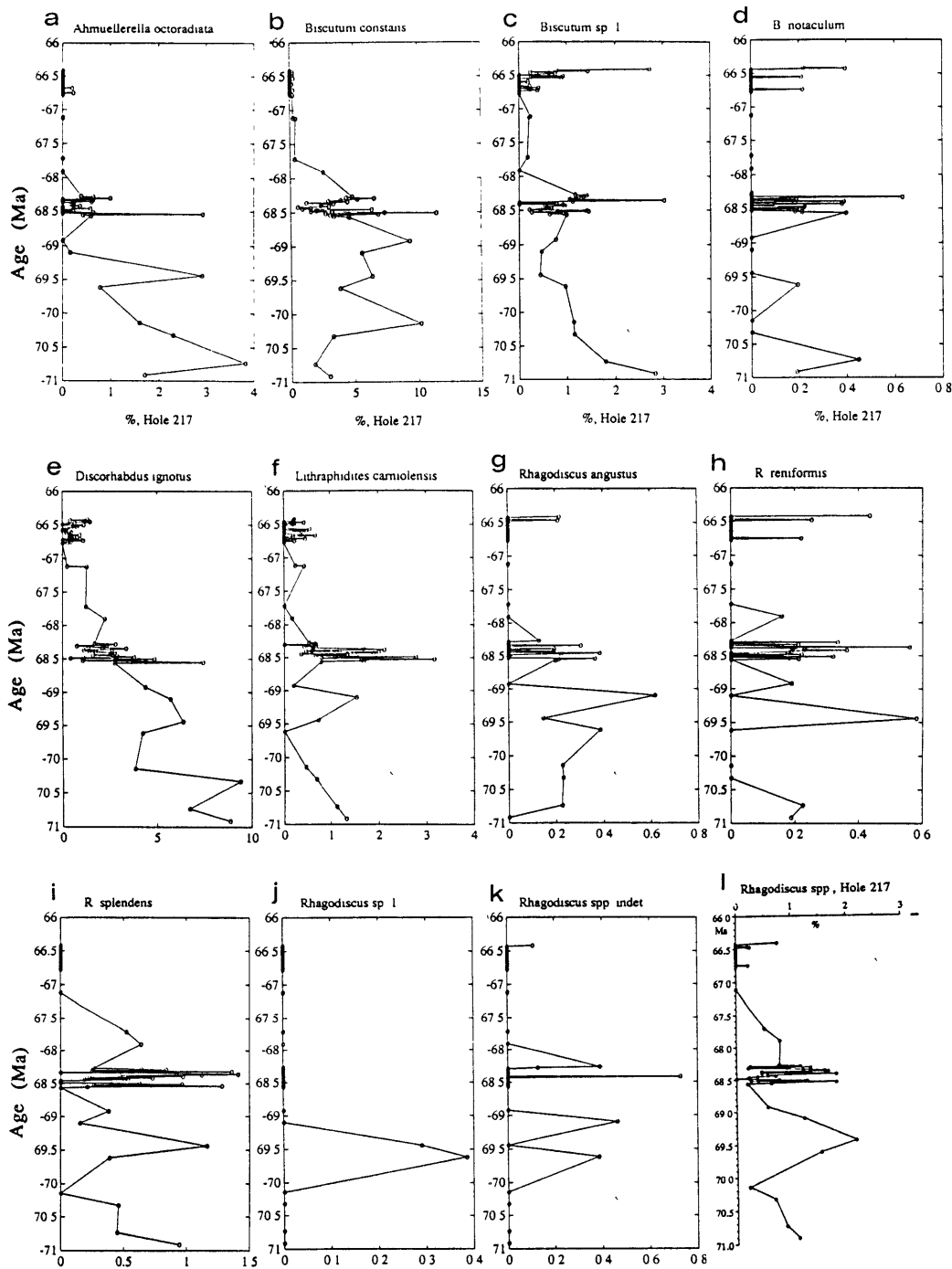


Figure 35: Relative abundance changes (%) of selected taxa during the late Maestrichtian in Hole 217. (All calculations exclusive of M. stauraphora).

abundance decreases to <1% between 455.19 and 450.49 mbsf (~68.56-68.27 Ma). It was absent from most counts above 450 mbsf (~68.27 Ma).

Biscutum constans (Figure 35b) is common to abundant (5-10%) below 455.19 mbsf (~68.56 Ma). In the interval of high sample density between 455.19 and 450.49 mbsf (~68.56-68.27 Ma) B. constans initially decreases in abundance from ~5% to <2% (between 455.19-453.30 mbsf), but then increases again to ~5% at 451.08 mbsf. It decreases again and is very rare (<1%) above 444.8 mbsf (~67.9 Ma).

Biscutum sp. 1 (Figure 35c) decreases in abundance from almost 3% to <1% throughout the lower half of the section (492.32 to 455.19 mbsf; ~70.9-68.56 Ma); similar to B. constans it increases in abundance between 453.9 and 450.49 mbsf (~68.48-68.27 Ma). Above 450.49 mbsf (68.27 Ma) it is present in very low abundance (<<1%). In contrast to B. constans, however, Biscutum sp. 1 increases in abundance again immediately below the K/P boundary to values >1% (between 423.2 and 421.2 mbsf; ~66.54-66.41 Ma).

Biscutum notaculum is always very rare (exceeding 0.5% only in one sample; Figure 35d). Below 451.30 mbsf (~68.3 Ma) it was recorded in almost each sample whereas above this level this species is so rare that it was recorded only in very few samples.

Discorhabdus ignotus decreases in abundance throughout the section (Figure 35e): it constitutes almost 10% of the assemblage below 480.14 mbsf (~70.14 Ma), but only around 1% above 432.4 mbsf (~67.1 Ma).

Lithraphidites carniolensis is comparatively rare (in most samples 1% and less) throughout the section (Figure 35f). Below 450.49 mbsf (~68.27 Ma) its abundance fluctuates considerably: peak abundances of >1% were recorded in several samples and >3% in one sample at 454.59 mbsf. Above 450.49 mbsf (~68.27 Ma) this species is always very rare (<1%).

Several species of Rhagodiscus were recorded. Although rare (individual species almost always <1%, Figures 35, g-k), all species displayed similar abundance patterns: they are more abundant and were more consistently recorded below 441.8 mbsf (~67.72 Ma); above 441.8 mbsf all species are very rare. This trend is especially obvious when the sum of all species of Rhagodiscus is considered (Figure 35l).

In the lowermost part of the section (between 492.32 and 480.14 mbsf; ~70.9-70.14 Ma) Ceratolithoides sp. cf. C. aculeus is rare (>2%); between 480.14 and 471.82 mbsf (~70.14-69.61) it increases abruptly in abundance from <2% to

~5% (Figure 36a), remains between 3% and 5% up to 432.22 mbsf (~67.1 Ma), decreases precipitously in abundance between 432.22 and 426.9 mbsf (~67.1-66.77 Ma) and is absent or very rare (<<1%) above 426.9 mbsf. Considerable inter-sample variability was recorded in the interval of very closely spaced samples between 455.19 and 450.49 mbsf (~68.56-68.27 Ma).

b) Taxa increasing in relative abundance

Below ~460 mbsf (~68.9 Ma) C. gallicus is recorded only in one sample (Figure 36f). In the closely sampled interval (455.19 - 450.49 mbsf; 68.56 to 68.27 Ma) this species increases in abundance from ~0.5% to ~1% and maintains this abundance throughout the remainder of the section. An exceptionally high abundance of almost 3% is recorded at 422.6 mbsf (~66.5 Ma). This is >1% higher than the abundances in either of its adjacent samples which are comparatively high (>~1.5%; Figure 36f). I suspected that the outlier value of 3% resulted from enrichment through dissolution. Cylindralithus gallicus is not included in the dissolution ranking of Thierstein (1980), but a structurally very similar form, Cylindralithus serratus is ranked as very slightly solution resistant. Cylindralithus gallicus consists of more massive elements than C. serratus and I assume that it is more solution resistant. In the same sample where C. gallicus is unusually abundant, higher abundance values of the two most dissolution resistant taxa in this assemblage, M. staurophora (29%, vs. 14% and 16%) and W. barnesae (27%, vs. 22% and 20%) were also recorded than in the adjacent samples. Thus it appears that the relative abundance of C. gallicus at 422.6 mbsf is increased by dissolution.

The relative abundance of G. fessus is ~2% below 444.8 mbsf (~67.9 Ma; Figure 36g). Above this level abundance values increase and throughout the uppermost 5.7 m of the section (~66.77 - 66.41 Ma) they vary around 4%, fluctuating strongly. Relative abundance values exceeding 6% were recorded in two samples in the uppermost Maestrichtian, at 422.0 mbsf and at 425.49 mbsf. These elevated values are isolated within the abundance pattern of G. fessus and do not correspond to unusually high or low values in dissolution resistant taxa. Thus it appears that they cannot be explained as preservational artifacts; their paleoceanographic significance is not understood at the moment.

Lithraphidites praequadratus is very rare (<<1%) below 463.65 mbsf (69.1 Ma; Figure 36h). Between 469.06 and 463.65 mbsf (~69.44 - 69.1 Ma) its

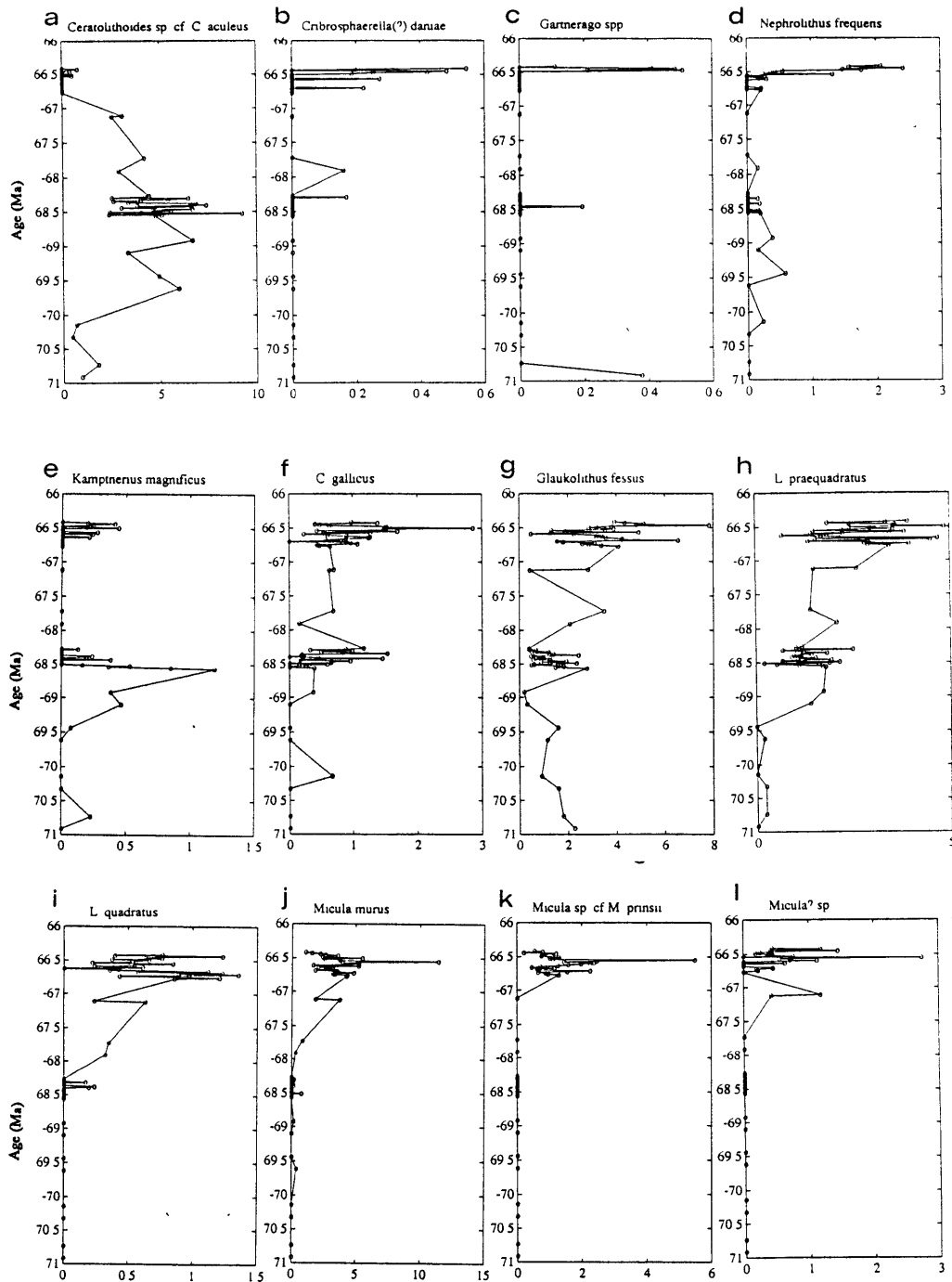


Figure 36: Relative abundance changes (%) of selected taxa during the late Maestrichtian in Hole 217. (All calculations exclusive of *M. staurophora*).

abundance increases sharply from 0 to ~1.5%, remains between ~1 and 2% up to 432.4 mbsf (~67.12 Ma), and then increases again to average values around 3% (and fairly high inter-sample variability) throughout the remainder of the Maestrichtian.

Lithraphidites quadratus was not recorded below to 452.5 mbsf (~68.39 Ma; Figure 36i). Between 452.5 and 426.9 mbsf (~68.39 - 66.73 Ma) its abundance increases steadily to values around 1%, subsequently decreases to around 0.5% between 426.9 and 424.9 mbsf (~66.73-66.65 Ma), and increases slightly below the K/P boundary (between 424.9 and 421.2 mbsf; ~66.65 - 66.41 Ma).

Below about 455.19 mbsf (~68.56 Ma) P. stoveri is fairly rare (<2%) except in the lowermost two samples where it reaches abundances >3% (Figure 37a). Above 455.19 mbsf this species increases steadily in abundance and at 444.8 mbsf (~67.9 Ma) its abundance is 4%. Throughout the remainder of the Maestrichtian P. stoveri remains at about 3-4%.

Tranolithus macleodae is rare in most samples (<0.5%, Figure 37b), but increased abundance values (1.5-2%) are recorded immediately below the K/P boundary (422.6 - 421.2 mbsf; ~66.5 - 66.41 Ma).

The relative abundance of Vagalapilla spp. is low (<0.5%) throughout most of the section; higher values (>1%) are recorded in two samples in the lowest part of the section (489.51 and 483.03 mbsf; ~70.73 - 70.32 Ma) as well as in several samples immediately below the K/P boundary (422.0, 421.6, 421.2 mbsf; ~66.46, 66.44, 66.41 Ma; Figure 37c).

Cribrosphaerella? daniae, Gartnerago spp., and N. frequens are absent or very rare in most samples, but increased in abundance in a few samples immediately below the K/P boundary (422.2 - 421.2 mbsf; ~66.48 - 66.41 Ma; Figures 36, b-d). Cribrosphaerella? daniae and Gartnerago spp. increase from virtually 0% to ~0.5%; Nephrolithus frequens is recorded in most samples in low abundances (<0.5%) and increases to ~2% below the K/P boundary.

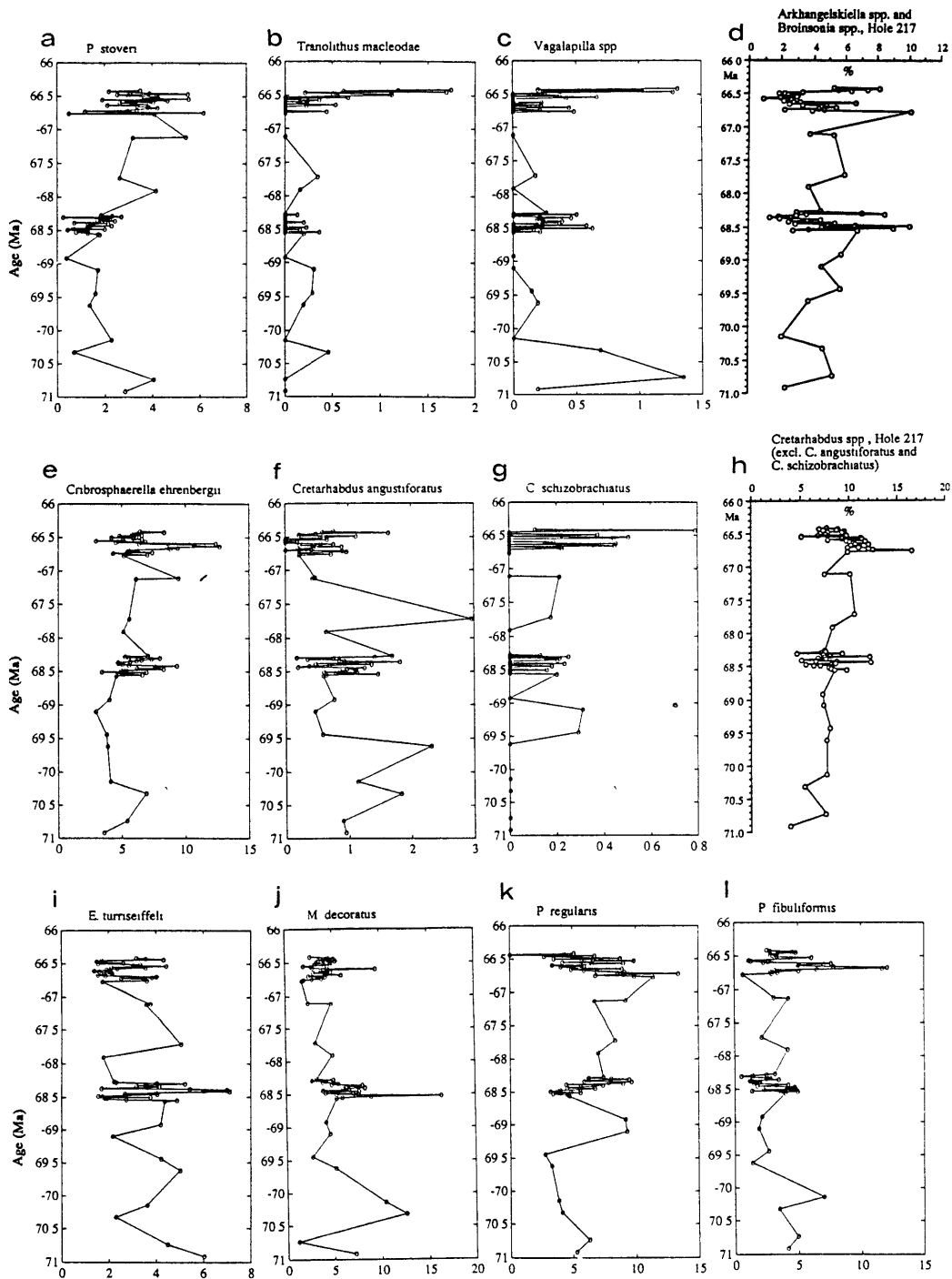


Figure 37: Relative abundance changes (%) of selected taxa during the late Maestrichtian in Hole 217. (All calculations exclusive of *M. staurophora*).

c) Other Fluctuations

Arkhangelskiella spp. and Broinsonia spp. have been grouped together because preservational differences between samples made it impossible to distinguish these taxa consistently. Below 455.19 mbsf (68.56 Ma) relative abundance values range from <2% to >6%, with steadily increasing values between 480.14 and 455.19 mbsf (~70.14 - 68.56 Ma; Figure 37d). The relative abundance fluctuates considerably (<3% to >10%) between 455.19 and 453.90 mbsf (~68.56 - 68.48 Ma), decreases to ~2% at 452.3 mbsf (68.38 Ma) and then increases slowly to ~4% at 450.49 mbsf. This gradual increase is interrupted by two very high abundance values (~8%) at 451.08 and 450.90 mbsf (~68.3 and 68.29 Ma). Between 450.49 and 432.22 mbsf abundance values vary between ~4 and 6%. One of the highest values (>10%) is recorded at 426.9 mbsf (~66.77 Ma). Between 426.7 and 424.9 mbsf (~66.76 - 66.65 Ma) relative abundances vary between ~5 and 2%; between 424.9 and 422.2 mbsf (66.65 - 66.48 Ma) they are slightly lower (~2%) and display low variability. Increased abundance (6-8%) is recorded in five samples immediately below the K/P boundary (422.0 - 421.2 mbsf; ~66.46 - 66.41 Ma).

Despite considerable variability between samples (e.g. between 455 and 452 mbsf) trends are only discernible in the intervals of high sample density. High sample density throughout the Maestrichtian would be required to determine trends in these two taxa.

Cribrosphaerella ehrenbergii is common to abundant in all samples (~>5%) below 425.49 mbsf (~66.68 Ma; Figure 37e). Between 425.49 and 424.1 mbsf its relative abundance increases to ~10%; above this interval the abundance decreases again to 5-7%.

Several species of Cretarhabdus were combined because different preservation made it impossible to distinguish them consistently (C. conicus, C. crenulatus, C. surirellus, Cretarhabdus spp. indet.). The abundance variations of Cretarhabdus angustiforatus (Figure 37f) and C. schizobrachiatus (Figure 37g) were plotted separately since the characteristic optical extinction pattern which results from the attachment of the central structure to the margin allows the unambiguous identification of these two species even when most of the central area is missing. The graph of the combined Cretarhabdus spp. (Figure 37h) shows an abundance increase throughout the section, from about 5% at 492.32 mbsf (~71Ma) to ~10% at 426.9 mbsf (~66.77 Ma). In the remainder of the section (426.9 - 421.2 mbsf; 66.77 - 66.41 Ma) the relative abundance of

this taxon decreases from ~10-13% to ~8%. An isolated abundance peak of almost 17% was recorded at 426.7 mbsf (~66.76 Ma). The relative abundance of Cretarhabdus angustiforatus never exceeds 3% and usually remains below 1%. It decreases from ~1% to values around 0.5% between 426.9 and 421.2 mbsf (66.77 -66.41 Ma). Cretarhabdus schizobrachiatus was very rare in all samples (hardly ever exceeding 0.5%; Figure 37g). It was absent from the lowest samples. Throughout its record no abundance changes were recorded.

The abundance values of E. turriseiffeli fluctuate between ~2 and 6% (Figure 37i). Below 455.19 mbsf (68.56 Ma) the sample density is insufficient to assess whether the recorded abundance fluctuations represent a genuine pattern. In the closely sampled interval between 455.19 and 450.49 mbsf (68.56 and 68.27 Ma) the abundance of this species lies mostly between ~2 and 4%. In four samples in the middle of this interval, however, elevated abundances of E. turriseiffeli (>5%) were recorded (452.89 - 452.3 mbsf; ~68.42 - 68.38 Ma; ~6% and more). No clear trend is discernible from the abundance fluctuations between 450.49 and 426.9 mbsf (68.27 and 66.77 Ma). In the uppermost 5.7 meters of the section increased abundance values were recorded in three intervals: 426.7-425.7 mbsf, 423.6-422.8, and immediately below the K/P boundary (421.6 - 421.2 mbsf; 66.76-66.70 Ma, 66.56-66.51 Ma, and ~66.44 - 66.41 Ma). In the intervening samples abundance values ~2% were recorded.

Kamptnerius magnificus was very rare in all samples (usually <0.5%) except for higher abundance values (around 1%) in two samples at 455.19 and 454.99 mbsf (~68.56 - 68.55 Ma; Figure 36e).

Microrhabdulus decoratus constitutes about 5% of the assemblage in most samples (Figure 37j). In the lower part of the section high abundance values (>10%) were recorded at 483.03 and 480.14 mbsf (~70.32 and 70.14 Ma). These high values may be indicative of a genuine increase of M. decoratus. Two other samples with comparatively high abundance values were recorded: at 454.59 mbsf this species exceed 15%, and at 424.1 mbsf (~66.60 Ma) it reaches almost 10%. These latter values are isolated outliers with background levels ~5%; the reason for their elevated abundance is not well understood; it may be related to preservation (see discussion below).

Micula murus and Micula sp. cf. M. prinsii were not recorded below 432.4 mbsf (67.12 Ma; Figure 36j); above this level they constitute between ~2-8% of the assemblage. Subtle abundance variations were recorded in the uppermost 5.7 m of the Maestrichtian where closely spaced samples were

examined (Figure 36k): relatively high abundance values (~5-6%) were recorded between 426.90 and 425.90 mbsf, followed by lower abundances (~3%) between 425.70 and 424.70 mbsf. Subsequently abundances rise again to ~6-8% between 424.50 and 423.40 mbsf. From there they decrease to ~2% at the K/P boundary.

Parhabdolithus regularis is common in most samples, constituting between about 5-10% of the assemblages (Figure 37k). Below 463.65 mbsf (~69.1 Ma) its abundance lies around 5%, fluctuating only slightly. At 463.65 and at 460.82 mbsf (~69.1 - 68.92 Ma) it increases in abundance to ~10% in two samples, but returns to ~5% at 455.19 mbsf (~68.56 Ma). Between 455.19 and 426.1 mbsf (~68.56 - 66.72 Ma) its abundance increases steadily from ~5% to a maximum values of >13%. Above this peak abundance values decrease again to <5% at the K/P boundary. A very similar pattern was recorded for P. cretacea (see below).

Placozygus fibuliformis constitutes around 3% of the assemblage (Figure 37l). However, increased values (>10%) were recorded at some levels in the uppermost Maestrichtian (425.49 and 425.30 mbsf; ~ 66.68 - 66.67 Ma). Above these maximum values its relative abundance decreases again to values around 3%.

Prediscosphaera cretacea is one of the most abundant taxa, constituting on average ~15% of the assemblage (Figure 38a). An abundance increase from <10% to ~20% was recorded between 455.19 and 426.9 mbsf (~68.56 - 66.77 Ma), followed by a decrease to ~12% between 426.9 mbsf and the K/P boundary.

Relative abundance values of P. spinosa never exceed 5%, and lie around 2% in most samples (Figure 38b). Between 455.19 and 450.49 mbsf (~68.56 - 68.27 Ma) an abundance increase from ~1% to ~2% was recorded.

Watznaueria barnesae is one of the most abundant taxa with relative abundance values between ~10-30% throughout most of the Maestrichtian (Figure 38c). In the lowest samples (492.32 - 480.14 mbsf; ~70.91 - 70.14 Ma) the relative abundance was conspicuously lower (~10%) than above where the abundance fluctuates around 20%. Very high percentages of this species (>25 to almost 30%) were recorded in several samples (at 454.30, 453.99, 453.90, 452.30, 424.10, and 423.80 mbsf). As W. barnesae is a very dissolution resistant taxon (Roth and Bowdler, 1981; Thierstein, 1980), these high values could be due to increased dissolution rather than reflect a primary signal (see discussion below).

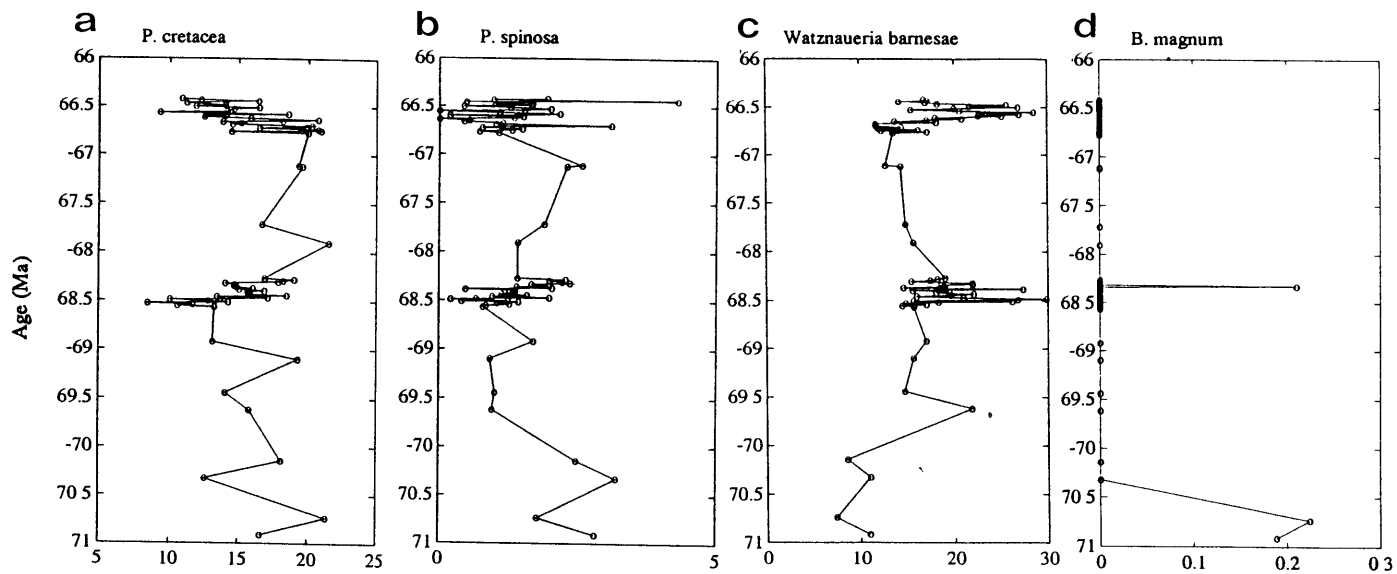


Figure 38: Relative abundance changes (%) of selected taxa during the late Maestrichtian in Hole 217. (All calculations exclusive of *M. staurophora*).

Biscutum magnum, a species very common in the lower Maestrichtian in high latitudes was observed in three samples in very low abundance (492.32, 489.51, and 451.49 mbsf; ~70.92, ~70.73, and ~68.33 Ma; Figure 38d).

B) Assessment of Preservation

Several dissolution resistant taxa were compared, and only a trend that is apparent in all these taxa should be considered indicative of dissolution. Micula staurophora, W. barnesae, Arkhangelskiella spp. and Broinsonia spp. were selected as representatives of the dissolution resistant taxa (following Thierstein, 1980). Combined in the group of dissolution susceptible taxa were C. ehrenbergii, E. turriseiffeli, P. regularis, Placozygus sp., P. bussonii, P. sigmoides, P. spinosa, and Vagalapilla spp. (following Thierstein, 1980).

No evidence indicative of increased dissolution was observed in the intervals of increased sample spacing (Figure 39). Especially the decrease in species richness between about 68.5 and 66.8 Ma cannot be explained as a consequence of increasing dissolution (compare e.g. the record of the dissolution susceptible taxa, which increase during the same interval: Figure 39g). Unusually high or low values of selected taxa (or groups of taxa) occurred in single samples, but lack of corresponding excursions in other taxa indicated that preservation could not be the explanation in these cases.

Graphs of the interval between ~66.80-66.40 Ma are presented in Figure 40. The species richness increased from values around 30 taxa per sample during the earlier part of this interval to values around 40 during the last 150 ky of the Maestrichtian (Figure 40a). Similarly, increased abundances during the later part of this interval were observed in the distribution of the absolute as well as the relative abundances of M. staurophora (Figure 40c, d), and also in the relative abundances of W. barnesae (Figure 40e). In contrast, this pattern was not present in the plot of Arkhangelskiella spp. and Broinsonia spp.: these two genera remained at comparatively low abundances throughout most of the latest Maestrichtian and increased in abundance only at about 66.47 Ma (Figure 40f). Virtually no changes between the earlier and the later part of this interval exist in the absolute abundance of calcareous nannofossils (Figure 40b) as well as in the dissolution susceptible taxa (Figure 40g). Because of the discrepancies between the abundance patterns of different dissolution

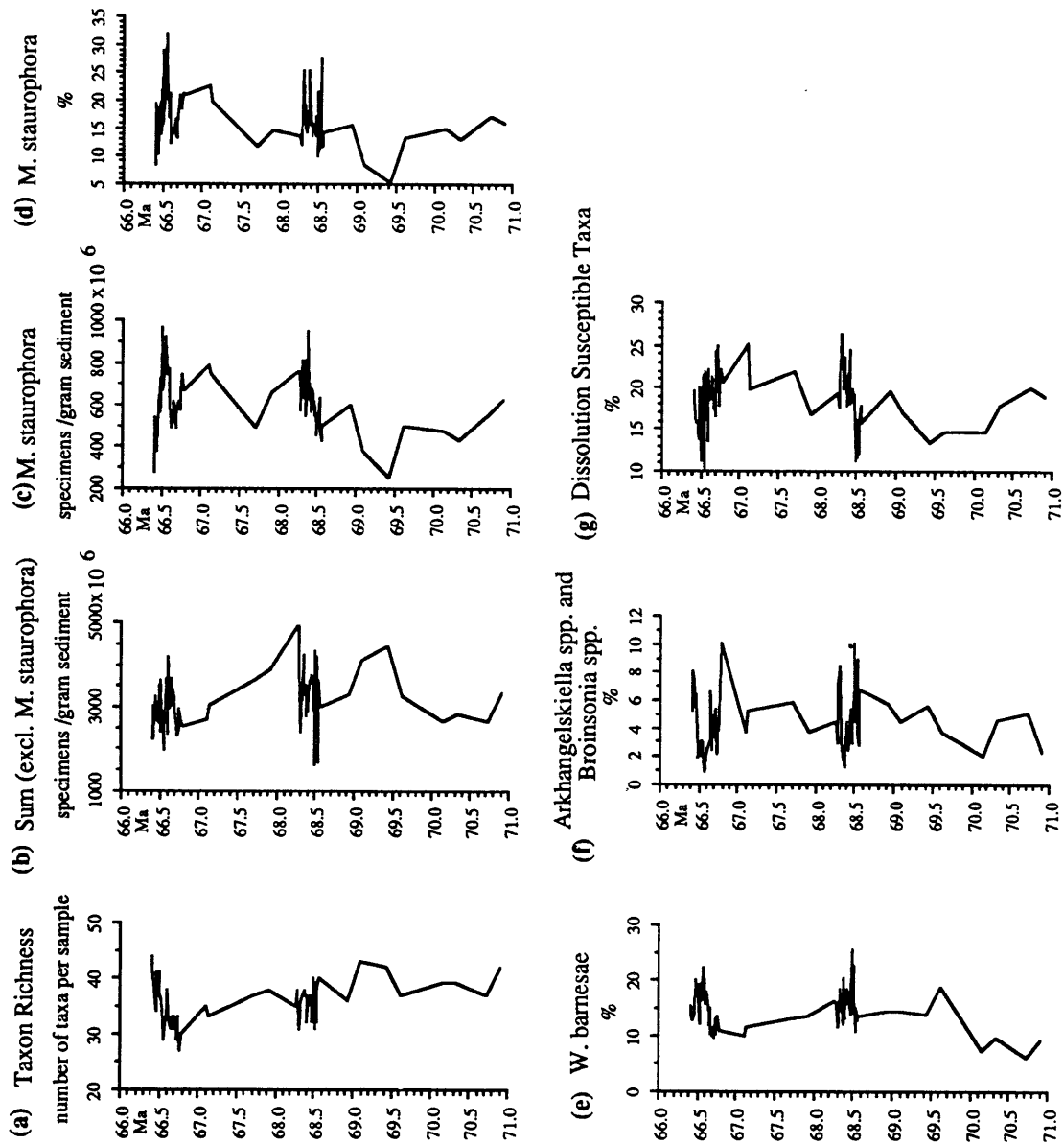


Figure 39: Parameters to assess the influence of dissolution on the nannofossil assemblages during the late Maestrichtian in Hole 217.

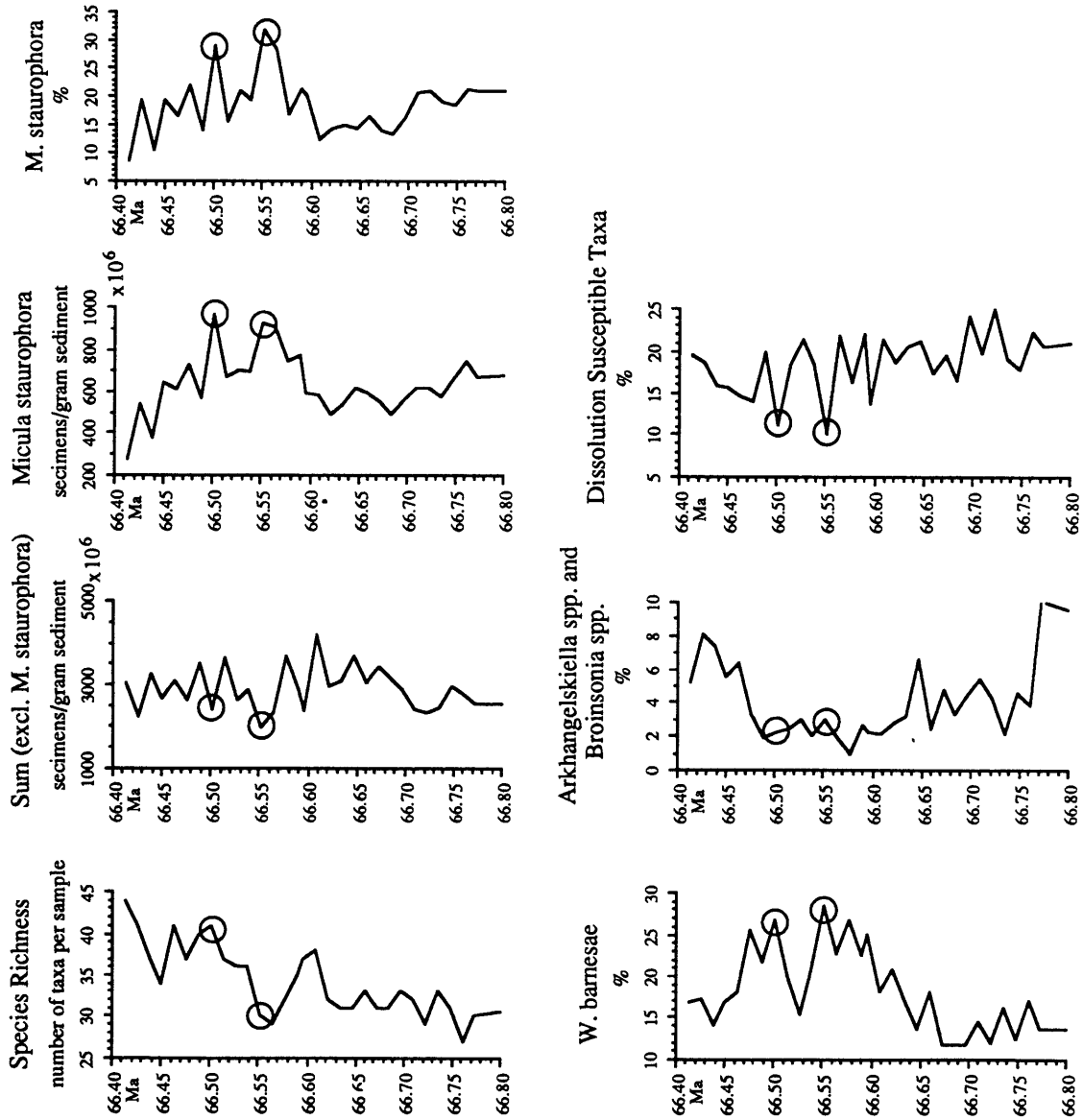


Figure 40: The same dissolution sensitive parameters as in Figure 39 plotted against age (latest Maestrichtian, Hole 217: K/P boundary at 66.40 Ma).

sensitive taxa, dissolution cannot be invoked as an explanation of the observed variations. Therefore the trends during the latest Maestrichtian are considered to be a genuine record of abundance fluctuations in the nannofossil assemblages.

However, in two instances in the uppermost Maestrichtian interval, exceptionally low abundances of dissolution susceptible taxa (Figure 40g) correspond to minimum values of absolute abundances of calcareous nannofossils (Figure 40b) and to peak values of dissolution resistant taxa (Figures 40d, e). The nannofossil distribution in these samples (marked with black circles in Figure 40) was apparently modified by above average dissolution. If this interpretation is correct, it would imply that 1) Arkhangelskiella and Broinsonia are not as dissolution resistant as previously assumed by Thierstein, 1980; and 2) it would indicate that dissolution was not sufficiently severe to eliminate certain taxa, since the species richness in these two samples appears not significantly different from the next higher and lower samples.

The other interval that was investigated at high resolution in Hole 217 was between about 68.6 and 68.2 Ma. Long term trends were only discernible in the absolute abundances of M. staurophora, which increase steadily during this interval, and an almost stepwise increase of the dissolution susceptible taxa from lower values between 10-15% prior to about 68.47 Ma to increased values (around 20%) thereafter. Due to lack of correlation with the other dissolution indicators neither of these trends is interpreted as a manifestation of changing preservation. Instead three samples were identified in this interval where the coincidence of unusually high or low values in several of the dissolution indicators suggests that increased dissolution has modified the nannofossil assemblages. These samples are marked with black circles. In none of these samples do all the dissolution indicators agree and it appears that in two of these samples the number of species was reduced.

Except for a few isolated samples where increased dissolution had altered the nannofossil assemblages, the abundance distributions of the calcareous nannofossil taxa seem to reflect genuine abundance changes

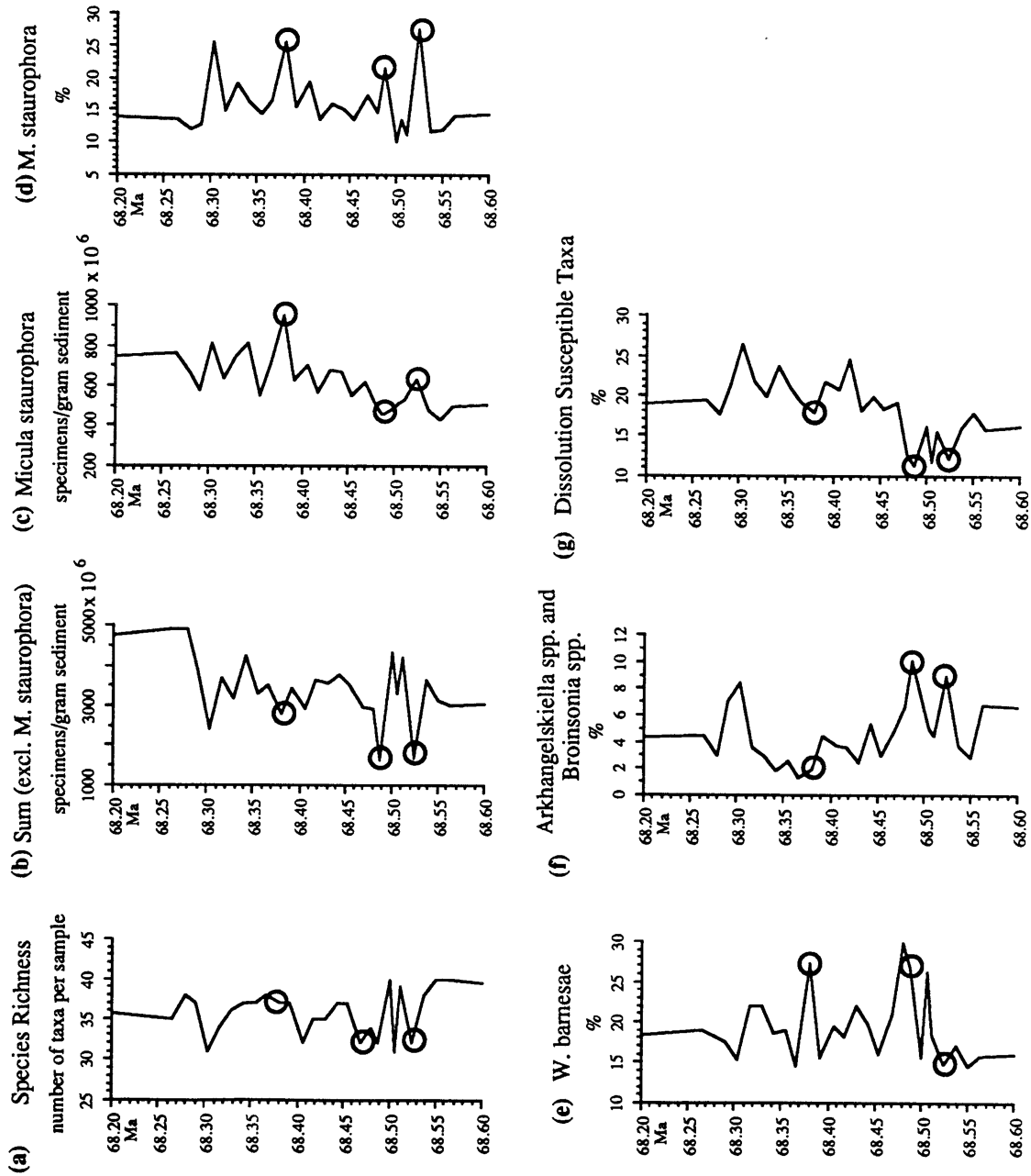


Figure 41: The same dissolution sensitive parameters as in Figure 39 plotted against age. Only the high resolution interval between 68.2 and 68.6 Ma is represented.

4) DSDP Hole 528

In DSDP Hole 528 a section 15.33 m thick, representing the last 800 ky (from about 67.2 to 66.4 Ma) of the Cretaceous was examined (Sections 528-32-1 to 528-33-4; 407.0 - 422.5 mbsf). The sediment is conspicuously coloured red and white, the thickness of each color band varies between about 20 and 50 cm (Shipboard Scientific Party, 1984: p. 390; see also Figure 42a).

Two unrelated questions were addressed in this study: 1) Are there differences in the calcareous nannofossil assemblages between different colored sediment layers? 2) Which abundance trends are discernible in calcareous nannofossil taxa during the last 800 ky of the Maestrichtian at this site?

1a) Differences Between Red and White Sediment

In the light sediment the carbonate content typically is >70% (and up to 90%) whereas in the dark red layers it is typically less than 60% (and may be as low as <50%; data from Shackleton et al., 1984, and from D'Hondt, unpublished data; Figure 42c). Herbert and D'Hondt (1991) suggested that the alternation of the sediment colors was an expression of precessional cyclicity in the latest Cretaceous. One of the goals of this study was to examine whether differences in nannofossil assemblages exist between the different colored sediment and whether they could be explained as consequences of the precessional cyclicity. Since carbonate dissolution on the seafloor can change nannofossil assemblages considerably due to the preferential removal of fragile, dissolution susceptible forms and enrichment of more robust, dissolution resistant forms it has to be established first whether dissolution of calcareous nannofossils occurred and may have overprinted original abundance variations. Several samples were taken from each color-band throughout Section 528-32-1 corresponding to sample spacing of about 5 cm (or about 3 ky).

Dissolution experiments performed on Cretaceous calcareous nannofossils by Thierstein (1980) allowed him to rank the taxa according to their dissolution resistance. Micula staurophora is by far the most dissolution resistant species in this list. It is also the most abundant taxon encountered in Hole 528 and its relative abundance was recorded with respect to all other taxa. The results from Section 528-32-1 are plotted in Figure 42e. Two intervals of

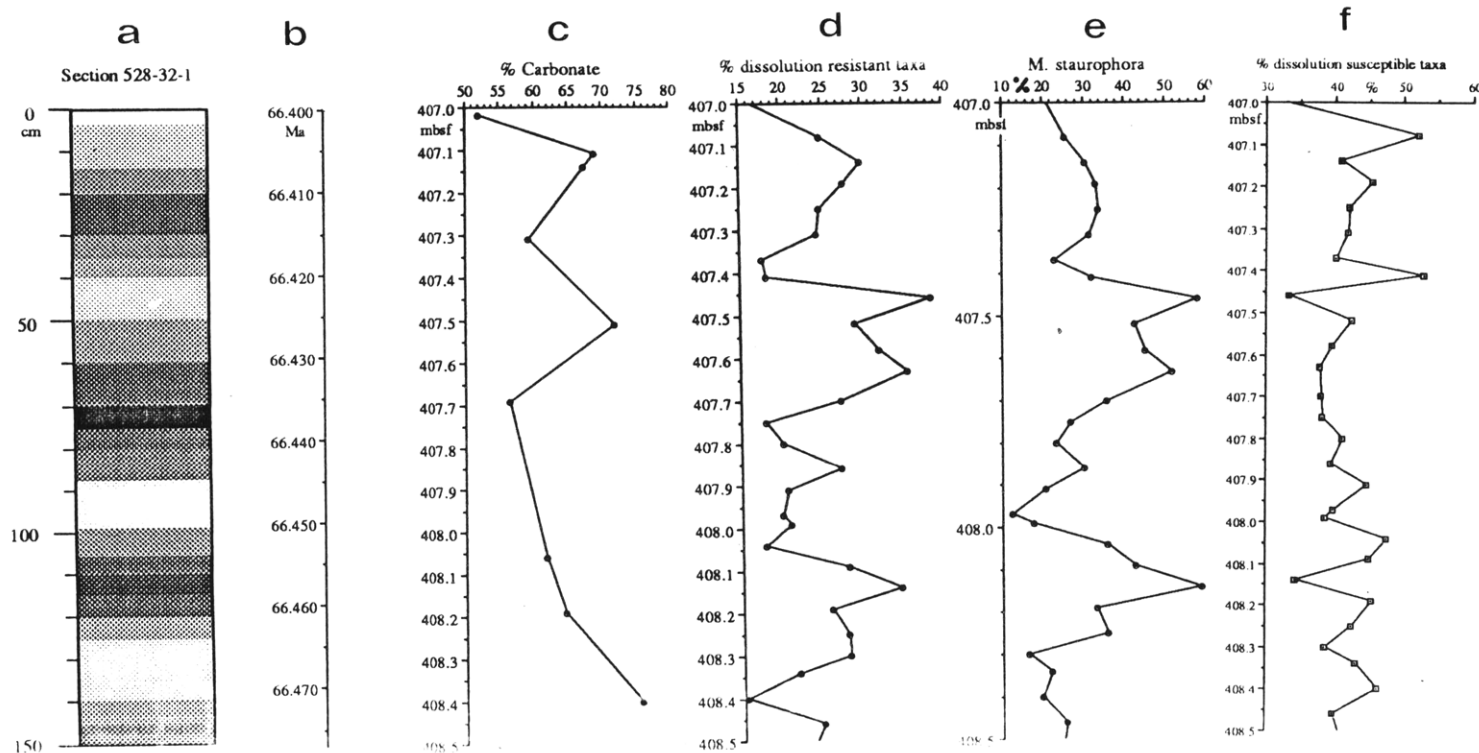


Figure 42: Sediment colors, carbonate contents, and nanofossil dissolution indicators in Section 528-32-1. The position of the Cretaceous/Paleocene (K/P) boundary lies at the very top of this section.

a) Schematic representation of sediment colors: darker shades of grey indicate deeper red sediment colors, lighter shades of grey indicate light-red, light brown or whitish-grey sediment colors. Drawing is based on colors of samples used in this study and on photograph in Shipboard Scientific Party (1984, p. 390). Scale on left hand side indicates cm level in this section.

b) Age estimates based on age model discussed in chapter "Chronology".

c) Carbonate data from Shackleton et al. (1984) and from D'Hondt (unpublished data).

d) Percentage of dissolution resistant taxa in Section 528-32-1.

e) Abundance of *M. staurophora* (%) relative to all other calcareous nanofossil taxa counted in this section. This dissolution resistant species is enriched in samples where other taxa were diagenetically removed.

f) Percentage of dissolution susceptible taxa (for further discussion see text).

maximum enrichment (>50% of all nannofossils counted) of M. staurophora are discernible: the first one peaks at about 408.15 mbsf, almost exactly coinciding with a dark red layer (Figure 42a). The other interval is really a double peak, one peak at 407.65 mbsf almost coinciding with the second dark red sediment layer in this section, the other one occurred at 407.45 mbsf in fairly light colored sediment. This later peak could be interpreted as an outlier among generally decreasing values of M. staurophora (possibly a consequence of the strong bioturbation of the sediment). A comparatively minor increase of the relative abundances of M. staurophora (from about 20% to >30%) coincides with the uppermost red layer at about 407.25 mbsf. Due to the imperfect correlation of the abundance peaks of M. staurophora with the red sediment layers abundance variations of other solution resistant and susceptible taxa were examined.

The inclusion of taxa in the dissolution resistant group was based on results of Thierstein (1980), but slightly modified: All dissolution resistant taxa of Thierstein (1980) were included as far as they were present in the material investigated, except for the persistent and the incoming taxa because they show a genuine (i.e. independent of preservation) abundance increase in the earliest Paleocene (beginning in some forms in the latest Maestrichtian). In addition, Ceratolithoides kamptneri was included, since it is closely related and morphologically similar to Tetralithus aculeus. The following taxa were included among the dissolution resistant forms:

Arkhangelskiella spp. and Broinsonia spp.

Ceratolithoides kamptneri

Cylindralithus spp. (mostly C. gallicus)

Kamptnerius magnificus

Lucianorhabdus cayeuxii

Micula spp. (except M. staurophora)

Watznaueria barnesae

The relative abundances of these taxa were calculated exclusive of M. staurophora, so that this abundant species did not influence (dampen) their percentages and the sum of their abundances were plotted against depth (Figure 42d). The same peaks are discernible as in M. staurophora, and again the abundance peaks of the solution resistant taxa are not restricted to the red sediment layers. It is noteworthy in this context that the individual abundance fluctuations of the taxa included in the dissolution resistant group (Figure 43)

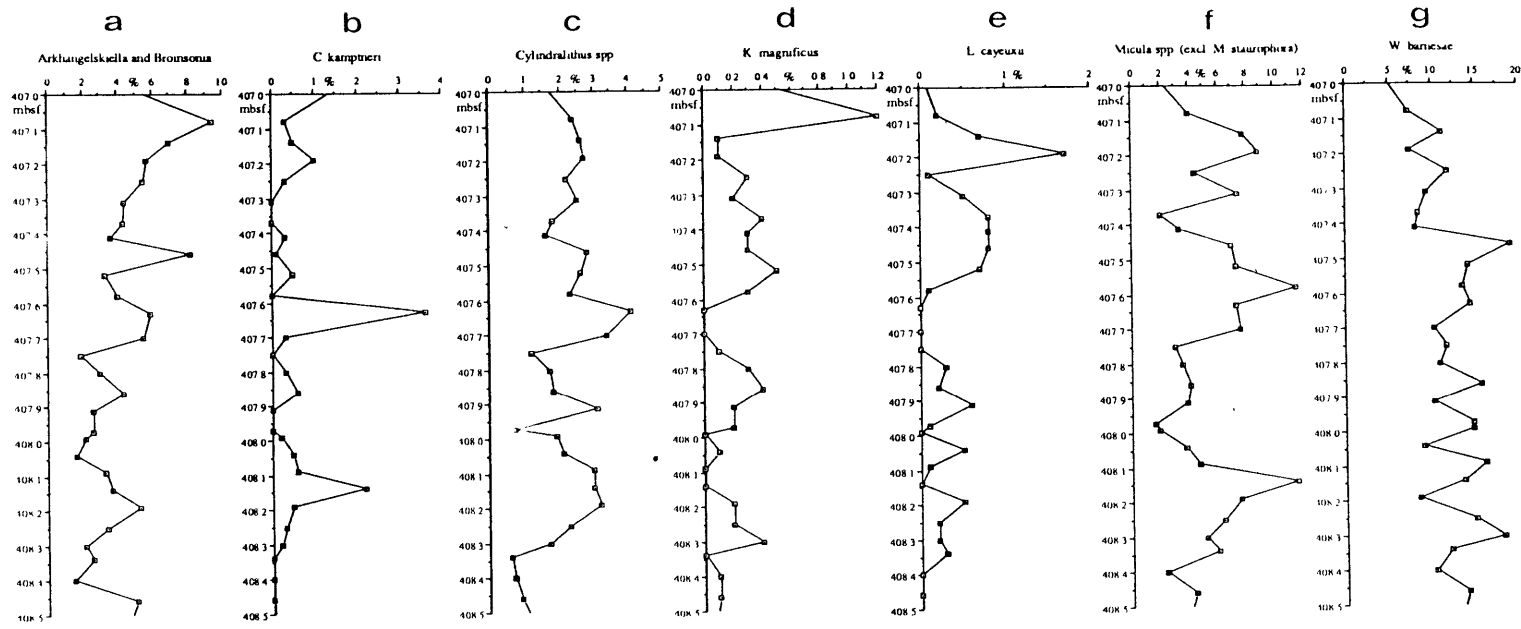


Figure 43: Individual plots of those taxa included in the dissolution resistant group.

do not all show the same peaks as their combined graph (except Micula spp., Figure 43f). This indicates that each taxon singly cannot be used as a preservational indicator, but when they are all combined their individual fluctuations (i.e. species-specific variations) are cancelled out and their common traits (i.e. dissolution resistance) become enhanced.

Particularly dissolution susceptible taxa were identified following Thierstein's (1980) dissolution ranking. Again, persistent taxa (Biscutum spp., Placozygus spp.) were omitted from the dissolution susceptible group which included:

Ahmuellerella octoradiata and Parhabdolithus regularis

Cribrosphaerella ehrenbergii

Discorhabdus ignotus

Eiffellithus turriseiffeli

Microrhabdulus decoratus

Nephrolithus frequens

Prediscosphaera creatcea

P. spinosa

Yagalpilla spp.

The abundance variations of the dissolution susceptible taxa were plotted in Figure 42f. Hardly any differences between the light and the red sediment layers are noticeable, but two minimum values of the dissolution susceptible group coincide with peak abundances of the dissolution resistant taxa (at about 407.45 and 408.15 mbsf). Apparently dissolution susceptible taxa are not very sensitive preservation indicators but only respond with anomalously low abundances in very strongly dissolved samples.

Abundance variations of the most solution resistant nannofossil taxa indicate that dissolution did affect the nannofossil assemblages. This is corroborated in at least two samples by an abundance decrease of solution susceptible taxa. The poor correlation of the abundance peaks of the solution resistant taxa with the sediment colors may either be due to problems of bioturbation, or may indicate that increased dissolution did also occur during the deposition of the white sediment layers and was not restricted to the red ones. In this case the increased clay content in the red sediment layers cannot be interpreted as residual enrichment due to the dissolution of carbonate but as a consequence of increased clay influx (due to increased wind strength?).

1b) Nannofossil Fluctuations During the Last 75 ky of the Maestrichtian

The high sample resolution during the last 7.5 m of the Maestrichtian (one sample every ~5cm, corresponding to a temporal resolution of about 3 ky) allowed the identification of very short term fluctuations in some taxa which seemed to be independent of preservational overprint. Relative abundance fluctuations are discussed in the following chapter. Some taxa show peculiar abundance variations throughout Section 528-32-1 (about 66.40 to 66.48 Ma). Placozygus fibuliformis decreased in abundance during the last 80 ky of the Maestrichtian (Figure 44a). Superimposed on this general trend are shorter fluctuations which do not coincide with the color bands (i.e. preservation). The fact that most of the peaks and troughs are defined by multiple data points and the observation that these fluctuations occur independent of preservational cycles suggest that these abundance variations are genuine. These fluctuations are particularly well developed between about 66.47 and 66.42 Ma and appear to be cyclical with a period of about 11-14 ky. This is about half of the precessional wavelength and thus may be a response to orbital forcing (D'Hondt, oral communication). This is particularly interesting since this species showed pronounced abundance variations during the latest Maestrichtian in ODP Hole 690C apparently as a response to changing water temperatures ($\delta^{18}\text{O}$) or changing nutrient levels ($\delta^{13}\text{C}$).

Prediscosphaera stoveri constituted about 5-10% of the nannofossil assemblage during the last 75 ky of the Maestrichtian (Figure 44b). Like P. fibuliformis this species shows short term, cyclical abundance fluctuations with period of ~10 ky. The values fluctuate over ~5%, which is much more than in P. fibuliformis, but they are less regularly spaced. Also the abundance fluctuations of D. ignotus (Figure 44c) resemble those of P. fibuliformis between about 66.46 and 66.40 Ma and may contain a cyclical signal of slightly less than 10ky. Since D. ignotus was quite rare throughout this interval (mostly <1.5%) it is difficult to assess the reliability of these abundance variations.

Increases in relative abundances during the last ~75 ky of the Maestrichtian were observed in Arkhangelskiella spp. and Broinsonia spp., C. ehrenbergii, Cylindralithus spp., E. parallelus, and M. murus and M. prinsii

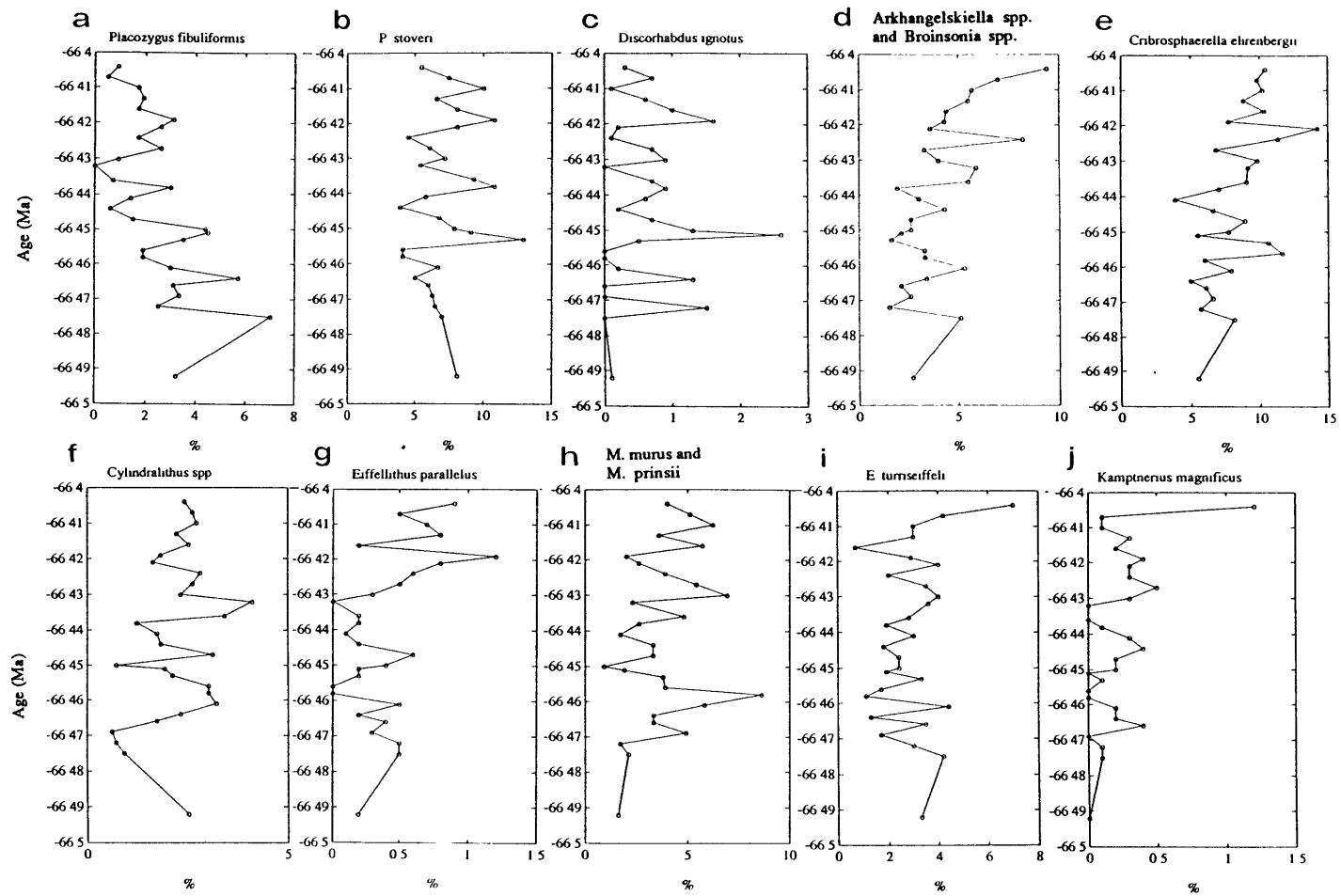


Figure 44: Fluctuations of relative abundances (%) of calcareous nannofossil taxa during the last 100 ky of the Maestrichtian in Hole 528. The Cretaceous/Paleocene boundary was drawn at 66.4 Ma (after Berggren et al., 1985).

(Figure 44d-h). Superimposed on the general abundance increase of Eiffellithus parallelus (Figure 44g) are short term variations that varied opposite to the abundance fluctuations of M. staurophora and of the dissolution resistant taxa which indicates that this species should be considered a dissolution susceptible taxon. The fact that it was not included in the dissolution susceptible group discussed above did not change the results since this species was very rare (<1%) in Section 528-32-1. Thus the abundance increases cannot be explained as preservational artifacts since dissolution susceptible (C. ehrenbergii, E. parallelus) as well as dissolution resistant (Arkhangelskiella and Broinsonia, Cylindralithus, M. murus and M. prinsii) taxa show similar patterns. Furthermore, not all dissolution resistant taxa increase in abundance during this time interval.

Eiffellithus turriseiffeli, K. magnificus and N. frequens (Figure 44i-j, 45a) displayed rather constant relative abundances during most of the last 100 ky of the Maestrichtian but all three species had increased abundance values immediately preceding the K/P boundary. Nephrolithus frequens has another peak of similar magnitude about 20 ky earlier. This common trend cannot be explained as dissolution artifact since E. turriseiffeli and N. frequens are more dissolution prone, whereas K. magnificus is rather dissolution resistant (based on Thierstein, 1980).

Generally decreasing relative abundances throughout the last ~75 ky of the Maestrichtian were observed in A. octoradiata and P. regularis, Lithastrinus spp., and P. fibuliformis (Figure 44a, 45b-c). Ahmuellerella octoradiata and P. regularis show generally lower values in samples where the solution resistant taxa were enriched, indicating that these forms are susceptible to dissolution. This observation supports Thierstein's (1980) ranking. Lithastrinus spp. is comparatively rare (<2%); its highest values were recorded in the same sample where M. staurophora had one of its abundance peaks (at about 66.46 Ma) which is interpreted here that Lithastrinus spp. are somewhat resistant to dissolution.

Creterhabdus spp., Cyclagelosphaera spp., G. fessus, and T. decorus all display increased abundances between about 66.45 and 6.43 Ma (Figure 45d-g). This time interval corresponds roughly to the interval of decreased abundances of the dissolution resistant taxa (particularly with low abundances

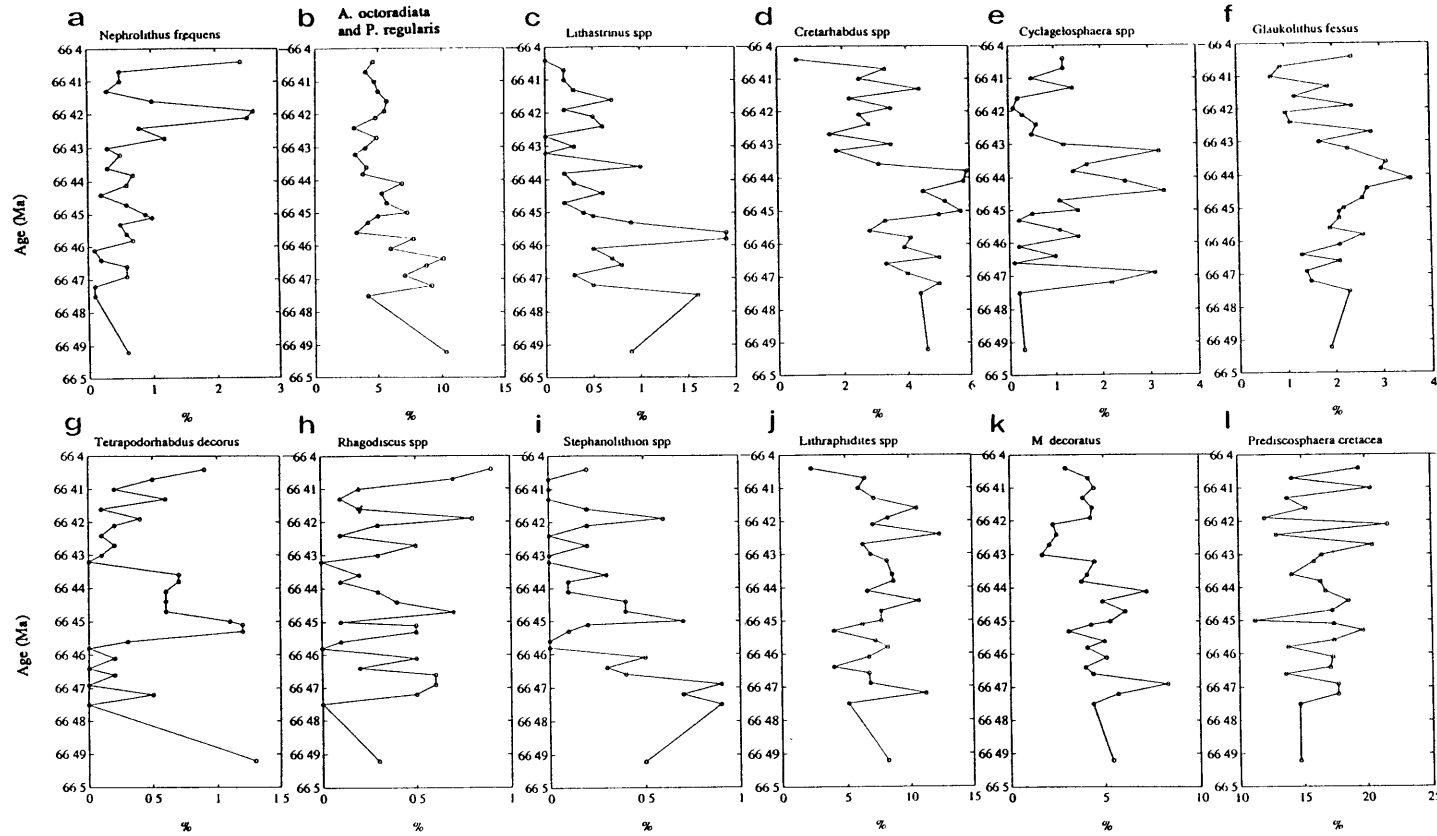


Figure 45: Fluctuations of relative abundances (%) of calcareous nannofossil taxa during the last 100 ky of the Maestrichtian in Hole 528. The Cretaceous/Paleocene boundary was drawn at 66.4 Ma (after Berggren et al., 1985).

of M. staurophora). This would indicate that these four taxa became relatively more abundant in comparatively well preserved sediment and that they should be considered as dissolution susceptible.

Rhagodiscus spp. and Stephanolithion spp. are very rare during the last 100 ky of the Maestrichtian (<1%, Figure 46h-i) but both taxa seem to be rather dissolution susceptible as they displayed especially low abundances (or were absent) in the samples from the red sediment layers.

Some of the most abundant taxa in Hole 528 did not show any conspicuous abundance trends during the last ~75 ky of the Maestrichtian. They include Lithraphidites spp., M. decoratus, P. cretacea, P. spinosa, and W. barnesae (Figure 46j-l, 47a-b). Microrhabdulus decoratus remained virtually constant with the exception of slightly lower values in the red sediment layers, which agrees with the dissolution ranking of this taxon as comparatively dissolution susceptible by Thierstein (1980). Prediscosphaera cretacea, P. spinosa, and W. barnesae displayed comparatively strong variability between adjacent samples which cannot be explained by different preservation. Except Lithraphidites spp. and W. barnesae all taxa mentioned above were included in the dissolution susceptible group discussed above. Their comparatively low variability between red and white layers is apparently the reason for the fact that the dissolution susceptible group do not vary significantly between the red and the white layers. This is in contrast to the dissolution resistant group where the combination of several taxa enhances the weak preservational signals contained in each individual taxon.

2) Nannofossil Variations Between 67.2 and 66.2 Ma

Below Section 528-32-1 samples were taken from the white intervals only since dissolution was less severe and nannofossil preservation accordingly better than in the red layers. The results described below are primarily fluctuations of relative abundances; absolute abundances were included for selected taxa when they showed abundance changes more conspicuously. Four samples were examined from the Core Catcher and from Section 7 of Core 528-31 because it was unclear whether the exact location of the K/P boundary was in 528-31-CC or whether it was between Cores 528-31 and 528-32. Ultimately the K/P boundary was placed between Cores 528-31 and 528-

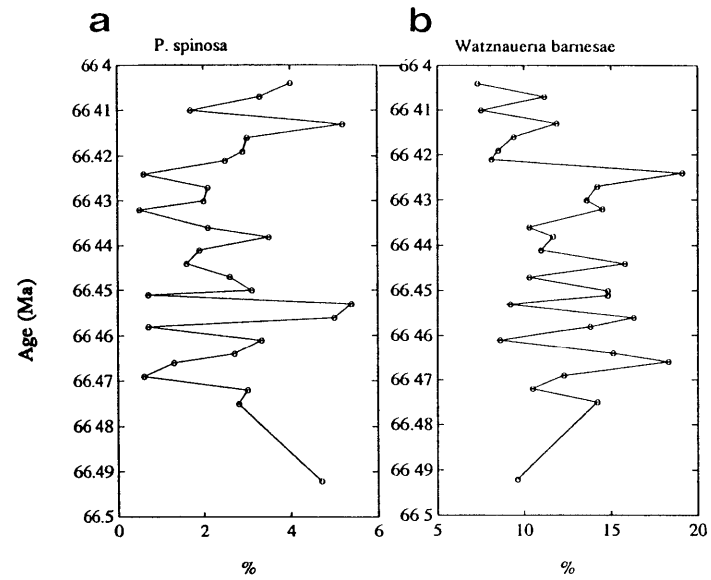


Figure 46: Fluctuations of relative abundances (%) of calcareous nannofossil taxa during the last 100 ky of the Maestrichtian in Hole 528. The Cretaceous/Paleocene boundary was drawn at 66.4 Ma (after Berggren et al., 1985).

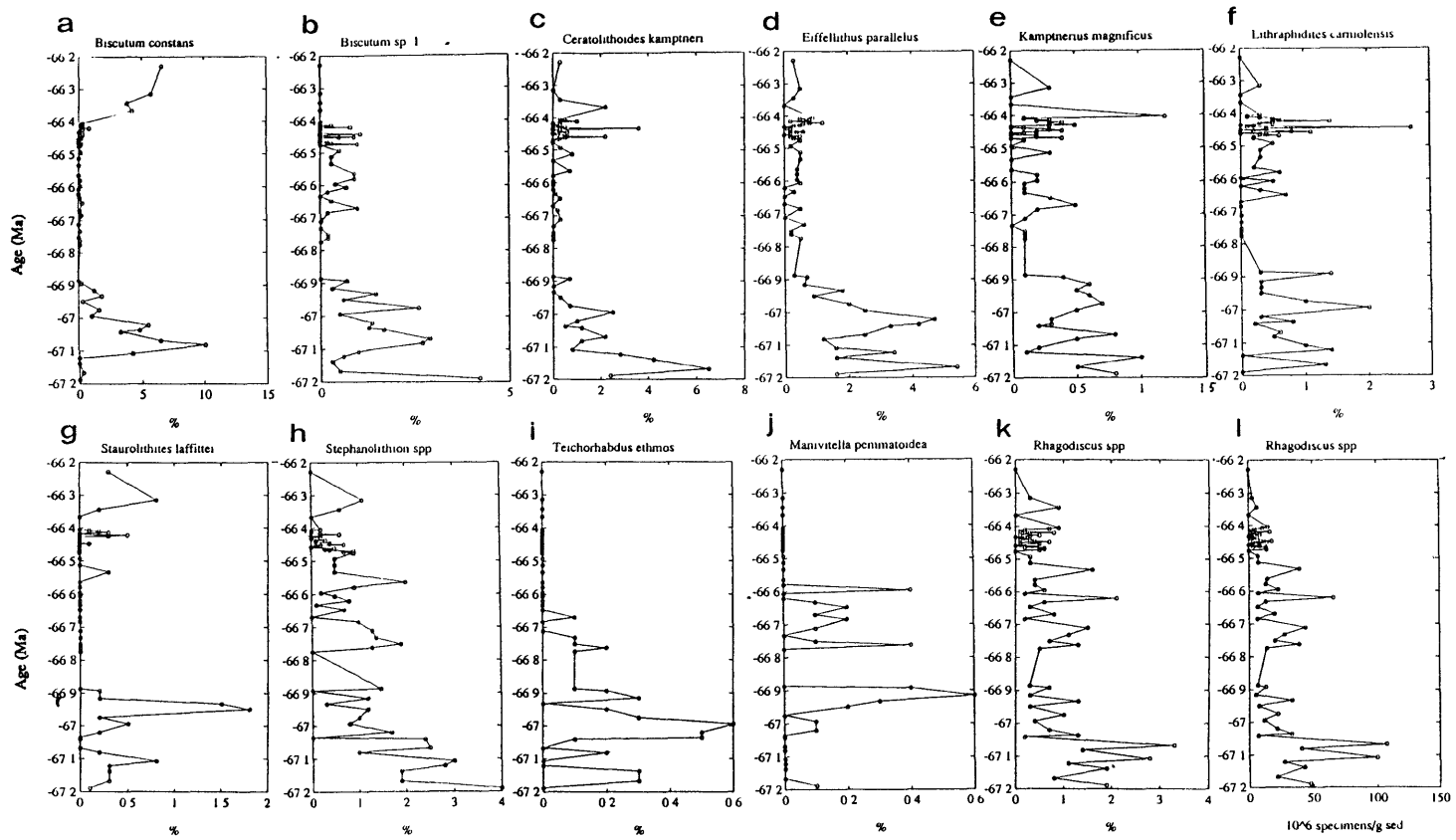


Figure 47: Fluctuations of relative abundances (%) of calcareous nannofossil taxa during the last 100 ky of the Maestrichtian. The Cretaceous/Paleocene boundary was drawn at 66.4 Ma (after Berggren et al., 1984).

32, resulting in a Paleocene age for four of the samples investigated (between 66.4 and 66.2 Ma).

The assemblage at this mid latitude site is more diverse than it was at high latitude Site 690C. On average 40 taxa per sample were encountered. This is more than in the latest Maestrichtian in Hole 690C where the number of taxa encountered per sample was only about 20.

Several taxa displayed higher abundance between about 67.2 and 66.9 Ma. Biscutum constans (Figure 47a) was very rare prior to ~67.1 Ma, then it increased very abruptly and reached peak abundances of >10% at 67.1 Ma; subsequently the abundance of this species decreased again to very low values (<1%) at about 66.9 Ma. During the remainder of the Maestrichtian B. constans was rare but its abundance increased again in the early Danian (66.4 to 66.2 Ma). Very similar is the abundance distribution of Biscutum sp. 1 (Figure 47b).

The abundance distribution of C. kamptneri resembles that of B. constans (Figure 47c) as it constituted up to >6% of the assemblage between ~67.2 and 67.1 Ma, decreased to very low values (<1%) at about 66.9 Ma and stayed very low for the remainder of the Maestrichtian. Eiffellithus parallelus displayed the same abundance variations (Figure 48d): between about 67.2 and 66.9 Ma its abundance was highest (up to >4%); it had decreased to values <1% by 66.9 Ma and remained at these low abundances for the remainder of the Maestrichtian. Kamptnerius magnificus was always rare (<1.5 %, Figure 47e) but its abundances were slightly higher prior to 66.9 Ma than thereafter. The abundance pattern of L. carniolensis was similar to that of K. magnificus with higher abundance prior to ~66.9 Ma (Figure 47f). Staurolithites laffittei was a comparatively rare component (always <2%, Figure 47g), but it was recorded in almost all samples prior to 66.9 Ma. After that its abundance became so rare that it was encountered only sporadically in the counts. Stephanolithion spp. decreased in abundance from >2% prior to about 67 Ma to values between 1-2% thereafter. Teichorhabdus ethmos was extremely rare in all samples investigated (<1%); it was recorded in most samples prior to about 66.65 Ma, but not in any younger sample. Also M. pemmatoidea is very rare (<0.6%, Figure 47j), but more frequent in the lower part of the section than in the upper part. The relative and the absolute frequencies of species of Rhagodiscus (Figure 47k, l) revealed that these species displayed an abundance peak around 67.1

Ma, whereafter they were encountered rarely (usually <1%) up to the K/P boundary.

The taxa illustrated in Figure 48 are those whose abundance decreased steadily during the last 800ky of the Maestrichtian. The trend was very conspicuous in D. ignotus (Figure 48a). In L. quadratus the plot of absolute frequency (Figure 48c) showed the decrease more clearly than the relative frequencies (Figure 48b); the same was true for N. frequens (Figure 48d, e) which was quite rare in most samples (<1%) in Hole 528.

All taxa whose abundance patterns were illustrated on Figure 49 had lower abundances in the earlier part of the section than in the later part. Whereas this trend is not very pronounced in A. octoradiata and P. regularis, it is fairly obvious in the other taxa. Cretarhabdus spp. displayed maximum values at about 66.9 Ma and declined in abundance until the K/P boundary. In G. fessus increased values were observed between ~67 and 66.6 Ma (in relative and in absolute abundances, Figure 49c, d), a decline occurred during the last 200 ky of the Maestrichtian. The patterns was slightly different in M. decoratus which reached peak values only later, at ~66.6 to 66.5 Ma; also in this species a decline occurred during the last 100 ky of the Maestrichtian. Micula murus and M. prinsii were combined due to the difficulty of consistent differentiation. Although present throughout the entire interval investigated both forms were too rare to be registered between about 67.2 and 67.05 Ma (Figure 49g). Between ~67.05 and 66.9 Ma these species increased to about 2-3% and maintain this abundance until about 66.5 Ma. Values increased to ~5% during the last 100 ky of the Maestrichtian. Tranolithus macleodae was virtually absent from the assemblages prior to about 67 Ma; thereafter it was recorded in almost all samples in strongly fluctuating abundances (between 0.1 and 3%, Figure 49h). Cylindralithus spp. (Figure 49i) also displayed lower abundances between about 67.2 and 66.9 Ma than thereafter.

The taxa on Figure 50 displayed isolated abundance peaks. Arkhangelskiella and Broinsonia displayed two abundance peaks, at ~67 Ma and at 66.7 Ma (Figure 50a, b). The relative abundances of C. ehrenbergii do not fluctuate very much (Figure 50c) but in the absolute abundances the variability is more pronounced (Figure 50d): abundance peaks are apparent at 67.1 Ma, around 66.8 Ma, and at about 66.6 Ma. Also E. trabeculatus showed increased abundances at ~67 Ma and at 66.6 Ma. Clearly enhanced relative abundances are present in Lithastrinus spp. at 67 Ma (Figure 50f). Watznaueria

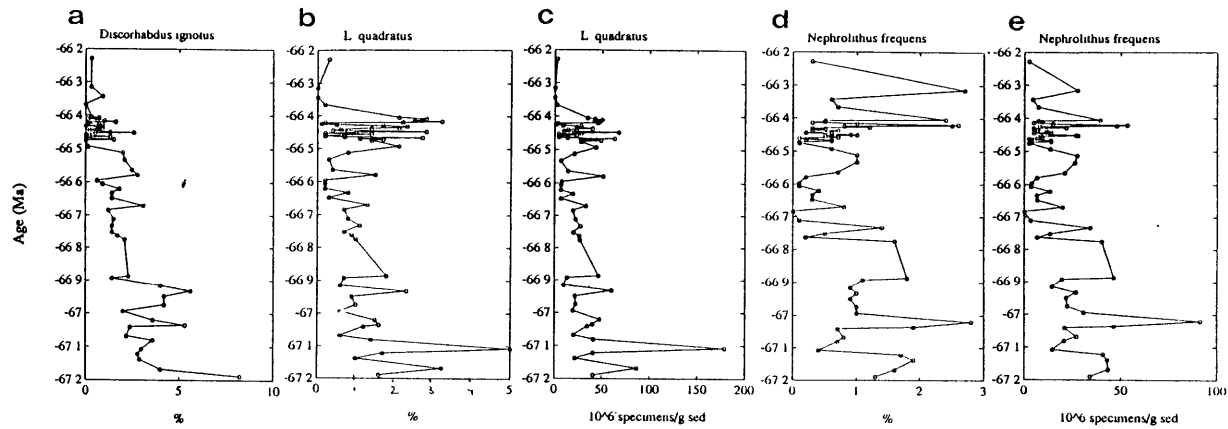


Figure 48: Abundance fluctuations of calcareous nannofossil taxa between 67.2 and 66.2 Ma in DSDP Hole 528 (Sections 528-31-7 to 528-33-4). The Cretaceous/Paleocene boundary was placed at 66.4 Ma (after Berggren et al., 1985). The abundances are either expressed as relative abundances (%) or as absolute abundances (10^6 x number of specimens per gram sediment).

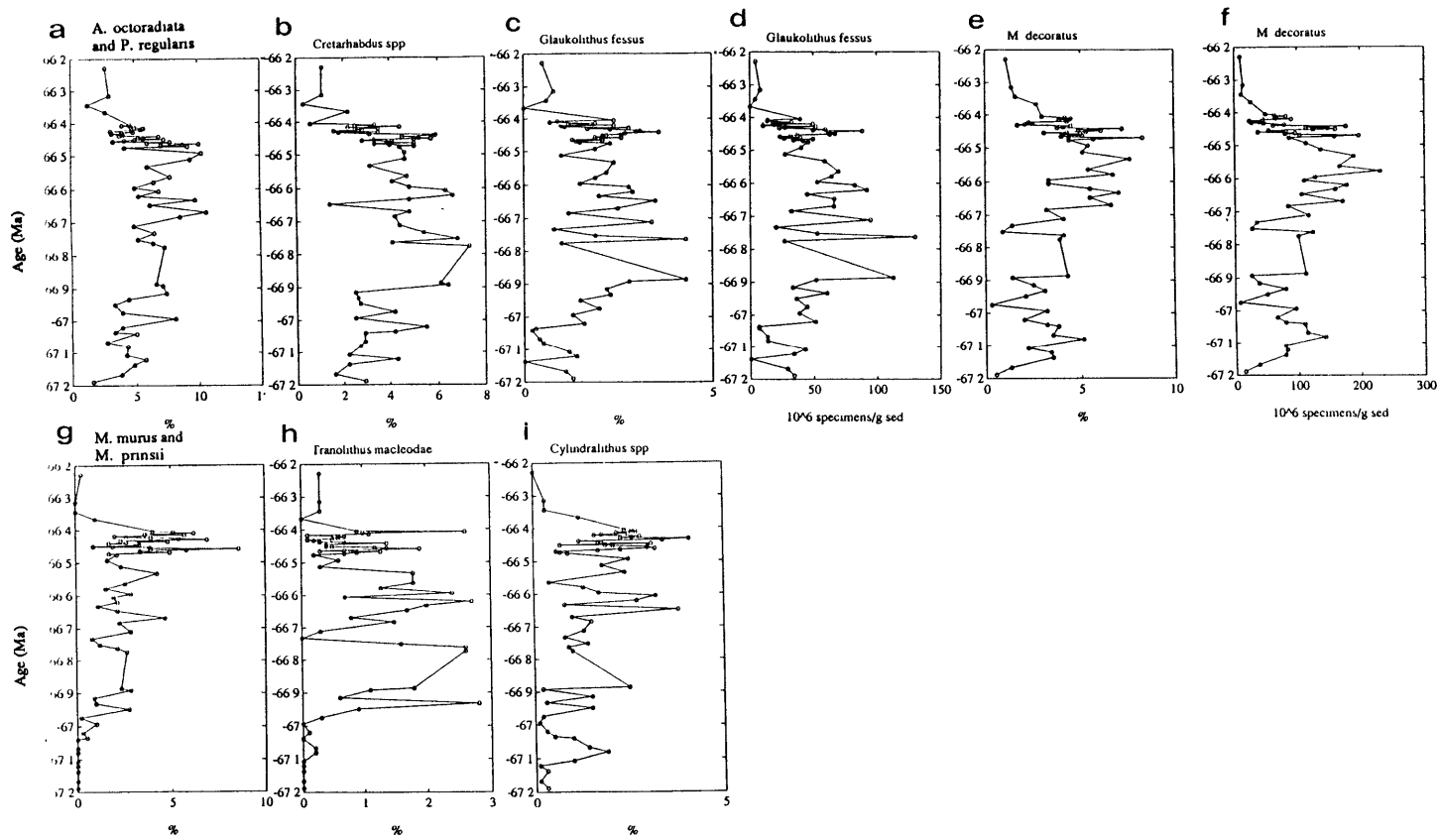


Figure 49: Abundance fluctuations of calcareous nannofossil taxa between 67.2 and 66.2 Ma in DSDP Hole 528 (Sections 528-31-7 to 528-33-4). The Cretaceous/Paleocene boundary was placed at 66.4 Ma (after Berggren et al., 1985). The abundances are either expressed as relative abundances (%) or as absolute abundances (10⁶ x number of specimens per gram sediment).

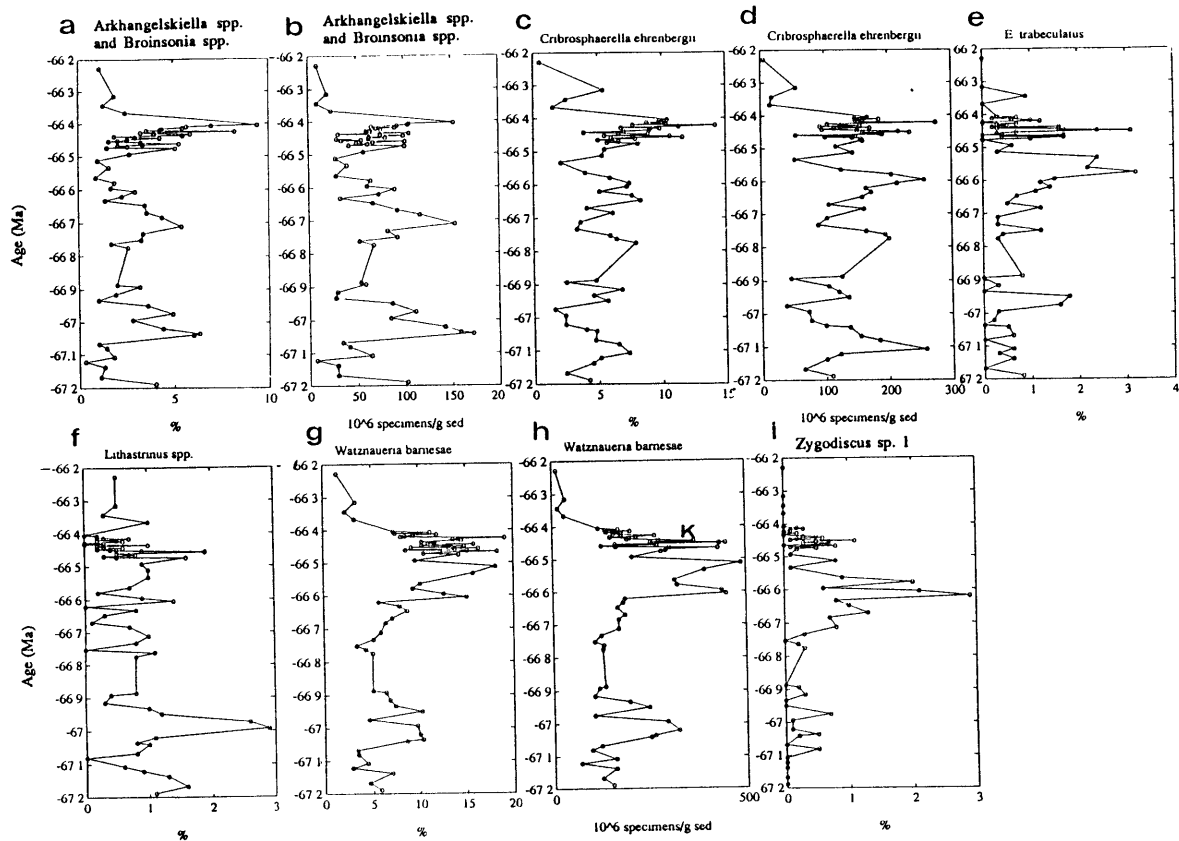


Figure 50: Abundance fluctuations of calcareous nannofossil taxa between 67.2 and 66.2 Ma in DSDP Hole 528 (Sections 528-31-7 to 528-33-4). The Cretaceous/Paleocene boundary was placed at 66.4 Ma (after Berggren et al., 1985). The abundances are either expressed as relative abundances (%) or as absolute abundances (10^6 x number of specimens per gram sediment).

barnesae was one of the most abundant species in Hole 528: abundance peaks are conspicuous at ~67 Ma and between ~66.6 and 66.5 Ma (Figure 50g, h). Zygodiscus sp. 1 showed a conspicuous abundance peak at 66.6 Ma (Figure 50i).

In the relative abundance plot of P. fibuliformis (Figure 51a) several abundance peaks were registered: 67.2, 66.9, 66.75, 66.6 and 66.5 Ma. Since a tentative cyclicity of about 11-14 ky was identified in this species in the high resolution study, these abundance peaks were possibly a consequence of aliasing (especially as their amplitude is comparable to the amplitude of the 11-14 ky cycles). In the absolute abundance plot (Figure 51b) only three (and possibly four) abundance peaks remained: at 67.2 Ma, at 66.75 Ma, and at 66.6 Ma (and possibly a minor peak around 66.5 Ma). The fact that the amplitude of the peaks at 67.2 and at 66.6 Ma is considerably higher than the amplitude of the high frequency cycles makes aliasing as the cause of these peaks unlikely (but not impossible). I conclude therefore that the abundance peaks at 67.2, at 66.75 and at 66.6 Ma are genuine features. Prediscosphaera stoveri was one of the most abundant species in Hole 528. Its abundances decreased abruptly at ~66.7 Ma to about half their previous values (Figure 51c, d). Tetrapodorhabdus decorus showed a fairly pronounced abundance peak at 66.6 Ma. Eiffelithus turriseiffeli and L. praequadratus (Figure 52h-k) displayed considerable variability in their abundance records, but on average they hardly changed during the last 800 ky of the Maestrichtian.

The persistent and the incoming taxa are plotted in Figure 52a-h. The fact that Thoracosphaera was virtually absent during the Maestrichtian, but very abundant during the Paleocene (Figure 52g) indicates that bioturbation - although very conspicuous and ubiquitous in the sediment - did not cause extensive reworking of calcareous nannofossils downsection.

Prediscosphaera cretacea did not show any conspicuous abundance excursions in the interval studied (Figure 53a, b). A steady decline was registered in the absolute abundance plot of this species during the last 100 ky of the Maestrichtian (Figure 53b). The abundance distribution of P. spinosa was similar to that of P. cretacea, but the abundance decline in this species started already 200 ky prior to the K/P boundary (Figure 53c, d). The percentage of unidentifiable calcareous nannofossils remained fairly constant throughout the section (Figure 53e). The comparatively constant relative abundances of M. staurophora between 67.2 and 66.5 Ma indicated that the preservation of calcareous nannofossils varied within fairly narrow limits.

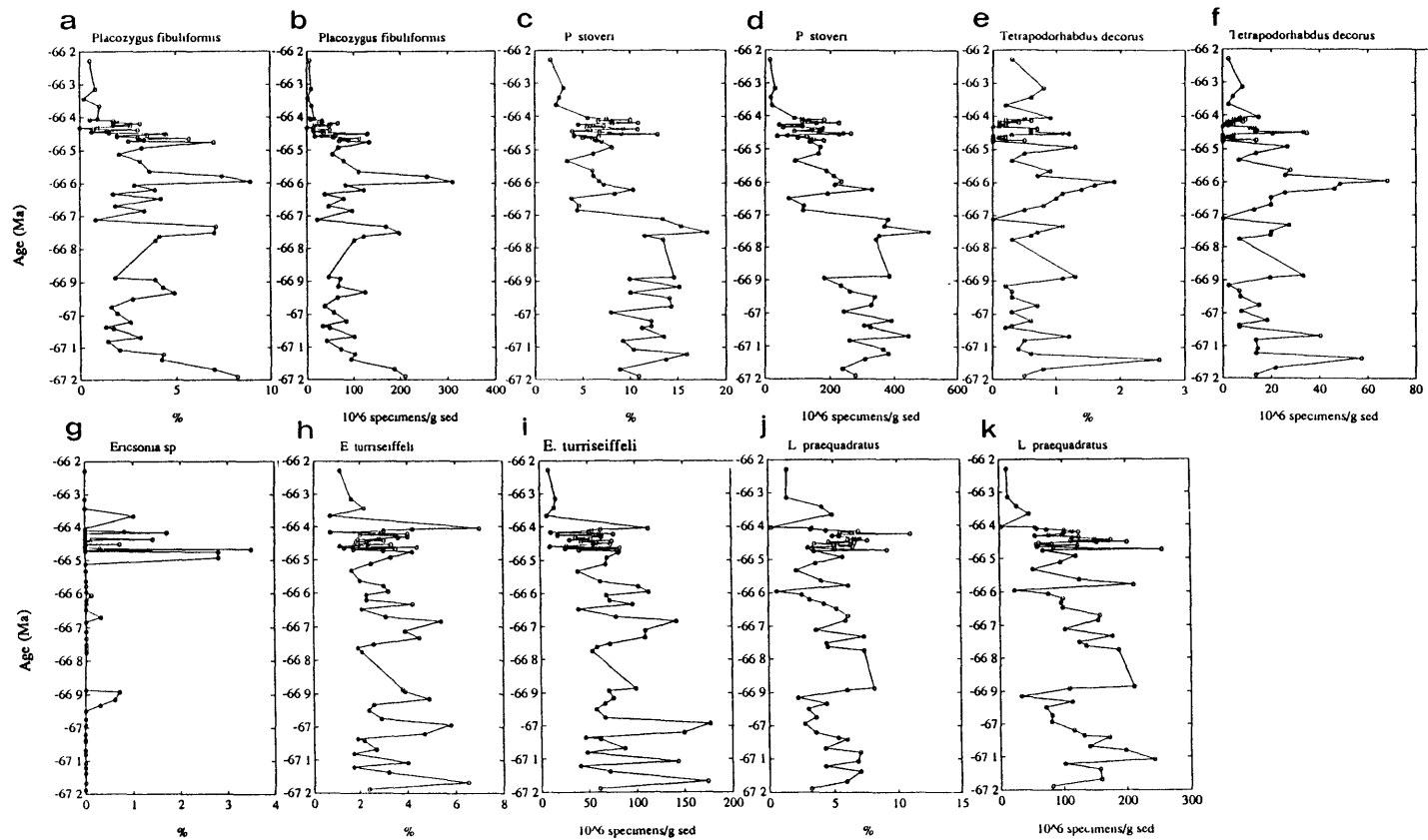


Figure 51: Abundance fluctuations of calcareous nannofossil taxa between 67.2 and 66.2 Ma in DSDP Hole 528 (Sections 528-31-7 to 528-33-4). The Cretaceous/Paleocene boundary was placed at 66.4 Ma (after Berggren et al., 1985). The abundances are either expressed as relative abundances (%) or as absolute abundances (10^6 x number of specimens per gram sediment).

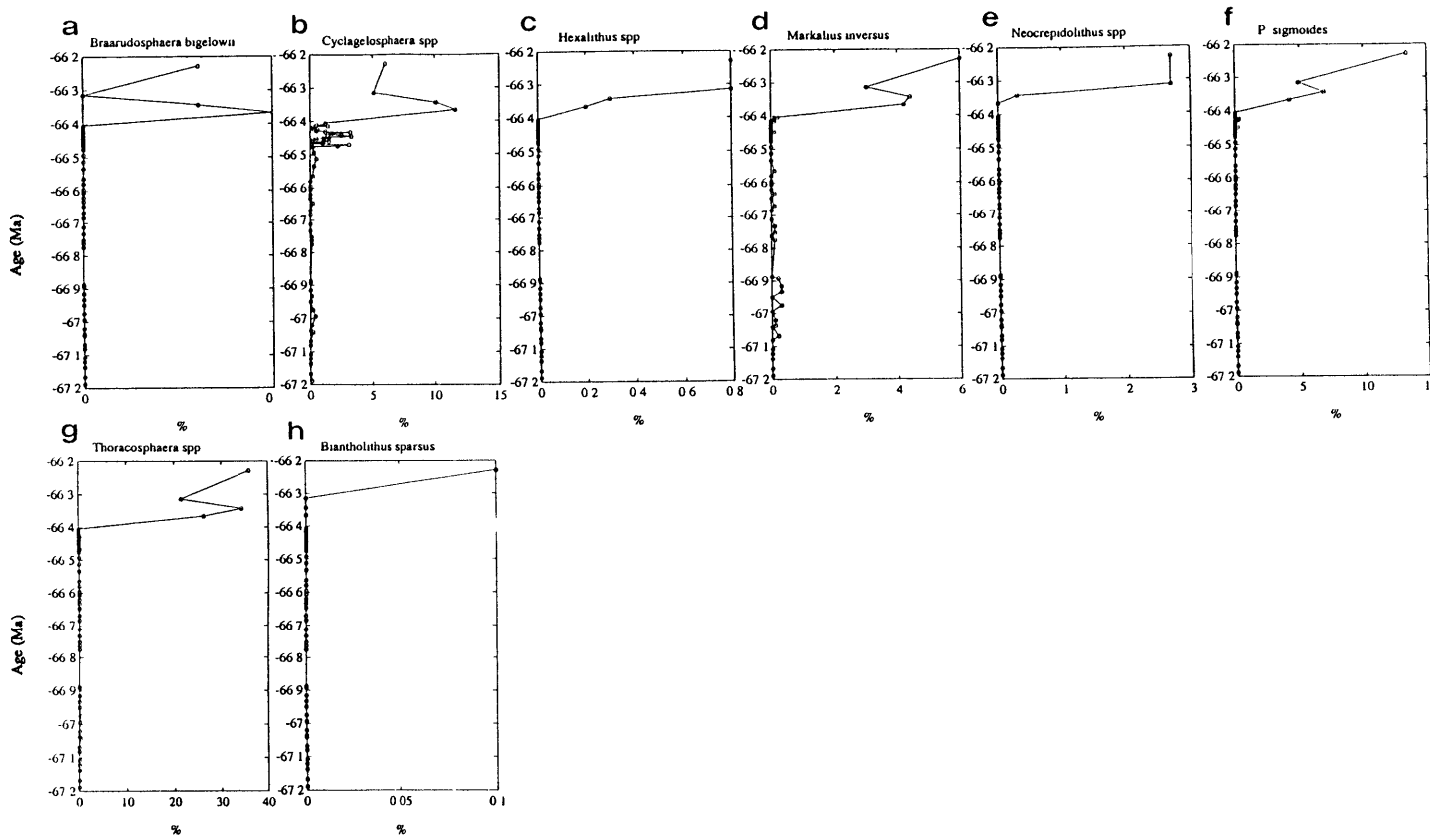


Figure 52: Abundance fluctuations of calcareous nannofossil taxa between 67.2 and 66.2 Ma in DSDP Hole 528 (Sections 528-31-7 to 528-33-4). The Cretaceous/Paleocene boundary was placed at 66.4 Ma (after Berggren et al., 1985). The abundances are either expressed as relative abundances (%) or as absolute abundances ($10^6 \times$ number of specimens per gram sediment).

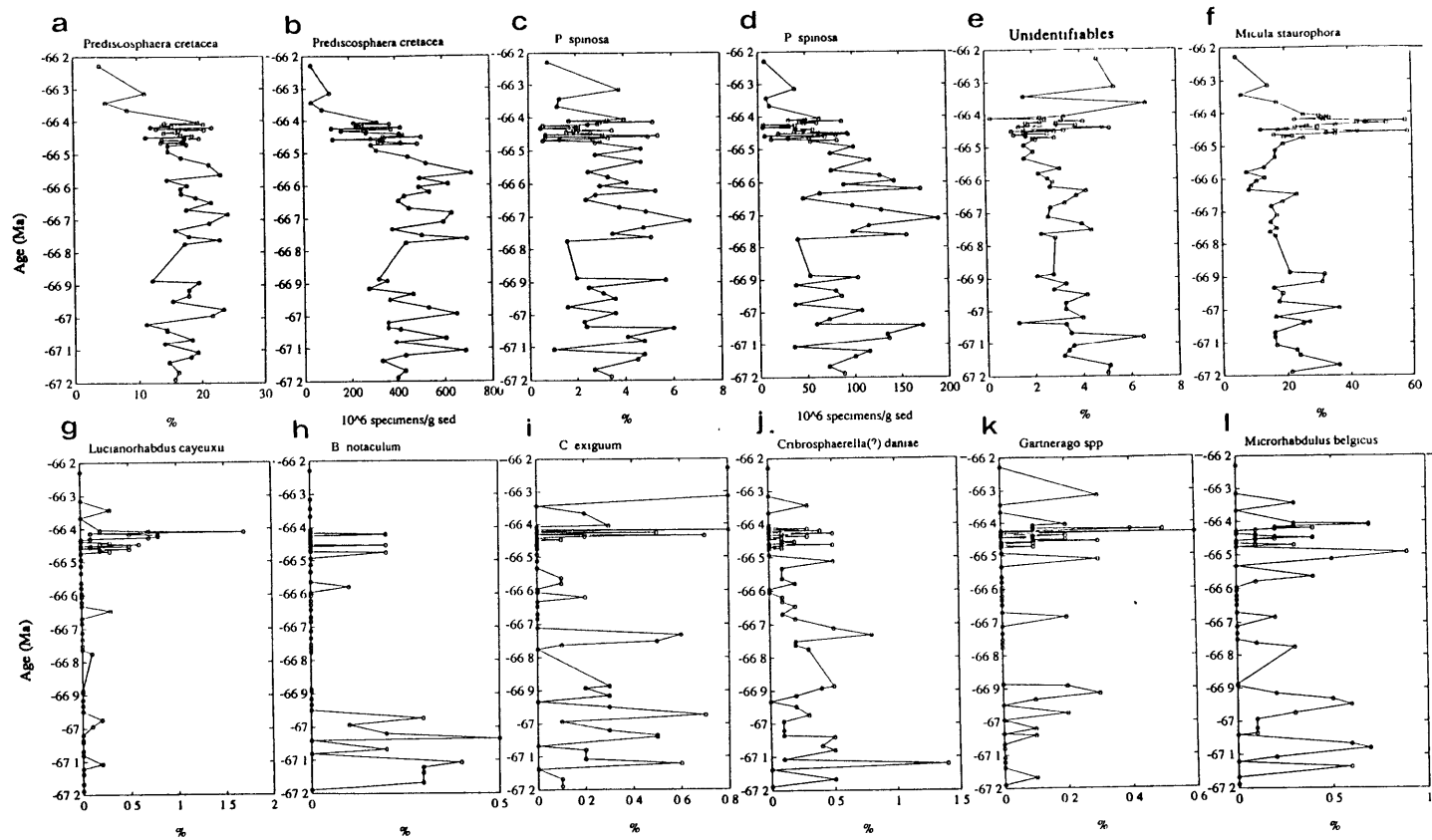


Figure 53: Abundance fluctuations of calcareous nannofossil taxa between 67.2 and 66.2 Ma in DSDP Hole 528 (Sections 528-31-7 to 528-33-4). The Cretaceous/Paleocene boundary was placed at 66.4 Ma (after Berggren et al., 1985). The abundances are either expressed as relative abundances (%) or as absolute abundances (10^6 x number of specimens per gram sediment).

5) Millers Ferry Section (Borehole 226), Alabama

The counts were performed on smear slides during an early stage of this study. The preservation between samples in this hole varies strongly with the lithology: in some of the clay rich samples it was excellent, while it was poor when the sand content was high.

Cribrosphaerella ehrenbergii (Figure 54a) increased in abundance throughout the section (from ~5% to ~20%). A high intraspecific variability was recorded in this species: elliptical, parallel sided, triangular, and round morphotypes were observed. The intraspecific variability did not change appreciably throughout the section.

Prediscosphaera stoveri (Figure 54b) decreased during the last ~250 ky of the Maestrichtian from ~15-20% to ~5%. An abundance peak of similar magnitude of this species was also recorded by Jiang and Gartner (1986) in the Brazos River Section.

The abundance of Prediscosphaera spinosa (Figure 54c) was very low prior to ~66.57 (<1%), it increased to almost 2% between ~66.57 and 66.52, and became very rare thereafter. Only in two samples at ~66.42 and ~66.4 Ma were higher values (~2%) recorded again.

The abundance pattern of C. exiguum (Figure 54d) was similar to that of P. spinosa. This species occurred more abundantly (~>2%) between ~66.57 and 66.50 Ma, and very rarely (<1%) before and after this abundance peak. A similar abundance pattern was recorded for the species of Cretarhabdus (Figure 54e): peak values occurred at ~66.55 Ma (~3%), with a gradual increase before and a gradual decrease afterwards.

Species of Thoracosphaera (Figure 54f) increased abruptly in abundance at ~66.5 Ma (from ~<2% to ~4%).

Watznaueria barnesae and M. staurophora (Figure 54g, h) were the most abundant taxa (10-30%) at this site. A gradual increase in the abundance of W. barnesae occurred between ~66.65 Ma and ~66.45 Ma. After 66.45 Ma the abundance of this species dropped abruptly from >20% to <10%. Micula staurophora did not display any gradual abundance changes during the last ~250 ky of the Maestrichtian but remained fairly constantly at ~10-15%. Isolated abundance peaks were recorded in isolated samples and are interpreted as a preservational artifact (see below).

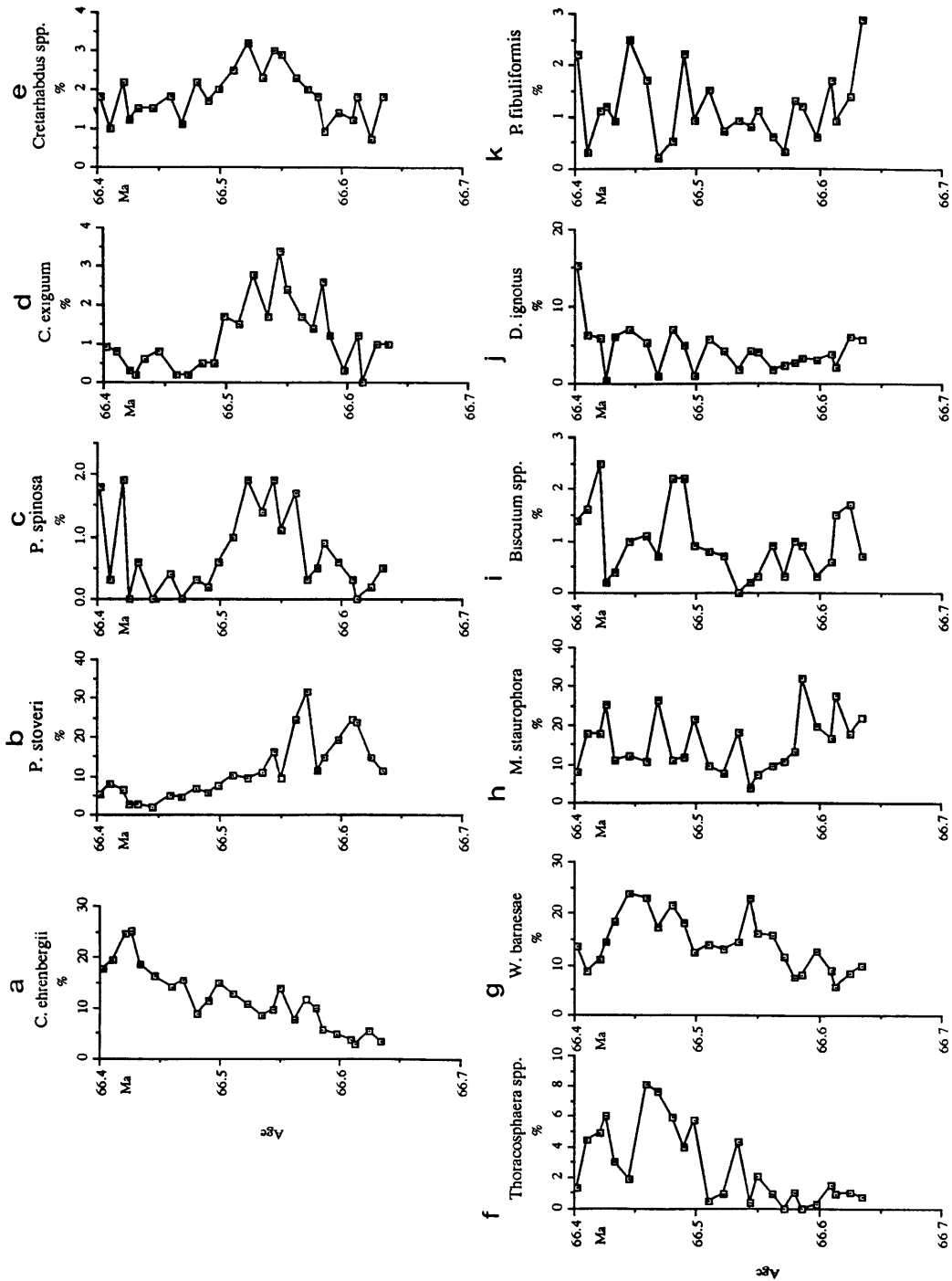


Figure 54: The relative abundance (%) of selected species recorded in the borehole from Millers Ferry are plotted against age.

The abundance of species of Biscutum (Figure 54i) remained around 1% in most samples. Only in three samples did this taxon exceed 2%.

Discorhabdus ignotus (Figure 54j) is common in the Millers Ferry Section (~5% in most samples). In some samples the abundance of this species is conspicuously lower than in the adjacent samples (almost 0%) and is interpreted as a preservational artifact. An outstanding high abundance (~15%) of D. ignotus was recorded in one sample at ~66.402 Ma.

The abundance of P. fibuliformis (Figure 54k) fluctuated between ~0.2 and 2% during the last ~250 ky of the Maestrichtian. Elevated abundance values (~2%) are concentrated between ~66.5 and ~66.45 Ma, but no conspicuous abundance peaks were recorded.

The most abundant taxa and sample preservation

The isolated abundance peaks of M. staurophora were recorded in samples where visual inspection revealed that the preservation was poor. Therefore these abundance peaks are considered to be preservational artifacts. Similarly, the isolated abundance decreases of D. ignotus were recorded in the same samples as the abundance peaks of M. staurophora and are therefore considered to be preservational artifacts as well. These patterns agree well with the solution ranking of Thierstein (1981). On the other hand, it is surprising that none of the other taxa described above show the same trends. This indicates that M. staurophora and D. ignotus are much more sensitive dissolution indicators than the other taxa.

CHAPTER 5 DISCUSSION

The abundance patterns described above can be grouped into (i) evolutionary (i.e. extinctions, originations) and (ii) biogeographic changes (migrations, increase and decrease of abundances). They are discussed below in latitudinal order, proceeding from high southern latitudes to mid- and low latitudes.

1) Maestrichtian Evolutionary and Biogeographic Events in High Latitudes

(A) Evolutionary Changes

(a) Extinctions

Biscutum boletum, B. coronum, B. dissimilis, B. magnum, Misceomarginatus spp., Monomarginatus spp., N. watkinsii, N. corystus, O. magnus, P. obscurus, P. firthii, and Reinhardtites spp., became extinct during the early and early late Maestrichtian (e.g. Pospichal and Wise, 1990; Watkins, 1992; Bralower and Siesser, 1992; this study). My data show that these twelve taxa represent about a third of all taxa present (~35-40), but constitute only ~20-25% of the assemblages. From the chronology derived for Hole 690C the extinctions occurred within a short stratigraphic interval from ~72.4 Ma to ~70.4 Ma (Figure 55). Many of these taxa were restricted to the southern hemisphere. Only B. coronum, B. dissimilis, B. magnum, Monomarginatus quaternarius, O. magnus and Reinhardtites spp. are also known from northern high latitudes (e.g. in Japan: Okada et al., 1987; in England and northern Germany: Burnett, 1990; in England: Black, 1972; in Poland: Deflandre, 1959).

(b) Originations

In high latitudes Nephrolithus frequens is the only taxon that originated during the Maestrichtian (between ~71.2 and 70.4 Ma in Hole 690C) and was one of the most abundant taxa in high latitudes (20-40%; Figure 18a; Table 6). During the late Maestrichtian this species occurred in progressively lower latitudes (Pospichal and Wise, 1990a; see also Chapter 3, Biohorizons)

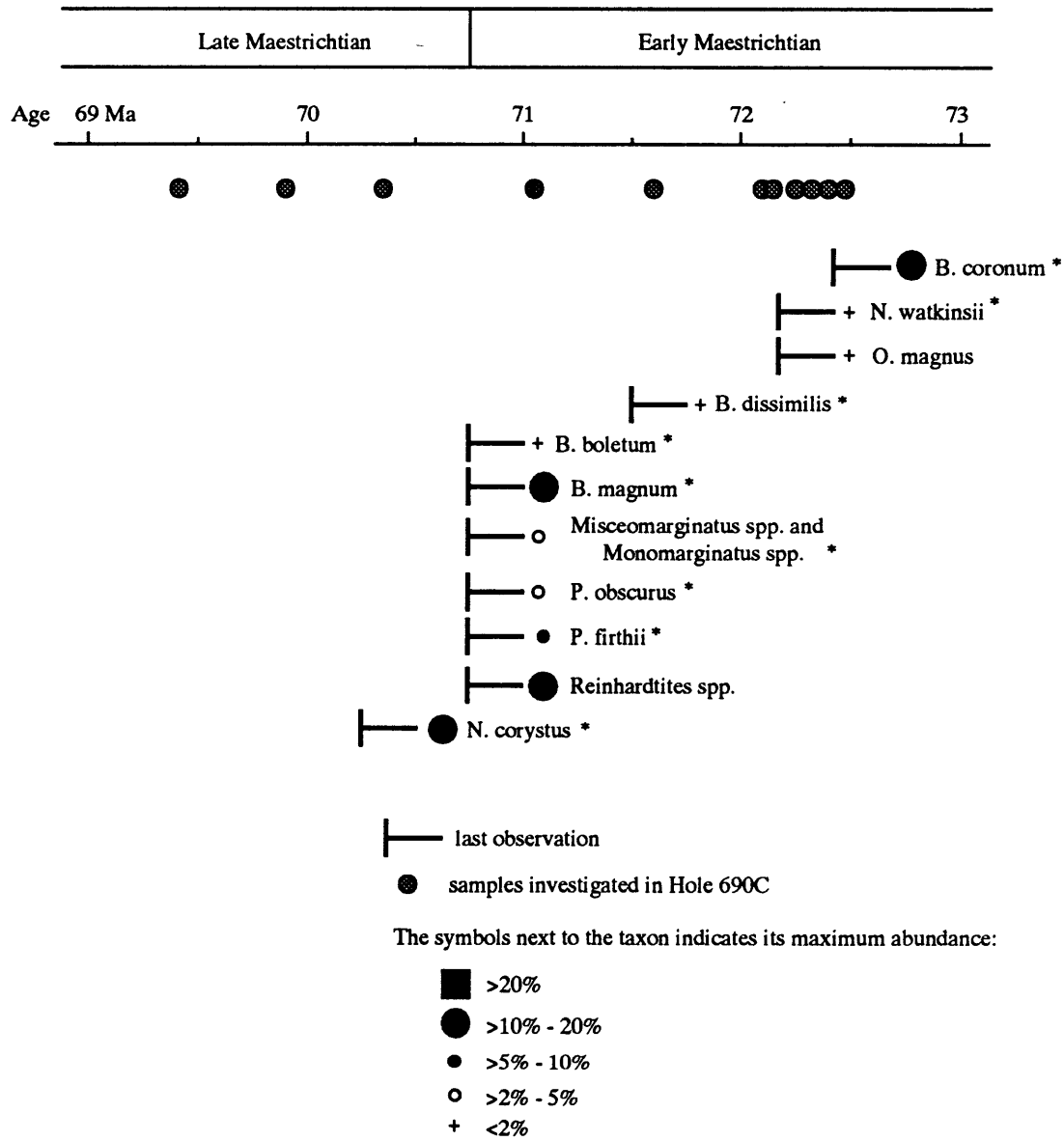


Figure 55: Sequence of extinctions around the early/late Maestrichtian boundary in high southern latitudes (ODP Hole 690C). All taxa marked with an asterisk (*) are considered to be austral taxa (see text).

	high lat.		mid (southern) latitudes			low/mid N. lat.
	690C		761B	528	217	Millers Ferry
	75-71 Ma	71 Ma K/P	761C			
<i>A. snydeni</i>	-	-	-	-	-	+
<i>A. octoradiata</i>	●	●	+	+	○	-
<i>Arkhangelskiella</i> spp. and <i>Bronsonia</i> spp.	●	●	●	●	●	●
<i>B. sparsus</i>	-	+	-	-(+)	-	-
<i>B. boletum</i>	+	-	-	-	-	-
<i>B. constans</i>	●	●	●	●	●	+
<i>B. coronum</i>	+	-	-	-	-	-
<i>B. dissimilis</i>	+	-	-	-	-	-
<i>B. magnum</i>	●	-	-	-	+	+
<i>B. notaculum</i>	■	○	+	+	+	+
<i>Biscutum</i> sp. 1	○	-	●	○	○	○
<i>Biscutum</i> sp. 2	○	-	-	-	-	-
<i>B. bigelowii</i>	-	-	-	-	-	+
<i>C. barbata</i>	+	+	+	-	-	-
<i>Ceratolithoides</i> spp.	-	-	●	●	●	+
<i>C. amphipons</i>	+	-	-	+	+	○
<i>C. garmsoni</i>	○	-	-	-	-	+
<i>Chastozygus</i> sp. 1	+	-	+	+	+	+
<i>C. exiguum</i>	-	-	+	+	-	○
<i>C. completum</i>	-	-	+	+	+	-
<i>C. angustifloratus</i>	-	-	○	○	○	-
<i>C. conicus</i>	-	+	+	+	+	○
<i>C. crenulatus</i>	-	+	+	○	○	+
<i>C. schizobrachiatus</i>	-	-	+	+	+	-
<i>C. sunrellii</i>	+	+	+	○	+	-
<i>Cretarhabdus</i> sp. 1	+	-	+	-	-	+
<i>Cretarhabdus</i> spp.	●	●	●	●	●	○
<i>C. ? daniae</i>	+	●	+	+	+	+
<i>C. ehrenbergii</i>	○	●	●	●	●	■
<i>Cruciplacolithus</i> spp.	-	+	-	+	-	-
<i>Cyclagelosphaera</i> spp.	+	+	+(■)	○	+	+
<i>C. biarcus</i>	-	-	+	-	○	-
<i>C. gallicus</i>	-	-	○	○	○	+
<i>C. serratus</i>	-	-	○	+	+	n.d.
<i>Cylindralithus</i> sp. 1	-	-	+	-	+	n.d.
<i>Cylindralithus</i> spp. indet.	-	+	-	-	+	-
<i>D. ignotus</i>	+	+	●	●	●	●
<i>E. eximius</i>	-	-	-	-	+	-
<i>E. parallelus</i>	-	-	○	●	+	+
<i>E. trabeculatus</i>	+	+	+	○	+	○
<i>E. turnseiffelii</i>	●	○	○	●	●	●
<i>Ericsonia</i> sp.	-	-	○	○	+	n.d.
<i>Gartnerago</i> spp.	○	●	+	+	+	n.d.
<i>G. fessus</i>	○	●	●	○	●	-
<i>Hornibrookina</i> spp.	-	+	-	-	-	-
<i>K. magnificus</i>	●	■	+	+	+	+
<i>Lapideacassis</i> spp.	+	-	+	-	-	-
<i>Lithastrinus</i> spp.	-	-	+	○	○	n.d.
<i>L. carniolensis</i>	+	-	+	○	●	+
<i>L. grossopectinatus</i>	-	-	+	+	+	+
<i>L. kennethii</i>	-	-	+	+	+	-
<i>L. praequadratus</i>	-	-	●	●	○	○
<i>L. quadratus</i>	-	-	○	○	+	○
<i>Lithraphidites?</i> sp. 1	-	-	+	-	+	n.d.
<i>L. cayeuxii</i>	■	●	+	+	+	+

■ >20%
 ● >10% - 20%
 ● >5% - 10%
 ○ >2% - 5%
 + <2%

Table 6: Schematic representation of the abundance of taxa recorded at different sites in this study. (n.d. - taxon not differentiated at time of counting; presence or absence cannot be confirmed)

	high lat.		mid (southern) latitudes			low/mid N. lat.
	690C		761B	528	217	Millers Ferry
	75-71 Ma	71 Ma K/P	761C			
M. pemmatoidea	-	+	○	+	+	?
M. apertus	-	-	+	+	+	n.d.
M. inversus	-	○	+	+	+	+
M. inconspicuus	-	-	-	-	-	+
M. belgicus	-	-	+	+	+	+
M. decoratus	+	+	●	●	●	●
M. praemurus	-	-	-	+	+	n.d.
M. murus	-	-	+	●	●	+
Micula sp. cf. M. prnsii	-	-	+	+	○	+
M. staurophora	+	○	■	■	■	■
Micula? sp	-	-	+	○	+	n.d.
Misceo- and Monomarginatus spp	○	-	-	-	-	-
N. watkinsii	+	-	-	-	-	-
Neocrepidolithus spp	-	+	-(+)	-(○)	-	-
N. corystus	●	+	-	-	-	-
N. frequens	-	■	●	○	○	+
O. magnus	+	-	-	-	-	-
P. embergen	-	-	+	-	+	-
P. regularis	-	-	●	●	●	○
P. pontolithuna	-	-	-	-	-	+
P. copularis	-	-	+	-	+	-
P. varius	-	-	+	-	-	-
P. obscurus	○	-	-	-	-	-
P. bussoni	●	+	+	+	+	-
P. fibuliformis	+	●	●	●	●	○
P. sigmoides	+	+(●)	+(○)	+(●)	+	+
Placozygus sp.	+	+	○	○	○	n.d.
Placozygus spp. indet.	-	-	-	-	-	○
P. arkhangel'skyn	○	○	-	-	+	-
P. cretacea	●	■	■	■	■	●
P. spinosa	■	●	●	●	○	○
P. grandis	-	-	+	+	+	n.d.
P. stoveri	■	■	●	●	●	■
P. firthii	●	-	-	-	-	-
Q. gartneri	+	-	+	+	+	-
Reinhardtites spp	●	+	○	-	+	-
R. angustus	+	+	+	+	+	○
R. asper	-	-	-	-	-	+
R. reniformis	-	-	+	+	+	+
R. splendens	-	-	○	○	+	+
Rhagodiscus sp. 1	-	-	+	-	+	-
Rhagodiscus spp	+	+	○	○	○	●
R. rhombicum	+	+	+	+	-	+
Scamparella spp	+	+	+	+	+	-
S. fossilis	+	+	+	-	+	-
S. laffitei	○	-	+	+	+	○
Stephanolithuon spp	-	-	○	○	+	○
T. stradneri	-	-	+	+	+	-
T. ethmos	+	+	+	+	+	-
T. decorus	-	-	○	○	+	+
Thoraacosphaera spp.	●	●	+(●)	-(■)	+	●
T. macleodae	-	-	+	○	+	○
T. phacelosus	-	-	-	-	+	-
Vagalapilla spp.	●	●	○	+	+	○
W. bamesae	+	+	■	●	■	■
W. biporta	-	-	+	+	+	-
Z. compactus	●	-	+	-	+	-
Z. diplogrammus	+	-	-	+	-	+
Z. lacunatus	-	-	+	+	+	+
Zygodiscus sp. 1	-	-	○	○	+	-

Table continued
6

indicating either (i) that high latitude surface water conditions extended into lower latitudes in the late Maestrichtian or (ii) that the ecological tolerance of this species increased to include low latitude conditions (see below).

(B) Biogeographic changes

(a) Emigrations

In addition to the twelve species that became extinct, twelve more taxa (Biscutum constans, B. notaculum, Biscutum sp. 1, C. garrisonii, C. amphipons, D. ignotus, R. rhombicum, S. fossilis, S. laffittei, W. barnesae, Z. compactus, and Z. diplogrammus) disappeared from high latitudes (or became extremely rare) during the Maestrichtian (Figure 56) but persisted into or throughout the late Maestrichtian at mid- and low latitudes (compare with range charts in e.g. Pospichal and Wise, 1990; Resiwati, 1991; Bralower and Siesser, 1992; this study). All of these taxa were fairly rare during the early Maestrichtian (<5%, Table 6) except for B. constans and B. notaculum which reached peak abundances of almost 10% and almost 40%, respectively (Table 6). Most of these disappearances (and abundance decreases) occurred during the same time interval (~72.4 to ~70.4 Ma) as the extinctions mentioned above.

(b) Abundance Changes

Decreasing abundance: Ahmuellerella octoradiata, P. spinosa and P. arkhangelskyi decreased in abundance during the early and early late Maestrichtian (~74-69 Ma; Figure 57a, b). Prediscosphaera arkhangelskyi was virtually absent after ~68.5 Ma whereas A. octoradiata and P. spinosa increased in abundance again after ~68 Ma (Figure 57a, b). Thoracosphaera spp. decreased gradually throughout the entire Maestrichtian (Figure 57d). Also Vagalapilla spp. decreased in abundance between the earliest and the latest Maestrichtian but between ~72-67 Ma its abundance remained virtually constant (Figure 57e). These taxa (except for Thoracosphaera spp.) were more abundant in high latitudes than in mid- or low latitudes.

Increasing abundance: Cribrosphaerella? daniae and N. frequens increased abruptly in abundance between ~71.1-70 Ma (Figure 58a, b). Kamptnerius magnificus, P. cretacea and P. stoveri also increased in abundance, but more gradually (Figure 58 c, d, e). Glaukolithus fessus displayed a fairly sudden abundance increase around 69 Ma (Figure 59a)

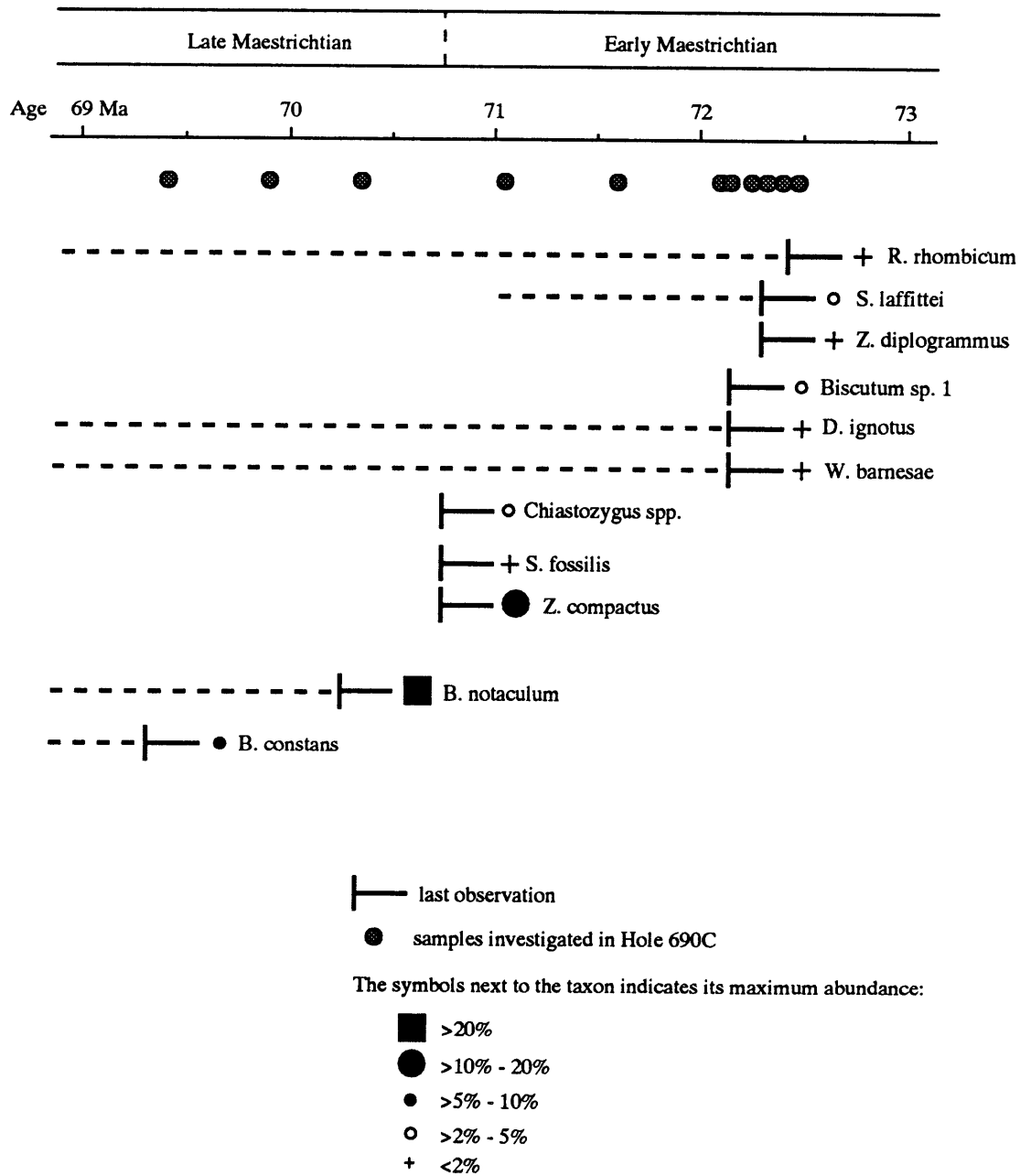


Figure 56: Sequence of regional disappearances of taxa around the early/late Maestrichtian boundary in high southern latitudes (ODP Hole 690C). The dashed lines indicate that some of these taxa were recorded very rarely in at least one sample in the upper Maestrichtian.

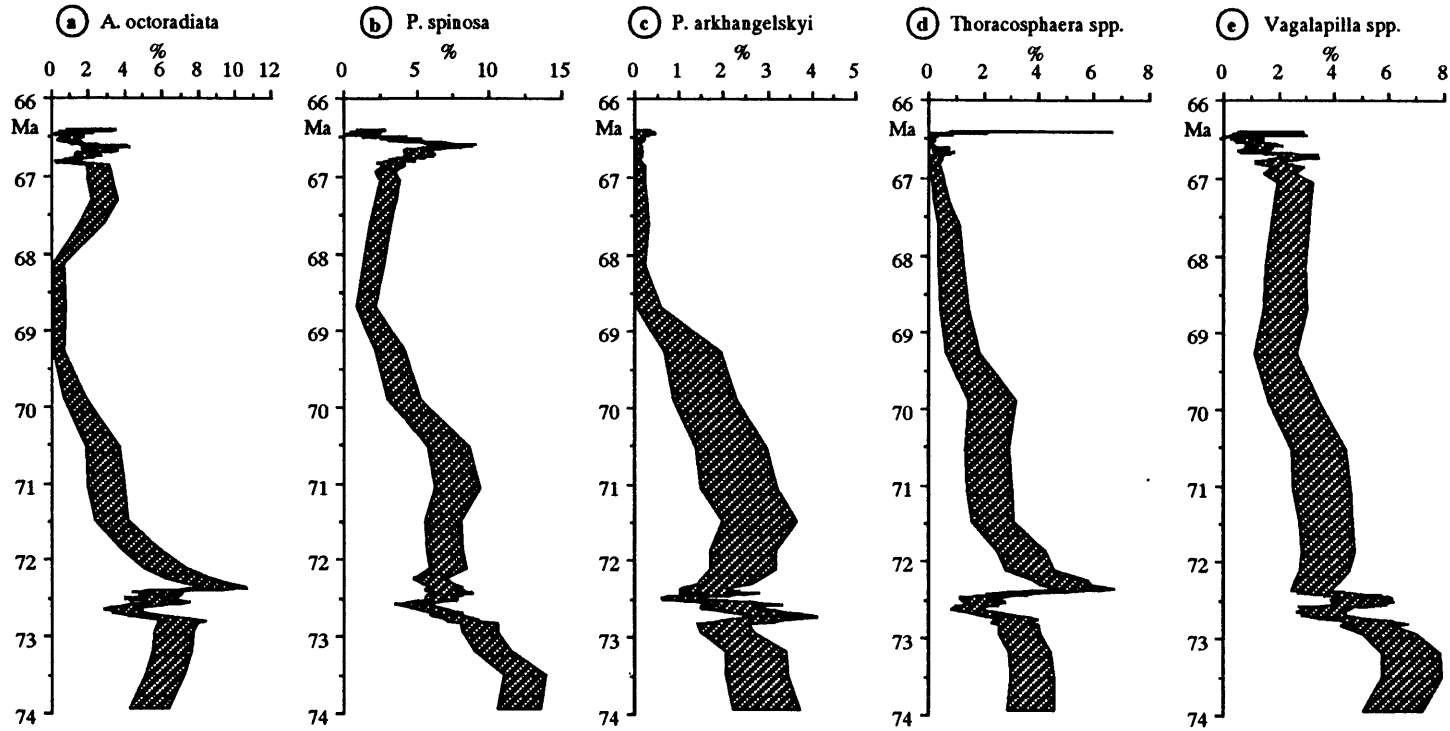


Figure 57: Calcareous nannoplankton taxa that decrease in abundance throughout the Maestrichtian in high southern latitudes (ODP Hole 690C).

Note: A five point running average was calculated from the raw data. The shaded band indicates the 95% confidence interval. The Cretaceous/Paleocene boundary lies at 66.4 Ma.

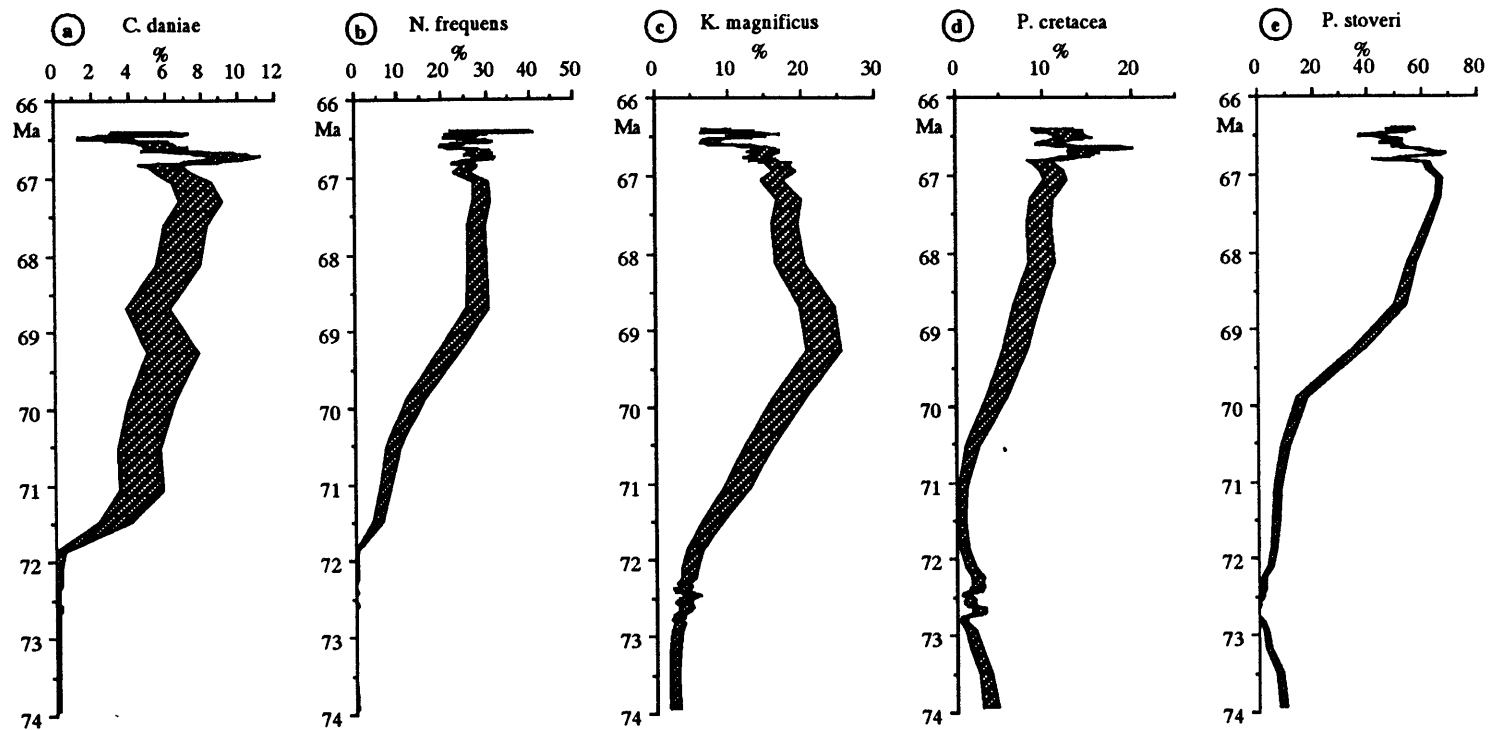


Figure 58: Calcareous nannoplankton taxa that increase in abundance throughout the Maestrichtian in high southern latitudes (ODP Hole 690C). See note in caption of Figure 57.

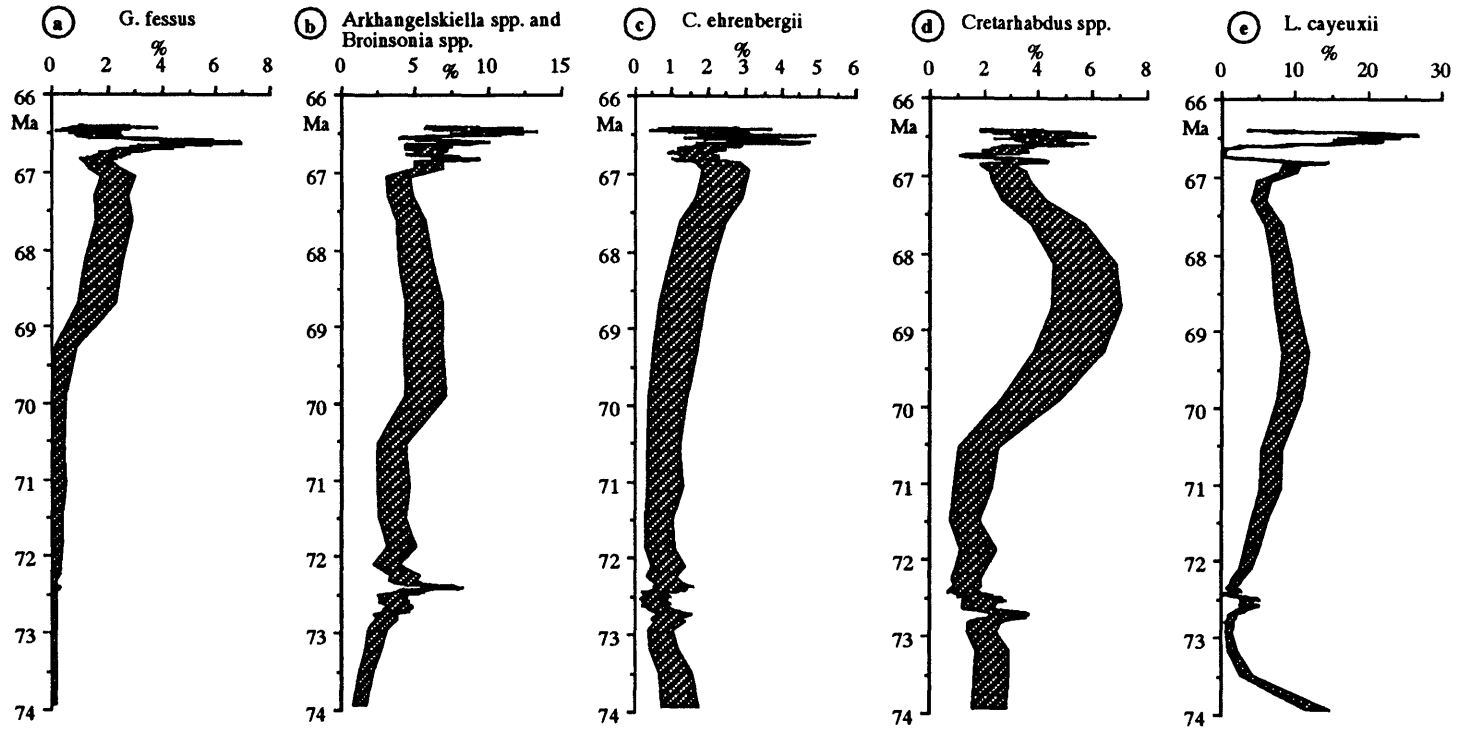


Figure 59: Calcareous nannoplankton taxa that increase in abundance throughout the Maestrichtian in high southern latitudes (ODP Hole 690C). See note in caption of Figure 57.

whereas Arkhangelskiella spp. and Broinsonia spp, C. ehrenbergii, Cretarhabdus spp. and L. cayeuxii increased in abundance gradually throughout the Maestrichtian (Figure 59b, c, d, e). These taxa dominated the late Maestrichtian nannoplankton assemblages.

In southern high latitudes conspicuous changes of the nannoplankton associations occurred close to the early/late Maestrichtian boundary (~71 Ma):

- (i) About one third of all taxa (corresponding to ~>20% of the specimens) became extinct within two million years (between ~72.4 and ~70.4 Ma).
- (ii) Another third of all taxa (corresponding to ~>40% of all specimens) disappeared from high southern latitudes (or became extremely rare) but persisted in mid- and low latitudes to the K/P boundary (66.4 Ma).
- (iii) Most of the dominant nannoplankton species in the late Maestrichtian were rare during the early Maestrichtian.
- (iv) Only one species (N. frequens) originated during the Maestrichtian (between ~71.2 and 70.4 Ma) in high southern latitudes.

2) Maestrichtian Evolutionary and Biogeographic Events in Mid/Low Latitudes

(A) Evolutionary Changes

(a) Extinctions

Five taxa (B. parca, Q. trifidum, T. phacelosus, R. levis, P. copulatus) became extinct during the early Maestrichtian in mid- and low latitudes and have been used for stratigraphic purposes (e.g. Bukry, 1973; Sissingh, 1977; Roth, 1978; Perch-Nielsen, 1979a, 1983; Bralower and Siesser, 1992). Because only upper Maestrichtian sediments were investigated from mid- and low latitude sites, it is not possible to evaluate the severity of the early Maestrichtian extinctions or to compare them with those in high latitudes. No extinctions were observed in mid- and low latitudes during the late Maestrichtian (after ~71 Ma).

(b) Originations

Three taxa (Lithraphidites quadratus, Micula murus, and M. prinsii) originated during the late Maestrichtian and have been used for stratigraphic purposes (e.g. Cepek and Hay, 1969; Bukry, 1973; Perch-Nielsen, 1979). Their first occurrences are at ~69.0 Ma, ~67.6 Ma and ~66.6 Ma, respectively (see Chapter 3, Biohorizons). Micula murus reached abundances of >5% in some sections (Table 6), whereas L. quadratus and M. prinsii never exceeded 5% (Table 6).

(B) Biogeographic Changes and Abundance Changes

Worsley (1974) reported that L. cayeuxii was restricted to the early Maestrichtian in tropical latitudes, but was still present in the late Maestrichtian in high latitudes.

Wind (1979a) examined Campanian and Maestrichtian nannoplankton abundance changes in the southern hemisphere (in mid- to high southern latitudes of the Atlantic and Indian Oceans). He documented primarily nannoplankton provincialism and indicated that a sharp boundary across the Falkland Plateau separated the high latitude taxa from the mid- latitude nannoplankton community (with abundant B. constans and M. staurophora). He also documented an abundance increase of W. barnesae and Cyclagelosphaera spp. from mid- to low latitudes. Wind (1979a) did not report abundance changes of individual species through time. Instead he examined changes in the dominance of assemblages (groups of taxa with similar latitudinal preferences) and changes of ratios of certain nannoplankton taxa (B. magnum and B. coronum vs. B. constans; M. staurophora vs. W. barnesae and Cyclagelosphaera spp.). Due to this grouping the abundance changes of individual taxa cannot be derived from the trends he reported. Comparison with his raw data, however, revealed some of the same trends recognized in this study (see below).

Only one study has attempted to investigate Maestrichtian nannoplankton biogeographic patterns on a global scale (Thierstein, 1981). The subsequent dearth of similar studies may be due, in part, to Thierstein's conclusion that no nannoplankton biogeographic or abundance changes occurred during the latest Cretaceous. Thierstein (1981) confirmed the results of previous authors (e.g. Worsley and Martini, 1970; Worsley, 1974; Thierstein, 1976; Wind, 1979a) that latitudinally defined, nannoplankton

paleoprovincialism was strongly developed during the latest Cretaceous. Wise (1988) interpreted this provincialism as a function of surface water temperatures.

Doeven (1983) investigated nanoplankton abundance patterns during the Campanian and Maestrichtian in the northwest Atlantic Ocean (Canadian Atlantic margin). He performed abundance counts on 29 samples from nine drillholes, and as a consequence the chronologic resolution is quite low (usually one sample per nannofossil zone). He reported only the abundance variations of the most abundant taxa (at least $\geq 2\%$ in one sample) but worked primarily at the generic level. He noted a pronounced abundance increase in A. cymbiformis from Campanian to Maestrichtian, a concurrent decrease of W. barnesae, and a frequency decrease of Biscutum spp. during the Maestrichtian. He considered these changes genuine, because preservation did not change significantly between samples and he interpreted them as reflecting a temperature decrease. No abundance changes of M. staurophora and W. barnesae were observed in this study, possibly due to the fact that only the late Maestrichtian was investigated (i.e. the abundance changes in these two taxa were not recorded because they occurred earlier).

In my study no change in the biogeographic distribution of any taxon during the late Maestrichtian has been observed (i.e. neither immigrations nor emigrations of taxa). A few taxa show abundance changes through the late Maestrichtian at all sites:

Ahmuellerella octoradiata was more abundant in high than in low latitudes during the Maestrichtian (Figure 60) which agrees with its classification as a high latitude taxon (e.g. Thierstein, 1981). At all sites its abundance decreased during the Maestrichtian and this species virtually disappeared from the records between ~68.5 and 68 Ma at mid-latitudes in the Indian Ocean (Hole 217 and 761B, respectively).

Biscutum constans reached peak abundances of ~6-8% at all sites, it decreased in abundance in all sections during the Maestrichtian (Figure 61). This decrease occurred at different times at different sites (~70-68 Ma in Hole 690C; ~67-66.7 Ma in Hole 761B; ~68-67 Ma in Hole 217; ~67.1 - 66.9 Ma in Hole 528).

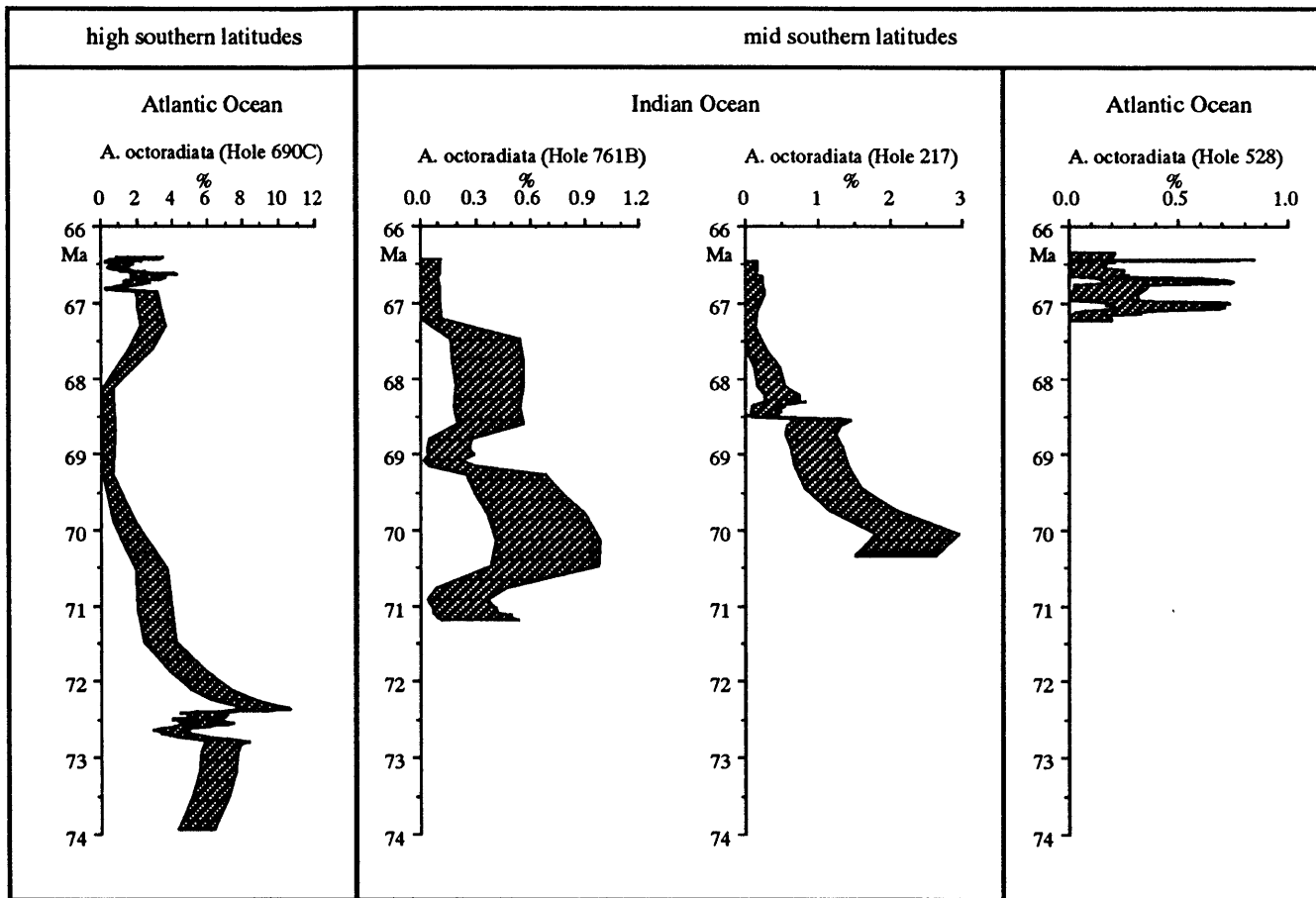


Figure 60: Comparison of abundance variations of *Ahmuellerella octoradiata* during the Maestrichtian between latitudes and Ocean Basins. See note in caption of Figure 57.

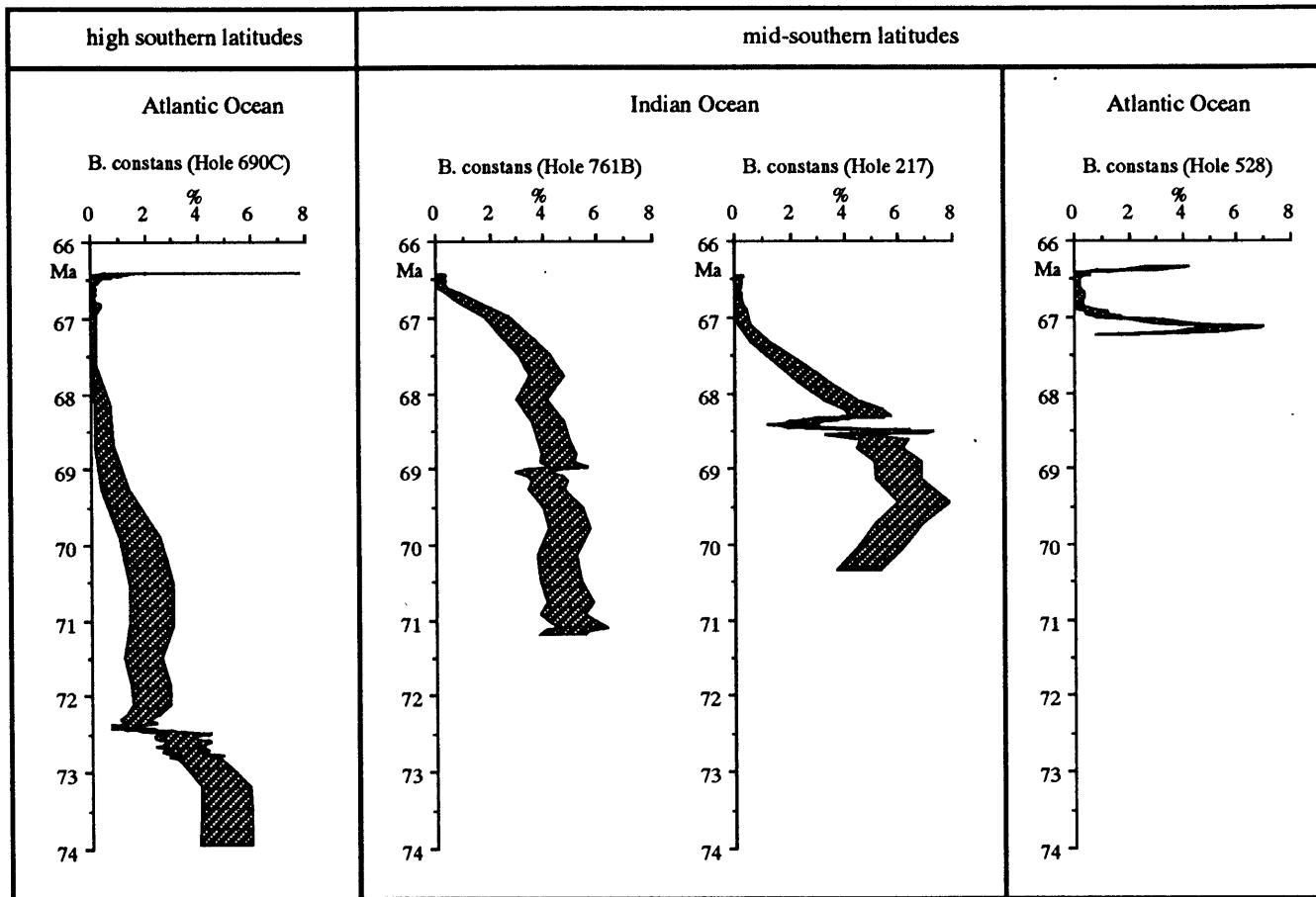


Figure 61: Comparison of abundance variations of *Biscutum constans* during the Maestrichtian between latitudes and Ocean Basins. See note in caption of Figure 57.

(3) **Maestrichtian Nannoplankton Biogeography: Arguments** against worldwide stable ecological conditions in the surface ocean during the latest Cretaceous.

(A) **The Austral Taxa**

(a) Which are the "austral" taxa?

Resiwati (1991) suggested the term "austral" to refer to late Campanian and early Maestrichtian taxa that were restricted to high southern latitudes. This definition is considered to be too restrictive: several taxa (e.g. N. corystus) that are characteristic of high southern latitudes extended into the late Maestrichtian. Others (e.g. B. coronum, B. dissimilis, B. magnum, M. quaternarius) occurred also in the northern hemisphere. I propose to extend the definition of the term "austral" to include taxa that were restricted to or particularly abundant in high southern latitudes from late Campanian to early late Maestrichtian. As a preliminary approach in this study the term austral taxa includes the following: Biscutum boletum, B. coronum, B. dissimilis, B. magnum, Misceomarginatus pleniporus, Monomarginatus pectinatus, M. quaternarius, Neocrepidolithus watkinsii, Nephrolithus corystus, Phanulithus obscurus, and Psyktosphaera firthii. Several new species of holococcoliths (Okkolithus australis, Orastrum asarotum, Phanulithus additus, Pharus simulacrum) were described by Wind and Wise (in Wise and Wind, 1977) from the same material in which many of the above listed austral taxa were first described. Due to their holococcolithic structure these forms are fairly susceptible to dissolution (Wind and Wise, 1978) which may explain why they are only very rarely reported from other austral sites. It is possible that (some of) these species share the stratigraphic and geographic distribution of the austral taxa and should be included in the austral assemblage. On the other hand, their absence may be due to ecologic exclusion since it has been suggested (Perch-Nielsen, 1985) that holococcoliths may be indicative of shallow water depths. A study of recent holococcolith species indicated that holococcolith species are most abundant under oligotrophic conditions (Kleijne, 1991). Despite its high abundance in the early Maestrichtian at high latitudes B. notaculum is not included in the austral assemblage because this

species also occurred in the late Maestrichtian at mid-latitudes (e.g. Holes 761B, 528, and 217, as well as Millers Ferry Section; Table 6).

In order to speculate about the causes of the extinctions of the austral taxa it is necessary to explore their paleoecological preferences. Their paleogeographic distribution is used below to infer these preferences.

(b) Paleogeographic distribution of austral taxa

Austral calcareous nanoplankton species have been reported extensively from the southern Atlantic and southern Indian Ocean (Table 7; Figure 62), but no reports of austral taxa from the southern Pacific Ocean could be located. No early Maestrichtian sediments have been recovered in the South Pacific, except maybe in DSDP Hole 208, where the exact age of the sediment is unclear. None of the ODP Legs in the extratropical South Pacific (Legs 133 and 135) recovered Cretaceous sediments. Five DSDP Legs (Legs 21, 28, 29, 35, and 90) took place in extratropical latitudes in the South Pacific Ocean. Only in one DSDP Hole (Hole 208, Lord Howe Rise, southwestern Pacific Ocean, Leg 21) were sediments recovered that are older than the N. frequens Zone (?L. quadratus Zone sensu Bukry, [1973a] which extends from the early to the early late Maestrichtian; Bukry, 1973b) and older than the A. mayaroensis Zone (Webb, 1973). Huber (1992b) studied the planktonic foraminifera in Hole 208 and concluded that the age of the Maestrichtian sediments was late early and early late Maestrichtian. Only the more abundant nannofossil taxa were listed (Edwards, 1973; Bukry, 1973b) and Bukry (1973) commented on the high latitude aspect of the assemblage which contained common A. cymbiformis, L. cayeuxii, and K. magnificus, while W. barnesae was absent (Bukry, 1973b). It is possible that austral nannofossil taxa are present in very low abundances in Hole 208.

In the North Sea region where Campanian and Maestrichtian calcareous nanoplankton assemblages have been thoroughly investigated, only few austral taxa occur. Biscutum dissimilis, B. magnum, and M. quaternarius have been reported from England and northern Germany (e.g. Burnett, 1990). Their first and last occurrences were used for a stratigraphic subdivision of the Campanian (Burnett, 1990). Burnett (1990) did not indicate the abundance of these three taxa, nor did she supply a species list to indicate whether any other austral taxa were observed. It appears that most of the austral taxa, if present, were much rarer in the northern hemisphere than in the southern. I

Table 7: List of sites where austral nannofossil taxa were reported. The sites are arranged in geographic order, from the western South Atlantic Ocean to the eastern Indian Ocean.

<u>Site</u>	<u>Location</u>	<u>Source</u>
DSDP Hole 327A	Falkland Plateau	Wise and Wind, 1977
DSDP Hole 511	Falkland Plateau	Wise, 1983
ODP Hole 700B	East Georgia Basin	Crux, 1991
ODP Holes 689B, 690C	Maud Rise	Pospichal and Wise, 1990
DSDP Hole 249	Mozambique Plateau	Wind, 1979
ODP Hole 738C	Kerguelen Plateau	Wei and Thierstein, 1991
ODP Holes 747A, 748C, 750A	Kerguelen Plateau	Watkins, 1992
ODP Holes 752B, 754A	Broken Ridge	Resiwati, 1991
ODP Holes 762C	Exmouth Plateau	Bralower and Siesser, 1992
DSDP Hole 217	Ninetyeast Ridge (8°N)	Wind, 1979
ODP Hole 758A	Ninetyeast Ridge (5°N)	Resiwati, 1991

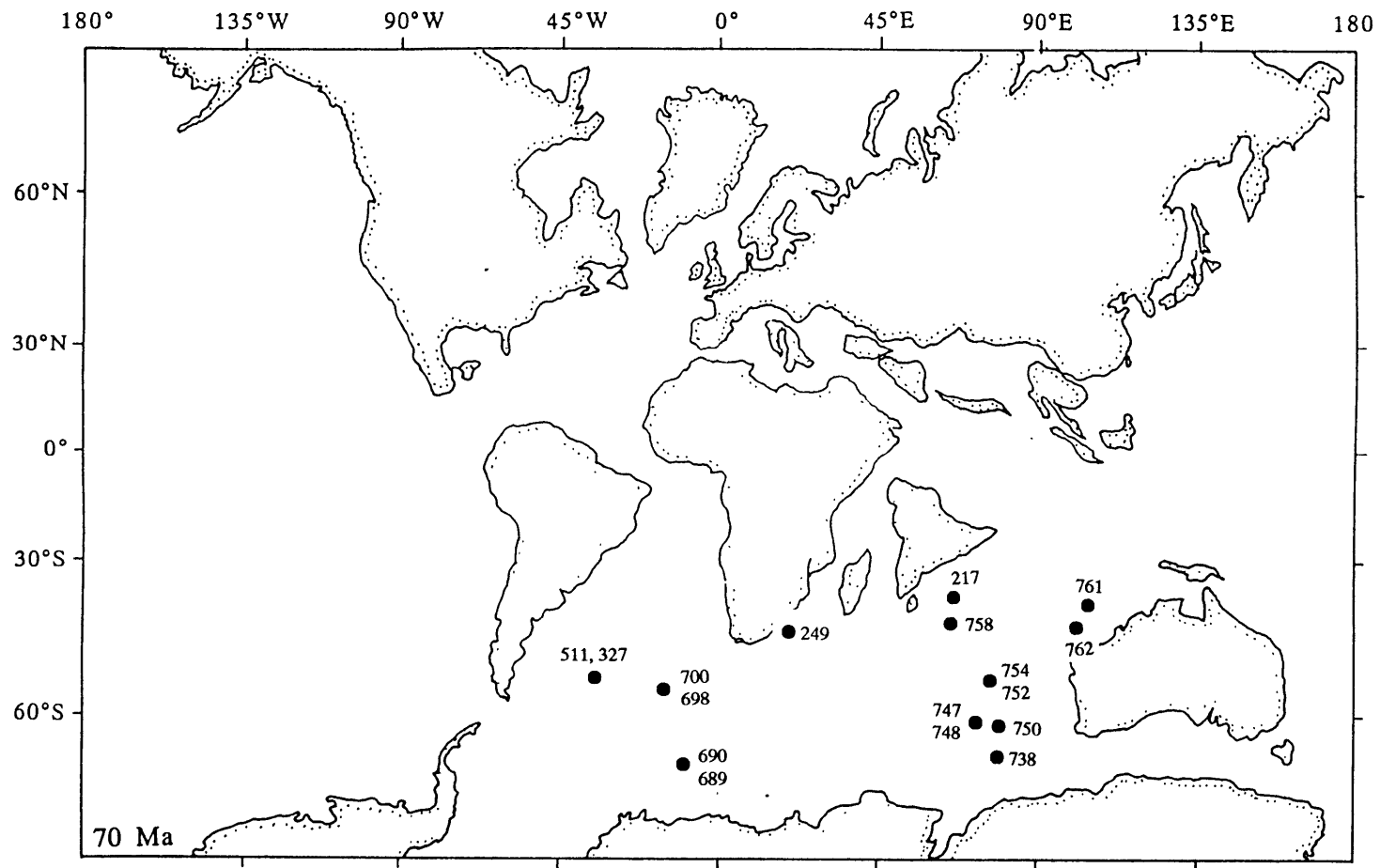


Figure 62: DSDP and ODP sites where austral taxa were recorded. Paleogeontinental reconstruction after Coffin et al. (1992).

encountered a single specimen of B. magnum in the upper Maestrichtian (M. prinsii Zone) of the Millers Ferry section (paleolatitude ~30° N). Biscutum dissimilis disappeared earlier in the northern hemisphere (late Campanian, Burnett, 1990) than in high southern latitudes (early Maestrichtian, this study). Crux (1991) indicates that the last occurrence of B. magnum was apparently synchronous in high latitudes in both hemispheres (in Chron C31R). Biscutum coronum was reported from upper Campanian sediments in Japan (Okada et al., 1987) where this species was commonly present (1-10% of the assemblage: Okada et al., 1987).

It appears that most austral calcareous nannoplankton taxa were restricted to the southern Atlantic and southern Indian Ocean during the late Campanian and early Maestrichtian. Some exceptions to this rule have been reported above and future investigations will possibly record other austral taxa from regions where they are still unknown (such as the southern Pacific Ocean).

(c) Why did austral calcareous nannoplankton species become extinct?

The paleogeographic restriction of the austral taxa and the cause of their disappearance are not fully understood. Apparently (i) the extinctions did not occur simultaneously among the austral taxa (although they were concentrated close to the end of the B. magnum Biochron; Figure 65) and (ii) at the same time numerous additional taxa disappeared from Hole 690C or became extremely rare.

In order to explain the pronounced changes that were observed in the Maestrichtian nannofossil assemblages in Hole 690C it is necessary to examine whether and in which way other organisms experienced changes around the early/late Maestrichtian boundary, and to integrate results from stable isotope investigations (planktonic foraminifera: Huber, 1990; benthic foraminifera: Thomas, 1990; stable isotopes: Barrera and Huber, 1990; Stott and Kennett, 1990).

Additional evidence

Planktonic Foraminifera: Planktonic foraminifera are excellently to well preserved in Maestrichtian sediments in Hole 690C. The slight changes in the proportion of benthic foraminifera throughout the Maestrichtian correlates with excellent preservation during most of the early Maestrichtian

and good preservation during the earliest and the late Maestrichtian (Barrera and Huber, 1990; Huber, 1990). The austral nature of the assemblage is documented by the presence of five species that were restricted to high latitudes (Archaeoglobigerina australis, A. mateola, Globigerinelloides impensus, Hedbergella sliteri, Rugotruncana circumnodifer; Huber, 1990), by low diversity (compared to tropical and subtropical assemblages), and by the absence or rareness of typical tropical taxa. The diversity of the planktonic assemblage was low during the early early Maestrichtian (around 10 species); it increased in the late early Maestrichtian to ~12-14 species and remained at that level during the late Maestrichtian (Huber, 1990). The diversity increased due to the first occurrences of five taxa (Globotruncana subcircumnodifer, G. bulloides, Globotruncanella petaloidea, Globigerinelloides subcarinatus, Globotruncanella citae, Pseudotextularia elegans; Huber, 1990, 1992b) which were known from lower latitudes where their first occurrences are (in some cases considerably) older than on Maud Rise. The poleward migrations of species typical of lower latitudes could be interpreted as warming pulses of surface waters at high latitudes. However, evidence from stable isotopes does not support such an interpretation (Huber, 1990). Paleooceanographic factors other than temperature, such as changes in nutrient supply, salinity, vertical stratification and/or surface water turbidity must be invoked to explain the planktonic foraminiferal patterns (Huber, 1990). Huber (1992a) and Huber and Watkins (1992) suggested that the poleward expansions of low latitude species may have been due to increased stratification of surface waters. Stable isotope records, however, do not seem to support this contention (see below).

Benthic Foraminifera: Benthic foraminiferal assemblages changed moderately between the early and the late Maestrichtian and the changes are sufficient to allow recognition of two assemblages (Thomas, 1990): assemblage 8 ranged throughout the early Maestrichtian and was replaced by assemblage 7 in the early late Maestrichtian (at ~69.4 Ma; boundary between subchrons 31R and 31N; Thomas, 1990). The differences between these assemblages were small compared to faunal changes at other times (Thomas, 1990) and the changes occurred gradually rather than abruptly. The differences between assemblages 8 and 7 include a slight increase in diversity, a decrease of the percentage of epifaunal species (from 52 to 43%) and an increase of infaunal and cylindrical species (from 43 to 51%; Thomas, 1990). In addition, the

proportion of benthic to planktonic foraminifera increases at the boundary between assemblages 8 and 7; this increase may reflect decreasing preservation of planktonic foraminifera in the late Maestrichtian (see above, and compare e.g. Huber, 1990; Barrera and Huber, 1990). Variations in relative abundances of infaunal and epifaunal species in recent assemblages reflect variations in the availability of organic carbon to the bottom-dwelling fauna (Corliss and Chen, 1988). Thus the increase of infaunal species may be used to argue for increased productivity in surface waters (Thomas, 1990) or low oxygen content in the bottom water (see Thomas [1990] for a more detailed discussion). Thomas (1990) noted that neither of these arguments was supported by sedimentologic (Robert and Maillot, 1990) or stable isotope evidence (Barrera and Huber, 1990).

Stable isotopes: Barrera and Huber (1990) measured stable isotopes from planktonic and benthic foraminifera as well as from bulk sediment to investigate paleoenvironmental changes at high southern latitudes during the Maestrichtian.

The general trend of oxygen isotope values of planktonic and benthic foraminifera is an increase throughout the Maestrichtian (except for a short negative excursion at the very top of the Maestrichtian; Figure 63a). This indicates a longterm temperature decrease. The increase of $\delta^{18}\text{O}$ values is not gradual but rather proceeds in a stepwise manner with steps at ~ 73.5 Ma and at about 71.0 Ma. The record of the benthic species Gavelinella beccariiformis shows both steps whereas only the earlier increase is evident in the $\delta^{18}\text{O}$ record of Globigerinelloides multispinatus. The second increase (at 71.0 Ma) is less apparent in G. multispinatus (only about 0.2‰). In contrast, the increase at ~ 73 Ma is not observed in the record of the planktonic species Archaeoglobigerina australis: its $\delta^{18}\text{O}$ values remained roughly constant (average -0.3‰) up to about 71 Ma, where an abrupt increase of about 0.5‰ occurred and subsequently a gradual increase to values similar to those of the benthic species.

The $\delta^{13}\text{C}$ records of benthic and planktonic species vary roughly in parallel, with a constant offset of about 1‰ (Figure 63b). A gradual $\delta^{13}\text{C}$ decrease occurred during the early Maestrichtian (from about 74.5 to 71.5 Ma); it culminated in a spike of very light $\delta^{13}\text{C}$ values at ~ 71 Ma. Carbon isotope ratios quickly rebounded from this negative excursion and around 70.2 Ma the

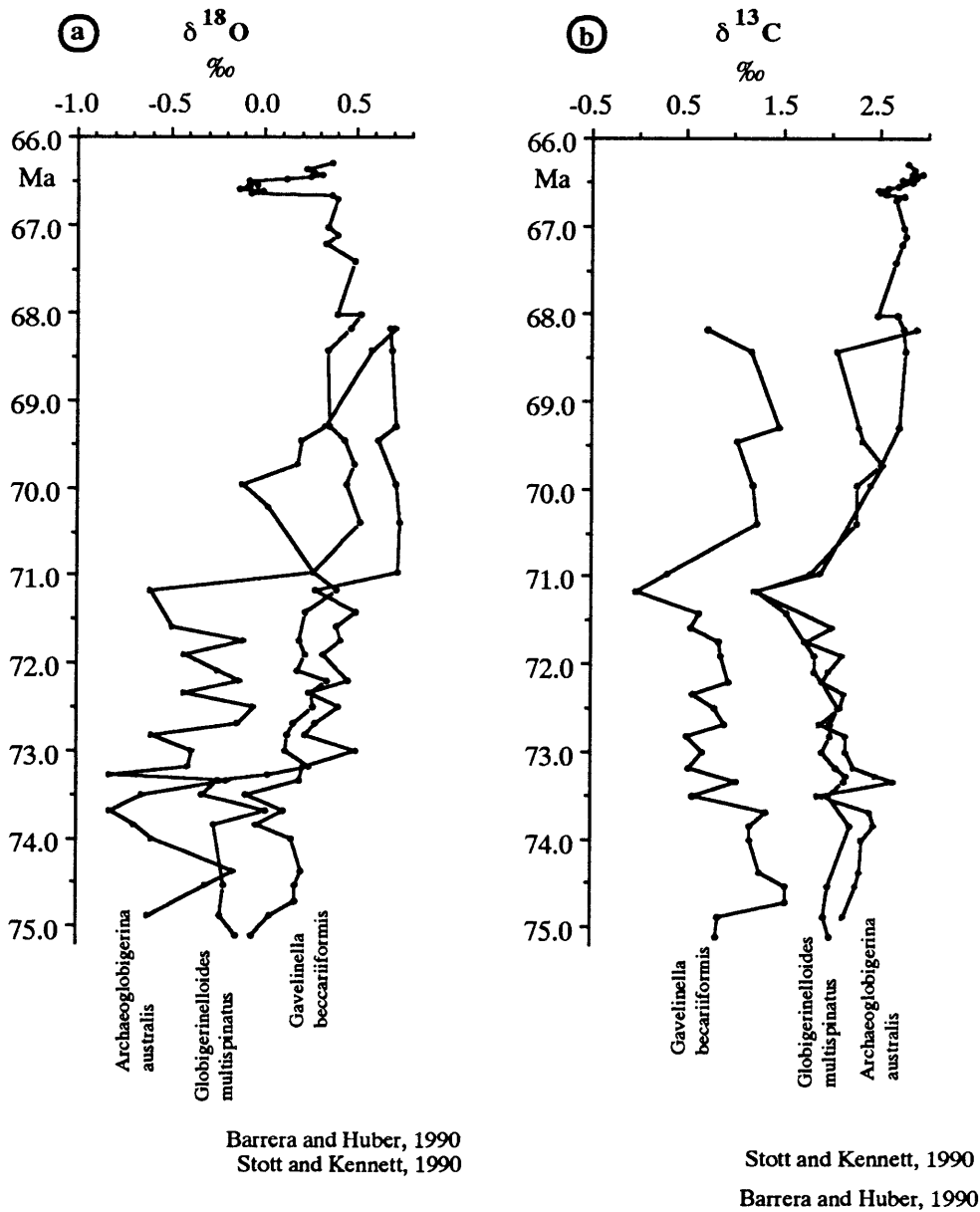


Figure 63: Stable isotope records from Maestrichtian sediments in southern high latitudes (ODP Hole 690C). Data from Barrera and Huber (1990) and Stott and Kennett (1990).

values were higher than during the early Maestrichtian. For the late Maestrichtian the benthic $\delta^{13}\text{C}$ record shows roughly constant values, while the planktonic record shows an increase that continued up to ~67.5 Ma (as recorded by Barrera and Huber, 1990).

Barrera and Huber (1990) discussed in detail the reliability of the stable isotope data from different foraminiferal species. They concluded that the isotopic values of A. australis and of G. beccariiiformis reflect changes, respectively, in surface and bottom waters. They argued that G. multispinatus lived very close to the surface (based on observations from Seymour Island, Antarctica, where G. multispinatus was recorded abundantly in shallow water sediments; Huber, 1988) and that its $\delta^{13}\text{C}$ record reflects surface water conditions, but that its $\delta^{18}\text{O}$ record was modified by vital effects.

I would suggest, however, that the carbon and oxygen isotope data from Hole 690C indicate that G. multispinatus lived in deeper waters than A. australis, except for an inversion of their respective $\delta^{18}\text{O}$ and $\delta^{13}\text{C}$ values between about 70 and 68.5 Ma. The oxygen isotope data indicate a cooling event at about 73.5 Ma that affected bottom waters and (possibly) the deeper thermocline. This cooling event did not affect surface waters (as recorded by A. australis). It should also be noted that a second cooling pulse occurred at about 71 Ma, which affected bottom and surface waters; the temperature decrease in surface waters was much more severe than that of bottom waters. This pronounced cooling of surface waters at 71 Ma coincides with the conspicuous diversity decrease among calcareous nannofossils observed at ODP Site 690.

The longterm shifts in both the benthic and the planktonic $\delta^{13}\text{C}$ data indicate changing carbon reservoirs, possibly reflecting changing paleocirculation patterns (e.g. better mixing of water masses of the southern high latitudes with the rest of the world's oceans).

A pronounced but brief negative excursion in the $\delta^{13}\text{C}$ record was documented in Hole 690C (Barrera and Huber, 1990): it began at the C32N/C31R boundary in the late early Maestrichtian (top of the G. havanensis Zone, top of the B. magnum Zone, ~71.2 Ma according to the age model herein; Figure 57). Its duration is difficult to assess due to incomplete core recovery, but it was probably no longer than ~0.8 m.y. (and could have been shorter, depending on the age estimated for the core catcher of Core 113-690C-18). The spike to

lighter $\delta^{13}\text{C}$ values at ~71 Ma occurred at the same time as the cooling event of the entire water column (as expressed by the $\delta^{18}\text{O}$ record) but a causal relation of these two trends is not apparent.

It is unlikely that this decline reflects decreased productivity (Berger and Vincent, 1986) because surface to deep water carbon isotope gradients remained unchanged (Barrera and Huber, 1990). Instead the negative $\delta^{13}\text{C}$ spike could have resulted from decreased storage of organic carbon in shallow shelf areas due to a sea level fall at the early/late Maestrichtian boundary (Haq et al., 1987). Barrera and Huber (1990) interpreted the ensuing increase in the $\delta^{13}\text{C}$ record as a consequence of the subsequent sea-level rise (via increased organic carbon burial on continental shelves).

If the negative carbon isotope spike is due to a global sea level fall, it should be a global feature. Only two sufficiently detailed Maestrichtian carbon isotope records are available for comparison (Figure 64). Mount et al. (1986) reported a negative carbon isotope excursion (Figure 64a) in the lowermost upper Maestrichtian (base of the *A. mayaroensis* Zone according to Herm, 1963; no paleomagnetic data available) from the Sopelana section in northern Spain. Also at Gubbio (Italy) the lowest $\delta^{13}\text{C}$ values in the Maestrichtian (Corfield et al., 1991; Figure 64b) occur in the mid-Maestrichtian (~71.5 Ma) shortly before the beginning of Magnetozone C31 (paleomagnetic data of Alvarez et al., 1977).

This suggests that the negative carbon isotope excursion may indeed be a global feature reflecting the sea level fall at the early/late Maestrichtian boundary. The carbon isotope data do not indicate a productivity increase (as suggested by benthic foraminiferal changes), since the offset between planktonic and benthic species remained constant throughout the record.

Summary: Numerous nannoplankton taxa disappear from high southern latitudes around the early/late Maestrichtian boundary (~71 Ma). Planktonic and benthic foraminifera suggest paleoceanographic changes during the Maestrichtian, but in these latter groups the changes are less pronounced than in the calcareous nannoplankton. No evidence is available to speculate about the influence of salinity changes on changes in calcareous nannoplankton. In the following the evidence for changes of temperature, nutrients, turbidity, and stratification of surface waters as causes for the observed biospheric changes will be briefly discussed.

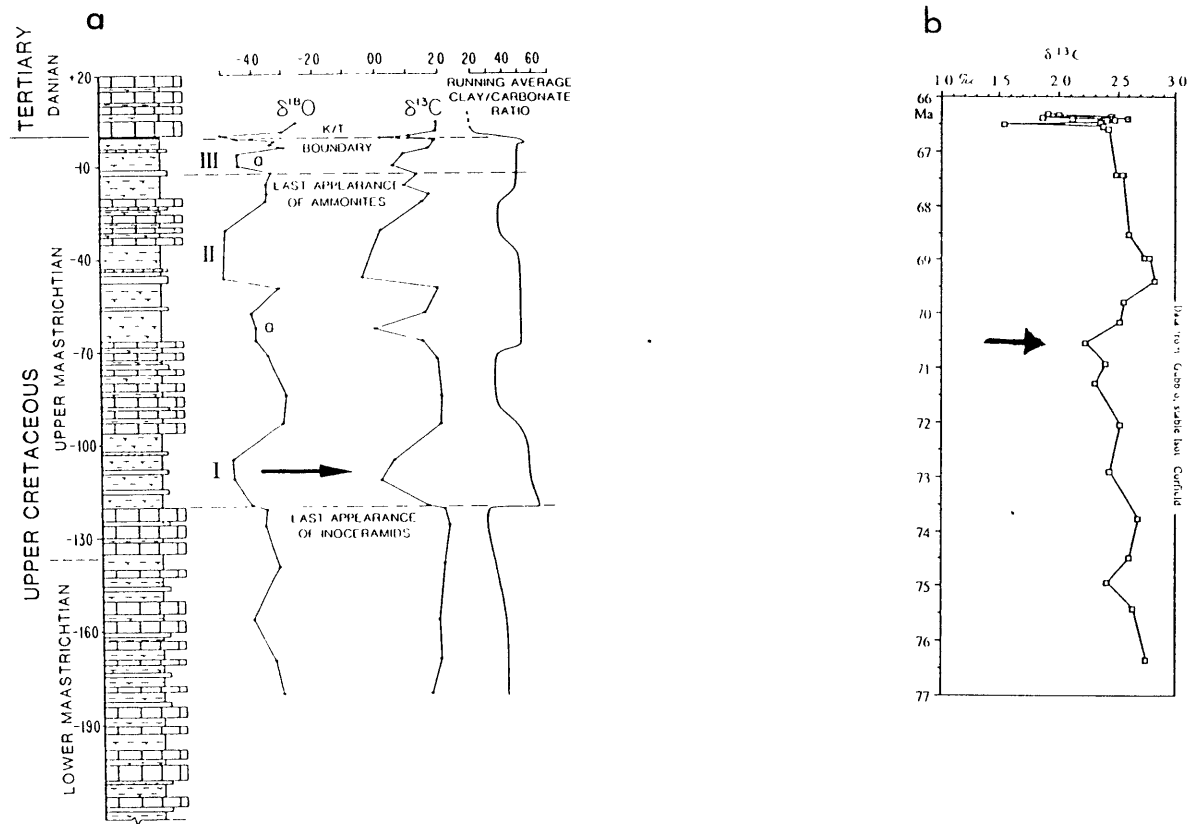


Figure 64: Stable carbon isotope records from the Maestrichtian in two low latitude sections. (a) Zumaya, northern Spain (data from Mount et al., 1986). (b) Gubbio, Italy (data from Corfield et al., 1991): The arrows marks the low $\delta^{13}C$ values that are thought to reflect the global sea level drop at the early/late Maestrichtian boundary.

Temperature: Huber (1990) pointed out that a discrepancy existed if the immigration of tropical planktonic taxa into high latitudes during the late Maestrichtian were interpreted as a warming signal, since the stable isotope record indicates cooling. Instead he suggested a solution to this dilemma by proposing that an oceanic front separated the austral realm from mid-latitudes during the late Campanian and early Maestrichtian (Huber, 1992a). He speculated that this oceanic front vanished at the early/late Maestrichtian boundary and that austral surface waters became more stratified. However, a decrease in the interspecific $\delta^{18}\text{O}$ gradient among planktonic foraminifera at the early/late Maestrichtian boundary (Barrera and Huber, 1990) seems to contradict this speculation (see below).

Several nannoplankton species disappeared from (or became very rare in) high latitudes around the early/late Maestrichtian boundary but persisted until the end of the Maestrichtian in mid- and low latitudes (as discussed above). This is interpreted here as a response to cooling in high latitudes as indicated by the oxygen isotope record. In contrast, the group of austral taxa became extinct at about the same time. I would suggest that the extinctions of the austral taxa were not a consequence of decreasing water temperature, because if they were temperature sensitive they would have migrated into lower latitudes. Instead I propose that the extinctions of the austral taxa were a consequence of changes in nutrient availability, stratification of the photic zone, turbidity or salinity changes brought about by circulation changes caused by a sea level fall.

A higher percentage of terrigenous components in early Maestrichtian sediments (compare Figure 6 in the chapter on Chronology) may indicate higher turbidity during this time and some changes among the calcareous plankton may be due to this fact. Comparison with other high latitude sites is needed to indicate whether mid-Maestrichtian changes correlate everywhere with sedimentologic changes.

A change in the stratification of surface waters from early to late Maestrichtian at high southern latitudes is inferred from the stable oxygen isotope record. If the $\delta^{18}\text{O}$ record of G. multispinatus is considered to reflect conditions in deeper surface waters and that of A. australis to reflect those in shallow surface waters, it seems that the temperature differences within the mixed layer were larger during the late early Maestrichtian than during the

early late Maestrichtian (Figure 63a). A higher temperature gradient in surface waters during the early Maestrichtian may indicate that the thermocline was shallower than during late Maestrichtian. This may imply that the stratification of surface waters decreased from the early to the late Maestrichtian. A decrease in the stratification of surface waters would have facilitated the advection of nutrients into the photic zone, and I would suggest that it was increased surface water fertility that caused the extinction of the austral taxa. This argument is consistent with investigations of recent calcareous nannoplankton: it has been documented that coccolithophorids dominate the phytoplankton under oligotrophic conditions (Smayda, 1980) and that nannoplankton diversity is higher in the oligotrophic open ocean than in eutrophic marginal seas (Okada and Honjo, 1975).

A decrease of surface water stratification is in contrast to the argument of Huber and Watkins (1992) who interpreted the migration of tropical planktonic foraminiferal species to high southern latitudes during the late Maestrichtian as a reflection of increased surface water stratification during the late Maestrichtian.

The following observations are summarized:

- (i) Eleven taxa are considered as "austral taxa". All of them were restricted to, or particularly abundant in, high southern latitudes, and all of them became extinct between ~72.4 and ~70.4 Ma (most of the extinctions were concentrated between 71.1 and 70.4 Ma).
- (ii) The austral taxa constituted about one third of all taxa present in southern high latitudes, and ~20% of the assemblage.
- (iii) I suggest that the extinctions of most of the austral taxa were a consequence of increased nutrient availability and decreased surface water stratification. The extinctions coincide with a $\delta^{13}\text{C}$ excursion that probably reflects a sea level fall.

(B) Nannoplankton Response to Environmental Perturbations During the Last 500 ky of the Cretaceous

a) High latitude evidence

The following discussion relies mostly on nannofossil and stable isotope data from ODP Hole 690C because no other record of comparable resolution or duration is available.

At high southern latitudes the following nannoplankton trends occurred during the last 500 ky of the Cretaceous (Figure 65): Between ~66.70 and 66.57 Ma Placozygus fibuliformis (Figure 65a) was more abundant in the nannoplankton association than either before or afterward. This species reached peak abundances of ~5-6%. An almost exactly opposite abundance pattern was recorded for the species Lucianorhabdus cayeuxii and Micula staurophora (Figure 65b, c). Both taxa were present prior to ~66.76 Ma, disappeared almost completely between ~66.76 and 66.62 Ma, and were present again between 66.62 Ma and 66.4 Ma.

A fairly detailed stable isotope record from the uppermost Maestrichtian in Hole 690C was presented by Stott and Kennett (1990). Direct comparison of this record with the nannoplankton abundance patterns is difficult because the resolution of the stable isotope study is much coarser than that of the nannoplankton abundance records in this study. In addition, the stable isotope changes measured on different foraminiferal species or on the fine fraction are not exactly synchronous. The highest resolution was achieved in the stable isotope record of the planktonic foraminifera Globigerinelloides multispinatus and this record was used for comparison with the nannoplankton abundance changes in the following discussion (Figure 65d, e).

A fairly abrupt decrease in $\delta^{18}\text{O}$ values (~0.5‰) occurred at ~66.65 Ma, values remained low until ~66.50 Ma, and then increased again abruptly (by ~0.5‰; compare Figure 65d). This brief negative excursion was observed in planktonic as well as in benthic foraminiferal species and was interpreted by Stott and Kennett (1990) as a warming pulse of ~2°C. Alternatively, this $\delta^{18}\text{O}$ excursion could indicate a brief episode of decreased salinity. A $\delta^{18}\text{O}$ decrease of 0.5‰ corresponds to a salinity decrease of ~1.7‰ according to Craig (1966), and ~0.8‰ according to Craig and Gordon (1965). Palynomorph evidence from Seymour Island (off the Antarctic Peninsula) suggests a brief warming interval in the latest Maestrichtian (Askin, 1989). The oxygen isotope excursion is interpreted here as a brief warming pulse rather than a salinity decrease. A warming pulse during the latest Maestrichtian (at the base of Magnetochron 29) was also reported from the North American interior based

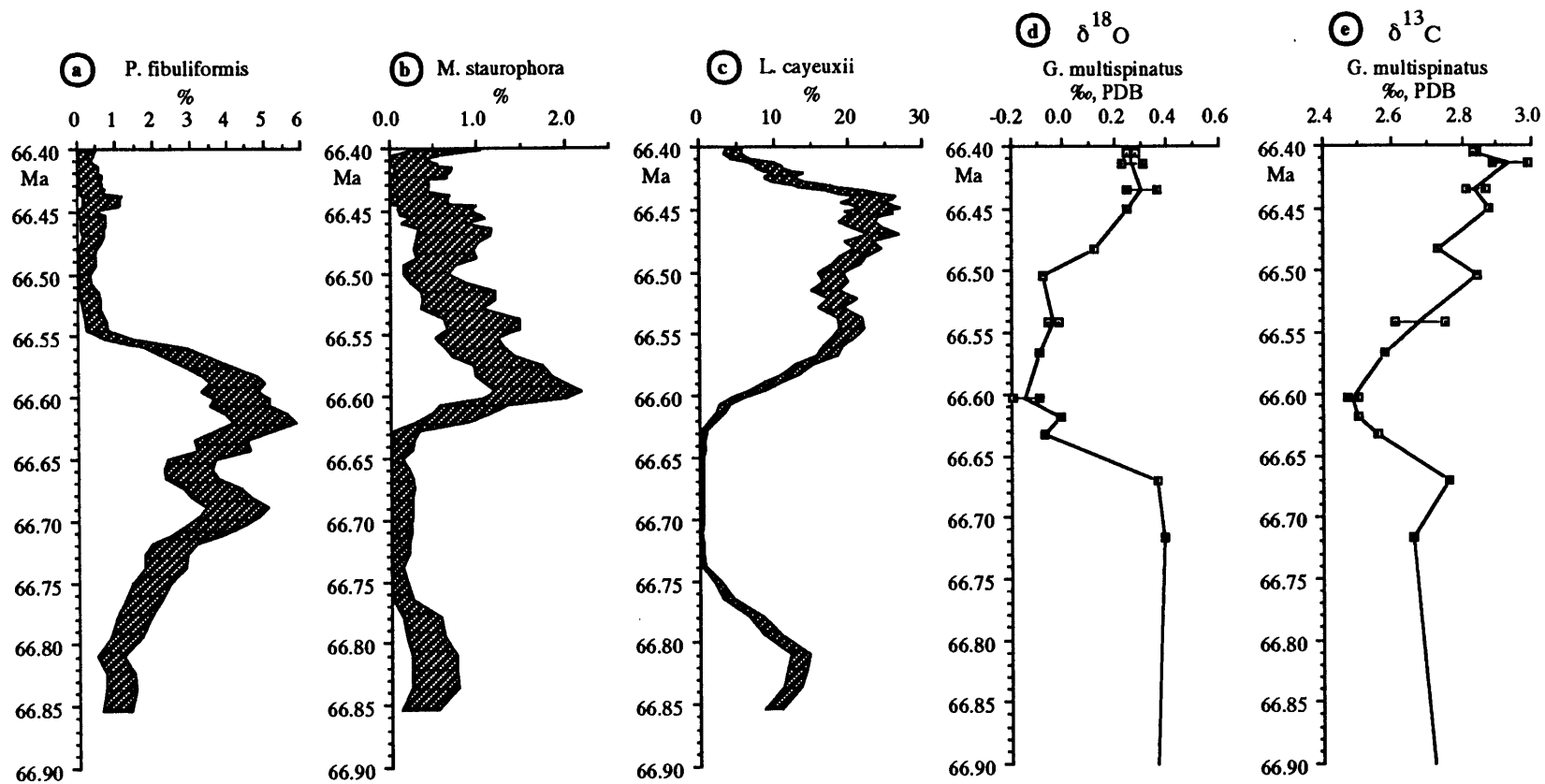


Figure 65: Abundance variations in three calcareous nannoplankton taxa (*Placozygus fibuliformis*, *Micula staurophora*, *Lucianorhabdus cayeuxii*) and stable isotope records from southern high latitudes (ODP Hole 690C). The relative abundance of the nannoplankton taxa were calculated under exclusion of *Prediscosphaera stoveri*. A running five point average was calculated and the shaded band represents the approximate 95% confidence interval (after Mosiman, 1965). Stable isotope data from Stott and Kennett, 1990).

on plant fossils (Johnson, 1992). This may indicate that the warming pulse in the latest Maestrichtian was not restricted to high southern latitudes.

The $\delta^{13}\text{C}$ record of G. multispinatus shows increasing values between ~66.6 and 66.4 Ma but the $\delta^{13}\text{C}$ record of A. mayaroensis decreased during the same interval; this latter record is discarded in this discussion because of very few data points. Stott and Kennett (1990) reported that the $\delta^{13}\text{C}$ increase prior to the K/P boundary in Hole 690C was part of a global pattern reflecting a redistribution of carbon between different reservoirs. Zachos et al. (1989) suggested that the positive $\delta^{13}\text{C}$ excursion prior to the K/P boundary in the equatorial Pacific (Site 577) may have been caused by changes in circulation.

The increased abundances of P. fibuliformis and its abrupt decline between ~66.60 and 66.55 Ma does not correlate with any of the observed stable isotope changes (Figure 65a). A similar lack of correlation of calcareous nannoplankton abundance patterns and stable isotope variations was also reported in the late Miocene of the North Atlantic (Beaufort and Aubry, 1990) and in the Miocene of the southern Indian Ocean (Beaufort and Aubry, 1992). Placozygus fibuliformis was observed more abundantly in mid- and low latitudes (this study), but it is unresolved whether this biogeographic pattern reflects temperature preferences.

Lucianorhabdus cayeuxii (Figure 65b) was present between ~66.85 and 66.75 Ma, it was absent between ~66.74 and 66.62 Ma. This species started to increase in abundance at ~66.62 Ma, reached maximum values (~20%) at ~66.55 Ma, remained at these high values 66.43 Ma, and decreased in abundance to comparatively low values (<5%) between 66.43 and 66.40 Ma. Insufficient stable isotope data points are available to elucidate the interval between 66.85 and 66.76 Ma (Figure 65d, e). The beginning of the abundance increase of L. cayeuxii started as soon as the warming pulse was fully established (based on the $\delta^{18}\text{O}$ record of G. multispinatus). No decline in the abundance of L. cayeuxii is observed between ~66.5 and 66.45 Ma when the $\delta^{18}\text{O}$ record of G. multispinatus indicated that surface water temperatures cooled again. An abundance decrease of L. cayeuxii was recorded only when temperatures had dropped to the same values as before the warming pulse (between ~66.45 and 66.40 Ma; $\delta^{18}\text{O}$ record of G. multispinatus). These patterns may indicate that L.

cayeuxii thrived during the maximum of the warming pulse and also during its decline, but that it decreased in abundance when temperatures fell below a certain threshold value. The implied temperature sensitivity of L. cayeuxii is not reflected by any abundance changes during the incipient phase of the warming pulse (between ~66.76 and 66.62 Ma), when the change in water temperature was almost the mirror image of that recorded between ~66.5 and 66.45 Ma. A similar, non-linear correlation of L. cayeuxii with temperature is also apparent from previously published abundance patterns of this species: due to its abundance peak in high latitudes Lucianorhabdus cayeuxii is considered a high latitude taxon possibly indicative of cooler surface waters (Thierstein, 1981) but Worsley (1974) pointed out that in high latitudes this species was present during the entire Maestrichtian, while in low latitudes it occurred only during the early Maestrichtian. My data indicate that this taxon did not disappear completely from mid- and low latitudes, since it was recorded very rarely in all mid- and low latitude sections (Table 6). Worsley (1974) did not report exactly at what time L. cayeuxii disappeared from (or became very rare in) low latitudes, but my data suggest that its disappearance/abundance decrease must have occurred prior to ~71 Ma. The reason for the disappearance of L. cayeuxii from low latitudes is unclear, because low latitude surface waters cooled during the Maestrichtian (e.g. Douglas and Savin, 1975) and should have become more hospitable for a high latitude dweller. I conclude that L. cayeuxii cannot be considered a temperature indicator exclusively.

The abundance pattern of L. cayeuxii could be explained as a consequence of circulation changes (and nutrient availability?) as expressed by the changes in the $\delta^{13}\text{C}$ record because the beginning abundance increase of L. cayeuxii at ~66.61 Ma coincides with the increase in the $\delta^{13}\text{C}$ of G. multispinatus (Figure 65b, e). However, no changes in the $\delta^{13}\text{C}$ record are discernible while L. cayeuxii decreased in abundance (between ~66.45 and 66.40 Ma).

Micula staurophora increased sharply in abundance at ~66.62 Ma (Figure 65c), reached peak abundances of almost 2% at 66.60 Ma and gradually decreased in abundance to <0.5% between 66.60 and 66.40 Ma. The peak abundance at 66.60 Ma coincided exactly with the beginning of the warming pulse indicated by the $\delta^{18}\text{O}$ record. It is possible that the increased abundance values of M. staurophora at 66.60 Ma were caused by increased water

temperatures. The interpretation of M. staurophora as a temperature sensitive taxon is in agreement with its latitudinal distribution during the Maestrichtian (Wind, 1979a; Thierstein, 1981) and has been proposed previously (Doeven, 1983). However, the decrease in abundance of M. staurophora between 66.60 and 66.50 Ma, when oxygen isotope data still indicated high surface water temperatures remains unexplained. It is possible that changes in the circulation pattern (suggested by the $\delta^{13}\text{C}$ record; Figure 65e) led to the establishment of deleterious environmental conditions for M. staurophora.

From the stable isotope results and the nannofossil patterns in the uppermost Maestrichtian in Hole 690C the following conclusions can be reached:

- (i) Stable isotope data of higher resolution are required to determine unambiguously the timing of the oxygen and carbon isotope changes.
- (ii) The negative $\delta^{18}\text{O}$ excursion between ~66.60 and 66.40 Ma is interpreted as a warming pulse of ~2°C and not as a low-salinity signal, because it affected the entire water column and independent evidence from plant fossils also suggests a short period of elevated temperatures.
- (iii) The abundance changes of most calcareous nannoplankton taxa do not correlate with the $\delta^{18}\text{O}$ variations ("warming pulse").
- (iv) The abundance increase of M. staurophora may be a consequence of increased surface water temperatures; its decrease during times of elevated surface water temperatures is not satisfactorily understood. It is possible that changes in ocean circulation as indicated by the $\delta^{13}\text{C}$ record led to environmental changes that were deleterious for this species.
- (v) The elevated abundances of L. cayeuxii between ~66.62 and ~66.45 can be interpreted as a consequence of increased nutrient availability. It is possible that the abundance decrease of L. cayeuxii between ~66.45 and 66.40 Ma reflects cooler surface waters.
- (vi) The abundance changes of P. fibuliformis, especially the abrupt decrease between 66.60 and 66.55 Ma does not correlate with variations in the stable isotope records suggesting that this species did not respond linearly to changes recorded by the stable isotopes (e.g. temperature changes, nutrient availability, etc).

(b) Mid-latitude trends

Changes in abundance of selected nanoplankton species were observed to occur in mid-latitudes but the species which displayed the most pronounced changes were different in the Atlantic and the Indian Ocean. In the mid-latitude Atlantic Ocean (Hole 528) the abundance changes of selected taxa occurred around 67.0 Ma (Figure 66). Biscutum constans, C. kamptneri, and E. parallelus (Figure 66a, b, c) decreased significantly in abundance at that time, whereas T. macleodae (Figure 66d) increased. Zygodiscus sp. 1 (Figure 66e) also fluctuated significantly in abundance; this species reached an abundance peak between ~66.70 and 66.60 Ma. No sufficiently detailed stable isotope records are available to compare with the nanoplankton abundance changes. Biscutum constans has been interpreted as a fertility indicator (Roth and Bowdler, 1981) and it is possible that its decrease in abundance between ~67.1 and 67.0 Ma reflects a reduction in nutrient availability at that time. If this is the case, then the abundance changes of C. kamptneri, E. parallelus and T. macleodae may also result from decreased nutrient availability. However, these conclusions are tentative until more detailed stable isotope records are available. No detailed nanoplankton records from the same time interval (~67 Ma) are available for comparison from the other sections studied. The cause for the abundance increase of Zygodiscus sp. 1 remains unclear at the moment.

In the sections investigated in the mid-latitude Indian Ocean (Holes 761B and 217) similar taxa display abundance variations: in both holes N. frequens, C. daniae, and Vagalapilla spp. increase in abundance during the last ~100 ky of the Maestrichtian (Figures 67 and 68). These three taxa are well known for their abundance maxima in high latitudes (e.g. Thierstein, 1981). There is some evidence (see discussion below) that N. frequens is indicative of cooler water temperatures and it is suggested that the abundance increase of this species in the mid-latitude Indian Ocean indicates cooling of surface waters during the last ~100 ky of the Maestrichtian. The concomitant abundance increase of two other high latitude taxa (C. daniae and Vagalapilla spp.) seems to support this argument.

An abundance decrease of P. fibuliformis was recorded in both Indian Ocean sites after ~66.65 Ma, but whereas this decrease occurs gradually (~66.65-66.40 Ma) in Hole 761B (Figure 67d) it is fairly abrupt (~66.65-66.60 Ma) in

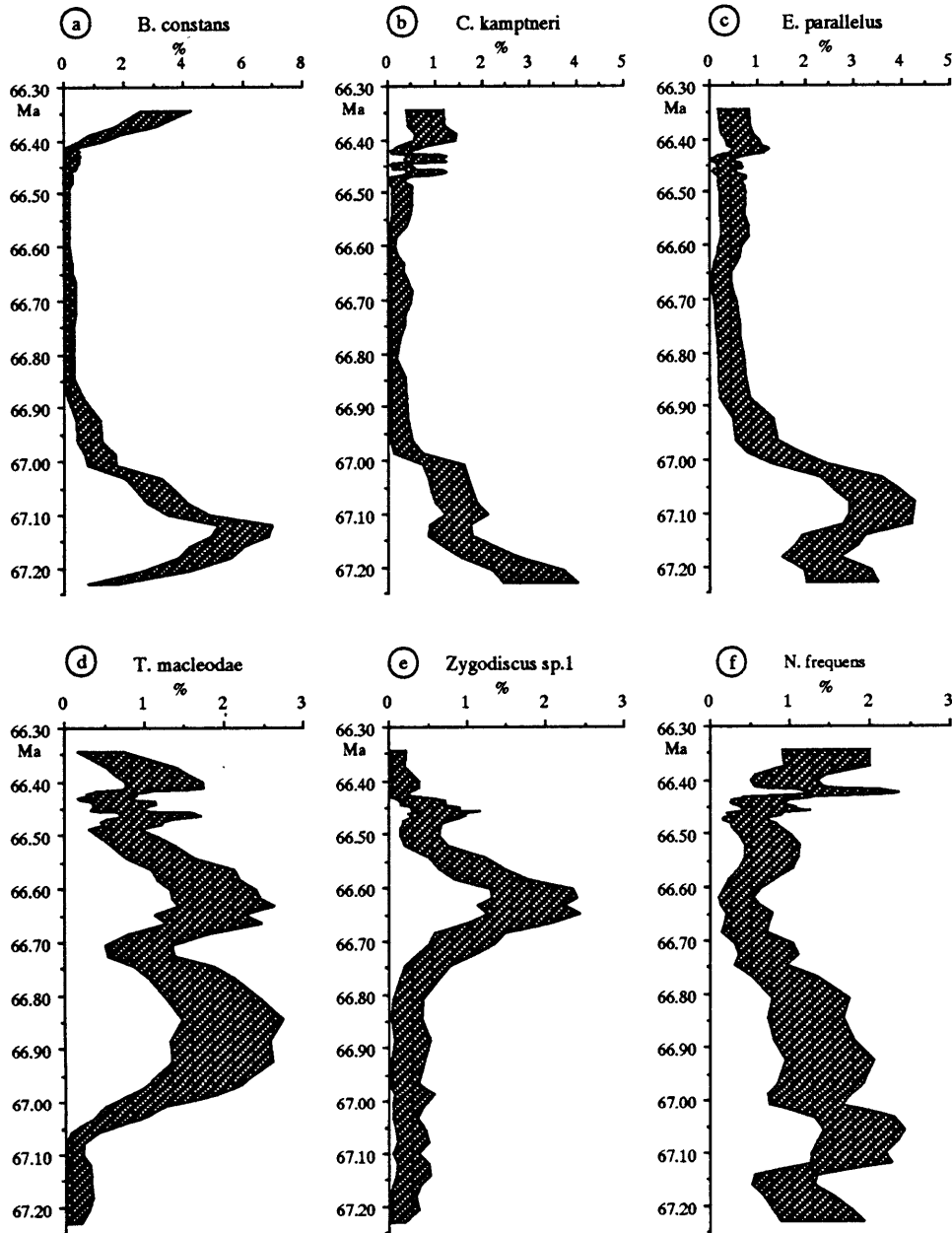


Figure 66: Abundance variations of selected calcareous nannoplankton taxa in mid-latitudes in the Atlantic Ocean (DSDP Hole 528). A running five point average was calculated on the data and the shaded band represents the 95% confidence interval. The Cretaceous/Paleocene boundary lies at 66.4 Ma.

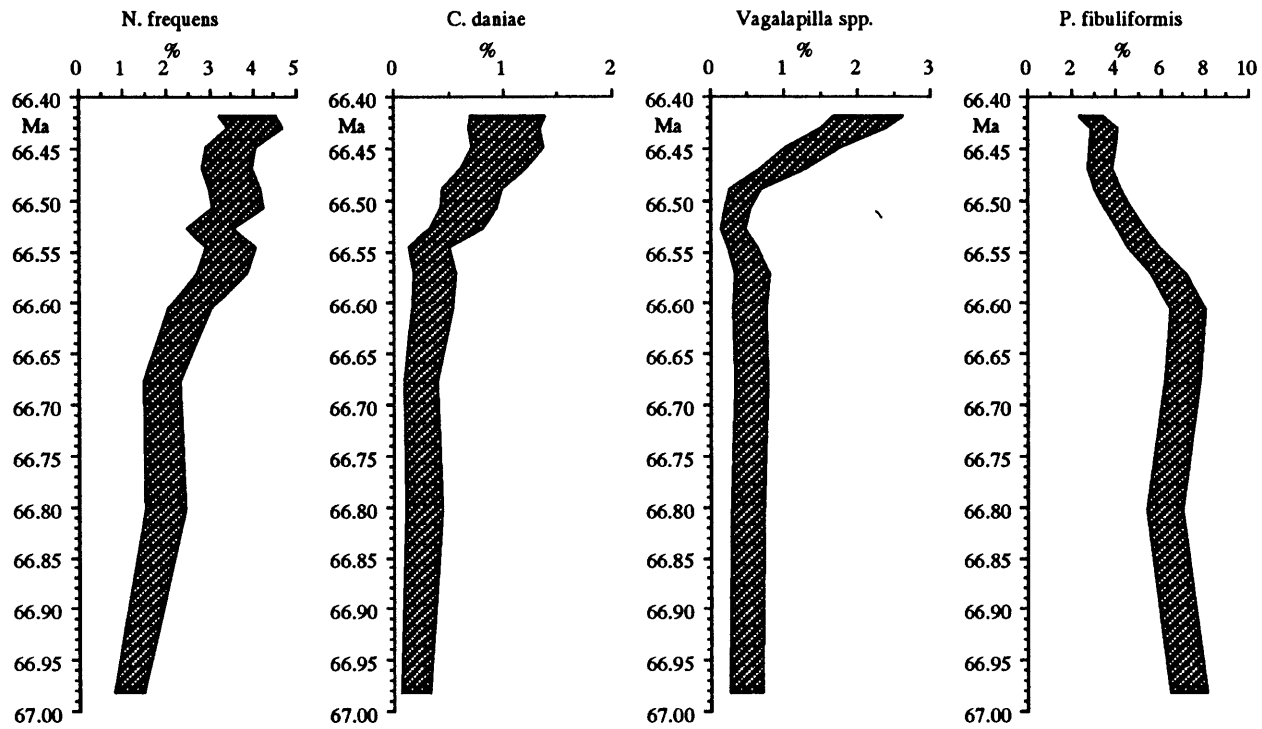


Figure 67: Abundance variations of selected calcareous nannoplankton taxa in mid-latitudes in the Indian Ocean (ODP Hole 761B). The Cretaceous/Paleocene boundary lies at 66.4 Ma. See note in caption of Figure 57.

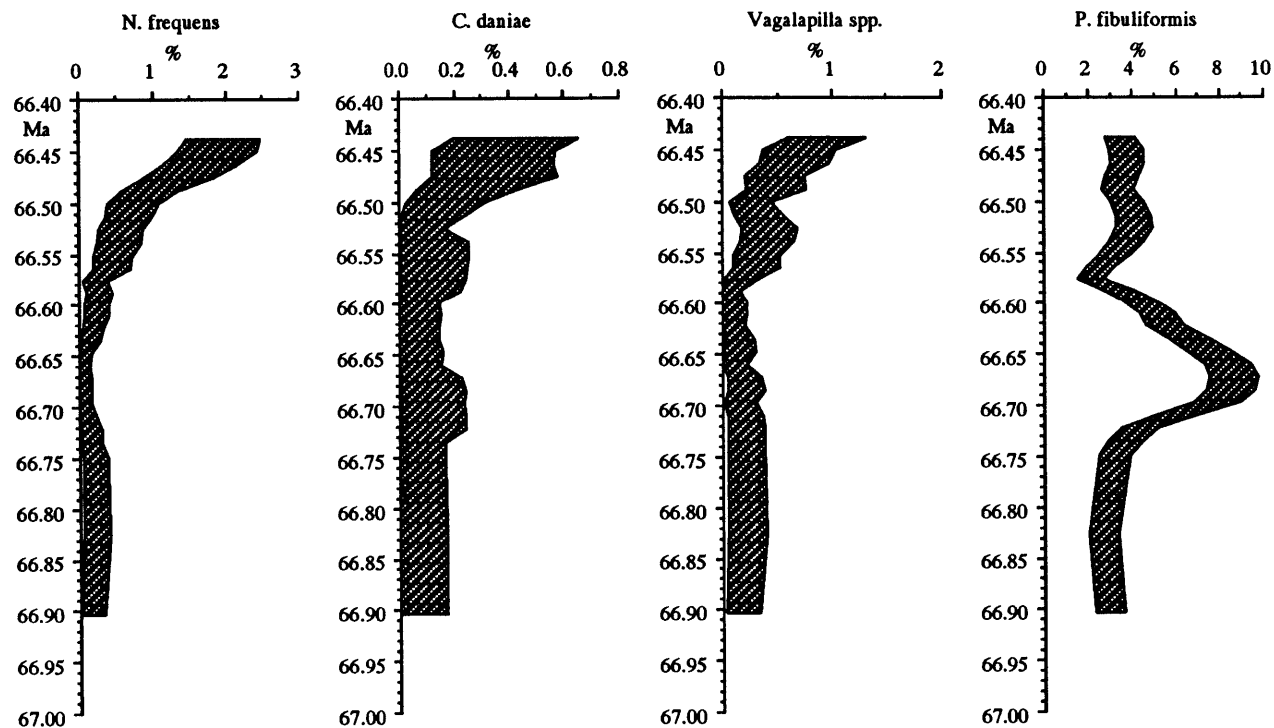


Figure 68: Abundance variations of selected calcareous nannoplankton taxa in mid-latitudes in the Indian Ocean (ODP Hole 217). The Cretaceous/Paleocene boundary lies at 66.4 Ma. See note in caption of Figure 57.

Hole 217 (Figure 68d). In fact the abundance pattern of P. fibuliformis in Hole 217 is similar to that observed in high southern latitudes (Hole 690C, Figure 65a); it also occurred virtually at the same time at these two sites. No comparable abundance fluctuations of this species were observed in the mid-latitude Atlantic Ocean.

The fact that different nanoplankton species displayed significant abundance fluctuations during the last ~500-800 ky of the Maestrichtian is interpreted here as a consequence of different environmental changes (possibly reflecting different water masses) in the high southern Atlantic Ocean, the mid-latitude Atlantic Ocean and the mid-latitude Indian Ocean. No species displayed comparable abundance variations during the latest Maestrichtian in the different ocean basins covered here. The similarity of the abundance record of P. fibuliformis between the high southern Atlantic Ocean and the mid-latitude Indian Ocean is considered an exception.

In contrast to the heterogeneous short term (~500-800 ky) abundance fluctuations, some species showed similar long term (throughout the entire Maestrichtian) abundance trends in all ocean basins. These trends are discussed below.

(C) Paleoenvironmental Significance of Selected Nanoplankton Species.

(a) Previous Studies

Geographic abundance gradients of Mesozoic nanoplankton species have been interpreted as a consequence of environmental differences. Latitudinal abundance gradients were most often explained as an expression of temperature preference (e.g. Thierstein, 1976; Thierstein, 1981; Wise, 1983). The other environmental parameters invoked were nutrient availability (e.g. Roth and Bowdler, 1981) and water depth (e.g. Thierstein, 1976).

Roth and Bowdler (1981) investigated mid-Cretaceous nanoplankton abundance patterns and observed abundance differences of numerous taxa between continental margin and oceanic associations. In neritic nanoplankton associations they observed comparatively rapid fluctuations of species abundances and monospecific horizons (which they explained as "blooms" of certain taxa during increased nutrient availability). These authors

explained the nanoplankton patterns in the neritic sites as a consequence of high nutrient availability near continental margins and denoted those taxa that were more abundant in neritic sections (B. constans, Z. erectus, Z. elegans, Z. diplogrammus, Corollithion sp.) as high fertility indicators. Based on inverse reasoning Roth and Bowdler (1981) identified nanoplankton species that they considered low fertility indicators (W. barnesae, R. splendens, R. asper, possibly L. carniolensis). Roth and Krumbach (1986) expanded the data set of Roth and Bowdler (1981) and applied more sophisticated statistical analyses, confirming the previous findings. In order to exclude poorly preserved samples from their data Roth and Bowdler (1981) and Roth and Krumbach (1986) discarded samples in which the solution resistant species W. barnesae constituted >40% of the nannofossil assemblage.

Watkins (1989) examined calcareous nannofossil assemblages from Cenomanian-Turonian rhythmically bedded pelagic carbonates of the Western Interior (Greenhorn Limestone). He compared assemblages from chalks with those from interbedded marlstones and concluded that significant differences existed in the abundances of some taxa as well as in diversity and species richness. The biogeographic abundance patterns of Z. erectus, Biscutum constans, and Zeugrhabdotus elegans were correlated with each other and occurred more frequently in the marls than in the chalks. Opposite abundance trends were observed in E. turriseiffeli, T. phacelosus, P. spinosa, D. ignotus, T. stradneri, and L. carniolensis. In interpreting these abundance trends Watkins (1989) followed Roth and Bowdler (1981) and Roth and Krumbach (1986) considering the first group of taxa as high fertility indicators and the second as low fertility indicators. Watkins (1989) did not observe a correlation of W. barnesae with any other taxa (nor with lithology). In addition, Watkins (1989) observed that nanoplankton diversity (as expressed by the Shannon diversity index) was higher in assemblages in which the low fertility taxa dominated.

Premoli Silva et al. (1989) investigated organic carbon rich sediments of the Aptian-Albian Furoid Marls in central Italy. Factor analyses performed on calcareous nannofossil assemblages showed that Biscutum constans, Discorhabdus ignotus and Zygodiscus spp. loaded high on the same factor. From comparison with the results of Roth and Bowdler (1981) and Roth and Krumbach (1986) they concluded that these three taxa were indicative of high fertility in areas of vigorous upwelling. Similarly, they interpreted

Rhagodiscus asper and Lithraphidites carniolensis as indicators of moderate fertility and warmer waters.

Erba et al. (1992) investigated calcareous nannofossil assemblages from the Albian Gault Clay Formation (southern England). Preservation of the calcareous nannofossils was good and she indicated that the abundance variations observed were not a consequence of differential dissolution. This was further supported by the fact that W. barnesae was never excessively abundant (<~25% in all samples). The abundance variations of W. barnesae and B. constans were inversely correlated in agreement with the results of Roth and Bowdler (1981). Consequently, Erba et al. (1992) interpreted these species as low and high fertility indicators, respectively.

All of the taxa interpreted as fertility indicators in studies of mid-Cretaceous nannoplankton were latitudinally restricted to mid and low latitudes during the Maestrichtian and some of them exhibited very conspicuous abundance changes during this time.

(b) Biscutum constans

Abundance decrease: An abundance decrease of this species has been observed in all sections investigated (Figure 69). It began in the early Maestrichtian in high latitudes and during the late Maestrichtian in mid-southern latitudes (Figure 69). A comparison with published data (Wind, 1979a; Thierstein, 1981; Doeven, 1983) also revealed decreasing abundances of B. constans throughout the Maestrichtian.

Geographic distribution of the abundance decrease: An investigation of the count data of Wind (1979a: table 6) reveals that the abundance decrease of B. constans occurred in several sections. In DSDP Hole 217 (Wind, 1979a) it occurred at exactly the same level where it was found in this study: >6% at and below Section 217-21-1; <1% at and above Section 217-19-1; in this study the decrease was observed between Sections 217-19-4 and 217-19-2. In DSDP Hole 216 a decrease at the same level (compare Wind, 1979a: figure 14, p. 110) was observed by Wind (1979a) although only two samples document this trend there. In DSDP Hole 249 an abundance decrease of B. constans (from >15% in most samples to <10%) was recorded in the lower Maestrichtian (compare Wind, 1979a: figure 14, p. 110). In DSDP Hole 357 an abundance decrease of B. constans is apparent from Wind's (1979a) data; its exact level is difficult to delineate due to a coring gap across which the

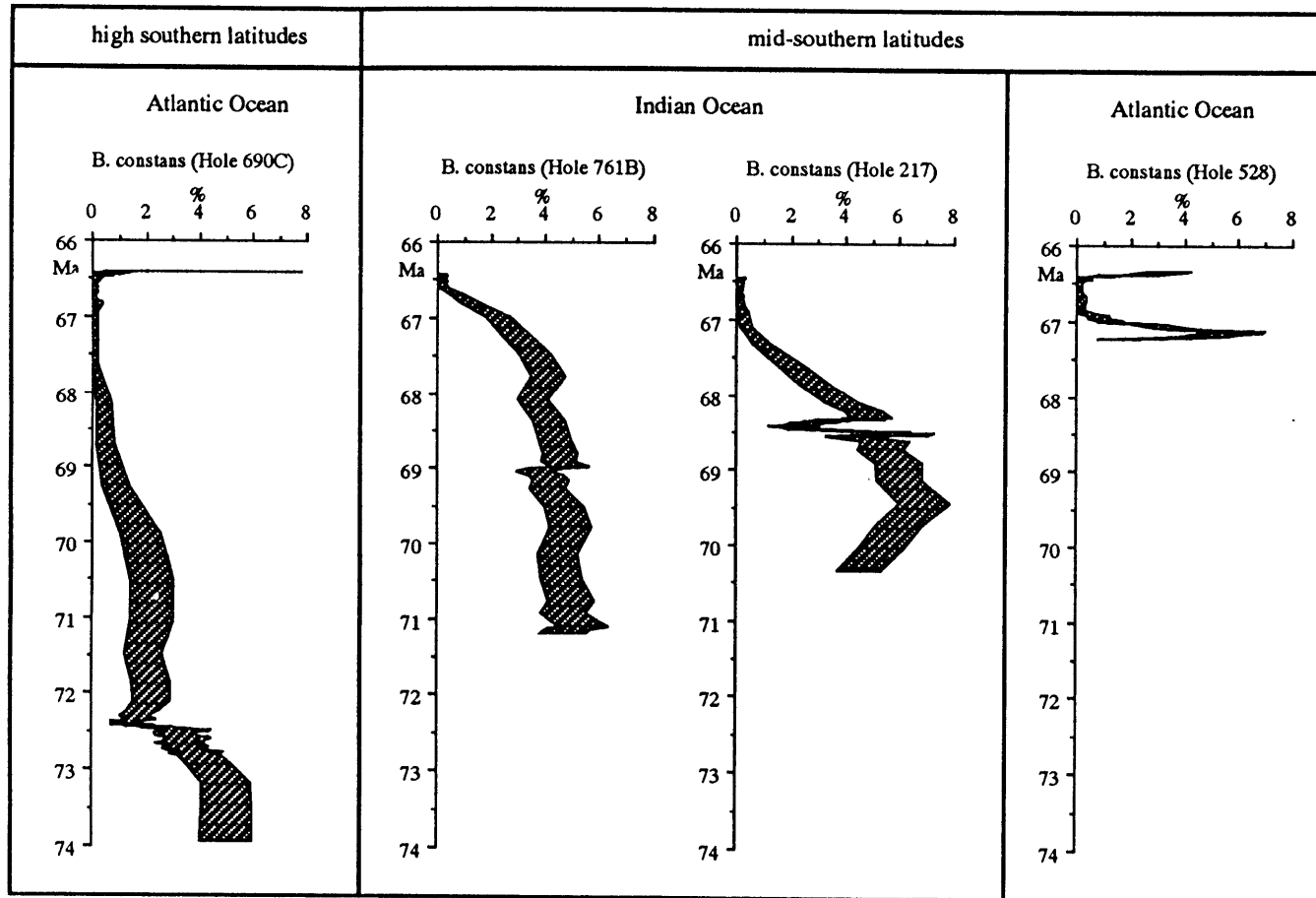


Figure 69: Comparison of the abundance variations of *Biscutum constans* in different latitudes and different ocean basins during the Maestrichtian. This species decreased in abundance in all holes, but the timing and abruptness of the decreases were different in all sections investigated. The K/P boundary lies at 66.4 Ma. *Biscutum constans* is a persistent species (i.e. survives the extinctions at the K/P boundary) and abruptly increased in abundance in the earliest Paleocene in Holes 690C and 528. No Paleocene samples were examined in Holes 761B and 217.

abundance change was recorded but it occurred near the boundary between Q. trifidum Zone and A. cymbiformis Zones (lower Maestrichtian; Perch-Nielsen, 1977; DSDP Vol. 39). In DSDP Hole 10 (central North Atlantic) the decrease of B. constans (from ~>4% to <1%) occurs at the base of the L. quadratus Zone (Data of Wind, 1979a).

An abundance decrease of B. constans is not apparent from Thierstein's (1981) study. In DSDP Hole 356 (South Atlantic), DSDP Hole 384 (North Atlantic), and in the low latitude shelf section at Braggs, Alabama, B. constans was recorded but did not change in abundance throughout the Maestrichtian (Thierstein, 1981). This species was not recorded from DSDP Hole 47.2 (tropical Pacific).

Doeven (1983) documented an abundance decrease of Biscutum spp. during the Maestrichtian, but it is not clear which species he observed, and his sample resolution is very low (see above).

The observations above indicate that although the abundance decrease of B. constans during the Maestrichtian was not restricted to the southern hemisphere, it did not occur worldwide. They also support my observation that this decrease did not occur simultaneously at different latitudes (Figure 69).

Biscutum constans has been interpreted alternatively as high fertility indicator (e.g. Roth and Bowdler, 1981) and as temperature indicator due to its highest abundances in high mid-latitudes (Wind, 1979a). My investigations showed that the abundance of B. constans decreased in high southern latitudes throughout the Maestrichtian. During the same time interval a cooling trend is indicated by the oxygen isotope record. This may be interpreted as a causal relation, indicating that B. constans decreased because surface waters became too cool and supporting Wind's (1979a) suggestion that this species is a (warm) temperature indicator.

At the same time there is evidence for increased surface water fertility during the late Maestrichtian (see discussion above) and the fact that B. constans did not increase in abundance seems to contradict its interpretation as a high fertility indicator (Roth and Bowdler, 1981). It is possible that abundance changes of this species reflect fertility changes as long as surface water temperatures remain within certain boundaries, but that this species disappears independent of nutrient availability if surface water temperatures exceed its ecological tolerance. It is suggested here that the abundance

decrease of B. constans in high southern latitudes was a consequence of cooling beyond the ecologic tolerances of this species, but that its decrease in mid-latitude sections could be due to decreasing nutrient availability.

(c) Discorhabdus ignotus

Decreasing abundances of D. ignotus in the late Maestrichtian were observed in two mid latitude sections (Holes 217 and 528) in this study but an increase in the epicontinental section at Millers Ferry is also observed. Like B. constans this species has also been interpreted as high fertility indicator (see above). Its abundance decrease supports the possibility of decreasing nutrient availability during the late Maestrichtian in mid latitudes.

In the Millers Ferry Section this species gradually increased in abundance between ~66.60 and 66.42 Ma (from ~3% to ~>5%). At ~66.41 Ma it increased almost threefold in abundance (from ~5% to ~15%). Since there is a hiatus at the K/P boundary, the true extent of this excursion is unknown.

(d) Nephrolithus frequens and other high latitude taxa

Nephrolithus frequens is more abundant in high than in mid- and low latitudes (e.g. Thierstein, 1981; Figure 70) and its abundance increased during the Maestrichtian in high southern latitudes in parallel with the temperature decrease indicated by the oxygen isotope record. This may indicate that N. frequens is indicative of comparatively cool surface water temperatures (e.g. Thierstein, 1981; Pospichal and Wise, 1990). The equatorward spread of the first appearance of N. frequens during the Maestrichtian (Figure 71) has usually been interpreted as reflecting progressive cooling of surface waters. On the other hand, no abundance decrease was observed at high southern latitudes during the warming pulse between ~66.65-66.50 Ma (Figure 72) suggesting that N. frequens is not a very sensitive temperature indicator and/or that abundance fluctuations of this taxon reflects changes in water mass structure or surface water fertility in addition to cooler temperatures.

The abundance increase of N. frequens during the last ~100 ky of the Maestrichtian at mid-latitudes in the Atlantic and Indian Oceans (Figure 70) possibly reflects decreasing surface water temperatures at these sites at the end of the Maestrichtian. Together with N. frequens, two other high latitude taxa also increased significantly in abundance during the last ~100 ky of the Maestrichtian in the mid-latitude Indian Ocean: C. daniae and Vagalapilla spp.

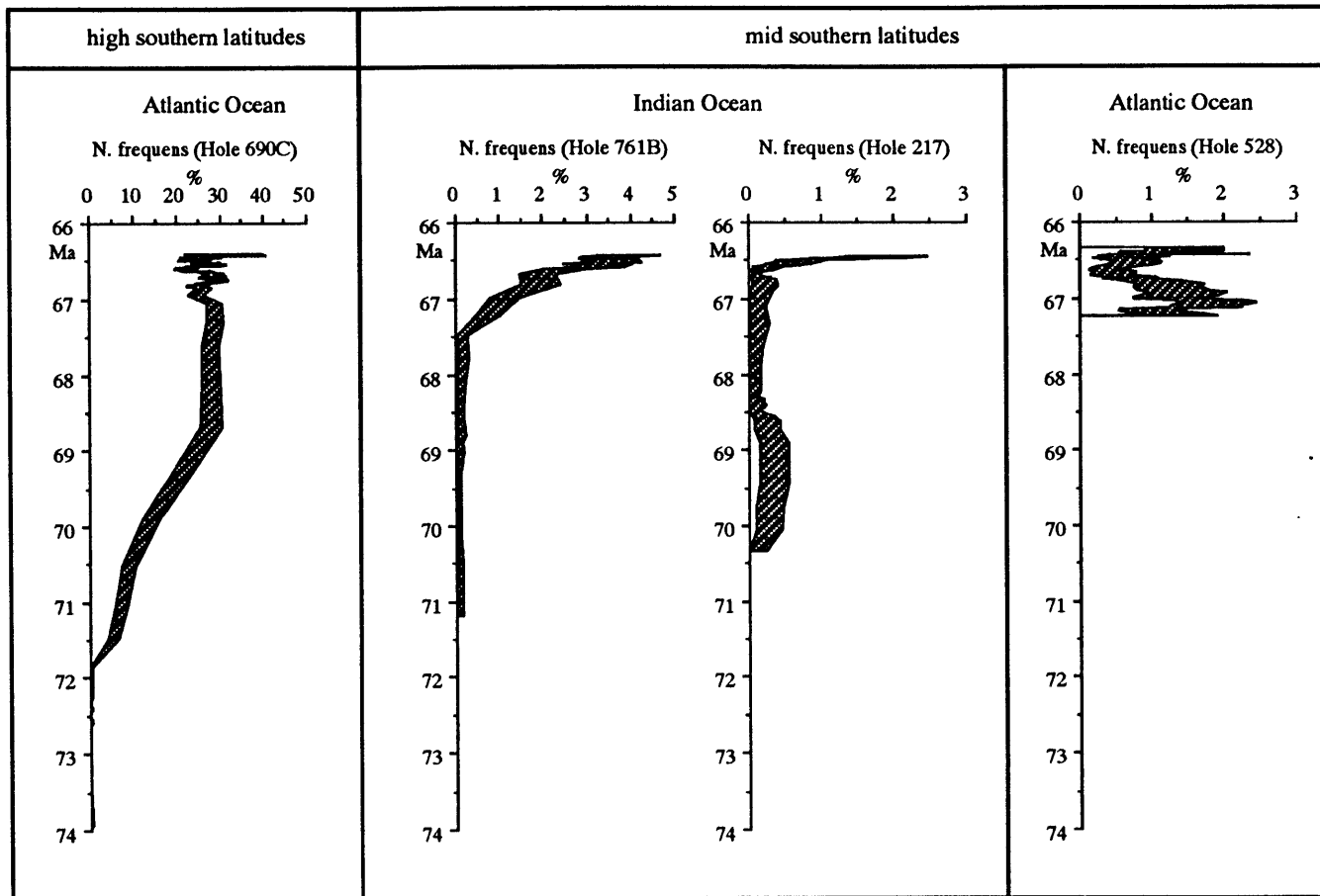


Figure 70: Comparison of the abundance variations of *Nephrolithus frequens* in different latitudes and different ocean basins during the Maestrichtian. This species increased in abundance much earlier in high southern latitudes than in the mid-latitude Indian Ocean.

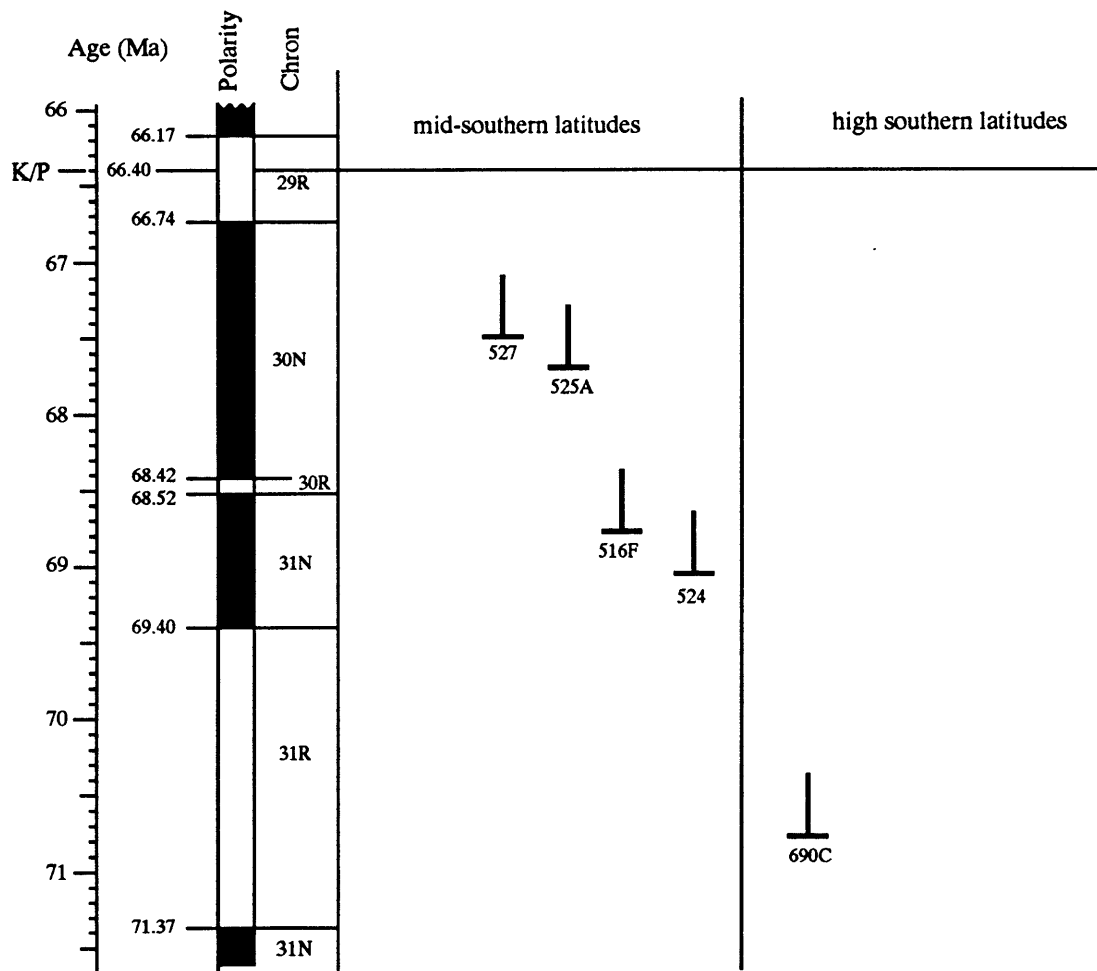


Figure 71: Comparison of the first appearances of *Nephrolithus frequens* compiled from DSDP- and ODP-Holes where magnetostratigraphic control is available.

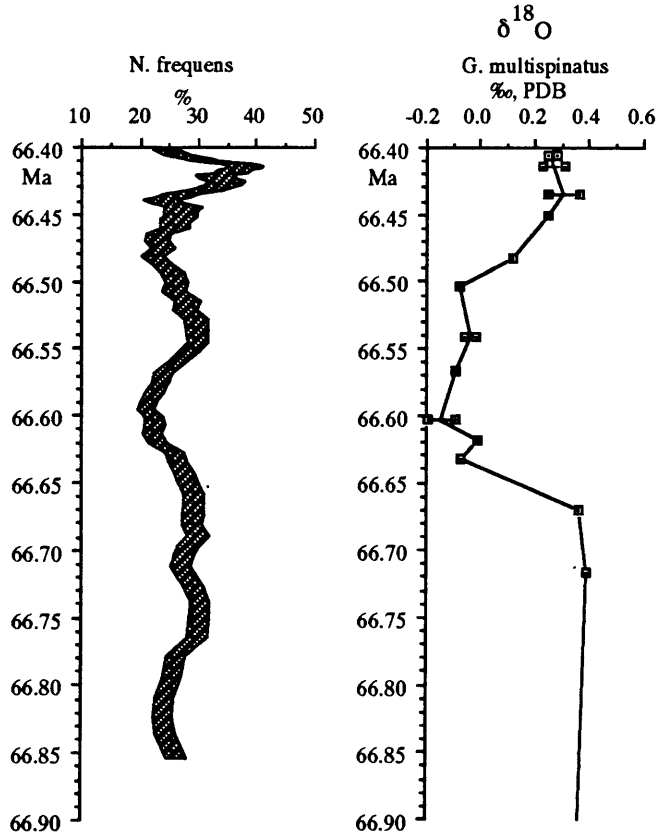


Figure 72: Abundance fluctuations of *Nephrolithus frequens* and the $\delta^{18}\text{O}$ record during the last ~500 ky of the Maestrichtian (66.9-66.4 Ma). The negative shift of the oxygen isotope values between ~66.65 and 66.50 Ma is interpreted as a warming pulse. No abundance decrease of the cool water indicator *N. frequens* is apparent during the warming pulse suggesting that this species is not a very sensitive temperature indicator and/or that its abundance fluctuations are not only reflecting temperature changes. Stable isotope data from Stott and Kennett (1990). The relative abundance of *N. frequens* was calculated exclusive of *P. stoveri*.

(Figures 67 and 68). Cribrosphaerella daniae increased in abundance in high southern latitudes throughout the Maestrichtian (in parallel with decreasing surface water temperatures); therefore its abundance increase in the latest Maestrichtian in the mid-latitude Indian Ocean may also suggest decreasing surface water temperatures. In contrast, Vagalapilla spp. decreased in abundance during the Maestrichtian suggesting that this high latitude taxon does not respond primarily (or exclusively) to changing surface water temperatures.

(f) Ahmuellerella octoradiata

This species was more abundant in high than in low latitudes during the Maestrichtian (e.g. Thierstein, 1981; this study; Table 6; Figure 73), which was sometimes interpreted as a preference for cooler waters. On the other hand, A. octoradiata decreased in abundance during the Maestrichtian in high and mid-latitudes (this study, Figure 73) when stable isotope records indicated global cooling and when most other high latitude taxa increased in abundance. The explanation for this abundance change is not obvious but is possibly related to fertility changes. Furthermore the abundance decrease through the Maestrichtian reinforces the warning that species with abundance peaks in high latitudes cannot automatically be interpreted as cool water indicators (e.g. Vagalapilla spp., see previous paragraph).

4) Implications of High Resolution Biogeographic Studies

Very closely spaced samples permitted a temporal resolution better than 5 ky for the last 60 ky of the Maestrichtian (represented by ~2.7m) in Hole 690C and during the last 75 ky (represented by ~7.5 m) in Hole 528.

Surprisingly high intersample variability was recorded in virtually all taxa in both holes. The sample spacing in Hole 690C was ~3-5cm and only minor abundance variability of individual nannoplankton taxa between samples had been expected, because (i) lithology (e.g carbonate content) and color are uniform (compare lithologic description in Chapter BIOCHRONOLOGY), and (ii) indications for intensive bioturbation are ubiquitous in the sediment (presumably obliterating any original short term abundance variations through sediment homogenization). The reason for the high intersample variability is not known. In most taxa this variability seems to be random and not cyclical (except maybe for C. ehrenbergii; compare Chapter RESULTS, HOLE

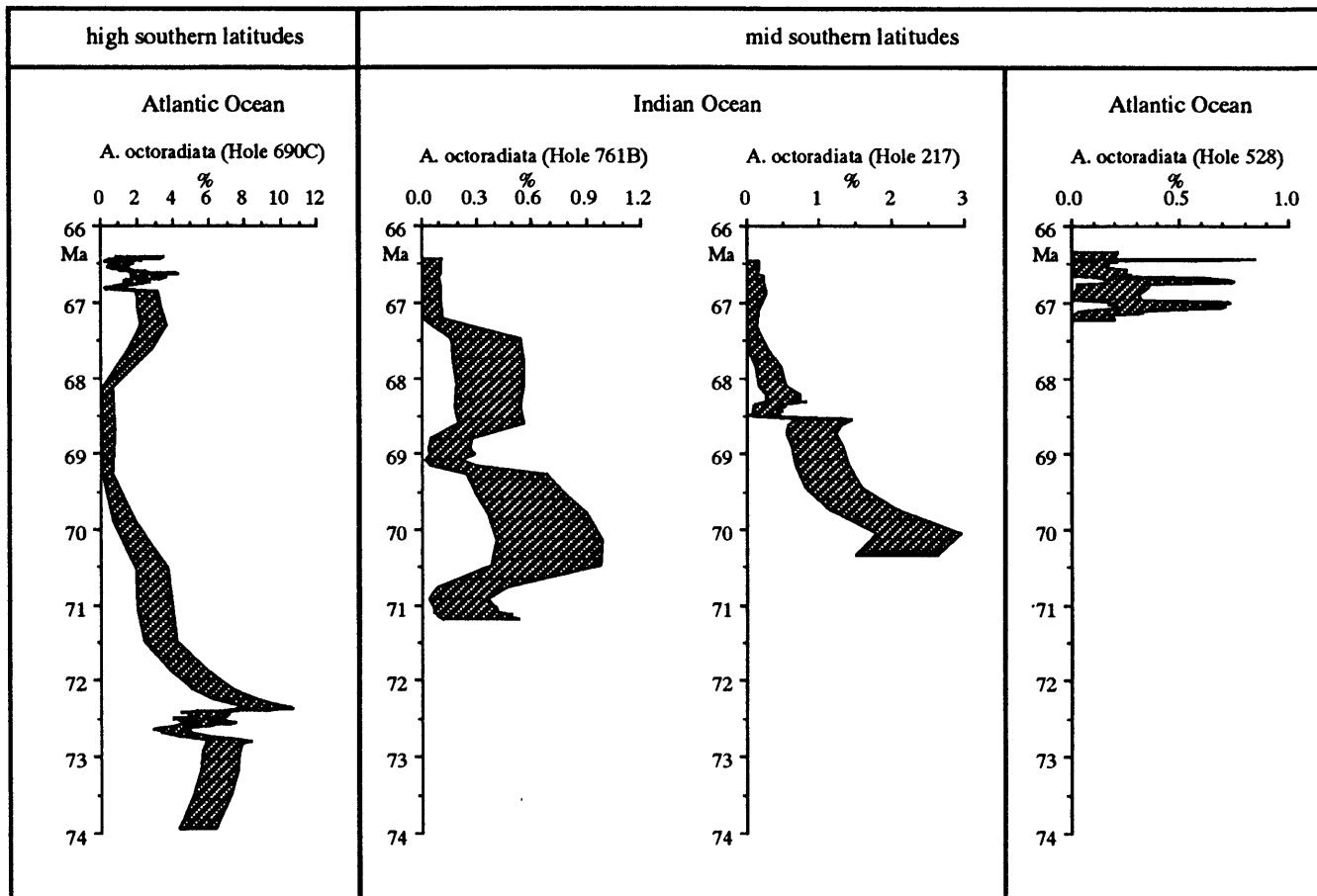


Figure 73: Comparison of the abundance variations of *Ahmuellerella octoradiata* at different latitudes and ocean basins. This species reached its highest abundances in high southern latitudes. Its abundance decreased throughout the Maestrichtian in all holes investigated when water temperatures decreased globally. *Ahmuellerella octoradiata* is therefore not interpreted as a cool water indicator, but possibly reflects changes in nutrient availability.

690C) but time series analyses will have to be used to decipher any genuine cyclicity.

Similar results of high intersample variability between closely spaced samples were obtained in Hole 528, where cyclical abundance variations were possibly recorded in *P. fibuliformis* and *P. stoveri* (but again, time series analyses will be necessary to evaluate these trends).

The high variability of nannoplankton species abundances between adjacent samples demonstrates the need of closely spaced samples to characterize genuine abundance trends. The abundance fluctuation of *P. fibuliformis* between ~66.85 and 66.4 Ma in Hole 690C (Figure 65a) is also apparent in the range chart of Pospichal and Wise (1990: table 2), but this interval is only covered by five samples and therefore the significance of these abundance changes was not recognized.

Similarly, in many cases it is impossible to interpret confidently the abundance fluctuations recorded in widely spaced samples (i.e. one sample every ~3 m) in Holes 690C, 761B, and 217 and only the most general trends can be derived.

High inter-sample variability was not restricted to the late Maestrichtian interval, but occurred in all time slices investigated. In order to recognize the statistically significant trends underlying this high variability a moving five-point average was calculated and is reported in the figures in this chapter.

5) IMPLICATIONS FOR CALCAREOUS NANNOPLANKTON EXTINCTIONS AT THE K/P BOUNDARY

My detailed investigations of abundance changes of calcareous nannoplankton taxa do not indicate a gradual loss of species nor stepwise extinctions during the last ~500 ky of the Cretaceous. The nannofossil data thus do not support sequential turnover and stepwise extinctions of planktonic foraminifera reported from several sections (El Kef, Tunisia: Keller, 1988; Brazos River, Texas: Keller, 1989). Conspicuous abundance changes of few taxa were demonstrated during this time interval (~67-66.4 Ma) which are believed to reflect environmental perturbations, but no extinctions could be demonstrated to occur at the same time. There is no evidence in my data that

the environmental perturbations inferred from fluctuations of stable isotopes and selected nannoplankton taxa imposed a stress on the calcareous nannoplankton rendering them particularly vulnerable to extinction: relative abundances of most taxa did not change systematically during the last ~500 ky of the Cretaceous.

The abundance fluctuations recorded during the last ~500 ky of the Maestrichtian are not unusual compared to abundance fluctuations recorded in intervals of high sample density earlier in the Maestrichtian (compare e.g. the abundance fluctuations of B. constans between ~68.6-68.3 Ma in Hole 217 with those between ~67.2-66.4 Ma in Hole 528; Figure 69c, d). This implies that environmental perturbations were not restricted to the last ~500 ky of the Cretaceous, but characterized the entire Maestrichtian. Judging from the nannoplankton results it would be expected that high-resolution stable isotope records during earlier parts of the Maestrichtian should document environmental perturbations similar to those during the latest Maestrichtian (~67-66.4 Ma).

There is no evidence in my data that calcareous nannoplankton associations in high latitudes were affected by environmental stress to a greater degree than in low latitudes during the last ~500 ky of the Maestrichtian. This contradicts the predictions of Stanley (1984) who argued that global cooling was the cause for the extinctions at the K/P boundary.

6) SUMMARY

Investigations of evolutionary and biogeographic patterns in Maestrichtian calcareous nannoplankton yield the following results.

1) Major differences in the early and the late Maestrichtian nannoplankton associations existed in high southern latitudes. Over 50% of all taxa became either extinct or restricted in their geographic distribution to mid- and low latitudes. Most of the extinctions and emigrations occurred in the late early and early late Maestrichtian (between ~71.4 and ~70.4 Ma). During this time interval less pronounced assemblage changes were also recorded in planktonic and benthic foraminifera.

2) Oxygen isotope records of planktonic and benthic foraminifera indicate progressive cooling of water masses during the entire Maestrichtian in high southern latitudes with a cooling pulse at ~71 Ma (early part of Chron 31R). A (possibly global) brief negative carbon isotope excursion occurred at ~71 Ma and may be a consequence of the sea-level fall in the mid-Maestrichtian.

3) Many of the nannoplankton taxa that became extinct between 72.4 and 70.4 Ma were restricted to or most abundant in high southern latitudes in the Atlantic and Indian Ocean (austral taxa). It would appear that they became extinct as a consequence of increases in nutrient availability, reduction in the stratification of the photic zone, or changes in salinity, caused by changes in surface circulation as a consequence of a sea level fall.

The emigrations of numerous taxa from high latitudes is interpreted as a response to progressive cooling in high latitudes.

4) In high southern latitudes an abundance increase of Micula staurophora coincided with the beginning of a warming pulse indicating that abundance changes of this species may be due to temperature fluctuations. Previously, abundance fluctuations of this highly solution resistant species have mostly been interpreted as an indicator of preservation.

5) Significant abundance fluctuations were recorded in several other nannoplankton taxa during the last ~500-800 ky of the Maestrichtian. Abundance fluctuations of similar magnitude were also recorded in the early and early late Maestrichtian, indicating that environmental perturbations were not restricted to the latest Maestrichtian.

6) A conspicuous feature of the calcareous nannoplankton assemblage is the lack of abundance changes in numerous high-latitude taxa (i.e. taxa that are most abundant in high latitudes and rare or absent from low latitudes) during a warming pulse of ~2°C. This may indicate that high-latitude taxa have wide temperature tolerances or that their abundance fluctuations are not exclusively due to temperature changes.

7) Abundance changes in two taxa are of particular interest. An abundance decrease of B. constans was recorded in all sections studied. It occurred

diachronously in different sections and is attributed to local decreases in surface water fertility.

Ahmuellerella octoradiata was more abundant in high than in low latitudes during the Maestrichtian but decreased in abundance throughout the Maestrichtian in all latitudes when stable isotope records indicated progressive cooling of surface waters. This indicates that the higher abundance of A. octoradiata in high latitudes does not reflect its preference for colder surface waters. This observation indicates that high latitude taxa should not automatically be interpreted as indicative of lower water temperatures.

8) No stepwise extinctions and no gradual loss of species were recorded among the calcareous nannoplankton during the last ~500 ky of the Cretaceous.

CHAPTER 6 SYNOPSIS

The following discussion summarizes the major findings of this study and highlights correlations between the biogeographic evolution of the marine calcareous plankton during the Maestrichtian and major oceanographic and climatic events. These events are graphically summarized in Figures 74 and 75.

Maestrichtian calcareous nannoplankton are characterized by pronounced latitudinal provincialism: numerous species display abundance gradients across latitudes and/or are endemic to high or low latitude regions (e.g. Wind, 1979a; Thierstein, 1981; this study). This study shows that a significant turnover occurred in the late early and early late Maestrichtian (between ~72.4 and 70.4 Ma) when about one third of all taxa in high southern latitudes became extinct (including all taxa endemic to the austral realm. During the same time interval another third disappeared regionally (Figure 74.2) restricting their geographic distribution to mid and low latitudes where they persisted until the end of the Cretaceous (66.4 Ma).

Ahmuellerella octoradiata and Nephrolithus frequens are both more abundant in high than in low latitudes and it has been implied (Thierstein, 1981) that high latitude taxa preferred colder water temperatures. These two species, however, have opposite abundance trends during the Maestrichtian (Figure 74). When stable isotope evidence suggests gradual global cooling of surface waters, the abundance of A. octoradiata decreased whereas that of N. frequens increased, suggesting that N. frequens may have preferred lower temperatures and that A. octoradiata was insensitive to the cooling. In addition, the first occurrence of N. frequens appears to be diachronous, occurring progressively later (calibrated against paleomagnetic stratigraphy) in mid- and low than in high latitudes, in agreement with the hypothesis that this species migrated equatorward in response to decreasing surface water temperatures (Pospichal and Wise, 1990).

Biscutum constans also decreased in abundance throughout the Maestrichtian (Figure 74). This abundance decrease occurred earlier in high than in low latitudes. According to Roth and Bowdler (1981) B. constans is a fertility indicator. Its abundance decrease during the Maestrichtian would suggest that nutrient availability decreased during the latest Cretaceous.

However, stable isotope records from high southern latitudes may be interpreted as a decrease in the stratification of surface waters, thus facilitating mixing of nutrients into the photic zone. The conflict in the interpretation of the abundance decrease of B. constans and the stable isotope record cannot be resolved with the data available, but it is likely that the abundance distribution of B. constans is not simply a fertility signal. Its distribution may also be influenced by temperature changes.

Pronounced provincialism during the late Campanian and early Maestrichtian was also reported for planktonic foraminifera (e.g. Huber, 1992) when austral, transitional, and tethyan assemblages were differentiated. The austral planktonic foraminiferal assemblages were characterized by low diversity, taxa endemic to high southern latitudes, and the absence or extreme rarity of keeled forms. During the late early and late Maestrichtian the differences between the austral, transitional, and tethyan foraminiferal assemblages became less pronounced partly due to the geographic expansion of low latitude, keeled species into high southern latitudes (see Figure 74).

Two Maestrichtian assemblages of benthic foraminifera can be distinguished in high southern latitudes (Thomas, 1990; Figure 74) but the differences between the assemblages are small compared to faunal changes at other times (Thomas, 1990). At ~69.4 Ma (magnetochron 31R/31N boundary) species diversity increased slightly, and the proportion of infaunal and cylindrical species increased at the expense of epifaunal species. The causes of the changes in the benthic foraminifera assemblages (changes in the availability of organic carbon due to productivity changes in surface waters or changes in the oxygen content of bottom waters) are not clear, since neither the stable isotope records nor the other microfossil groups exhibit coeval changes.

Stable isotope records indicate global cooling of surface and bottom waters as well as circulation changes. Oxygen isotope data from planktonic and benthic foraminifera from low (Saito and van Donk, 1974; Douglas and Savin, 1975; see summary in Savin, 1977) and high latitudes (Barrera et al., 1987; Barrera and Huber, 1990) indicate that surface and bottom water temperatures decreased throughout the Maestrichtian (see Figure 74). In high southern

Figure 74: Oceanographic and climatic events in the Maestrichtian as evidenced by calcareous nannoplankton, foraminifera, stable isotopes and seismic stratigraphy. Compiled from the following sources: (1) Kent and Gradstein (1985); Berggren et al. (1985); (2) this study; (3) Huber (1992a); (4) Thomas (1990); (5) Barrera and Huber (1990); Stott and Kennett (1990); Saito and van Donk (1974); Douglas and Savin (1975); (6) Barrera and Huber (1990); Corfield et al. (1991); Mount et al. (1986); (7) Vail et al. (1977); Bond (1978); Hancock and Kauffman (1979); Haq et al. (1987).

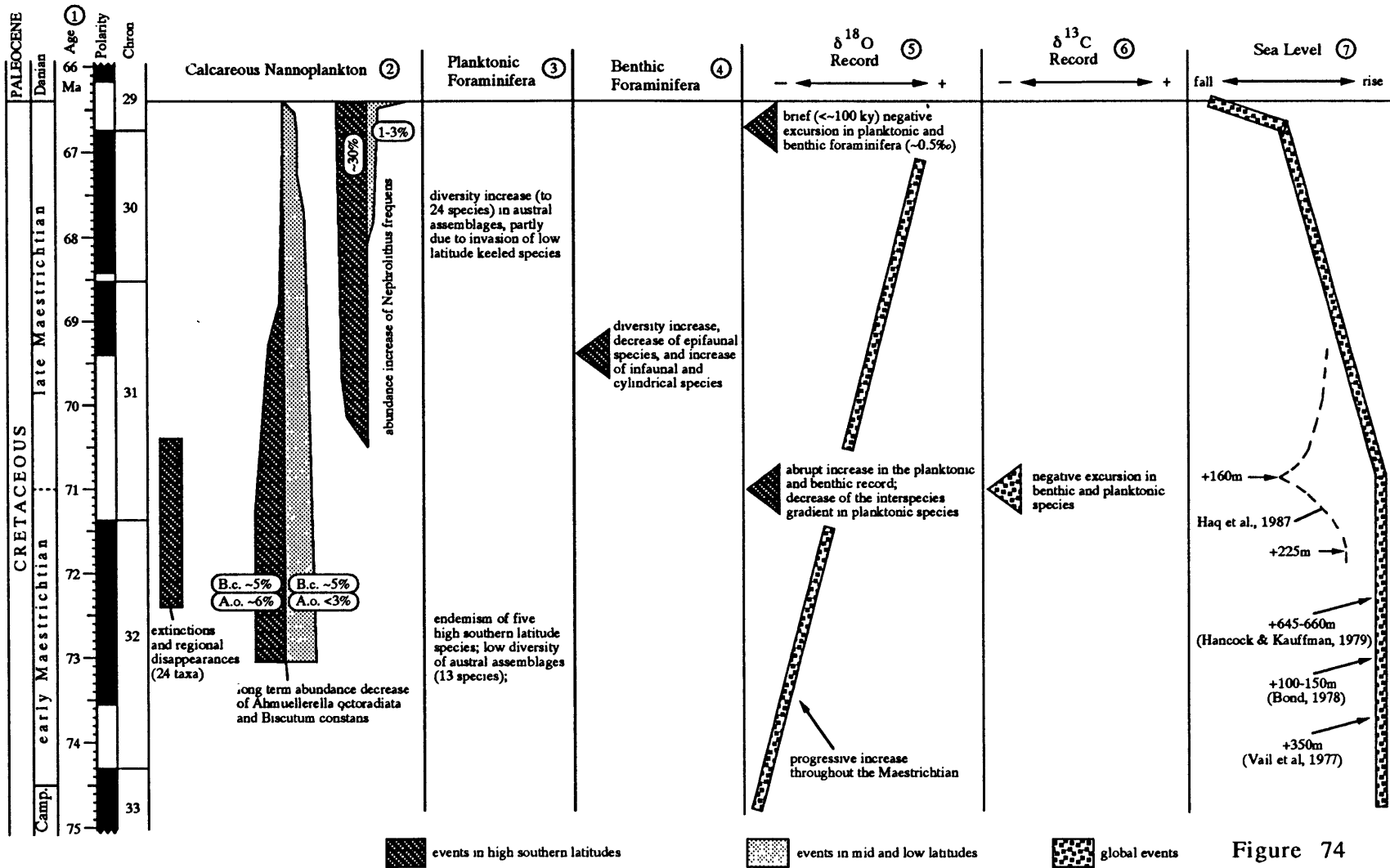


Figure 74

latitudes an abrupt cooling pulse was recorded at the early/late Maestrichtian boundary. I proposed that the temperature decrease of high latitude surface waters was the cause for the regional disappearance of twelve nannoplankton species and genera during the late early and early late Maestrichtian; these taxa persisted until the end of the Cretaceous in lower latitudes where surface water temperatures were warmer.

At the same time as the cooling pulse, the oxygen isotope gradient between planktonic species decreased implying decreased surface water stratification in the late Maestrichtian. This decrease of surface water stratification would have facilitated the mixing of nutrients into surface waters. Studies of recent nannoplankton have shown that coccolithophorid diversity is higher under oligotrophic than under eutrophic conditions (Kilham and Kilham, 1980). I propose that decreasing stratification of surface waters and increased nutrient concentrations in the photic zone resulted in the extinction of twelve taxa in high southern latitudes.

A negative excursion in the carbon isotope record was recorded at the early/late Maestrichtian boundary (~71 Ma; earliest part of magnetochron 31R) in high southern latitudes. This excursion was recorded in planktonic as well as in benthic foraminifera indicating that it affected the entire water column. A similar negative carbon isotope excursion was also observed in two tropical sections indicating a global phenomenon. This excursion may have resulted from an exchange of carbon reservoirs, possibly as a consequence of ocean circulation changes and/or a sea-level fall.

A sea level fall at the early/late Maestrichtian boundary has been suggested by several authors (e.g. Hancock and Kauffman, 1979; Haq et al., 1987), but opinions differ about its abruptness and amplitude. Hancock and Kauffman (1979) reported that the sea level during the late Campanian and early Maestrichtian was about 645-660 m higher than today, and that it fell during the late Maestrichtian (dotted bar in Figure 74.7). Haq et al. (1987) indicated a fairly abrupt and comparatively brief sea-level fall at the early/late Maestrichtian boundary (from ~225 m to ~160 m above present sea level) followed by a return to a high sea level stand during the late Maestrichtian (dashed line in Figure 74.7). Vail et al. (1977) reported that the sea-level in the latest Cretaceous was 300-350 m above present sea level. These authors did not report any details on Cretaceous sea-level changes because these results had not been released for publication (Vail et al., 1977). Bond

(1978) argued that the sea-level during the late Campanian and early Maestrichtian was only ~100-150 m higher than today; he suggested that higher estimates derived from North America and Africa were exaggerated due to uplift of these continents since the latest Cretaceous.

During the last ~800 ky of the Maestrichtian pronounced abundance changes occurred in calcareous nannoplankton in all sections investigated. The abundance changes in the mid-latitude Indian Ocean Sites (Site 217 and 761) affected the same species and occurred at approximately the same time; in contrast, the abundance patterns at the other sites strongly differ from those at Sites 217 and 761 and they occurred at different times. This indicates that environmental perturbations occurred in all ocean basins, but apparently were of different nature and timing. It is concluded that the mid-latitude South Atlantic Ocean, the mid-latitude Indian Ocean, and the high-latitude Southern Ocean were occupied by different water masses with different environmental characteristics.

At southern high latitudes stable isotope records from planktonic and benthic foraminifera (Stott and Kennett, 1990) indicate environmental perturbations (warming pulse or low-salinity pulse; ocean circulation changes) but none of the nannoplankton abundance changes exactly correlate with the stable isotope changes.

The planktonic foraminifer Pseudotextularia elegans first appeared in high southern latitudes in the latest Maestrichtian (at ~66.5 Ma on Maud Rise: Huber, 1990; Huber, 1992b). This is much younger than the first appearance datum of this species in low latitudes (late Campanian; see Huber and Watkins, 1992: fig. 16). Huber and Watkins (1992) interpreted the poleward migration of P. elegans in the latest Maestrichtian as a consequence of a brief (~<100 ky) warming pulse indicated by a negative excursion in the oxygen isotope records at that time on Maud Rise.

During the same general time Courtillot (1990) placed three major eruption events of the Deccan Trap volcanism. The temporal constraints on these eruption pulses are derived from the paleomagnetic data and are only approximate but they suggest that the bulk of the eruptions occurred during the last ~500 ky of the Cretaceous (Courtillot, 1990). It has been suggested that the eruptions of the Deccan Traps caused environmental (acid rain) and climatic perturbations which leading to the biospheric turnover across the

Figure 75: Oceanographic and climatic events during the last 800 ky of the Cretaceous based on evidence from calcareous nannoplankton, planktonic foraminifera, stable isotopes, volcanism, seismic stratigraphy, and fossil plant records. Compiled from the following sources: (1) (1) Kent and Gradstein (1985); Berggren et al. (1985); (2) this study; (3) Huber (1990, 1992a); (4) and (5) Stott and Kennett (1990); (6) Courtillot (1990); (7) Vail et al. (1977), Haq et al. (1987), Brinkhuis and Zachariasse (1988).

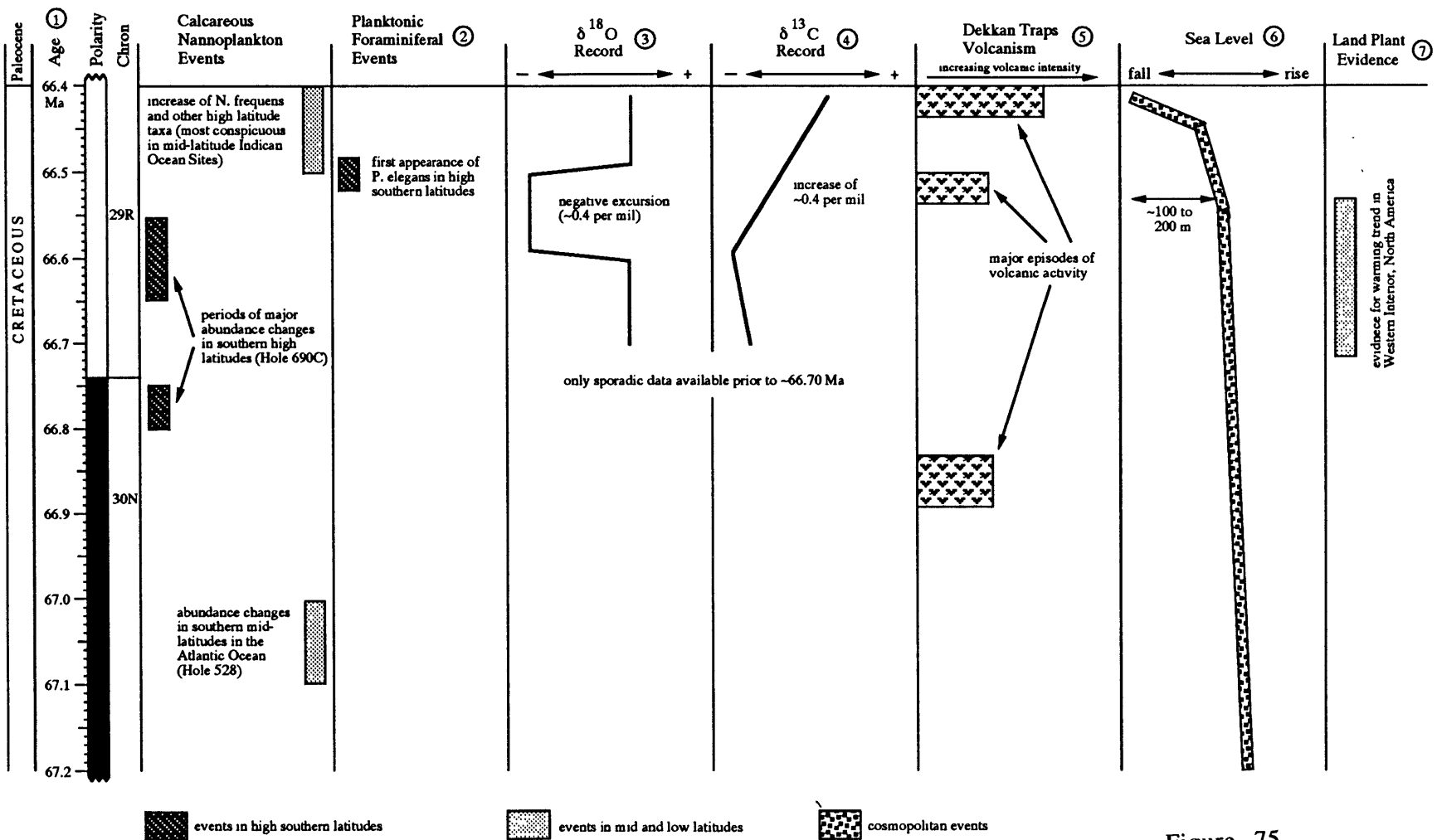


Figure 75

K/P boundary (Officer et al., 1987). However, no gradual or stepwise extinctions of calcareous nannoplankton during the postulated eruption pulses in the latest Maestrichtian could be documented in this study.

At the Cretaceous/Paleocene boundary the sea-level fell ~200 m according to Vail et al. (1977), and ~100 m according to Haq et al. (1987). Brinkhuis and Zachariasse (1988) reported changes in dinoflagellate associations, number of sporomorphs and changing amounts of land derived organic matter from the El Haria section (Tunisia) and regarded them as indicative of rapidly falling sea level during the last 17 ky of the Cretaceous.

Physiognomic and taxonomic changes of land plant macrofossils from the interior of North America indicate a warming trend beginning at the base of Magnetochron 29 (Johnson, 1992). The correlation of this warming trend with the warming pulse deduced from the oxygen isotope record in high southern latitudes remains tentative at present.

LITERATURE

- Alvarez, L. W., Alvarez, W., Asaro, F., and Michel, H. V., 1980. Extraterrestrial Cause for the Cretaceous-Tertiary Extinction. Science, 208, 1095-1108.
- Alvarez, W., 1986. Toward A Theory of Impact Crisis. Eos, 67, 649-658.
- Alvarez, W., Arthur, M. A., Fischer, A. G., Lowrie, W., Napoleone, G., Premoli Silva, I., and Roggenthen, W. M., 1977. Upper Cretaceous-Paleocene magnetic stratigraphy at Gubbio, Italy, V. Type section for the Late Cretaceous-Paleocene geomagnetic reversal time scale. Geol. Soc. Am. Bull., 88, 367-389.
- Askin, R. A., 1989. Endemism and heterochroneity in the Late Cretaceous (Campanian) to Paleocene palynofloras of Seymour Island, Antarctica: Implications for origins, dispersal and palaeoclimates of southern floras. In Origins and Evolution of the Antarctic Biota, Spec. Publ. Geol. Soc. London, 147, 107-119.
- Aubry, M.-P., 1988. Phylogeny of the Cenozoic calcareous nannoplankton genus Helicosphaera. Paleobiology, 14(1), 64-80.
- Barrera, E., Huber, B. T., Savin, S. M., and Webb, P.-N., 1987. Antarctic marine temperatures: late Campanian through early Paleocene. Paleoceanography, 2(1), 21-47.
- Barrera, E., and Huber, B. T., 1990. Evolution of Antarctic waters during the Maestrichtian: foraminifer oxygen and carbon isotope ratios, Leg 113. In Barker, P. F., Kennett, J. P., et al., Proc. ODP, Sci. Results, 113: College Station, TX (Ocean Drilling Program), 813-827.
- Barron, E. J., Thompson, S. L., and Schneider, S. H., 1981. An Ice-Free Cretaceous? Results from Climate Model Simulations. Science, 212, 501-509.
- Beaufort, L. E., 1991: Adaptation of the random settling method for quantitative studies of calcareous nannofossils. Micropaleontology, 37, 415-418.
- Beaufort, L. E., and Aubry, M.-P., 1990. Fluctuations in the composition of late Miocene calcareous nannofossil assemblages as a response to orbital forcing. Paleoceanography, 5(6), 845-865.
- Beaufort, L. E., and Aubry, M.-P., 1992. Paleoceanographic implications of a 17-m.y.-long record of high-latitude Miocene calcareous nannoplankton fluctuations. In Wise, S. W., Jr., Schlich, R., et al., 1992. Proc. ODP, Sci. Results, 120: College Station, TX (Ocean Drilling Program), 539-549.
- Berggren, W. A., Kent, D. V., and Flynn, J. J., 1985. Jurassic to Paleogene: Part 2 Paleogene geochronology and chronostratigraphy. In Snelling, N. J., (ed), The Chronology of the Geological Record, Memoir No 10, Geological Society, Blackwell Scientific Publications, Oxford, 141-195.

- Black, M., 1972. British Lower Cretaceous coccoliths. I. Gault Clay. Part 2. Paleontological Society Monographs. The Paleontological Society, London. 49-112, plates 17-33.
- Blackman, R. B., and Tukey, J. W., 1958. The measurement of power spectra. New York, Dover Publishers, 190 pp.
- Boersma, A., 1984a. Cretaceous-Tertiary planktonic foraminifers from the southeastern Atlantic, Walvis Ridge area, Deep Sea Drilling Project Leg 74. In Moore, T. C., Jr., Rabinowitz, P. D., et al., Init. Repts. DSDP, 74: Washington (U.S. Govt. Printing Office), 501-523.
- Boersma, A., 1984b. Campanian through Paleocene paleotemperature and carbon isotope sequence and the Cretaceous-Tertiary boundary in the Atlantic Ocean. In: Berggren, W. A. and Van Couvering, J. A. (eds). Catastrophes and Earth History, Princeton University Press, Princeton, 247 - 277.
- Borella, P. E., 1984. Sedimentology, petrology, and cyclic sedimentation patterns, Walvis Ridge Transect, Leg 74, Deep Sea Drilling Project. In Moore, T. C., Jr., Rabinowitz, P. D., et al., Init. Repts. DSDP, 74: Washington (U.S. Govt. Printing Office), 645-662.
- Bralower, T. J., and Siesser, W. G., 1992. Cretaceous calcareous nannofossil biostratigraphy of Sites 761, 762, and 763, Exmouth and Wombat Plateaus, Northwest Australia. In von Rad, U., Haq, B. U., et al., 1992. Proc. ODP, Sci. Results, 122: College Station, TX (Ocean Drilling Program), 529-556.
- Bramlette, M. N., and Martini, E., 1964. The great change in calcareous nannoplankton fossils between the Maestrichtian and the Danian. Micropaleontology, 10(3), 291-322.
- Brass, G. W., Southam, J. R., and Peterson, W. H., 1982. Warm saline bottom water in the ancient ocean. Nature, 296, 620-623.
- Brinkhuis H., and Zachariasse, W. J., 1988. Dinoflagellate cysts, sea level changes and planktonic foraminifers across the Cretaceous-Tertiary boundary at El Haria, northwest Tunisia. Marine Micropaleontology, 13, 153-191.
- Bromley, R. G., 1979. Chalk and bryozoan limestone: facies, sediments and depositional environments. In: Christensen, W. K., and Birkelund, T., (eds.), Cretaceous-Tertiary boundary events, I. Proceedings, University of Copenhagen, 16-32.
- Bukry, D. 1969. Upper Cretaceous coccoliths from Texas and Europe. University of Kansas Paleontological Contributions, Art. 51, 1-79, 40 pls.
- Bukry, D., and Bramlette, M. N., 1970. Coccolith age determinations Leg 3, Deep Sea Drilling Project. In Maxwell, A. E., et al., Init. Repts. DSDP, 3: Washington (U.S. Govt. Printing Office), 589-611.

- Bukry, D., 1973. Low-latitude coccolith biostratigraphic zonation. In Edgar, N. T., Saunders, J. B., et al., Init. Repts. DSDP, 15: Washington (U.S. Govt. Printing Office), 685-703.
- Bukry, D., 1974. Coccolith and silicoflagellate stratigraphy, eastern Indian Ocean, Deep Sea Drilling Project, Leg 22. In von der Borch, C. C., Sclater, J. G., et al., Init. Repts. DSDP, 22: Washington (U.S. Govt. Printing Office), 601-607.
- Cepek, P., and Hay, W. W., 1969. Calcareous nannoplankton and biostratigraphic subdivision of the Upper Cretaceous. Transactions - Gulf Coast Assoc. Geological Societies, 19, 323-336.
- Channell, J. E. T., and Dobson, J. P., 1989. Magnetic stratigraphy and magnetic mineralogy at the Cretaceous-Tertiary boundary section, Braggs, Alabama. Palaeogeography, Palaeoclimatology, Palaeoecology, 69, 267-277.
- Chave, A. D., 1984. Lower Paleocene-Upper Cretaceous magnetostratigraphy, Sites 525, 527, 528, and 529, Deep Sea Drilling Project Leg 74. In Moore, T. C., Jr., Rabinowitz, P. D., et al., Init. Repts. DSDP, 74: Washington (U.S. Govt. Printing Office), 525-531.
- Chepstow-Lusty, A., Backman, J. and Shackleton, N. J., 1989. Comparison of upper Pliocene *Discoaster* abundance variations from North Atlantic Sites 552, 607, 658, 659, and 662: further evidence for marine plankton responding to orbital forcing. In Ruddiman, W., Samthein, M., et al., Proc. ODP, Sci. Results, 108: College Station, TX (Ocean Drilling Program), 121-141.
- Christensen, W. K., 1976. Palaeobiogeography of Late Cretaceous belemnites of Europe. Paläont. Z., 50, 113-129.
- Christensen, W. K., and Birkelund, T., (eds), 1979. Cretaceous - Tertiary boundary events. Symposium. Part II. Proceedings. University of Copenhagen. 262 pp.
- Ciesielski, P. F., Sliter, W. V., Wind, F. H., and Wise, S. W., Jr., 1977. Paleoenvironmental analysis and correlation of a Cretaceous Islas Orcadas core from the Falkland Plateau, southwest Atlantic. Marine Micropaleontology, 2, 27-34.
- Clemens, W. A., Archibald, J. D., and Hickey, L. J., 1981. Out with a whimper not a bang. Paleobiology, 7(3), 293-298.
- Clauser, S., 1987. Evolution de la composition isotopique de l'oxygène des carbonates durant le Campanien-Maastrichtien. Données préliminaires issues de la série de Bidart (Pyrénées-Atlantiques). C. N. Acad. Sc. Paris, 304, Série 2 (11), 579-584.
- Cobban, W. A., and Scott, G. R., 1972: Stratigraphy and ammonite fauna of the Graneros Shale and Greenhorn Limestone near Pueblo, Colorado. U. S. Geol. Surv. Prof. Paper, 645, 1-108.

Coffin, M. F., Gahagan, L. M., Lawver, L. A., Lee, T.-Y., and Rosencrantz, E., 1992. Atlas of Mesozoic/Cenozoic reconstructions (200 Ma to Present Day), PLATES Progress Report No. 1-0192, University of Texas Institute for Geophysics Technical Report No. 122, 49 pp.

Copeland, C. W., and Mancini, E. A., 1986. Cretaceous-Tertiary boundary southeast of Braggs, Lowndes County, Alabama. In: T. L. Neathery (ed), Southeastern Section of the Geological Society of America, Centennial Field Guide, 6, 369-372.

Corfield, R. M., Cartlidge, J. E., Premoli-Silva, I., and Housley, R. A., 1991. Oxygen and carbon isotope stratigraphy of the Palaeogene and Cretaceous limestones in the Bottacione Gorge and the Contessa Highway sections, Umbria, Italy. Terra Nova, 3, 414-422.

Courtillot, V., 1990. Deccan volcanism at the Cretaceous-Tertiary boundary: past climatic crises as a key to the future? Palaeogeography, Palaeoclimatology, Palaeoecology (Global and Planetary Change section), 189, 291-299.

Courtillot, V., Besse, J., Vandamme, D., Montigny, R., Jaeger, J. J., and Cappetta, H., 1986. Deccan flood basalts at the Cretaceous-Tertiary boundary? Earth and Planetary Science Letters, 80, 361-374.

Craig, H., 1966. Isotopic composition and origin of the Red Sea and Salton Sea geothermal brines. Science, 154, 1544-1548.

Craig, H., and Gordon, 1965. Deuterium and oxygen-18 variations in the ocean and the marine atmosphere. In: Stable Isotopes in Oceanographic Studies and Paleotemperatures. Spoleto, July 26-27, 1965. Consiglio Nazionale delle Ricerche, Laboratorio di Geologia Nucleare, Pisa, 1-22.

Crux, J. A., 1991. Calcareous nannofossils recovered by Leg 114 in the subantarctic South Atlantic Ocean. In Ciesielski, P. F., Kristofferson, Y., et al., 1991. Proc. ODP, Sci. Results, 114: College Station TX (Ocean Drilling Program), 155-177.

Deflandre, G., 1959. Sur les nannofossiles calcaires et leur systématique. Extr. de la Rev. de Micropaléont., 2, 127-152.

Doeven, P. H., 1983. Cretaceous nannofossil stratigraphy and paleoecology of the Canadian Atlantic margin. Canadian Geological Survey Bulletin, 356, 1-70.

Douglas, R. G., and Savin, S. M., 1971. Isotopic analyses of planktonic foraminifera from the Cenozoic of the Northwestern Pacific, Leg 6. In A. G. Fischer, and others (Ed.), Init. Repts. DSDP (pp. 1123-1127). Washington, D. C.: U.S. Govt. Printing Office.

Douglas, R. G., and Savin, S. M., 1973. Oxygen and carbon isotope analyses of Cretaceous and Tertiary foraminifera from the central North Pacific. In E. L. Winterer, J. I. Ewing, and others (Ed.), Init. Repts. DSDP (pp. 591-605). Washington, D. C.: U.S. Govt. Printing Office.

- Douglas, R. G., and Savin, S. M., 1975. Oxygen and carbon isotope analyses of Tertiary and Cretaceous microfossils from Shatsky Rise and other sites in the North Pacific Ocean. In R. L. Larson Moberly, R. et al. (Ed.), Init. Repts. DSDP (pp. 509-520). Washington: U.S. Government Printing Office.
- Erba, E., Castradori, D., Guasti, G., Ripepe, M., 1992. Calcareous nannofossils and Milankovitch cycles: the example of the Albian Gault Clay Formation (southern England). Palaeogeogr., Palaeoclimatol., Palaeoecol., 93, 47-69.
- Firstbrook, P. L., Funnell, B. M., Hurley, A. M., and Smith, A. G., 1979. Paleocene reconstructions 160-0 Ma. University of California, Scripps Institute of Oceanography, 41pp.
- Fütterer, D. K., 1990. Distribution of calcareous dinoflagellates at the Cretaceous-Tertiary boundary of Queen Maud Rise, Eastern Weddell Sea, Antarctica (ODP Leg 113). In Barker, P. F., Kennett, J. P., et al., Proc. ODP, Sci. Results, 113: College Station, TX (Ocean Drilling Program), 533-548.
- Galbrun, B., 1992. Magnetostratigraphy of Upper Cretaceous and lower Tertiary sediments, 761 and 762, Exmouth Plateau, northwest Australia. In von Rad, U., Haq, B. U., et al., 1992. Proc. ODP, Sci. Results, 122: College Station, TX (Ocean Drilling Program), 699-716.
- Gartner, S., Jr., 1974. Nannofossil Biostratigraphy, Leg 22, Deep Sea Drilling Project. In von der Borch, C. C., Sclater, J. G., et al., Init. Repts. DSDP, 22: Washington (U.S. Govt. Printing Office), 577-599.
- Hallam, A., and Perch-Nielsen, K., 1990. The biotic record of events in the marine realm at the end of the Cretaceous: calcareous, siliceous and organic-walled microfossils and macroinvertebrates. Tectonophysics, 171, 347-357.
- Hamilton, N., 1990. Mesozoic magnetostratigraphy of Maud Rise, Antarctica. In Barker, P. F., Kennett, J. P., et al., Proc. ODP, Sci. Results, 113: College Station, TX (Ocean Drilling Program), 255-260.
- Hamilton, N., Suzyumov, A. E., and Shirshov, P. P., 1983. Late Cretaceous magnetostratigraphy of Site 516, Rio Grande Rise, southwestern Atlantic Ocean, Deep Sea Drilling Project, Leg 72. In Barker, P. F., Carlson, R. L., and Johnson, D. A. Init. Repts. DSDP, 72: Washington (U.S. Govt. Printing Office), 723-730.
- Haq, B. U., Hardenbol, J., and Vail, P., 1987. Chronology of fluctuating sea levels since the Triassic. Science, 235, 1156-1167.
- Herbert, T. D., and D'Hondt, S. L., 1990. Precessional climate cyclicity in Late Cretaceous-Early Tertiary marine sediments: a high resolution chronometer of Cretaceous-Tertiary boundary events. Earth and Planetary Science Letters, 99, 263-275.
- Hildebrand, A. R., Penfield, G. T., Kring, D. A., Pilkington, M., Carmago Z., A., Jacobsen, S. B., and Boynton, W. V., 1991. Chicxulub Crater: A possible Cretaceous/Tertiary boundary impact crater on the Yucatán Peninsula, Mexico. Geology, 19, 867-871.

Hsü, K. J., 1980. Terrestrial catastrophe caused by cometary impact at the end of Cretaceous. Nature, 285, 201-203.

Hsü, K. J., He, Q., McKenzie, J. A., Weissert, H., Perch-Nielsen, K., Oberhänsli, H., Kelts, K., LaBrecque, J., Tauxe, L., Krähenbühl, U., Percival, S. F., Jr., Wright, R., Karpoff, A. M., Petersen, N., Tucker, P., Poore, R. Z., Gombos, A. M., Pisciotto, K., Carman, M. F., Jr., and Schreiber, E., 1982. Mass Mortality and Its Environmental and Evolutionary Consequences. Science, 216, 249-256.

Huber, B. T., 1990. Maestrichtian planktonic foraminifer biostratigraphy of the Maud Rise (Weddell Sea, Antarctica): ODP Leg 113 Holes 689B and 690C. In Barker, P. F., Kennett, J. P., et al., Proc. ODP, Sci. Results, 113: College Station, TX (Ocean Drilling Program), 489-513.

Huber, B. T., 1992a. Paleobiogeography of Campanian-Maestrichtian foraminifera in the southern high latitudes. Palaeogeography, Palaeoclimatology, Palaeoecology, 92, 325-360.

Huber, B. T., 1992b. Upper Cretaceous planktic foraminiferal biozonation for the Austral Realm. Marine Micropaleontology, 20, 107-128.

Huber, B. T., and Watkins, D. K., 1992. Biogeography of Campanian-Maestrichtian calcareous plankton in the region of the Southern Ocean: Paleogeographic and paleoclimatic implications. Antarctic Research Series, 56, 31-60.

Hutchison, J. H. and Archibald, J. D., 1986. Diversity of turtles across the Cretaceous/Tertiary boundary in northeastern Montana. Paleogeography, Paleoclimatology, Paleoecology, 55, 1-22.

Jiang, M. J., and Gartner, S., 1986. Calcareous nannofossil succession across the Cretaceous/Tertiary boundary in east-central Texas. Micropaleontology, 32, 232-255.

Johnson, K. R., 1992. Foliar Physiognomy of Maestrichtian leaf floras from the northern Great Plains: implications for paleoclimate. Abstracts, SEPM 1992 Theme Meeting, Ft. Collins, Colorado, 36.

Johnson, K. R., and Hickey, L. J., 1990. Megafloral change across the Cretaceous/Tertiary boundary in the northern Great Plains and Rocky Mountains, U.S.A. GSA Spec. Paper, 247, 433-444.

Katz, M. E., and Miller, K. G., 1991. Early Paleogene benthic foraminiferal assemblages and stable isotopes in the Southern Ocean. In Ciesielski, P. F., Kristofferson, Y., et al., 1991. Proc. ODP, Sci. Results, 114: College Station TX (Ocean Drilling Program), 481-512.

Kauffman, E. G., 1984. The fabric of Cretaceous marine extinctions. In Berggren, W. A., and Van Couvering, J. A. (eds.), Catastrophes and Earth History, 151-246, Princeton University Press.

- Keller, G., 1988. Extinction, Survivorship and Evolution of Planktic Foraminifera across the Cretaceous/Tertiary Boundary at El Kef, Tunisia. Mar. Micropaleontol., 13, 239-263.
- Keller, G., 1989. Extended Cretaceous/Tertiary boundary extinctions and delayed population change in planktonic foraminifera from Brazos River, Texas. Paleoceanography, 4, 287-332.
- Kent, D. V., and Gradstein, F. M., 1985. A Cretaceous and Jurassic geochronology. Geological Society of America Bulletin, 96, 1419-1427.
- Kerr, R. A., 1991. Dinosaurs and Friends Snuffed Out? Science, 251, 160-162.
- Kilham, P., and Kilham, S. S., 1980. The evolutionary ecology of phytoplankton. In Morris, I., (ed.), The Physiological Ecology of Phytoplankton. Los Angeles (University of California Press), 571-597.
- Kitchell, J. A., Clark, D. L., and Gombos, A. M., 1986. Biological Selectivity of Extinction: A Link Between Background and Mass Extinction. Palaeos, 1, 504-511.
- Kleijne, A., 1991. Holococcolithophorids from the Indian Ocean, Red Sea, Mediterranean Sea and North Atlantic Ocean. Mar. Micropaleontol., 17, 1-76.
- Ledbetter, M. T., and Ellwood, B. B., 1976. Selection of sample intervals in deep-sea sedimentary cores. Geology, 4, 303-304.
- Liu, Chengjie, 1992. Uppermost Cretaceous - lower Paleocene stratigraphy and turnover of planktonic foraminifera across the Cretaceous-Paleogene boundary. Dissertation, State University of New Jersey, New Brunswick Rutgers.
- Loeblich, Jr., A. R., and Tappan, H., 1957. Correlation of the Gulf and Atlantic Coastal Plain Paleocene and Lower Eocene formations by means of planktonic Foraminifera. J. Paleontology, 31, 1109-1137.
- Luterbacher, H. P., and Premoli Silva, I., 1964. Biostratigrafia del limite Cretaceo-Terziario nell'Appennino centrale. Rivista Italiana di Paleontologia e Stratigrafia, 70, 67-128.
- MacLeod, N., and Keller, G., 1991. Hiatus distributions and mass extinctions at the Cretaceous/Tertiary boundary. Geology, 19, 497-501.
- Mancini, E. A., Tew, B. H., and Smith, C. C., 1989. Cretaceous-Tertiary contact, Mississippi and Alabama. Journal of Foraminiferal Research, 19(2), 93-104.
- Manivit, H., 1984. Paleogene and Upper Cretaceous calcareous nannofossils from Deep Sea Drilling Project Leg 74. In Moore, T. C., Jr., Rabinowitz, P. D., et al., Init. Repts. DSDP, 74: Washington (U.S. Govt. Printing Office), 475-499.

- Margolis, S. V., Kroopnick, P. M., and Goodney, D. E., 1977. Cenozoic and late Mesozoic paleoceanographic and paleoglacial history recorded in circum-Antarctic deep-sea sediments. Marine Geology, 25, 131-147.
- McGowran, B., 1974. Foraminifera. In von der Borch, C. C., Sclater, J. G., et al., Init. Repts. DSDP, 22: Washington (U.S. Govt. Printing Office), 609-627.
- Michel, H. V., Asaro, F., Alvarez, W., and Alvarez, L. W., 1985. Elemental profile of iridium and other elements near the Cretaceous/Tertiary boundary in Hole 577B. In Heath, G. R., Burckle, L. H., et al., Init. Repts. DSDP, 86: Washington (U.S. Govt. Printing Office), 533-538.
- Michel, H. V., Asaro, F., Alvarez, W., and Alvarez, L. W., 1990. Geochemical studies of the Cretaceous-Tertiary boundary in ODP Holes 689B and 690C. In Barker, P. F., Kennett, J. P., et al., Proc. ODP, Sci. Results, 113: College Station, TX (Ocean Drilling Program), 159-168.
- Miller, K. G., and Fairbanks, R. G., 1987. Tertiary oxygen synthesis, sea level history, and continental margin erosion. Paleoceanography, 2, 1-19.
- Monechi, S., 1985. Campanian to Pleistocene calcareous nannofossil stratigraphy from the northwest Pacific Ocean, Deep Sea Drilling Project Leg 86. In Heath, G. R., Burckle, L. H., et al., Init. Repts. DSDP, 86: Washington (U.S. Govt. Printing Office), 301-336.
- Monechi, S., and Thierstein, H. R., 1985. Late Cretaceous - Eocene nannofossil and magnetostratigraphic correlations near Gubbio, Italy. Mar. Micropaleontol., 9, 419-440.
- Mosimann, J. E., 1965. Statistical methods for the pollen analyst: Multinomial and negative multinomial techniques. In Kummel, B., and Raup, D., (eds.), Handbook of Paleontological Techniques. W. H. Freeman, San Francisco, California, 636-673.
- Mount, J. F., Margolis, S. V., Showers, W., Ward, P., Doehne, E., 1986. Carbon and Oxygen Isotope Stratigraphy of the Upper Maestrichtian, Zumaya, Spain: A Record of Oceanographic and Biologic Changes at the End of the Cretaceous Period. Palaeos, 1, 87-92.
- Nederbragt, A. J., 1990. Biostratigraphy and paleoceanographic potential of the Cretaceous planktonic foraminifera Heterohelicidae. (Ph. D. Thesis). Centrale Huisdrukkerij Vrije Univ., Amsterdam.
- Noël, D., 1970. Coccolithes Crétacés. Centre National de la Recherche Scientifique, Paris, 129 pp., 48 pls.
- Officer, C. B., Hallam, A., Drake, C. L. and Devine, J. D., 1987. Late Cretaceous and paroxysmal Cretaceous/Tertiary extinctions. Nature, 326, 143-149.
- Okada, H., and Honjo, S., 1975. Distribution of Coccolithophores in Marginal Seas along the Western Pacific Ocean and in the Red Sea. Mar. Biology, 31, 271-285.

- Okada, H., Yamada, M., and Matsuoka, H., 1987. Calcareous nannofossils and biostratigraphy of the Upper Cretaceous and lower Paleogene Nemuro Group, eastern Hokkaido, Japan. J. Geol. Soc. Japan, 93(5), 329-348.
- Olsson, R. K., Liu, C., Aubry, M.-P., Ehrendorfer, T., 1992. A biostratigraphically continuous Cretaceous/Paleogene section at Millers Ferry, Alabama: support for a bolide impact. GSA Abstr. w. Prgm., Annual Meeting, Cincinnati, Ohio, A28.
- Parrish, J. T., and Spicer, R. A., 1988. Late Cretaceous terrestrial vegetation: A near-polar temperature curve. Geology, 16, 22-25.
- Perch-Nielsen, K., 1968. Der Feinbau und die Klassifikation der Coccolithen aus dem Maastrichtien von Dänemark. Kongelige Danske Videnskabernes Selskab, Biologiske Skrifter, 16(1), 1-96, 32 pls.
- Perch-Nielsen, K., 1983. Recognition of Cretaceous stage boundaries by means of calcareous nannofossils. In T. Birkelund, et al. (eds), Symposium on Cretaceous Stage Boundaries, Copenhagen, Abstracts, 152-156.
- Perch-Nielsen, K., McKenzie, J. A., and He, Q., 1982: Biostratigraphy and isotope stratigraphy and the 'catastrophic' extinction of calcareous nannoplankton at the Cretaceous/Tertiary boundary. Spec. Pap. geol. Soc. Amer., 190, 353-371.
- Percival, S. F., Jr., 1984. Late Cretaceous to Pleistocene calcareous nannofossils from the South Atlantic, Deep Sea Drilling Project Leg 73. In Hsü, K. J., LaBrecque, J. L., et al., Init. Repts. DSDP, 73: Washington (U.S. Govt. Printing Office), 391-424.
- Percival, S. F., and Fischer, A. G., 1977. Changes in calcareous nannoplankton in the Cretaceous-Tertiary biotic crisis at Zumaya, Spain. Evol. Theory, 2, 1-35.
- Pessagno, E. A., Jr., and Michael, F. Y., 1974. Mesozoic foraminifera, Leg 22, Site 217. In von der Borch, C. C., Sclater, J. G., et al., Init. Repts. DSDP, 22: Washington (U.S. Govt. Printing Office), 629-634.
- Pospichal, J. J., 1991. Calcareous nannofossils across Cretaceous/Tertiary boundary at Site 752, eastern Indian Ocean. In Weissel, J., Peirce, J., Taylor, E., Alt, J., et al., 1991. Proc. ODP, Sci. Results, 121: College Station, TX (Ocean Drilling Program), 395-410.
- Pospichal, J. J., and Wise, S. W., Jr., 1990a. Maastrichtian calcareous nannofossil biostratigraphy of Maud Rise ODP Leg 113 Sites 689 and 690, Weddell Sea. In Barker, P. F., Kennett, J. P., et al., Proc. ODP, Sci. Results, 113: College Station, TX (Ocean Drilling Program), 465-487.
- Pospichal, J. J., and Wise, S. W., Jr., 1990b. Calcareous nannofossils across the K/T boundary, ODP Hole 690C, Maud Rise, Weddell Sea. In Barker, P. F., Kennett, J. P., et al., Proc. ODP, Sci. Results, 113: College Station, TX (Ocean Drilling Program), 515-532.

Pospichal, J. J., Wise, S. W., Jr., Asaro, F., and Hamilton, N., 1990. The effects of bioturbation across a biostratigraphically complete high southern latitude Cretaceous/Tertiary boundary. In Sharpton, V. L., and Ward, P. D. (eds.), Global Catastrophes in Earth History: An Interdisciplinary Conference on Impacts, Volcanism, and Mass Mortality. GSA Spec. Paper 247, 497-507.

Pospichal, J. J., and Bralower, T. J., 1992. Calcareous nannofossils across the Cretaceous/Tertiary boundary, Site 761, northwest Australian margin. In von Rad, U., Haq, B. U., et al., Proc. ODP, Sci. Results, 122: College Station, TX (Ocean Drilling Program), 735-751.

Premoli Silva, I., Erba, E., Tornaghi, M. E., 1989. Paleoenvironmental signals and changes in surface fertility in mid Cretaceous Corg-rich pelagic facies of the Fucoïd Marls (central Italy). Geobios, Special Vol. 11, 225-236.

Raup, D. M., and Sepkoski, J. J., Jr., 1984. Periodicity of extinctions in the geologic past. Proc. Natl. Acad. Sci. USA, 81, 801-805.

Resiwati, P., 1991. Upper Cretaceous calcareous nannofossils from Broken Ridge and Ninetyeast Ridge, Indian Ocean. In Weissel, J., Peirce, J., Taylor, E., Alt, J., et al., 1991. Proc. ODP, Sci. Results, 121: College Station, TX (Ocean Drilling Program), 141-170.

Robert, C, and Maillot, H., 1990. Paleoenvironments in the Weddell Sea area and Antarctic climates, as deduced from clay mineral associations and geochemical data, ODP leg 113. In Barker, P. F., Kennett, J. P., et al., Proc. ODP, Sci. Results, 113: College Station, TX (Ocean Drilling Program), 51-70.

Rocchia, R., Boclet, D., Bonté, P., Froget, L., Galbrun, B., Jéhanno, C., and Robin, E., 1992. Iridium and other element distributions, mineralogy, and magnetostratigraphy near the Cretaceous/Tertiary boundary in Hole 761C. In von Rad, U., Haq, B. U., et al., Proc. ODP, Sci. Results, 122: College Station, TX (Ocean Drilling Program), 753-762.

Romein, A. J. T., 1979. Lineages in early Paleogene calcareous nannoplankton. Utrecht Micropaleontol. Bull., 22, 1-231.

Roth, P. H., and Bowdler, J. L., 1981. Middle Cretaceous calcareous nannoplankton biogeography and oceanography of the Atlantic Ocean. SEPM Special Publication, 32, 517-546.

Roth, P. H., and Krumbach, K. R., 1986. Middle Cretaceous calcareous nannofossil biogeography and preservation in the Atlantic and Indian Oceans: implications for paleoceanography. Mar. Micropaleontol., 10, 235-266.

Royer, J.-Y., Peirce, J. W., and Weissel, J. K., 1991. Tectonic constraints on the hotspot formation of Ninetyeast Ridge. In Weissel, J., Peirce, J., Taylor, E., Alt, J., et al., 1991. Proc. ODP, Sci. Results, 121: College Station, TX (Ocean Drilling Program), 763-776.

Russell, D. A., 1977. The biotic crisis at the end of the Cretaceous Period. Syllogus, 12, 11-23.

- Saltzman, E. S., and Barron, E. J., 1982. Deep circulation in the Late Cretaceous: oxygen isotope paleotemperatures from *Inoceramus* remains in D.S.D.P. cores. Palaeogeography, Palaeoclimatology, Palaeoecology, 40, 167-181.
- Savin, S. M. 1977. The history of the earth's surface temperature during the past 100 millio years. Ann. Earth Sci. Rev., 5, 319-355.
- Saito, T., and Van Donk, J., 1974. Oxygen and carbon isotope measurements of Late Cretaceous and Early Tertiary foraminifera. Micropaleontology, 20(2), 152-177.
- Shackleton, N. J., and Boersma, A., 1984. Oxygen and carbon isotope data from Leg 74 foraminifers. In Moore, T. C, Jr., Rabinowitz, P. D., et al., Init. Repts. DSDP, 74: Washington (U.S. Govt. Printing Office), 599-612.
- Shipboard Scientific Party, 1974. Site 217. In von der Borch, C. C., Sclater, J. G., et al., Init. Repts. DSDP, 22: Washington (U.S. Govt. Printing Office), 267-324.
- Shipboard Scientific Party, 1977. Site 327. In Barker, P. F., Dalziel, I. W. D., et al., Init. Repts. DSDP, 36: Washington (U.S. Govt. Printing Office), 27-86.
- Shipboard Scientific Party, 1983. Site 516: Rio Grande Rise. In Barker, P. F., Carlson, R. L., and Johnson, D. A. Init. Repts. DSDP, 72: Washington (U.S. Govt. Printing Office), 155-338.
- Shipboard Scientific Party, 1984. Site 528. In Moore, T. C., Jr., Rabinowitz, P. D., et al., Init. Repts. DSDP, 74: Washington (U.S. Govt. Printing Office), 307-405.
- Shipboard Scientific Party, 1988. Site 690. In Barker, P. F., Kennett, J. P., et al., Proc. ODP, Init. Repts., 113: College Station, TX (Ocean Drilling Program).
- Shipboard Scientific Party, 1990. Site 761. In Haq, B. U., von Rad, U., O'Connell, S., et al., Proc. ODP, Init. Repts., 122: College STation, TX (Ocean Drilling Program), 161-211.
- Signor, P. W., III, and Lipps, J. H., 1982. Sampling bias, gradual extinction patterns, and catastrophes in the fossil record. GSA Special Paper, 190, 291-296.
- Sissingh, W., 1977. Biostratigraphy of Cretaceous calcareous nannoplankton. Geologie en Mijnbouw, 56(1), 37-65.
- Smayda, T. J., 1980. Phytoplankton species succession. In Morris, I. (ed), The physiological ecology of phytoplankton. Studies in Ecology, 7, 493-570.
- Smit, J., 1990. Meteorite impact, extinctions and the Cretaceous-Tertiary Boundary. Geologie en Mijnbouw, 69, 187-204.
- Smith, A. G., Hurley, A. M., and Briden, J. C., 1981. Phanerozoic paleocontinental world maps. Cambridge University Press, Cambridge, 102 pp.

- Smith, C. C., and Poore, R. Z., 1984. Upper Maestrichtian and Paleocene planktonic foraminiferal biostratigraphy of the northern Cape Basin, Deep Sea Drilling Project Hole 524. In Hsü, K. J., LaBrecque, J. L., et al., Init. Repts. DSDP, 73: Washington (U.S. Govt. Printing Office), 449-457.
- Stanley, S. M., 1984. Temperature and biotic crises in the marine realm. Geology, 12, 205-208.
- Stott, L. D., and Kennett, J. P., 1990a. Antarctic Paleogene planktonic foraminifer biostratigraphy: ODP Leg 113, Sites 698 and 690. In Barker, P. F., Kennett, J. P., et al., Proc. ODP, Sci. Results, 113: College Station, TX (Ocean Drilling Program), 549-569.
- Stott, L. D., and Kennett, J. P., 1990b. The paleoceanographic and paleoclimatic signature of the Cretaceous/Paleogene boundary in the Antarctic: stable isotopic results from ODP leg 113. In Barker, P. F., Kennett, J. P., et al., Proc. ODP, Sci. Results, 113: College Station, TX (Ocean Drilling Program), 829-848.
- Tauxe, L., Tucker, P., Petersen, N. P., LaBrecque, J. L., 1984. Magnetostratigraphy of Leg 73 sediments. In Hsü, K. J., LaBrecque, J. L., et al., Init. Repts. DSDP, 73: Washington (U.S. Govt. Printing Office), 609-621.
- Thierstein, H. R., 1976. Mesozoic calcareous nannoplankton biostratigraphy of marine sediments. Mar. Micropaleontol., 1, 325-362.
- Thierstein, H. R., 1980. Selective dissolution of late Cretaceous and earliest Tertiary calcareous nannofossils: experimental evidence. Cretaceous Research, 2, 165-176.
- Thierstein, H. R., 1981. Late Cretaceous nannoplankton and the change at the Cretaceous-Tertiary boundary. SEPM Special Publication, 32, 355-394.
- Thierstein, H. R., 1982. Terminal Cretaceous plankton extinctions: A critical assessment. GSA Special Paper, 190, 385-399.
- Thomas, E., 1990. Late Cretaceous through Neogene deep-sea benthic foraminifers (Maud Rise, Weddell Sea, Antarctica). In Barker, P. F., Kennett, J. P., et al., Proc. ODP, Sci. Results, 113: College Station, TX (Ocean Drilling Program), 571-594.
- Van Valen, L., and Sloan, Robert E., 1977. Ecology and the extinction of the dinosaurs. Evol. Theory, 2, 37-64.
- Watkins, D. K., 1989. Nannoplankton productivity fluctuations and rhythmically-bedded pelagic carbonates of the Greenhorn Limestone (Upper Cretaceous). Palaeogeography, Palaeoclimatology, Palaeoecology, 74, 75-86.
- Watkins, D. K., 1992. Upper Cretaceous nannofossils from Leg 120, Kerguelen Plateau, Southern Ocean. In Wise, S. W., Jr., Schlich, R., et al., 1992. Proc. ODP, Sci. Results, 120: College Station, TX (Ocean Drilling Program), 343-370.

Wei, W., and Thierstein, H. R., 1991. Upper Cretaceous and Cenozoic calcareous nannofossils of the Kerguelen Plateau (southern Indian Ocean) and Prydz Bay (East Antarctica). In Barron, J., Larsen, B., et al., 1991. Proc. ODP, Sci. Results, 119: College Station, TX (Ocean Drilling Program), 467-493.

Weiss, W., 1983. Upper Cretaceous planktonic foraminiferal biostratigraphy from the Rio Grande Rise: Site 516 of Leg 72, Deep Sea Drilling Project. In Barker, P. F., Carlson, R. L., and Johnson, D. A. Init. Repts. DSDP, 72: Washington (U.S. Govt. Printing Office), 715-721.

Wiedmann, J., 1964. Le Crétacé supérieur de l'Espagne et du Portugal et ses Céphalopodes. Estud. Geol., 20, 107-148.

Wind, F. H., 1979a. Late Campanian and Maestrichtian calcareous nannoplankton biogeography and high-latitude biostratigraphy. Ph. D. Thesis. Florida State University, Tallahassee, 333 pp.

Wind, F. H., 1979b. Maestrichtian-Campanian Nannofloral Provinces of the Southern Atlantic and Indian Oceans. In Talwani, M., Hay, W., and Ryan, W. B. F. (eds.), Deep Drilling Results in the Atlantic Ocean: Continental Margins and Paleoenvironment. AGU, Washington D. C., 123-137.

Wind, F. H., and Wise, S. W., 1983. Correlation of upper Campanian-lower Maestrichtian calcareous nannofossil assemblages in drill and piston cores from the Falkland Plateau, southwest Atlantic Ocean. In Ludwig, W. J., Krasheninnikov, V., et al., Init. Repts. DSDP, 71: Washington (U.S. Govt. Printing Office), 551-563.

Wise, S. W., Jr., 1983. Mesozoic and Cenozoic calcareous nannofossils recovered by Deep Sea Drilling Project Leg 71 in the Falkland Plateau region, southwest Atlantic Ocean. In Ludwig, W. J., Krasheninnikov, V., et al., Init. Repts. DSDP, 71: Washington (U.S. Govt. Printing Office), 481-550.

Wise, S. W., Jr., 1988. Mesozoic-Cenozoic history of calcareous nannofossils in the region of the Southern Ocean. Palaeogeogr., Palaeoclimatol., Palaeoecol., 67, 157-179.

Wise, S. W., Jr., and Wind, F. H., 1977. Mesozoic and Cenozoic calcareous nannofossils recovered by DSDP Leg 36 drilling on the Falkland Plateau, southwest Atlantic sector of the Southern Ocean. In Barker, P. F., Dalziel, I. W. D., et al., Init. Repts. DSDP, 36: Washington (U.S. Govt. Printing Office), 269-491.

Wonders, A. A. H., 1992. Cretaceous planktonic foraminiferal biostratigraphy, Leg 122, Exmouth Plateau, Australia. In von Rad, U., Haq, B. U., et al., 1992. Proc. ODP, Sci. Results, 122: College Station, TX (Ocean Drilling Program), 587-599.

Worsley, T., 1974. The Cretaceous-Tertiary boundary event in the ocean. SEPM Special Publication, 20, 94-125.

Worsley, T., and Martini, E., 1970. Late Maestrichtian Nannoplankton Provinces. Nature, 225, 1242-1243.

Zachos, J. C., and Arthur, M. A., 1986. Paleocyanography of the Cretaceous/Tertiary boundary event: inferences from stable isotopic and other data. Paleocyanography, 1(1), 5-26.

Zachos, J. C., Arthur, M. A., and Dean, W. E., 1989. Geochemical evidence for suppression of pelagic marine productivity at the Cretaceous/Tertiary boundary. Nature, 337, 61-64.

APPENDIX I TAXONOMY

Different levels of taxonomic identification were possible depending on preservation. In the data tables (Appendix II) the highest taxonomic resolution achieved is given for each sample: in well preserved samples most taxa could be identified at the species level, whereas in many moderately to poorly preserved samples only generic identification was possible in certain taxa. When identification at the species level could not be maintained in all samples it was necessary to group species at the generic level for comparison between samples and between sections. The following is a list of the species identified in this study; included are discussions of the grouping of taxa for inter-sample comparison.

Ahmuellerella octoradiata (Gorka, 1957) Reinhardt (1964)

Angulofenestrellithus snyderi Bukry (1969)

Arkhangelskiella cymbiformis Vekshina (1959)

A. specillata Vekshina (1959): In poorly preserved samples it was not always possible to differentiate between A. cymbiformis and A. specillata because the pores in the central area were covered due to recrystallization. (see also comments under Broinsonia enormis).

Biantholithus sparsus Bramlette and Martini, 1964

Biscutum Black in Black and Barnes, 1959

B. boletum Wind and Wise in Wise and Wind (1977)

B. constans (Gorka, 1957) Black, 1967: In this study B. constans and B.

castrorum are considered synonymous. According to Perch-Nielsen (1968) B. constans has priority over B. testudinarium Black (1959) which is a younger synonym. Biscutum constans and B. castrorum are considered synonyms (following Noël, 1970), although some researchers indicate that these may be indeed two distinct genera, based on coccolith size and number of marginal elements (Perch-Nielsen, 1968) or on coccolith size and the construction of the central area (Romein, 1979). According to Romein (1979) the elements of the proximal shield extend into and close the central area in B. castrorum, whereas in B. constans the central area is filled with granular elements which are clearly separate from the shield elements. The light microscope expression of

these two types of construction is not demonstrated satisfactorily: in B. castrorum the entire central area is birefringent (Romein, 1979; pl. 9, fig. 1), but no light microscope picture was supplied of B. constans. Pospichal (1991; pl. 2, fig. 1-2 and pl. 3, fig. 3) gave light microscope illustrations of both species: the central area of B. castrorum is completely bright in cross-polarized light, whereas only a narrow birefringent ring lines the central area in B. constans. No electron microscope pictures of the proximal sides of these two forms were provided so that the correspondence of the light-microscope pictures to the ultra structure as described by Romein (1979) is still unproven. In my investigations both of the forms illustrated by Pospichal (1991) as B. castrorum and as B. constans were encountered; both were recorded as B. constans because I interpreted the forms with a birefringent ring in the central area as incomplete (broken) specimens of those with a completely birefringent area.

B. coronum Wind and Wise in Wise and Wind (1977): The species illustrated by Bralower and Siesser (1992: pl. 1, figs. 23, 24) is not included with B. coronum in this study, but would probably be classified as B. constans.

B. dissimilis Wind and Wise in Wise and Wind (1977)

B. magnum Wind and Wise in Wise and Wind (1977)

Biscutum sp. cf. B. magnum: This species is very similar to B. magnum except that its margin is much narrower than typical specimens of this species.

B. notaculum Wind and Wise in Wise and Wind (1977)

Biscutum sp. 1 (Pospichal and Bralower; 1992; pl.3, fig. 1-2): This taxon is common in all sections studied. It is smaller than other species of this genus observed in this investigation (with the exception of B. notaculum). In normal light a ring of high relief surrounds the central area; this ring is bright in cross polarized light. Biscutum sp. 1 differs from B. constans in having a fairly narrow margin (the diameter of the central area is bigger than the width of the margin).

Biscutum sp. 2 This species is characterized by a narrow margin and a cross like (?) structure spanning the central opening. It was only observed in Hole 690C.

Braarudosphaera bigelowii (Gran and Braarud, 1935) Deflandre, 1947

Broinsonia Bukry, 1969: This genus differs from Arkhangelskiella in the presence of a second, outer, narrow marginal cycle on the distal side (Bukry, 1969). This cycle is clearly visible only in well preserved material. In moderately and poorly preserved material the outer marginal cycle cannot be distinguished in most cases. Bralower and Siesser (1992) used the presence/absence of pores as well as the extinction pattern of the central area to distinguish between Arkhangelskiella and Broinsonia. This practice is not adopted here since observations in well preserved material (where Broinsonia can be recognized based on the outer marginal cycle) indicate that both of these characteristics are very variable and do not allow consistent differentiation between the genera.

Broinsonia bevieri Bukry, 1969

Broinsonia enormis (Shumenko, 1969) Manivit (1971): In size and in ratio of margin to central area this species is very similar to Arkhangelskiella cymbiformis. In many cases it was impossible to determine whether the margin consisted of one or of two cycles; A. cymbiformis and B. enormis were then recorded as one taxon.

Broinsonia parca (Stradner, 1963) Bukry, 1969: Because of the small size of the central area this species could be identified consistently.

Centosphaera barbata Wind and Wise in Wise and Wind, 1977

Ceratolithoides aculeus (Stradner, 1961) Prins and Sissingh in Sissingh, 1977

C. kamptneri Bramlette and Martini, 1964

Ceratolithoides sp. 1: This form has broad, parallel arms that touch each other in many specimens. It is not clear whether these forms are recrystallized specimens of C. kamptneri or of C. aculeus, or whether they represent a separate taxon.

Chiastozygus Gartner, 1968

C. amphipons (Bramlette and Martini, 1964) Gartner, 1968: This species has a fairly wide margin which does not display sharp extinction lines in cross-polarized light. The central X consists of arms that are as wide as the margin; under cross-polarized light the arms are divided lengthwise.

C. garrisonii Bukry, 1969: A small square is visible at the central juncture of the arms; it is interpreted as the base of a central stem which in most cases is not preserved.

Chiastozygus sp. 1: This taxon is characterized by a narrow margin (compared to C. amphipons); in cross polarized light well defined, strongly curved extinction lines occur in the margin. The central crossbars do not intersect at one point, but rather form a distorted H. This species differs from C. amphipons in having a narrower margin, in the extinction pattern of the margin, and in the fact that in C. amphipons the central crossbars form a perfect X. This form differs from C. garrisonii in lacking an opening at the intersection point of the crossbars.

Corollithion? completum Perch-Nielsen, 1973

Corollithion exiguum Stradner, 1961

Cretarhabdus Bramlette and Martini, 1964: The distinction between C. conicus, C. crenulatus, C. surirellus, and Cretarhabdus sp. 1 is based on the construction of the central area. Species identification was thus not possible when the central area was incompletely preserved. On the other hand, identification of C. angustiforatus and of C. schizobrachiatus was still possible when most of the central area was missing: the points where the central arms were connected to the margin were still recognizable. Species identification was possible because of the characteristic number (eight in C. angustiforatus) and position (groups of three in C. schizobrachiatus) of these points on the margin. Thus, the forms included in this group are mostly C. conicus, C. crenulatus, C. surirellus and Cretarhabdus sp. 1. Because distinction between these species was so dependent on preservation, these four species and Cretarhabdus spp. were added and treated as one taxon for plotting purposes.

Cretarhabdus angustiforatus (Black, 1971) Bukry, 1973: A species of Cretarhabdus with eight radial arms in the central area: four longer arms are aligned with the ellipse; the other four arms are somewhat shorter and lie at an angle of about 45° to the ellipse axes.

C. conicus Bramlette and Martini, 1964: Included in this species are forms with more than one row of central perforations (as explicitly stated by Bukry, 1969), i.e. the central area appears to be covered by a porous grid. Cretarhabdus conicus may have a central cross aligned with the ellipse axes.

C. crenulatus Bramlette and Martini, 1964: Like C. surirellus, this species has only one row of openings in the central area, i.e. its central area

appears to be spanned by short buttresses/rods. The relative size of the central area was used to distinguish C. crenulatus from C. surirellus. In C. crenulatus the diameter of the central area is smaller than or equal to the width of the margin (measured along the short ellipse axis). In C. surirellus the diameter of the central area is larger than the width of the margin.

C. schizobrachiatus (Gartner, 1968) Bukry, 1969

C. surirellus (Deflandre, 1964), Reinhardt, 1970: see comments under C. crenulatus

Cretarhabdus sp. 1: This species is characterized by numerous pores in the central area (similar to the central area of C. ehrenbergii), but with a margin typical of Cretarhabdus. It was observed in the Millers Ferry section, in Hole 690C and in Hole 761C.

Cribrosphaerella? daniae Perch-Nielsen, 1973

Cribrosphaerella ehrenbergii (Arkhangelskii, 1912) Deflandre in Piveteau, 1952: Included in this species are elliptical, triangular, as well as almost circular morphotypes.

Cruciplacolithus Hay and Mohler in Hay et al, 1967: Rare representatives of this genus have been observed in the uppermost Maestrichtian samples in Hole 690C where they are considered to be contamination due to bioturbation.

Cyclagelosphaera alta Perch-Nielsen, 1979a

C. margerelii Noel, 1965

C. reinhardtii (Perch-Nielsen, 1968) Romein, 1977

Cyclagelosphaera sp. 1: In size and extinction pattern this species is similar to C. margerelii but in brightfield 4 or 5 ridges are visible radiating from the center of the coccolith and extending about halfway to its periphery.

Cylindralithus Bramlette and Martini, 1964

C. biarcus Bukry, 1969

C. gallicus (Stradner, 1963) Bramlette and Martini, 1964: Round and elliptical morphotypes were observed.

C. serratus Bramlette and Martini, 1964: Included in this species are all specimens that have a narrow margin in comparison to C. gallicus.

Cylindralithus sp. 1: This form consists of wide, thick, numerous, strongly overlapping elements. It is distinguished from C. gallicus by having

more numerous elements, from C. serratus by being thicker. In cross polarized light this form is highly birefringent, blue and orange interference colors are characteristic. Monechi (1985, pl. 2, figs. 6, 10A, 10B) illustrated this form as Cylindralithus sp.

Discorhabdus ignotus (Gorka, 1957) Perch-Nielsen, 1968

Eiffellithus parallelus Perch-Nielsen, 1973

E. trabeculatus (Gorka, 1957) Reinhardt and Gorka (1967)

E. turriseiffeli (Deflandre in Deflandre and Fert, 1954) Reinhardt (1965): The size variation within this species is considerable, but continuous.

Ericsonia Black, 1964

Ericsonia sp.: Included in this taxon are circular forms with a large central opening with white to light yellow interference colors.

Gartnerago Bukry, 1969

Gartnerago spp.: Thierstein (1974) used the number and arrangement of pores in the central area to distinguish between G. segmentatus, G. obliquum, and G. segmentatum, but he reports that the pores get easily obliterated as a consequence of recrystallization. This observation is corroborated in this study. As a consequence it was not possible here to differentiate between different species.

Glaukolithus fessus (Stover, 1966) Perch-Nielsen, 1968

Hexalithus Gardet, 1955: Forms with six and with eight rays were observed.

Hornibrookina Edwards, 1973

Kamptnerius magnificus Deflandre, 1959: Included in this species are also the perforated forms (K. punctatus) that were occasionally encountered.

Lapideacassis Black, 1971 spp indet: Due to fragmentation rigorous and consistent species identification was impossible in this genus.

Lithastrinus Stradner, 1962

Lithastrinus spp.: I have assigned to this genus small circular forms that usually have high interference colors (orange-red).

Lithraphidites carniolensis Deflandre, 1963

L. grossopectinatus Bukry, 1969

Lithraphidites sp. cf. L. kennethii Perch-Nielsen, 1984: Specimens included in this taxon are almost as wide as they are long, resembling L. quadratus that has been reduced to about half its length without changing the width.

L. praequadratus Roth, 1978

L. quadratus (Bramlette and Martini, 1964) Roth, 1978

Lithraphidites (?) sp. 1: This form is tentatively assigned to Lithraphidites.

Under the light-microscope it consists of two parallel rods which overlap for about one third of their length. The overlapping portions are somewhat thicker than the parts that form the two tips of this form.

Lucianorhabdus cayeuxii Deflandre (1959): Acuturris scotus is also included in this taxon. Both taxa occurred mostly as fragments which made consistent species identification impossible.

Manivitella pemmatoidea (Deflandre ex Manivit, 1965) Thierstein, 1971

Markalius apertus Perch-Nielsen, 1979

M. inversus (Deflandre in Deflandre and Fert, 1954) Bramlette and Martini, 1964

Microrhabdulus decoratus Deflandre, 1959

M. belgicus Hay and Towe, 1963

Micula murus (Martini, 1961) Bukry 1973

M. praemurus (Bukry, 1973) Stradner and Steinmetz, 1984

Micula sp. cf. M. prinsii Perch-Nielsen, 1979: Micula prinsii s. str. is characterized by curved arms with a delicate, terminal bifurcation that tends to recrystallize and overgrow. Specimens with long, curved arms were observed, but the characteristic bifurcation at the tips of the arms was absent. In some cases the tips of the arms were thickened and of higher birefringence than the remainder of the nannofossil, possibly due to recrystallization of the delicate terminal bifurcation.

M. staurophora (Gardet, 1955) Stradner, 1963

Micula? sp.: Pospichal and Bralower (1992, pl. 4, figs. 7, 8) illustrate this species: the fact that it consists of four crystals and its extinction pattern suggest that it belongs to the genus Micula. The triangular outline of this form is unusual for Micula. It was encountered only at mid and low latitudes, its stratigraphic range is the uppermost Maestrichtian (approximately the M. murus Zone).

Misceomarginatus Wind and Wise in Wise and Wind, 1977

Misceomarginatus pleniporus Wind and Wise in Wise and Wind, 1977: Species identification of Misceomarginatus and of Monomarginatus was not consistently possible due to susceptibility of these species to dissolution and recrystallization. For plotting purposes species from both genera were added together.

Monomarginatus Wind and Wise in Wise and Wind, 1977

Monomarginatus pectinatus Wind and Wise in Wise and Wind, 1977

M. quaternarius Wind and Wise in Wise and Wind, 1977

Neocrepidolithus Romein, 1979 spp indet.: Included here are all species of Neocrepidolithus that were encountered in the immediate vicinity of the K/P boundary (e.g. N. crassus, N. cruciatus, etc). Never included is N. watkinsii.

Neocrepidolithus watkinsii Pospichal and Wise, 1990

Nephrolithus frequens Gorka, 1957: Frequently specimens were observed with a highly birefringent crystal in the center of the distal side of the coccolith. It is possible that this bright spot was caused by a piece of calcite debris lying on top of the nannofossils; this is improbable considering that the "bright spot" occurred consistently in the center of the central area. Alternatively, the "bright spot" could be the expression of a genuine structural feature, like a knob or short stem, similar to the stems observed in N. corystus. Watkins (1992: pl. 4, fig. 1) has indeed illustrated N. frequens with a short stem in material from the Kerguelen Plateau.

N. corystus Wind, 1983

Octocyclus magnus Black, 1972

Parhabdolithus sp. cf. P. embergeri (Noël, 1958) Stradner, 1963: Specimens included in this taxon differ from P. embergeri in lacking a clear bipartition of the transverse bar, which is usually massive and diamond shaped. The specimens are virtually always very recrystallized, with high relief, outline of individual elements never discernible, and high interference colors (red, blue). The openings in the central area are often completely closed due to overgrowth.

Parhabdolithus regularis (Gorka, 1957) Bukry, 1969

Pervilithus varius Crux, 1981: This species occurs very rarely in the upper Maestrichtian (N. frequens Zone) in Hole 690C and upper Maestrichtian M. murus Zone in Hole 217. This extends the range originally assigned to this species (Santonian to Campanian; Crux, 1981) into the upper Maestrichtian.

Petrarhabdus copulatus (Deflandre, 1959) Wind and Wise in Wise (1983):

Phanulithus obscurus (Deflandre, 1959) Wind and Wise in Wise and Wind (1977)

Placozygus fibuliformis (Reinhardt, 1964) Hoffmann, 1970

P. bussonii Perch-Nielsen, 1968

P. sigmoides (Bramlette and Sullivan, 1961) Romein, 1979

Placozygus sp: This species was illustrated by Pospichal and Bralower (1992, pl. 4, figs 11-12) as Zygodiscus sp. The basal plate and the flange (sensu Aubry, 1988) of this form are usually present, the transverse bar in virtually all cases absent. The basal plate is quite narrow. The flange is always well developed and consists of strongly overlapping, distally flaring elements. The sutures in this cycle are easily discernible under the light microscope (bright field). In many forms it appears as if an additional cycle is present in the central area, adjacent to the basal plate and the flange, usually extending all the way around. The provenance of this cycle is unclear: it may either correspond to the blocky elements at the junction of transverse bar and basal plate in P. sigmoides, or may be an artifact of recrystallization and overgrowth of the basal plate extending into the central opening. The size of this species is quite variable; it is fairly common in the Maestrichtian at middle and low latitudes.

Prediscosphaera arkhangel'skyi (Reinhardt, 1965) Perch-Nielsen, 1984

P. cretacea (Arkhangelsky, 1912) Gartner, 1968: Considerable size variation is conspicuous within this species. It did not appear, however, that distinct size classes justify the separation of subspecies, or morphotypes. A quantitative study may be necessary to investigate this issue. Round morphotypes of Prediscosphaera were included in this species.

P. grandis Perch-Nielsen, 1979

P. spinosa (Bramlette and Martini, 1964) Gartner, 1968

P. stoveri (Perch-Nielsen, 1968) Shafik and Stradner, 1971

Prinsius tenuiculum (Okada and Thierstein, 1979) Perch-Nielsen, 1984

Psyktosphaera firthii Pospichal and Wise, 1990: The perforate inner central area of this species is elliptical and has a granulate appearance in cross polarized light. Some specimens were encountered in which the perforate part of the central area was extremely narrow.

Quadrum gartneri Prins and Perch-Nielsen in Manivit et al, 1977

Q. trifidum (Stradner in Stradner and Papp, 1961) Prins and Perch-Nielsen in Manivit et al, 1977

Reinhardtites aff. anthophorus Prins and Sissingh in Sissingh, 1977

R. levis Prins and Sissingh in Sissingh, 1977

Rhagodiscus Reinhardt, 1967

Rhagodiscus angustus (Stradner, 1963) Reinhardt, 1971

R. reniformis Perch-Nielsen, 1973

R. splendens (Deflandre, 1953) Verbeek, 1977

Rhagodiscus sp. 1: This species is characterized by an extremely narrow central area.

Rhombolithion rhombicum (Stradner and Adamiker, 1966) Black, 1973

Rucinolithus hayi Stover, 1966

Scampanella Forchheimer and Stradner, 1973

S. asymmetrica Perch-Nielsen, 1977

S. wisei Perch-Nielsen in Perch-Nielsen and Franz, 1977

Scapholithus fossilis Deflandre in Deflandre and Fert, 1954

Staurolithites laffittei Caratini, 1963

Stephanolithion Deflandre, 1939 spp indet.: Different species of this genus are recognized based on the number of central spokes and peripheral knobs. In less than well preserved material the central spokes are unrecognizable and the knobs on the outside of the nannofossil are partly dissolved. The consistent recognition of species was therefore impossible.

Tegumentum stradneri Thierstein in Roth and Thierstein, 1972

Teichorhabdus ethmos Wind and Wise in Wise and Wind, 1977

Tetrapodorhabdus decorus (Deflandre in Deflandre and Fert, 1954) Wind and Wise in Wise and Wind, 1977

Thoracosphaera Kamptner, 1927 spp: included are T. operculata, T. saxea

Tranolithus macleodae (Bukry, 1969) Perch-Nielsen, 1984: includes T. minimus

Tranolithus phacelosus Stover, 1966

Vagalapilla Bukry, 1969

Watznaueria barnesae (Black in Black and Barnes, 1959) Perch-Nielsen, 1968

W. biporta Bukry, 1969

Zygodiscus compactus Bukry, 1969

Z. diplogrammus (Deflandre in Deflandre and Fert, 1954) Gartner, 1968

Z. lacunatus Gartner, 1968

Zygodiscus sp. 1: This is a small form of Zygodiscus? with a cross aligned with the ellipse axes spanning the central opening. Under the light

microscope a small dark spot at the intersection of the cross arms is a very distinct feature.

APPENDIX II
DATA

The counting results are listed in the following tables. The following abbreviations are used:

Preservation: G - good
 M - moderate
 P - poor
 PP- very poor

Abundance: A - abundant
 C - common
 R - rare

Carbonate content: n.d. - not determined

An asterisk (*) or a 'P' in the data tables indicates that this taxon was observed at this level during the additional scanning after the counts were performed.

Sample Number	1	2	3	4	5	6	7	8	9
ODP Hole 690C	690C	690C	690C	690C	690C	690C	690C	690C	690C
Core - Section	15-4	15-4	15-4	15-4	15-4	15-4	15-4	15-4	15-4
cm - level	38	41	43.5	47	50	53	56.5w	56.5b	60.5
Depth (mbsf)	247.78	247.81	247.835	247.87	247.9	247.93	247.965	247.965	248.005
<i>Placozygus bussonii</i>
<i>P. fibuliformis</i>	1	P	.	.	P
<i>P. sigmoides</i>	52	19	9	80	5	1	1	16	5
<i>Placozygus</i> sp.
<i>Prediscosphaera arkhangel'skyi</i>
<i>P. cretacea</i>	36	20	29	65	19	18	19	18	35
<i>P. spinosa</i>	.	2	2	14	1	P	6	4	4
<i>Psyktosphaera firthii</i>
<i>Quadrum gartneri</i>
<i>Reinhardtites</i> spp.
<i>Rhagodiscus angustus</i>
<i>Rhagodiscus</i> spp.
<i>Rhombolithion rhombicum</i>
<i>Scampanella asymmetrica</i>
<i>S. wisai</i>
<i>Scampanella</i> spp.	.	P
<i>Scapholithus fossilis</i>
<i>Staurolithites laffitei</i>
<i>Teichorhabdus ethmos</i>
<i>Thoracosphaera</i> spp.	5	16	3	44	3	3	1	4	3
<i>Vagalapilla</i> spp.	.	1	1	8	3	2	4	3	8
<i>Watznaueria barnesae</i>	1
<i>Zygodiscus compactus</i>
<i>Z. diplogrammus</i>
Unidentifiable	6	5	4	18	5	5	5	3	9
Total (exclusive of <i>P. stoveri</i>):	383	174	153	625	169	150	186	162	353
<i>Prediscosphaera stoveri</i>	366	148	190	187	192	199	169	178	518
Total of <i>P. stoveri</i> - count(s)	750	322	343	345	361	351	355	340	871
<i>P. stoveri</i> , fields	153.9	99.2	34	42	33	32	18	28	67

Sample Number	10	11	12	13	14	15	16	17	18	19	20	21
Hole	690C	690C	690C	690C	690C	690C	690C	690C	690C	690C	690C	690C
Core - Section	15-4	15-4	15-4	15-4	15-4	15-4	15-4	15-4	15-4	15-4	15-4	15-4
cm - level	62	64	67	70	73	76	79	82.5	85	88	92	95
Depth (mbsf)	248.02	248.04	248.07	248.1	248.13	248.16	248.19	248.225	248.25	248.28	248.32	248.35
<i>P. bussonii</i>
<i>P. fibuliformis</i>	1	1	.	.	.	P	.	3
<i>P. sigmoides</i>	3	.	.	.
<i>Placozygus</i> sp.
<i>P. arkhangel'skyi</i>
<i>P. cretacea</i>	20	26	23	21	17	19	26	14	19	24	17	17
<i>P. spinosa</i>	1	1	3	2	1	6	2	.	2	4	.	2
<i>P. firthii</i>
<i>Q. gartneri</i>
<i>Reinhardtites</i> spp.
<i>R. angustus</i>
<i>Rhagodiscus</i> spp.
<i>R. rhombicum</i>
<i>S. asymmetrica</i>
<i>S. wisei</i>	2
<i>Scampanella</i> spp.
<i>S. fossilis</i>
<i>S. laffitei</i>
<i>T. ethmos</i>
<i>Thoracosph.</i> spp.	2	2	2	.	1	1	.	.	.	1	1	.
<i>Vagalapilla</i> spp.	1	1	1	2	1	4	7	1	2	1	.	3
<i>W. bamesae</i>
<i>Z. compactus</i>
<i>Z. diplogrammus</i>
Unidentifiable	1	4	4	4	5	2	1	7	3	5	6	4
Total (excl. <i>P. stoveri</i>)	173	133	205	187	160	174	177	140	188	184	151	148
<i>P. stoveri</i>	175	205	226	189	178	215	148	175	158	160	174	171
Total (<i>P. stoveri</i> .count)	348	338	431	376	338	389	325	315	346	344	325	319
<i>P. stoveri</i> , fields	22	25	23	25	24	21	19	49	46	19	42	34

Sample Number	22	23	24	25	26	27	28	29	30	31	32	33
Hole	690C	690C	690C	690C	690C	690C	690C	690C	690C	690C	690C	690C
Core - Section	15-4	15-4	15-4	15-4	15-4	15-4	15-4	15-4	15-4	15-4	15-4	15-5
cm - level	98	100-101	103-104	106-107	110-111	113-114	118	121	129	140	149	3
Depth (mbsf)	248.38	248.4	248.43	248.46	248.5	248.53	248.58	248.61	248.69	248.8	248.89	248.93
<i>P. bussonii</i>
<i>P. fibuliformis</i>	.	.	P	.	.	P	P	.	.	1	1	P
<i>P. sigmoides</i>	1	.	1	.	?	.	.
<i>Placozygus sp.</i>
<i>P. arkhangel'skyi</i>
<i>P. cretacea</i>	28	17	22	21	24	22	14	68	22	60	21	61
<i>P. spinosa</i>	.	2	7	2	.	2	P	P	.	2	2	26
<i>P. firthii</i>
<i>Q. gartneri</i>
<i>Reinhardtites spp.</i>
<i>R. angustus</i>
<i>Rhagodiscus spp.</i>
<i>R. rhombicum</i>
<i>S. asymmetrica</i>	P
<i>S. wisei</i>
<i>Scampanella spp.</i>	.	.	.	1	.	.	P
<i>S. fossilis</i>
<i>S. laffitei</i>
<i>T. ethmos</i>
<i>Thoracosph. spp.</i>
<i>Vagalapilla spp.</i>	P	2	10	2	.	1	P	2	.	.	.	9
<i>W. bamesae</i>
<i>Z. compactus</i>
<i>Z. diplogrammus</i>
Unidentifiable	3	3	5	8	3	10	4	21	3	13	6	16
Total (excl. <i>P. stoveri</i>)	171	193	184	186	199	150	135	520	168	472	196	458
<i>P. stoveri</i>	186	222	221	200	153	178	189	192	157	134	110	181
Total (<i>P. stoveri</i> .count)	357	415	405	386	352	328	324	345	325	301	306	312
<i>P. stoveri</i> , fields	47	43	30	47	36	16	34	44	44	80	101	34

Sample Number	34	35	36	37	38	39	40	41	42	43	44	45
Hole	690C	690C	690C	690C	690C	690C	690C	690C	690C	690C	690C	690C
Core - Section	15-5	15-5	15-5	15-5	15-5	15-5	15-5	15-5	15-5	15-5	15-5	15-5
cm - level	11-12.0	22-23	31	39-40	49-50	60-61	70-71	79-80	90-91	101	110-111	120
Depth (mbsf)	249.01	249.12	249.21	249.29	249.39	249.5	249.6	249.69	249.8	249.91	250	250.1
<i>P. bussonii</i>
<i>P. fibuliformis</i>	1	.	.	P	P	2	1	2	2	3	19	41
<i>P. sigmoides</i>	.	.	.	P	2	.	P	.	.	1	1	1
<i>Placozygus</i> sp.
<i>P. arkhangel'skyi</i>
<i>P. cretacea</i>	80	37	27	71	46	42	35	75	63	70	66	58
<i>P. spinosa</i>	6	13	2	24	17	12	6	32	7	36	50	49
<i>P. firthii</i>
<i>Q. gartneri</i>
<i>Reinhardtites</i> spp.
<i>R. angustus</i>
<i>Rhagodiscus</i> spp.
<i>R. rhombicum</i>
<i>S. asymmetrica</i>
<i>S. wisei</i>	.	.	.	P	P	.	P
<i>Scampanella</i> spp.	P	.	.	P	P	.	P	1	.	.	1	.
<i>S. fossilis</i>
<i>S. laffittei</i>
<i>T. ethmos</i>
<i>Thoracosph.</i> spp.
<i>Vagalapilla</i> spp.	1	3	.	6	2	3	2	7	.	6	23	8
<i>W. bamesae</i>
<i>Z. compactus</i>
<i>Z. diplogrammus</i>
Unidentifiable	15	3	4	10	5	4	4	20	11	13	22	11
Total (excl. <i>P. stoveri</i>)	634	207	256	488	294	329	315	609	432	624	629	676
<i>P. stoveri</i>	297	172	145	166	188	314	269	189	151	176	220	254
Total (<i>P. stoveri</i> count)	931	379	401	318	482	646	585	352	310	341	433	495
<i>P. stoveri</i> , fields	101.4	22	86.9	17	32	30	30	30	43	30	32	30

Sample Number	46	47	48	49	50	51	52	53	54	55	56	57
Hole	690C	690C	690C	690C	690C	690C	690C	690C	690C	690C	690C	690C
Core - Section	15-5	15-5	15-5	15-6	15-6	15-6	15-6	15-6	15-6	15-6	15-6	15-6
cm - level	130-131	140-141	150	4. - 5	10	20	30-31	40-41	50-51	59-60	70	80
Depth (mbsf)	250.2	250.3	250.4	250.44	250.5	250.6	250.7	250.8	250.9	250.99	251.1	251.2
<i>P. bussonii</i>
<i>P. fibuliformis</i>	19	24	8	23	30	27	12	30	24	22	11	18
<i>P. sigmoides</i>	1	1	1	2	1	1	.
<i>Placozygus sp.</i>
<i>P. arkhangel'skyi</i>
<i>P. cretacea</i>	79	55	34	62	68	47	45	74	86	144	115	84
<i>P. spinosa</i>	35	42	26	73	11	45	31	40	40	33	26	17
<i>P. firthii</i>
<i>Q. gartneri</i>
<i>Reinhardtites spp.</i>
<i>R. angustus</i>
<i>Rhagodiscus spp.</i>
<i>R. rhombicum</i>	1
<i>S. asymmetrica</i>
<i>S. wisei</i>
<i>Scampanella spp.</i>	P	1	.	.
<i>S. fossilis</i>
<i>S. laffitei</i>
<i>T. ethmos</i>
<i>Thoracosph. spp.</i>	.	.	.	1	.	2	6	2	.	1	1	4
<i>Vagalapilla spp.</i>	3	11	1	10	4	5	9	6	7	2	5	3
<i>W. bamesae</i>	1
<i>Z. compactus</i>
<i>Z. diplogrammus</i>
Unidentifiable	9	21	12	19	33	19	12	18	20	19	11	11
Total (excl. <i>P. stoveri</i>)	568	601	269	620	536	562	361	502	535	692	549	457
<i>P. stoveri</i>	424	233	139	222	187	314	298	352	413	313	354	428
Total (<i>P. stoveri</i> .count)	829	474	410	462	329	644	659	602	802	567	715	885
<i>P. stoveri</i> , fields	30	30	27	30	35	30	30	30	30	30	30	30

Sample Number	70	71	72	73	74	75	76	77	78	79	80	81
Hole	690C	690C	690C	690C	690C	690C	690C	690C	690C	690C	690C	690C
Core - Section	16-1	16-1	16-1	16-1	16-1	16-1	16-1	16-1	16-3	16-4	17-1	17-3
cm - level	9-10	21-22	30-31	40-41	50-51	59-60	70	100-101	20-21	80	31-32	29-30
Depth (mbsf)	252.59	252.71	252.8	252.9	253	253.09	253.2	253.5	255.7	257.8	262.11	265.09
<i>P. bussonii</i>	1	.
<i>P. fibuliformis</i>	3	4	4	6	3	10	4	.	4	2	6	3
<i>P. sigmoides</i>	6	.	1
<i>Placozygus sp.</i>	1
<i>P. arkhangel'skyi</i>	1
<i>P. cretacea</i>	75	69	35	53	11	92	59	30	53	23	30	28
<i>P. spinosa</i>	29	24	3	37	1	19	14	21	13	10	5	1
<i>P. firthii</i>
<i>Q. gartneri</i>
<i>Reinhardtites spp.</i>	1	.
<i>R. angustus</i>	1
<i>Rhagodiscus spp.</i>	1	.	.
<i>R. rhombicum</i>
<i>S. asymmetrica</i>
<i>S. wisei</i>
<i>Scampanella spp.</i>	1	1
<i>S. fossilis</i>
<i>S. laffitei</i>
<i>T. ethmos</i>	.	.	.	?	.	.	P	.	P	1	.	1
<i>Thoracosph. spp.</i>	3	1	.	1	.	2	.	1	.	.	.	1
<i>Vagalapilla spp.</i>	6	13	2	20	1	16	9	11	8	14	7	2
<i>W. barnesae</i>
<i>Z. compactus</i>
<i>Z. diplogrammus</i>
Unidentifiable	17	34	15	10	19	16	20	10	15	5	6	2
Total (excl. <i>P. stoveri</i>)	600	547	512	564	402	596	477	409	357	411	345	245
<i>P. stoveri</i>	293	308	281	437	79	588	1004	1066	622	677	461	111
Total (<i>P. stoveri</i> .count)	631	544	793	780	481	932	1482	1476	979	1088	806	356
<i>P. stoveri</i> , fields	30	30	273.2	30	142.8	30	30	30	15.8	20.2	59.7	64.1

Sample Number	82	83	84	85	86	87	88	89	90	91	92	93
Hole	690C	690C	690C	690C	690C	690C	690C	690C	690C	690C	690C	690C
Core - Section	18-1	18-3	18-5	19-1	19-3	19-6	19-7	20-1	20-1	20-1	20-1	20-2
cm - level	107-108	106	54	107	137	110-111	20-21	68-69	130	136	145	4-5
Depth (mbsf)	272.47	275.46	277.94	282.17	285.47	289.7	290.3	291.48	292.1	292.16	292.25	292.34
Sed. rate (m/m.y.)	5.7	5.7	5.7	5.7	8.9	8.9	8.9	8.9	8.9	8.9	8.9	8.9
Age (Ma)	69.439	69.968	70.407	71.156	71.604	72.080	72.147	72.280	72.350	72.357	72.367	72.377
Pres. (G, M, P)	P-M	PP	M-P	M	M	PP	M	M	M-G	M-G	M-G	M-G
Abund. (A, C, R)	C-R	C	A-C	C	A	R	A	A	A	A	A	A
Fields counted	65.9	24.6	40	54.9	20.2	23.7	20.6	23.3	29	35.1	59.7	36.4
mg sediment	21.0	21.1	21.2	20.5	20.4	20.4	20.3	20.8	21.1	20.0	19.7	20.1
Carbonate (wt-%)	89.9	81.3	76.3	62.7	61.5	83.1	76.3	47.8	53.1	52.2	54.3	55.3
Beaker Constant	2.7	2.7	2.7	2.7	2.7	2.7	2.7	2.7	2.7	2.7	2.7	2.7
<i>A. octoradiata</i>	1	.	.	26	36	.	25	42	58	64	53	51
<i>A. cymbiformis</i>	7	2	2	.	.	4	.	.	.	19	12	7
<i>A. cymbif./specill.</i>	1	6	.	.	.
<i>A. specillata</i>	4	1	2
<i>B. sparsus</i>
<i>B. boletum</i>	.	.	.	2	1	.	1
<i>B. constans</i>	4	.	4	10	8	2	3	10	13	3	2	10
<i>B. coronum</i>
<i>B. dissimilis</i>	3	.	2	1	1	.	.	2
<i>B. magnum</i>	.	.	.	12	45	5	37	31	21	25	13	29
<i>B. notaculum</i>	.	.	10	50	42	7	40	54	50	51	75	66
<i>Biscutum sp. 1</i>	3	.	1	.	1	2
<i>Biscutum sp. 2</i>	.	.	.	2	1	1	3	3
<i>B. cf bevieri</i>	5	5	3	4	3	16
<i>Broinsonia spp.</i>	.	.	.	27	4	1	8	9	6	.	.	.
<i>C. barbata</i>	1	.	2	6	3	.	.	4	10	10	11	1
<i>C. amphipons</i>	.	.	.	?	?	1	1	.	.	.	1	.
<i>C. garrisonii</i>	.	.	.	3	3	.	7	6	4	6	3	7
<i>Chiastozygus sp. 1</i>	2	1
<i>C. conicus</i>	1	.	1	2	2	3	.	4
<i>C. crenulatus</i>
<i>C. surirellus</i>	.	.	.	6	2	.	1	2	.	.	4	1
<i>Cretarhabdus sp. 1</i>	1	.	1	1	1	.	.	.
<i>Cretarhabdus spp.</i>	4	3	.	3	1	.	1	4	3	.	1	.
<i>C. daniae</i>	3	7	44	1	.	.	1
<i>C. ehrenbergii</i>	.	.	.	3	5	.	.	1	8	2	6	3
<i>Cruciplacolithus spp.</i>
<i>Cyclagelosph. spp.</i>	1	.	.	.	1
<i>Cylindralithus spp.</i>
<i>D. ignotus</i>	.	.	.	1	1	.	.
<i>E. trabeculatus</i>
<i>E. turriseiffeli</i>	.	1	16	6	16	1	31	15	21	23	15	14
<i>Gartnerago spp.</i>	.	P	10	5	8	.	3	2	12	8	7	5
<i>G. fessus</i>	1	1
<i>Hornibrookina spp.</i>
<i>K. magnificus</i>	54	21	63	27	12	6	9	29	22	10	6	20
<i>Lapideacassis spp.</i>
<i>L. carniolensis</i>	.	.	.	1
<i>L. cayeuxii</i>	15	24	17	10	21	5	24	1	1	4	7	9
<i>M. inversus</i>
<i>M. decoratus</i>
<i>M. staurophora</i>	1	.	.	3	1	1
<i>M. pleniporus</i>	1	.	.	1	4	.	.	.
<i>Misceomarg. sp.</i>
<i>M. pectinatus</i>	1	1	1	.	3
<i>M. quaternarius</i>	.	.	.	7	7	.	10	2	2	.	5	4
<i>Monomarg. sp.</i>
<i>Misceo/Monomg sp.</i>	1
<i>N. watkinsii</i>	2	3	.	2
<i>Neocrepidol. spp.</i>
<i>N. corystus</i>	.	.	4	14	27	2	47	50	39	36	33	34
<i>N. frequens</i>	29	5	75
<i>O. magnus</i>	5	1	.	.	1	1
<i>P. obscurus</i>	.	.	.	3	7	2	11	1	3	2	2	3

Sample Number	82	83	84	85	86	87	88	89	90	91	92	93
Hole	690C	690C	690C	690C	690C	690C	690C	690C	690C	690C	690C	690C
Core - Section	18-1	18-3	18-5	19-1	19-3	19-6	19-7	20-1	20-1	20-1	20-1	20-2
cm - level	107-108	106	54	107	137	110-111	20-21	68-69	130	136	145	4-5
Depth (mbsf)	272.47	275.46	277.94	282.17	285.47	289.7	290.3	291.48	292.1	292.16	292.25	292.34
<i>P. bussorii</i>	.	.	.	1	.	3	2	1	1	.	.	.
<i>P. fibuliformis</i>	.	.	5	4	2	2	3
<i>P. sigmoides</i>	1	.	.	1	4	1	1	.
<i>Placozygus</i> sp.	1
<i>P. arkhangel'skyi</i>	.	2	11	3	10	.	17	7	6	6	4	9
<i>P. cretacea</i>	14	2	.	4	1	.	3	5	18	15	6	7
<i>P. spinosa</i>	1	1	27	15	47	.	13	34	28	26	32	30
<i>P. firthii</i>	.	.	.	5	38	.	19	15	18	12	8	12
<i>Q. gartneri</i>
<i>Reinhardtites</i> spp.	.	.	.	18	6	2	4	20	38	28	39	16
<i>R. angustus</i>	7	.	.	.
<i>Rhagodiscus</i> spp.
<i>R. rhombicum</i>	2	1	P	.	.	1
<i>S. asymmetrica</i>
<i>S. wisei</i>
<i>Scampanella</i> spp.	.	.	1
<i>S. fossilis</i>	.	.	4	.	1	.	3	1	2	7	1	2
<i>S. laffitei</i>	.	.	.	1	1	4
<i>T. ethmos</i>	1	.	?	.	.	.	1	.	P	1	.	.
<i>Thoracosph.</i> spp.	.	.	1	12	3	.	10	17	15	16	9	27
<i>Vagalapilla</i> spp.	2	1	8	14	17	.	16	12	16	14	9	15
<i>W. barnesae</i>	1	1	2	.	2
<i>Z. compactus</i>	.	.	.	12	.	6	8
<i>Z. diplogrammus</i>
Unidentifiable	5	1	12	16	14	.	31	9	9	26	7	22
Total (excl. <i>P. stoveri</i>)	143	70	316	333	393	49	412	405	457	435	382	449
<i>P. stoveri</i>	53	.	17	26	43	1	13	3	12	7	5	9
Total (<i>P. stoveri</i> .count)	196	70	333	359	436	50	425	408	468	442	387	458
<i>P. stoveri</i> , fields	65.9	24.6	40	54.9	20.2	23.7	20.6	23.3	29	35.1	59.7	36.4

Sample Number	94	95	96	97	98	99	100	101	102	103	104	105
Hole	690C	690C	690C	690C	690C	690C	690C	690C	690C	690C	690C	690C
Core - Section	20-2	20-2	20-2	20-2	20-2	20-2	20-2	20-2	20-2	20-2	20-2	20-2
cm - level	10-11	19-20	29-30	38-39	47-48	51-52	61.1	70-71	80	90	100	110-111
Depth (mbsf)	292.4	292.49	292.59	292.68	292.77	292.81	292.91	293	293.1	293.2	293.3	293.4
Sed. rate (m/m.y.)	8.9	8.9	8.9	8.9	8.9	8.9	8.9	8.9	8.9	8.9	8.9	8.9
Age (Ma)	72.383	72.394	72.405	72.415	72.425	72.430	72.441	72.451	72.462	72.473	72.485	72.496
Pres. (G, M, P)	M-G	M	M-G	M	M-G	G	M-G	M	M	M-P	M-P	M-G
Abund. (A, C, R)	C-A	A	A	A	C	A	A	A	A	C	C-R	A
Fields counted	70.7	52.7	20	41	73.3	20.2	22	17.6	22	45.7	56.2	12.7
mg sediment	18.3	18.5	18.6	18.0	17.1	21.1	19.0	21.8	20.4	20.4	21.0	20.0
Carbonate (wt-%)	55.9	53.3	56.7	52.9	52.7	50.4	58.2	60.3	62.5	70.1	70.5	68.7
Beaker Constant	2.7	2.7	2.7	2.7	2.7	2.7	2.7	2.7	2.7	2.7	2.7	2.7
<i>A. octoradiata</i>	29	32	12	18	34	31	41	50	38	33	30	26
<i>A. cymbiformis</i>	23	17	9	11	11	8	8	11	9	6	4	1
<i>A. cymbif./specill.</i>	2	.
<i>A. specillata</i>	.	.	P	1	1	5	2	4	2	.	2	?
<i>B. sparsus</i>
<i>B. boletum</i>	2
<i>B. constans</i>	1	6	3	3	6	10	6	10	14	11	14	16
<i>B. coronum</i>	.	.	P	.	1	P
<i>B. dissimilis</i>	.	1	.	.	.	2	1	4	1	1	.	4
<i>B. magnum</i>	29	29	13	22	16	27	24	22	33	39	21	28
<i>B. notaculum</i>	67	58	23	56	97	45	77	69	77	84	96	66
<i>Biscutum</i> sp. 1	.	1	.	.	.	2	.	3
<i>Biscutum</i> sp. 2	.	2	.	.	.	3	2	8	2	1	.	2
<i>B. cf bevieri</i>	10	15	11	9	.	7	10	8	8	2	5	5
<i>Broinsonia</i> spp.	5	1	5	5
<i>C. barbata</i>	3	4	1	5	2	1	2	3	1	1	.	1
<i>C. amphipons</i>	.	.	P	2	.	1	.	1	.	.	1	.
<i>C. garrisonii</i>	1	P	6	1	3	4	10	3	8	1	.	10
<i>Chiastozygus</i> sp. 1	1	2	1	2	.	.	.
<i>C. conicus</i>	1	2	P	.	1	1	.	.
<i>C. crenulatus</i>
<i>C. surirellus</i>	3	3	1	2	2	3	3	4	2	1	5	1
<i>Cretarhabdus</i> sp. 1	3	2	4	1	.	P
<i>Cretarhabdus</i> spp.	3	.	1	1	2	1	1	1	.	3	3	.
<i>C. daniae</i>
<i>C. ehrenbergii</i>	4	2	2	6	1	3	2	2	.	3	3	1
<i>Cruciplacolithus</i> spp.
<i>Cyclagelosph.</i> spp.
<i>Cylindralithus</i> spp.
<i>D. ignotus</i>	1
<i>E. trabeculatus</i>	1
<i>E. turriseiffeli</i>	14	23	10	15	6	18	16	21	17	3	4	12
<i>Gartnerago</i> spp.	8	12	1	2	8	4	10	15	20	8	8	12
<i>G. fessus</i>	.	.	.	1
<i>Hornibrookina</i> spp.
<i>K. magnificus</i>	14	15	10	12	11	24	20	20	25	19	10	21
<i>Lapideacassis</i> spp.	1	.	1
<i>L. camiolensis</i>	.	.	.	1
<i>L. cayeuxii</i>	9	9	5	P	1	1	2	5	13	19	15	13
<i>M. inversus</i>
<i>M. decoratus</i>
<i>M. staurophora</i>	.	.	1	2	2	2
<i>M. pleniporus</i>	.	.	1	1	1	1	1	.
<i>Misceomarg.</i> sp.
<i>M. pectinatus</i>	1	2	.	.	.	1	.
<i>M. quaternarius</i>	3	7	2	3	6	.	3	2	5	3	2	4
<i>Monomarg.</i> sp.
<i>Misceo/Monomg</i> sp.
<i>N. watkinsii</i>	.	1	1	.	6	2	.	4	1	2	2	P
<i>Neocrepidol.</i> spp.
<i>N. corystus</i>	36	36	23	43	37	42	34	51	23	25	28	22
<i>N. frequens</i>
<i>O. magnus</i>	.	1	.	P	.	.	.	1
<i>P. obscurus</i>	.	.	1	1	1	2	3	2	2	5	3	3

Sample Number	94	95	96	97	98	99	100	101	102	103	104	105
Hole	690C	690C	690C	690C	690C	690C	690C	690C	690C	690C	690C	690C
Core - Section	20-2	20-2	20-2	20-2	20-2	20-2	20-2	20-2	20-2	20-2	20-2	20-2
cm - level	10-11	19-20	29-30	38-39	47-48	51-52	61.1	70-71	80	90	100	110-111
Depth (mbsf)	292.4	292.49	292.59	292.68	292.77	292.81	292.91	293	293.1	293.2	293.3	293.4
<i>P. bussonii</i>	P
<i>P. fibuliformis</i>	1	.	.	1	1	1	2	4	1	1	1	.
<i>P. sigmoides</i>	2	3	2	2	2	.	.	1	3	1	.	2
<i>Placozygus sp.</i>	.	1	1	3	.
<i>P. arkhangel'skyi</i>	7	4	7	5	3	11	11	6	3	1	2	8
<i>P. cretacea</i>	7	11	4	11	6	7	4	2	4	4	4	3
<i>P. spinosa</i>	26	22	15	39	22	29	31	34	32	21	22	24
<i>P. firthii</i>	13	10	9	15	8	18	10	10	18	7	7	13
<i>Q. gartneri</i>	2	.	.
<i>Reinhardtites spp.</i>	24	32	10	23	22	19	17	9	9	6	9	10
<i>R. angustus</i>	.	1	1	2	.	.	.	1
<i>Rhagodiscus spp.</i>
<i>R. rhombicum</i>	1	.	1	1	.	2	.	1	1	.	1	3
<i>S. asymmetrica</i>	1	.	P
<i>S. wisei</i>
<i>Scampanella spp.</i>	.	.	P
<i>S. fossilis</i>	1	.	1	2	3	2	7	5	3	.	.	6
<i>S. laffitei</i>	2	3	.	3	3	3	6	5	5	3	3	4
<i>T. ethmos</i>	.	.	P	P	P	2	1
<i>Thoracosph. spp.</i>	9	9	2	9	9	11	9	6	7	3	2	9
<i>Vagalapilla spp.</i>	13	22	6	13	20	23	21	14	26	23	21	12
<i>W. barnesae</i>	3	.	.	2	1	1	2	.	2	.	.	.
<i>Z. compactus</i>	1	.	.	2	.	9	13	1
<i>Z. diplogrammus</i>	.	.	P	1	P
Unidentifiable	24	10	17	26	13	13	13	15	19	6	17	20
Total (excl. <i>P. stoveri</i>)	394	402	211	370	367	392	420	445	447	363	372	371
<i>P. stoveri</i>	9	6	.	6	4	13	2	4	2	10	2	.
Total (<i>P. stoveri</i> .count)	403	408	211	376	371	405	422	449	449	373	374	371
<i>P. stoveri</i> , fields	70.7	52.7	20	41	73.3	20.2	22	17.6	22	45.7	56.2	12.7

Sample Number	106	107	108	109	110	111	112	113	114	115	116	117
Hole	690C	690C	690C	690C	690C	690C	690C	690C	690C	690C	690C	690C
Core - Section	20-2	20-2	20-2	20-2	20-3	20-3	20-3	20-3	20-3	20-3	20-3	20-3
cm - level	120	129-130	140-141	149	10.1	30.1	52	70	90-91	107-108	130	150
Depth (mbsf)	293.5	293.59	293.7	293.79	293.9	294.1	294.32	294.5	294.7	294.87	295.1	295.3
Sed. rate (m/m.y.)	8.9	8.9	8.9	8.9	8.9	8.9	8.9	8.9	8.9	8.9	8.9	8.9
Age (Ma)	72.507	72.517	72.530	72.540	72.552	72.575	72.599	72.620	72.642	72.661	72.687	72.710
Pres. (G, M, P)	M-G	M-P	M	M-P	M	M	P-M	PP	M	M	M	M
Abund. (A, C, R)	A	A-C	A	A-C	A	A	A	A	A	A	A	A
Fields counted	20.6	29.9	14.5	19.8	21.1	30.7	26.3	58.8	21.1	22.4	20.2	20.6
mg sediment	21.6	20.4	20.7	21.0	20.0	20.7	19.8	19.7	20.6	21.2	19.5	20.6
Carbonate (wt-%)	65.5	65.3	65.2	63.3	62.3	63.3	75	77.4	69.5	65	62.8	61.6
Beaker Constant	2.7	2.7	2.7	2.7	2.7	2.7	2.7	2.7	2.7	2.7	2.7	2.7
<i>A. octoradiata</i>	32	43	38	38	43	36	22	25	23	32	34	47
<i>A. cymbiformis</i>	4	2	5	6	4	.	8	13	3	4	4	.
<i>A. cymbif./specill.</i>	.	1	2	1	3	3	3	4
<i>A. specillata</i>	2	.	1	1	.	.	.	1	1	.	.	1
<i>B. sparsus</i>
<i>B. boletum</i>	1	4	2	8	5	3
<i>B. constans</i>	14	11	7	9	18	13	13	11	13	18	17	7
<i>B. coronum</i>	P	1	.	.	1	1	1
<i>B. dissimilis</i>	2	1	1	1	1	.	.	3	1	1	2	4
<i>B. magnum</i>	30	25	22	11	32	28	25	22	31	38	43	44
<i>B. notaculum</i>	61	112	75	119	81	116	96	138	102	86	72	71
<i>Biscutum sp. 1</i>	1	.	8	4	.
<i>Biscutum sp. 2</i>	.	.	2	.	.	2	.	.	.	5	.	1
<i>B. cf bevieri</i>	5	4	5	6	5	2	5	3	3	12	5	7
<i>Broinsonia spp.</i>	4	3	3	1	5	5	.	2	2	8	7	2
<i>C. barbata</i>	6	3	2	1	2	2	2	3	.	5	7	7
<i>C. amphipons</i>	1	1
<i>C. garrisonii</i>	7	3	9	3	4	.	3	1	4	4	7	6
<i>Chiastozygus sp. 1</i>	1	.	1	.	3	.	.	.	2	2	1	1
<i>C. conicus</i>	1	.	1	.	1
<i>C. crenulatus</i>
<i>C. surirellus</i>	7	6	1	1	6	5	3	1	1	7	7	9
<i>Cretarhabdus sp. 1</i>	3	.	.	1	2	1	.	.	2	3	1	5
<i>Cretarhabdus spp.</i>	5	2	2	2	1	2	5	1	2	1	4	9
<i>C. daniae</i>	1
<i>C. ehrenbergii</i>	3	1	1	.	5	1	2	1	2	1	6	4
<i>Cruciplacolithus spp.</i>
<i>Cyclagelosph. spp.</i>
<i>Cylindralithus spp.</i>
<i>D. ignotus</i>
<i>E. trabeculatus</i>	1
<i>E. turriseiffeli</i>	13	14	18	10	4	8	15	6	7	7	9	10
<i>Gartnerago spp.</i>	19	10	13	6	13	6	10	4	12	7	7	6
<i>G. fessus</i>
<i>Homibrookina spp.</i>
<i>K. magnificus</i>	19	12	13	15	11	15	14	19	18	19	13	19
<i>Lapideacassis spp.</i>	1	.	.
<i>L. camiolensis</i>
<i>L. cayeuxii</i>	19	18	2	12	17	17	9	23	9	8	6	5
<i>M. inversus</i>
<i>M. decoratus</i>	.	.	7
<i>M. staurophora</i>	.	1	.	.	1	.	1	.	.	2	4	.
<i>M. pleniporus</i>	1	.
<i>Misceomarg. sp.</i>
<i>M. pectinatus</i>
<i>M. quaternarius</i>	1	.	3	5	3	1	2	2	.	2	6	9
<i>Monomarg. sp.</i>	1	.	.	.
<i>Misceo/Monomg sp.</i>
<i>N. watkinsii</i>	.	1	2	.	1	.	2	1	.	.	2	1
<i>Neocrepidol. spp.</i>
<i>N. corystus</i>	25	22	31	19	18	22	27	21	39	39	44	30
<i>N. frequens</i>
<i>O. magnus</i>
<i>P. obscurus</i>	5	5	6	10	6	7	4	10	5	7	9	3

Sample Number	106	107	108	109	110	111	112	113	114	115	116	117
Hole	690C	690C	690C	690C	690C	690C	690C	690C	690C	690C	690C	690C
Core - Section	20-2	20-2	20-2	20-2	20-3	20-3	20-3	20-3	20-3	20-3	20-3	20-3
cm - level	120	129-130	140-141	149	10.1	30.1	52	70	90-91	107-108	130	150
Depth (mbsf)	293.5	293.59	293.7	293.79	293.9	294.1	294.32	294.5	294.7	294.87	295.1	295.3
<i>P. bussonii</i>	1	.	.	.	1	2	2	2
<i>P. fibuliformis</i>	.	.	3	.	2	.	1	.	.	.	2	1
<i>P. sigmoides</i>	.	2	2	.	1	5	2
<i>Placozygus</i> sp.	3	1	.	.	.	1	1	1	1	1	.	.
<i>P. arkhangel'skyi</i>	5	3	6	12	12	8	10	1	9	13	20	15
<i>P. cretacea</i>	7	8	4	5	6	1	12	.	7	14	22	10
<i>P. spinosa</i>	33	30	24	18	14	17	19	12	34	31	35	32
<i>P. firthii</i>	15	16	14	16	11	10	11	4	10	30	26	8
<i>Q. gartneri</i>
<i>Reinhardtites</i> spp.	7	11	12	9	4	5	6	8	9	6	12	5
<i>R. angustus</i>	1	1	.
<i>Rhagodiscus</i> spp.
<i>R. rhombicum</i>	6	1	2	1	1	1	3	.	6	2	2	6
<i>S. asymmetrica</i>
<i>S. wisai</i>
<i>Scampanella</i> spp.	P	.	.	.
<i>S. fossilis</i>	3	3	.	5	.	.	3	.	1	2	7	5
<i>S. laffittei</i>	5	6	5	2	2	1	2	1	5	1	5	3
<i>T. ethmos</i>	P	.	.	P	.	.	.	1	.	P	.	2
<i>Thoracosph.</i> spp.	5	4	8	3	8	2	5	1	3	3	6	9
<i>Vagalapilla</i> spp.	20	21	28	14	14	17	7	13	21	15	16	15
<i>W. bamesae</i>	.	.	.	1	.	.	.	1	.	.	1	1
<i>Z. compactus</i>
<i>Z. diplogrammus</i>	.	.	.	1	.	.	1
Unidentifiable	7	16	6	8	21	10	22	14	21	22	22	15
Total (excl. <i>P. stoveri</i>)	405	422	380	373	387	367	376	374	413	482	510	446
<i>P. stoveri</i>	12	1	.	.	.	1	.	.	1	.	.	.
Total (<i>P. stoveri</i> count)	417	423	380	373	387	368	376	374	414	482	510	446
<i>P. stoveri</i> , fields	20.6	29.9	14.5	19.8	21.1	30.7	26.3	58.8	21.1	22.4	20.2	20.6

Sample Number	118	119	120	121	122	123	124	125	126	127	128
Hole	690C	690C	690C	690C	690C	690C	690C	690C	690C	690C	690C
Core - Section	20-4	20-4	20-4	20-4	20-4	20-4	20-4	21-1	21-4	22-1	22-4
cm - level	8-9	31	50	70-71	89-90	109	115-116	123-124	121	46-47	119-120
Depth (mbsf)	295.38	295.61	295.8	296	296.19	296.39	296.45	301.63	306.11	310.56	315.79
Sed. rate (m/m.y.)	8.9	8.9	8.9	8.9	8.9	8.9	8.9	8.9	8.9	8.9	8.9
Age (Ma)	72.719	72.745	72.766	72.788	72.810	72.832	72.839	73.422	73.925	74.425	75.013
Pres. (G, M, P)	M-P	M	M-G	M	M	M	M	G-M	M-P	M-P	P-M
Abund. (A, C, R)	A	A	A	A	A	A	A	A	A	C	C
Fields counted	26.3	20.2	19.3	20.2	21.1	34.2	21.1	25.5	30.7	55.3	47.4
mg sediment	20.0	20.4	20.4	21.5	20.0	20.6	19.9	19.8	21.0	20.8	21.3
Carbonate (wt-%)	60.8	56.2	56.5	56.1	53.8	58	59.4	52.5	46.7	43.8	55
Beaker Constant	2.7	2.7	2.7	2.7	2.7	2.7	2.7	2.7	2.7	2.7	2.7
<i>A. octoradiata</i>	30	52	47	52	52	52	32	65	65	17	.
<i>A. cymbiformis</i>	3
<i>A. cymbif./specill.</i>	3	2	3	.	2	1	1	.	1	1	1
<i>A. specillata</i>	1	.	1	.	.	1	1
<i>B. sparsus</i>
<i>B. boletum</i>	5	3	5	3	1	1	.	4	.	.	.
<i>B. constans</i>	24	17	9	21	18	12	23	20	34	11	4
<i>B. coronum</i>	P	.	1
<i>B. dissimilis</i>	.	.	1	2	.	1	2	.	.	2	.
<i>B. magnum</i>	28	30	26	19	20	26	19	2	7	22	.
<i>B. notaculum</i>	102	76	51	51	58	92	58	100	11	4	6
<i>Biscutum sp. 1</i>	1	.	3	1	1	2	1	.	2	3	6
<i>Biscutum sp. 2</i>	1	.	3	2	2	2	.	2	.	.	.
<i>B. cf bevieri</i>	8	8	5	6	5	10	5	3	.	.	.
<i>Broinsonia spp.</i>	2	5	6	2	3	2	5	2	.	.	.
<i>C. barbata</i>	6	5	3	6	2	2	6	3	5	3	.
<i>C. amphipons</i>	1
<i>C. garrisonii</i>	10	4	9	5	11	6	3	25	3	1	2
<i>Chiastozygus sp. 1</i>	1	.	.	2	.	1	1	4	1	.	.
<i>C. conicus</i>	.	.	1	1	9	2	1
<i>C. crenulatus</i>
<i>C. surirellus</i>	8	3	2	5	.	1	.	1	7	4	P
<i>Cretarhabdus sp. 1</i>	.	2	.	1	1	.	2	6	4	.	.
<i>Cretarhabdus spp.</i>	5	4	5	3	1	4	2	1	7	3	2
<i>C. daniae</i>
<i>C. ehrenbergii</i>	5	4	5	3	1	4	6	.	5	6	5
<i>Cruciplacolithus spp.</i>
<i>Cyclagelosph. spp.</i>	1	.
<i>Cylindralithus spp.</i>
<i>D. ignotus</i>	.	.	1	.	1	2	1	.	1	1	.
<i>E. trabeculatus</i>
<i>E. turriseiffeli</i>	11	14	8	7	14	6	11	10	18	8	1
<i>Gartnerago spp.</i>	4	3	6	5	4	4	5	8	4	1	.
<i>G. fessus</i>
<i>Homibrookina spp.</i>
<i>K. magnificus</i>	11	16	13	14	9	12	20	7	7	3	12
<i>Lapideacassis spp.</i>	1	.	.
<i>L. carniolensis</i>
<i>L. cayeuxii</i>	10	3	5	5	2	4	9	2	15	39	185
<i>M. inversus</i>
<i>M. decoratus</i>
<i>M. staurophora</i>	.	.	1	.	1	1	1	.	.	4	.
<i>M. pleniporus</i>	.	.	.	9	.	.	.	3	.	.	.
<i>Misceomarg. sp.</i>	2
<i>M. pectinatus</i>	1	2	.	.	.
<i>M. quaternarius</i>	1	3	5	3	5	3	6
<i>Monomarg. sp.</i>	1	.
<i>Misceo/Monomg sp.</i>	1	.	1	.
<i>N. watkinsii</i>	3	3	.	3	.	1	1	2	.	.	2
<i>Neocrepidol. spp.</i>
<i>N. corystus</i>	32	40	48	41	31	30	30	33	8	.	.
<i>N. frequens</i>
<i>O. magnus</i>	.	.	1	1	1	.	.
<i>P. obscurus</i>	2	2	4	4	2	1	9	1	.	1	.

Sample Number	118	119	120	121	122	123	124	125	126	127	128
Hole	690C	690C	690C	690C	690C	690C	690C	690C	690C	690C	690C
Core - Section	20-4	20-4	20-4	20-4	20-4	20-4	20-4	21-1	21-4	22-1	22-4
cm - level	8-9	31	50	70-71	89-90	109	115-116	123-124	121	46-47	119-120
Depth (mbsf)	295.38	295.61	295.8	296	296.19	296.39	296.45	301.63	306.11	310.56	315.79
<i>P. bussonii</i>	8	6	4	1	4	.	2	3	2	3	.
<i>P. fibuliformis</i>	.	.	1	3	2	1	2	.	3	3	3
<i>P. sigmoides</i>	1	.	2	4	.	.
<i>Placozygus sp.</i>	.	2	5	.	2	1	2	1	1	.	.
<i>P. arkhangel'skyi</i>	10	17	14	8	7	7	5	18	21	4	7
<i>P. cretacea</i>	7	3	1	1	5	5	2	20	15	22	12
<i>P. spinosa</i>	32	33	33	45	35	35	51	41	64	66	8
<i>P. firthii</i>	14	15	20	27	37	38	36
<i>Q. gartneri</i>
<i>Reinhardtites spp.</i>	8	5	5	9	7	12	6	18	17	.	.
<i>R. angustus</i>
<i>Rhagodiscus spp.</i>
<i>R. rhombicum</i>	.	8	3	2	1	.	2
<i>S. asymmetrica</i>
<i>S. wisoi</i>
<i>Scampanella spp.</i>
<i>S. fossilis</i>	1	4	2	3	2	1	.	6	2	.	.
<i>S. laffitei</i>	12	8	7	4	5	13	3	2	.	.	.
<i>T. ethmos</i>	1	.	.
<i>Thoracosph. spp.</i>	5	7	13	10	9	7	10	17	19	5	2
<i>Vagalapilla spp.</i>	15	30	22	32	18	23	15	44	48	9	.
<i>W. bamesae</i>	3	5	2	1	.	.	3	.	.	1	.
<i>Z. compactus</i>	.	.	.	1	7	1	4
<i>Z. diplogrammus</i>	.	.	.	1	.	1	2
Unidentifiable	19	24	19	16	18	8	13	12	15	10	11
Total (excl. <i>P. stoveri</i>)	449	466	428	440	408	440	415	492	426	261	279
<i>P. stoveri</i>	5	8	15	21	31	93	16
Total (<i>P. stoveri</i> .count)	449	466	428	440	413	448	430	513	457	354	295
<i>P. stoveri</i> , fields	26.3	20.2	19.3	20.2	21.1	34.2	21.1	25.5	30.7	55.3	47.4

	1	2	3	4	5	6	7	8	9	10
ODP Hole 761 B	761 B	761 B	761 B	761 B	761 B	761 B	761 B	761 B	761 B	761 B
Core-Section	21-4	21-4	21-4	21-5	21-5	21-5	21-5	21-5	21-6	21-6
cm-level	130	140	145	10	45	80	115	150	11	45
Depth (mbaf)	176.00	176.10	176.15	176.30	176.65	177.00	177.35	177.70	177.81	178.15
Age (Ma)	66.403	66.409	66.412	66.422	66.445	66.468	66.491	66.514	66.521	66.543
Sedimentation Rate (m/m.y.)	15.32	15.32	15.32	15.32	15.32	15.32	15.32	15.32	15.32	15.32
Carbonate content (weight-%)	82.7	n.d.	86.7	89.3	n.d.	n.d.	n.d.	n.d.	90	n.d.
Preservation	M	M	M	M	M	M	M	M	M	M
Abundance	A	A	A	A	A	A	A	A	A	A
Fields counted	20	20	20	20	20	20	20	20	20	20
mg sediment used	20.7	20.8	20.9	21	20.8	20.6	20.4	20.9	20.3	20.8
<i>Ahmullerella octoradiata</i>
<i>Arkhangelskiella</i> spp.	11	16	22	12	20	14	18	7	14	10
<i>Biscutum constans</i>	.	.	2	.	1	2	1	1	.	3
<i>B. magnum</i>
<i>B. notaculum</i>	2	3	4	2	.	1
<i>Biscutum</i> sp. 1	27	72	32	49	42	51	65	7	4	15
<i>Broinsonia</i> spp.	4	6	7	12	3	9	5	1	8	7
<i>Arkhangelskiella/Broinsonia</i>
<i>Centosphaera barbata</i>
<i>Ceratolithoidea</i> sp. cf. <i>C. aculeus</i>	1	1	1	2	2	1	.	1	.	3
<i>Chiastozygus</i> sp. 1	1
<i>Corollithion exiguum</i>	1	9	1	2	3	4	2	.	.	.
<i>Corollithion?</i> completum	1
<i>Chiastozygus</i> sp cf. <i>C. amphipons</i>
<i>Cribrosphaerella(?) damiae</i>	2	11	5	10	5	4	13	1	2	4
<i>Cribrosphaerella ehrenbergii</i>	48	56	53	66	33	44	53	19	32	35
<i>Cretarhabdus angustiforatus</i>	2	1	1	3	14	8	10	3	8	6
<i>C. conicus</i>	.	.	2	1	.	.	.	2	1	1
<i>C. crenulatus</i>
<i>C. schizobrachiatus</i>	1	.	.	1	.	1	2	1	.	1
<i>C. surirellus</i>	1	.	.	.
<i>Cretarhabdus</i> sp. 1
<i>Cretarhabdus</i> spp. indet	20	33	12	27	27	47	71	35	38	35
<i>Cyclagelosphaera alta</i>
<i>C. margerelii</i>	2	1	.	4	2	2
<i>C. reinhardtii</i>	2	3	2	.	5	.	.	1	.	.
<i>Cylindralithus biarcus</i>
<i>C. gallicus</i>	2	3	2	3	9	3	11	12	6	11
<i>C. serratus</i>
<i>D. ignotus</i>	8	28	9	21	11	32	20	3	11	10
<i>Eiffelithus parallelus</i>	7	13	5	6	4	7	8	11	9	4
<i>E. trabeculatus</i>	3	1	.	8	5	2	2	2	2	3
<i>E. turiseiffelii</i>	21	47	14	39	36	44	35	25	34	37
<i>Ericsonia</i> sp.	3	2	2	3	3	6	2	21	2	9
<i>Gartnerago</i> spp.	1	1	.	.	.
<i>Glaukolithus fesusus</i>	11	37	25	23	24	27	37	22	54	21
<i>Hexalithus hexalithus</i>
<i>Kamptnerius magnificus</i>	.	1	.	1	1	.	.	2	.	.
<i>Lapideacassis</i> spp.
<i>Lithastrinus</i> spp.	.	.	1	1	2	3	5	1	2	3
<i>Lithraphidites carniolensis</i>	.	3	2	4	.	6	5	2	1	.
<i>L. grossopectinatus</i>	1
<i>L. kennethii</i>	1	1	2	1	1
<i>L. praequadratus</i>	29	32	13	20	22	28	39	18	18	11
<i>L. quadratus</i>	4	4	7	1	1	4	6	4	5	4
<i>Lithraphidites?</i> sp. 1
<i>Manivitella pemmatoidea</i>	.	.	1	.	1	.	.	1	.	1
<i>Markalius apertus</i>
<i>M. inversus</i>	2
<i>Microrhabdulus belgicus</i>	3	9	4	2	2	9	11	2	4	3
<i>M. decoratus</i>	16	30	15	25	32	12	34	44	32	35
<i>Micula murus</i>	.	3	2	3	1	2	2	6	2	1

	11	12	13	14	15	16	17	18	19	20	21
ODP Hole 761B	761 B	761 B	761 B	761 B	761 B	761 B	761 B	761 B	761 B	761 B	761 B
Core-Section	21-6	21-6	21-CC	22-1	22-2	22-3	22-4	22-5	22-6	23-1	23-2
cm-level	80	101	31-32	80	80	80	79	70	56-57	70	72
Depth (mbsf)	178.50	178.71	179.70	180.50	182.00	183.50	184.99	186.40	187.76	189.90	191.42
Age (Ma)	66.566	66.580	66.644	66.696	66.900	67.190	67.477	67.750	68.012	68.425	68.719
Sed. Rate (m/m.y.)	15.32	15.32	15.32	15.32	5.18	5.18	5.18	5.18	5.18	5.18	5.18
Wt.-% Carbonate	n.d.	n.d.	n.d.	88.4	n.d.	86.5	n.d.	88.5	n.d.	91	n.d.
Preservation	M	M	M	M	M	M	M	M	M	M	M
Abundance	A	A	A	A	A	A	A	A	A	A	A
Fields counted	20	20	20	20	20	20	20	20	20	20	20
mg sediment used	21	19.5	19.9	19.5	19.8	20.8	20.7	20.1	19.1	19.6	20.2
<i>A. octoradiata</i>	10	1	2
<i>Arkhangelskiella</i> spp.	17	9	20	7	4	10	1	.	27	16	23
<i>Biscutum constans</i>	.	.	3	1	19	20	34	24	24	41	14
<i>B. magnum</i>
<i>B. notaculum</i>	.	.	1	.	1	.	2	2	.	.	.
<i>Biscutum</i> sp. 1	21	25	19	71	26	10	8	8	3	8	6
<i>Broinsonia</i> spp.	7	7	6	2	.	1	.	.	4	1	1
<i>Arkhang./Broinsonia</i>
<i>Centosphaera barbata</i>
<i>C. cf aculeus</i>	2	1	2	.	6	8	22	6	8	18	11
<i>Chiasozygus</i> sp. 1	.	1	4	.	5	1
<i>Corolithion exiguum</i>	.	1
<i>C.? completum</i>
<i>C. cf amphipons</i>
<i>C.(?) daniae</i>	.	3	3	2	1
<i>C. ehrenbergii</i>	30	32	37	43	55	30	38	34	20	31	20
<i>C. angustifloratus</i>	14	7	6	6	4	5	3	9	10	4	4
<i>C. conicus</i>	1	3	.	1	1	.	.	2	.	1	1
<i>C. crenulatus</i>	1	1	7
<i>C. schizobrachiatus</i>	2	.	2	2	.	2	2
<i>C. surirellus</i>	.	.	.	1
<i>Cretarhabdus</i> sp. 1
<i>Cretarhabdus</i> spp. indet	75	30	29	41	61	39	34	41	62	65	49
<i>C. alta</i>
<i>C. margerelii</i>	.	4	4	4	4	5	3	1	3	4	4
<i>C. reinhardtii</i>	1	.	1	.	.	.	2	2	4	.	3
<i>C. biarcus</i>
<i>C. gallicus</i>	11	14	11	10	.	5	1	.	2	2	4
<i>C. serratus</i>
<i>D. ignotus</i>	13	29	22	29	18	14	15	17	23	31	75
<i>E. parallelus</i>	6	8	4	6	9	12	6	6	19	30	26
<i>E. trabeculatus</i>	4	9	2	1	5	.	3	2	13	6	7
<i>E. turrisseiffelii</i>	43	21	15	19	27	10	14	23	26	26	21
<i>Ericaonia</i> sp.	5	2	4	2	1	1	8	8	8	17	4
<i>Gartnerago</i> spp.	.	.	.	2
<i>G. fessus</i>	26	26	39	42	12	7	8	6	21	45	42
<i>H. hexalithus</i>
<i>K. magnificus</i>	2	1
<i>Lapideacassus</i> spp.	1
<i>Lithastrinus</i> spp.	.	5	.	6	4	1	1	.	1	1	.
<i>L. carniolensis</i>	.	2	1	4	3	.	6	6	2	2	.
<i>L. grosospectinatus</i>	.	1
<i>L. kennethii</i>	1
<i>L. praequadratus</i>	25	23	8	24	44	17	45	11	18	21	29
<i>L. quadratus</i>	3	3	2	4	9	.	7	1	3	.	4
<i>Lithraphidites?</i> sp. 1
<i>M. pemmatoidea</i>	3	.	.	2	1	.	.
<i>M. apertus</i>	.	.	.	1
<i>M. inversus</i>	.	.	1	.	.	1
<i>M. belgicus</i>	4	5	2	7	2	1	1	5	2	1	1
<i>M. decoratus</i>	53	31	28	37	16	18	9	19	16	13	21
<i>Micula murus</i>	4	2	9	1

	33	34	35	36	37	38	39	40	41	42
ODP Hole 761B	761 B	761 B	761 B	761 B	761 B	761 B	761 B	761 B	761 B	761 B
Core-Section	24-2	24-3	24-4	24-4	24-4	24-4	24-4	24-4	24-4	24-4
cm-level	80	80	10	31-32	49-50	70	80	90	110	130
Depth (mbsf)	201.00	202.50	203.30	203.51	203.69	203.90	204.00	204.10	204.30	204.50
Micula? sp.
Neocrepidolithus spp.
N. frequens
P. regularis	19	40	19	20	21	10	18	15	19	16
P. cf embergeni	.	1
P. copulatus	.	.	1	.	1
P. bussonii	1	2	.
P. fibuliformis	11	9	11	7	8	64	21	22	57	13
P. sigmoides	.	.	1	2	1
Placozygus sp.	2	1	10	4	8	5	4	7	8	3
P. arkhangelskyi
P. cretacea	84	161	71	78	100	138	131	81	152	113
P. grandis	.	1	1	3	2	.
P. spinosa	7	35	6	10	11	18	28	25	25	8
P. stoven	12	14	10	6	6	7	19	4	12	12
Q. gartneri
R. levis	.	.	3	11	8
R. angustus	1	2	.	.	2	.
R. reniformis	3	1	.	1	.	1	2	.	2	.
R. splendens	1	1	1	1	1	.	2	1	2	2
Rhagodiscus sp. 1	.	.	1
Rhagodiscus spp. indet.
R. rhombicum
Scampanella spp.
S. fossilis
S. laffittei
Stephanolithion spp.	1	2	.	.	.	6	1	.	1	.
T. stradneri
T. ethmos	1	1	.	.	1
T. decorus	.	2	1	1	1	6	7	3	6	4
Thoracosphaera spp.	.	.	1
T. macleodae
T. phacelosus
Vagalapilla spp.	.	.	1	1	1	1
W. barnesae	33	39	33	35	40	35	38	60	43	51
W. biporta
Z. compactus	.	.	.	1	3	1
Z. lacunatus
Zygodiscus sp. 1	1	.	2	.	2	3
Unidentifiables	9	6	8	9	10	6	6	5	10	4
Sum (excl. M. stauroph.)	795	883.5	717.3	685.51	704.69	848.9	839	732.1	931.3	792.5
Micula staurophora	177	78	151	175	160	51	56	102	53	113
Sum of M. staur. counts	972	961.5	868.3	860.51	864.69	899.9	895	834.1	984.3	905.5
Fields of M. staur. counts	30	20	30	30	30	20	20	30	20	20

	1	2	3	4	5	6	7	8	9	10
DSDP Hole 217	217	217	217	217	217	217	217	217	217	217
Core-Section	17-1	17-1	17-1	17-1	17-1	17-1	17-1	17-2	17-2	17-2
cm-level	20-21	40-41	60-61	80-81	100-101	120-121	140-141	10.-11	30-31	50-51
Depth (mbsf)	421.20	421.40	421.60	421.80	422.00	422.20	422.40	422.60	422.80	423.00
Age (Ma)	66.413	66.425	66.438	66.451	66.463	66.476	66.489	66.501	66.514	66.527
Sedimentation Rate (m/m.y.)	15.81	15.81	15.81	15.81	15.81	15.81	15.81	15.81	15.81	15.81
Carbonate content (weight-%)	91.5	90.2	n.d.	n.d.	n.d.	n.d.	n.d.	n.d.	n.d.	n.d.
Preservation	M	M	M	M	M	M	M	M	M	M
Abundance	A	A-C	A	A	A	A	A	A	A	A
Fields counted	40.0	30.0	20.0	20.0	20.0	20.0	20.0	25.0	20.0	20.0
mg sediment used	20.5	20.3	20.2	20.9	20.6	20.4	20.6	20.6	20.0	20.5
Ahmullerella octoradiata
Arkhangelskiella spp.	16	20	18	14	18	5	6	2	1	2
Biscutum constans	.	.	1	.	1	1
B. magnum
B. notaculum	2	2
Biscutum sp. 1	25	4	7	1	3	3	2	.	5	1
Broinsonia spp.	31	21	18	9	12	8	4	8	12	10
Arkhangelskiella/Broinsonia	1
Ceratolithoides sp. cf. C. aculeus	.	4	2	1	.	.	.	2	.	2
Chiasozygus sp. 1	1
Corollithion completum	1	.	1	.
Chiasozygus sp. cf. C. amphipons	2
Cribrosphaerella(?) daniae	5	1	.	2	2	1	1	.	.	.
Cribrosphaerella ehrenbergii	59	42	30	24	31	19	33	19	32	26
Cretarhabdus angustiforatus	7	3	8	2	1	1	6	3	3	.
C. conicus	2	1	1	.	1	3	.	1	2	.
C. crenulatus	.	.	4	1	.	1	3	3	4	.
C. schizobrachiatus	1	4	1	.	.	.	2	1	.	2
C. surirellus	8	3	1	1	2	1
Cretarhabdus spp. indet.	61	31	37	34	42	32	39	28	35	27
Cyclagelosphaera alta
C. reinhardtii	.	.	1	1	.
Cylindralithus biarcus
C. gallicus	9	7	2	2	3	6	8	13	8	6
C. serratus	1	.	.
Cylindralithus sp. 1
Cylindralithus spp. indet.
Discorhabdus ignotus	12	2	6	6	3	1	.	5	3	3
Eiffellithus eximius	1
E. parallelus	5	.	1	.	1	.	1	.	.	2
E. trabeculatus	3	1	1	.
E. turmseiffelii	29	18	21	7	7	7	14	7	20	12
Ericsonia sp.	10	8	2	2	4	4	8	9	7	2
Gartnerago spp.	1	.	2	2	1	2
Glaukolithus fessus	36	22	25	20	37	15	17	13	21	14
Kamptnerius magnificus	.	1	2	1	1	.	1	2	.	.
Lithastrinus spp.	29	15	3	5	7	11	8	16	13	7
Lithraphidites carniolensis	2	1	1	.	2	.	1	1	.	.
L. grossopectinatus	.	.	.	1
L. kennethii	2	1	.	2
L. praequadratus	36	17	9	10	17	14	26	11	16	14
L. quadratus	7	2	6	3	3	3	2	3	3	2
Lithraphidites(?) sp. 1
Lucianorhabdus cayeuxii
Manivitella pemmatoidea	1
Markalius apertus
M. inversus
Microrhabdulus belgicus	1
M. decoratus	24	23	25	17	17	21	26	17	17	19
Micula praemurus
Micula murus	10	8	11	11	17	12	13	25	14	15
Micula sp. cf. M. prinsii	5	4	1	5	4	3	4	5	7	4

	1	2	3	4	5	6	7	8	9	10
DSDP Hole 217	217	217	217	217	217	217	217	217	217	217
Core-Section	17-1	17-1	17-1	17-1	17-1	17-1	17-1	17-2	17-2	17-2
cm-level	20-21	40-41	60-61	80-81	100-101	120-121	140-141	10.-11	30-31	50-51
Depth (mbsf)	421.20	421.40	421.60	421.80	422.00	422.20	422.40	422.60	422.80	423.00
Micula? sp	4	6	2	6	2	1	1	2	2	3
Nephrolithus frequens	19	8	9	10	7	7	3	2	2	1
Parhabdolithus embergeni	.	.	1	.	1	1
P. regularis	47	22	.	28	13	20	47	16	36	39
Petrarhabdus copulatus
Placozygus bussoni	4	3	1	1	.	.
P. fibuliformis	23	14	22	20	16	11	16	15	20	24
P. sigmoides
Placozygus sp.	10	6	.	3	4	1	3	5	2	.
Prediscosphaera arkhangelskyi
P. cretacea	100	62	80	58	53	50	75	54	89	58
P. spinosa	18	5	21	2	8	4	9	2	7	8
P. grandis	.	1	.	.	1	1	.	.	2	.
P. stoven	32	11	15	16	26	10	16	19	23	14
Quadrum gartneri	.	1	1	.	.
Reinhardtites sp aff. R. anthophorus
Reinhardtites levis
Rhagodiscus angustus	2	.	.	.	1
R. reniformis	4	1
R. splendens
Rhagodiscus sp. 1
Rhagodiscus spp. indet	1
Scapanella spp.	.	1	1	.	.
Scapholithus fossilis
Staurolithes laffittei
Stephanolithion spp.	7	.	.	.	1	1	1	1	2	2
Tegumentum stradneri
Teichorhabdus ethmos
Tetrapodorhabdus decorus	6	4	6	.	2	2	3	1	4	2
Thoracosphaera spp.	2	2	3	3	1
Tranolithus macleodae	16	6	3	7	1	2	6	5	3	.
T. phacelosus
Vagalapilla spp.	12	1	5	1	6	1	.	1	2	.
Watznauena barnesae	154	87	69	70	86	101	116	122	108	61
W. biporta	1	.	2	.	1	.	1	2	1	1
Zygodiscus compactus
Z. lacunatus	.	1	.	2	.	.	1	.	2	2
Zygodiscus sp. 1	2	3	.	.	.	1	2	1	.	.
Unidentifiable	17	3	7	10	6	3	5	5	7	5
Sum (excl. M. staurophora)	919	507	488	414	473	395	536	455	541	396
Micula staurophora	84	122	57	99	93	110	86	185	99	106
Sum of M. staurophora counts	1003	629	545	513	566	505	622	640	640	502
Fields of M. staurophora counts	40.0	30.0	20.0	20.0	20.0	20.0	20.0	25.0	20.0	20.0

	11	12	13	14	15	16	17	18	19	20	21
DSDP Hole 217	217	217	217	217	217	217	217	217	217	217	217
Core-Section	17-2	17-2	17-2	17-2	17-2	17-3	17-3	17-3	17-3	17-3	17-3
cm-level	70-71	90-91	110-111	130-131	149-150	10.-11	30-31	50-51	70-71	90-91	110-111
Depth (mbaf)	423.20	423.40	423.60	423.80	423.99	424.10	424.30	424.50	424.70	424.90	425.10
Age (Ma)	66.539	66.552	66.564	66.577	66.589	66.596	66.609	66.621	66.634	66.647	66.659
Sed. Rate (m/m.y.)	15.81	15.81	15.81	15.81	15.81	15.81	15.81	15.81	15.81	15.81	15.81
Carbonate (wt-%)	n.d.	n.d.	n.d.	n.d.	n.d.	n.d.	n.d.	n.d.	n.d.	n.d.	n.d.
Preservation	M	M	M	M	M	M	M	M	M	M	M
Abundance	A	A	A	A	A	A	AA	A	A	AA	A
Fields counted	20.0	30.0	20.0	20.0	20.0	30.0	20.0	20.0	20.0	20.0	20.0
mg sediment used	21.1	21.5	21.4	20.1	19.7	20.5	21.2	20.3	20.6	20.6	20.0
<i>A. octoradiata</i>
<i>Arkhangelskiella</i> spp.	6	5	3	1	5	3	4	2	5	10	3
<i>Biscutum constans</i>	1
<i>B. magnum</i>
<i>B. notaculum</i>	.	1
<i>Biscutum</i> sp. 1	4	1	1
<i>Broinsonia</i> spp.	3	9	4	4	6	9	10	10	10	27	8
<i>Arkhang./Broinsonia</i>
<i>C. cf. aculeus</i>
<i>Chiastozygus</i> sp. 1	1
<i>C. completum</i>	1
<i>C. cf. amphipons</i>
<i>C.(?) daniae</i>	.	.	1
<i>C. ehrenbergi</i>	23	14	25	25	52	34	70	47	60	48	42
<i>C. angustiforatus</i>	3	.	.	1	.	3	5	1	2	5	2
<i>C. conicus</i>	.	1	1	.	1	1	.	.	.	1	.
<i>C. crenulatus</i>	2	1	9	4	3	4	5	3	2	2	.
<i>C. schizobrachiatus</i>	2	1	1	2	.	2	2
<i>C. surirellus</i>	.	.	2
<i>Creterhabdus</i> spp. indet.	42	22	29	47	44	37	72	40	46	56	54
<i>C. alta</i>
<i>C. reinhardtii</i>	2	1	.	.	1	.
<i>C. biarcus</i>
<i>C. gallicus</i>	2	8	2	7	1	3	4	4	6	7	4
<i>C. serratus</i>	1	1	.	.
<i>Cylindralithus</i> sp. 1	.	1	.	.	1	2	1	.	.	1	1
<i>Cylindralithus</i> spp. indet.
<i>D. ignotus</i>	2	1	.	1	.	1	3	2	1	5	2
<i>E. eximius</i>
<i>E. parallelus</i>	1	.	1	.	.
<i>E. trabeculatus</i>	1	1	1
<i>E. turris Eiffelii</i>	20	10	13	13	8	11	9	7	10	12	8
<i>Ericsonia</i> sp.	2	2	4	9	6	6	5	2	4	1	.
<i>Gartnerago</i> spp.
<i>G. fessus</i>	6	9	18	7	2	12	21	15	15	20	19
<i>K. magnificus</i>	.	.	1	.	1	.	.	.	1	.	.
<i>Lithastrinus</i> spp.	11	18	6	10	4	15	9	5	7	5	1
<i>L. carniolensis</i>	.	.	2	.	2	2	.	.	.	2	3
<i>L. grossopectinatus</i>
<i>L. kennethii</i>	1	1	.	.	1	.	1	.	.	.	1
<i>L. praequadratus</i>	10	7	14	19	6	12	12	3	8	12	21
<i>L. quadratus</i>	1	4	2	3	1	2	4	.	2	2	5
<i>Lithraphidites(?)</i> sp. 1
<i>L. cayeuxii</i>
<i>M. pemmatoidea</i>	.	1	.	2	.	1	3
<i>M. apertus</i>
<i>M. inversus</i>
<i>M. belgicus</i>
<i>M. decoratus</i>	19	9	10	16	19	51	30	17	23	17	19
<i>M. praemurus</i>
<i>M. murus</i>	17	24	19	22	22	24	11	23	10	18	12
<i>M. cf. prinsii</i>	5	6	9	8	10	12	13	7	6	4	2

	11	12	13	14	15	16	17	18	19	20	21
DSDP Hole 217	217	217	217	217	217	217	217	217	217	217	217
Core-Section	17-2	17-2	17-2	17-2	17-2	17-3	17-3	17-3	17-3	17-3	17-3
cm-level	70-71	90-91	110-111	130-131	149-150	10.-11	30-31	50-51	70-71	90-91	110-111
Depth (mbaf)	423.20	423.40	423.60	423.80	423.99	424.10	424.30	424.50	424.70	424.90	425.10
Micula? sp	.	4	2	4	3	6	.	.	3	.	.
N. frequens	6	.	1	.	1	1	2
P. embergeri	1
P. regularis	26	20	33	36	24	20	39	18	24	50	22
P. copulatus
P. bussoni	1	2	2	.	1	1	2
P. fibuliformis	20	14	4	7	11	12	50	31	24	28	35
P. sigmoides
Placozygus sp.	3	2	5	3	3	5	10	3	2	5	1
P. arkhangel'skyi
P. cretacea	65	67	34	102	53	75	82	70	98	102	62
P. spinosa	7	.	4	12	6	1	10	6	.	3	2
P. grandis	.	2	.	5	3	6	.	1	1	2	4
P. stoveri	25	9	17	16	17	14	21	17	10	21	17
Q. gartneri	.	.	1	2	.	.	.
R. aff. anthophorus
R. levis	1
R. angustus
R. reniformis
R. splendens
Rhagodiscus sp. 1
Rhagodiscus spp. indet
Scampanella spp.
S. fossilis
S. laffitei
Stephanolithion spp.
T. stradneri	.	.	.	1	.	.	.	1	.	.	.
T. ethmos
T. decorus	6	1	3	4	1	.	4	1	1	.	1
Thoracosphaera spp.	1	.	.	.	1	1	4	1	.	.	.
T. macleodae	3	.	.	2	1	.	1	1	.	3	1
T. phacelosus
Vagalapilla spp.	3	2	1	.	.	1
W. barnesae	93	135	83	148	95	134	118	92	81	77	81
W. biporta	.	.	.	1	1	.	.	.	1	.	.
Z. compactus
Z. lacunatus	3	2	.	3	1	.	1	1	.	.	.
Zygodiscus sp. 1	.	.	3	3	2	1	6	.	3	1	3
Unidentifiable	5	3	2	4	2	6	9	5	5	11	6
Sum (excl. M. staur.)	452	415	366	550	421	534	656	442	474	562	448
Micula staurophora	108	221	144	111	113	134	91	73	82	94	88
Sum of M. staur. counts	560	636	510	661	534	668	747	515	556	656	536
Fields of M. staur. counts	20.0	30.0	20.0	20.0	20.0	30.0	20.0	20.0	20.0	20.0	20.0

	22	23	24	25	26	27	28	29	30	31	32
DSDP Hole 217	217	217	217	217	217	217	217	217	217	217	217
Core-Section	17-3	17-3	17-4	17-4	17-4	17-4	17-4	17-4	17-4	18-2	18-2
cm-level	130-131	149-150	20-21	40-41	60-61	80-81	100-101	120-121	140-141	22	40-42
Depth (mbsf)	425.30	425.49	425.70	425.90	426.10	426.30	426.50	426.70	426.90	432.22	432.40
Age (Ma)	66.672	66.684	66.697	66.710	66.723	66.735	66.748	66.761	66.773	67.110	67.121
Sed. Rate (m/m.y.)	15.81	15.81	15.81	15.81	15.81	15.81	15.81	15.81	15.81	15.81	15.81
Carbonate (wt-%)	n.d.	n.d.	n.d.	n.d.	n.d.	n.d.	n.d.	n.d.	n.d.	n.d.	n.d.
Preservation	M	M	M	M	M	M	M	M	M	M	M
Abundance	A	A	A	A-C	C-A	A-C	A-C	A	A	A	A
Fields counted	20.0	20.0	20.0	25.0	30.0	25.0	20.0	20.0	25.0	20.0	20.0
mg sediment used	20.7	20.8	21.1	20.1	20.2	20.4	20.8	20.3	19.8	21.1	21.2
<i>A. octoradiata</i>	1	1
<i>Arkhangelskiella</i> spp.	7	3	7	4	7	7	5	4	13	3	11
<i>Biscutum constans</i>	.	.	1	1	1	2
<i>B. magnum</i>
<i>B. notaculum</i>	1
<i>Biscutum</i> sp. 1	.	2	.	1	2	1	1
<i>Broinsonia</i> spp.	18	13	13	20	15	3	16	12	34	13	14
<i>Arkhang./Broinsonia</i>
<i>C. cf aculeus</i>	13	12
<i>Chiastozygus</i> sp. 1
<i>C. completum</i>
<i>C. cf amphipons</i>
<i>C.(?) daniae</i>	.	.	1
<i>C. ehrenbergii</i>	46	27	28	24	38	20	24	29	24	40	29
<i>C. angustiforatus</i>	1	2	.	4	5	1	1	3	1	2	2
<i>C. conicus</i>	56	.	.	.	1	.	.	3	.	.	.
<i>C. crenulatus</i>	.	1	2	1	.	2	.
<i>C. schizobrachiatus</i>	.	1	1	1
<i>C. surirellius</i>	1
<i>Cretarhabdus</i> spp. indet.	.	49	50	44	56	56	54	65	46	30	48
<i>C. alta</i>	1
<i>C. reinhardtii</i>	2	2	.	1	2	.	.
<i>C. biarcus</i>
<i>C. gallicus</i>	3	4	.	4	5	5	2	2	3	3	3
<i>C. serratus</i>
<i>Cylindralithus</i> sp. 1
<i>Cylindralithus</i> spp. indet.
<i>D. ignotus</i>	2	3	1	4	.	5	2	1	.	1	6
<i>E. eximius</i>
<i>E. parallelus</i>	3	9
<i>E. trabeculatus</i>	.	.	.	2	.	1
<i>E. turrisseiffelii</i>	8	9	18	17	13	16	16	15	8	16	17
<i>Ericonia</i> sp.	4	1	1	1	5	2	.	.	1	4	3
<i>Gartnerago</i> spp.
<i>G. feassus</i>	22	32	7	8	16	12	13	14	19	12	2
<i>K. magnificus</i>
<i>Lithastrinus</i> spp.	4	4	6	11	8	8	7	16	7	2	1
<i>L. carniolensis</i>	1	.	.	2	.	.	1	.	.	1	2
<i>L. grossopectinatus</i>
<i>L. kennethii</i>	1	.	1	1	.
<i>L. praequadratus</i>	8	22	13	6	15	13	18	12	16	11	7
<i>L. quadratus</i>	3	6	4	6	5	2	4	5	4	1	3
<i>Lithraphidites(?)</i> sp. 1
<i>L. cayeuxii</i>	1	.	.
<i>M. pemmatoidea</i>	.	1	.	1	1
<i>M. apertus</i>	.	.	1
<i>M. inversus</i>	.	.	.	1
<i>M. belgicus</i>
<i>M. decoratus</i>	23	29	11	19	18	18	13	8	8	10	23
<i>M. praemurus</i>
<i>M. murus</i>	17	9	16	16	25	15	17	18	20	8	18
<i>M. cf prinsii</i>	6	3	3	10	8	3	4	4	6	.	.

	22	23	24	25	26	27	28	29	30	31	32
DSDP Hole 217	217	217	217	217	217	217	217	217	217	217	217
Core-Section	17-3	17-3	17-4	17-4	17-4	17-4	17-4	17-4	17-4	18-2	18-2
cm-level	130-131	149-150	20-21	40-41	60-61	80-81	100-101	120-121	140-141	22	40-42
Depth (mbsf)	425.30	425.49	425.70	425.90	426.10	426.30	426.50	426.70	426.90	432.22	432.40
Micula? sp	.	.	2	2	1	1	1	.	.	5	2
N. frequens	1	1	.	1	.	.
P. embergeni
P. regularis	31	34	41	38	69	42	31	41	53	39	32
P. copulatus
P. bussoni	4	1	1	.	.
P. fibuliformis	63	57	29	14	26	13	17	12	3	13	20
P. sigmoides	.	.	2	1	.	.	.
Placozygus sp.	7	5	4	3	5	2	4	1	5	1	5
P. arkhangel'skiyi
P. cretacea	79	71	91	88	85	96	95	60	93	82	93
P. spinosa	6	5	14	5	4	7	6	3	5	11	11
P. grandis	2	2	1	3	1	1	2	.	.	1	.
P. stoveri	22	19	15	13	6	14	28	2	19	23	15
Q. garteri	.	1	1	.	1	.	.
R. aff. anthophorus
R. levis
R. angustus
R. reniformis	1
R. splendens
Rhagodiscus sp. 1
Rhagodiscus spp. indet
Scampanella spp.
S. fossilis
S. laffitei
Stephanolithion spp.	1	1	.	.	.	1	2
T. stradneri	1
T. ethmos	.	.	.	1	1
T. decorus	3	.	3	.	2	1	3	1	.	4	4
Thoracosphaera spp.
T. macleodae	2
T. phacelosus
Vagalapilla spp.	.	.	2	.	.	1	.	2	.	.	.
W. barnesae	61	57	53	64	62	75	56	71	63	54	68
W. biporta	.	1	1	1	.
Z. compactus
Z. lacunatus	.	.	1	1	.	1	3
Zygodiscus sp. 1	1	7	1	2	1	.	.	.	1	1	.
Unidentifiable	11	8	8	6	8	18	6	7	6	10	5
Sum (excl. M. staur.)	522	489	450	444	516	464	455	415	466	425	475
Micula staurophora	84	75	87	115	138	109	102	112	123	123	117
Sum of M. staur. counts	606	564	537	559	654	573	557	527	589	548	592
Fields of M. staur. counts	20.0	20.0	20.0	25.0	30.0	25.0	20.0	20.0	25.0	20.0	20.0

	33	34	35	36	37	38	39	40	41	42	43
DSDP Hole 217	217	217	217	217	217	217	217	217	217	217	217
Core-Section	19-2	19-4	20-1	20-1	20-1	20-2	20-2	20-2	20-2	20-2	20-2
cm-level	30	30	99-100	120-121	140-141	8-9	30	49-50	70-71	90	109-110
Depth (mbsf)	441.80	444.80	450.49	450.70	450.90	451.08	451.30	451.49	451.70	451.90	452.09
<i>Micula?</i> sp
<i>N. frequens</i>	.	1	1	.	.
<i>P. embergeri</i>	2	.	1	1	.	.	.	1	.	1	1
<i>P. regularis</i>	48	44	57	49	48	38	37	28	63	39	48
<i>P. copulatus</i>	1	.	.
<i>P. bussoni</i>	2	4	.	2	.	.	4	.	.	2	.
<i>P. fibuliformis</i>	12	26	24	19	8	2	8	13	16	17	6
<i>P. sigmoides</i>	.	.	.	1
<i>Placozygus</i> sp.	3	5	8	9	6	6	9	11	8	9	9
<i>P. arkhangel'skyi</i>
<i>P. cretacea</i>	96	135	130	149	109	72	83	70	96	74	86
<i>P. spinosa</i>	11	9	11	18	12	9	14	8	13	7	11
<i>P. grandis</i>	1	1	1	.
<i>P. stoveri</i>	15	26	14	18	16	1	13	10	11	12	10
<i>Q. gartneri</i>
<i>R. aff. anthophorus</i>
<i>R. levis</i>	.	.	1	.	1	1
<i>R. angustus</i>	.	.	1	2	.	.
<i>R. reniformis</i>	.	1	.	.	2	.	.	1	.	1	3
<i>R. splendens</i>	3	4	2	5	5	1	8	.	6	7	6
<i>Rhagodiscus</i> sp. 1
<i>Rhagodiscus</i> spp. indet	.	.	3	1
<i>Scampanella</i> spp.	1
<i>S. fossilis</i>
<i>S. laffitei</i>
<i>Stephanolithion</i> spp.	.	2	1	4	2	.	1	2	3	1	2
<i>T. stradneri</i>
<i>T. ethmos</i>	1	1
<i>T. decorus</i>	7	8	6	11	5	.	3	2	7	5	4
<i>Thoracosphaera</i> spp.	.	.	2	.	1	.	1	.	.	.	1
<i>T. macleodae</i>	2	1	.	1
<i>T. phacelosus</i>
<i>Vagalapilla</i> spp.	1	.	2	.	3	.	.	1	3	1	1
<i>W. barnesae</i>	85	98	146	142	104	62	129	104	121	94	78
<i>W. biporta</i>	.	.	2
<i>Z. compactus</i>
<i>Z. lacunatus</i>	1	.	.	2	.	1	.	1	.	.	.
<i>Zygodiscus</i> sp. 1	1	1	.
Unidentifiable	5	6	11	11	6	2	8	7	2	8	14
Sum (excl. <i>M. staur.</i>)	575	628	770	784	598	403	590	475	654	497	536
<i>Micula staurophora</i>	82	108	120	107	88	138	103	112	125	83	106
Sum of <i>M. staur.</i> counts	652	734	890	891	686	540	692	587	779	580	642
Fields of <i>M. staur.</i> counts	20.0	20.0	20.0	20.0	20.0	22.0	20.0	20.0	20.0	20.0	20.0

	44	45	46	47	48	49	50	51	52	53	54
DSDP Hole 217	217	217	217	217	217	217	217	217	217	217	217
Core-Section	20-2	20-2	20-3	20-3	20-3	20-3	20-3	20-3	20-3	20-3	20-4
cm-level	130	150	21-22	39-40	60-61	80-81	99-100	120	140-141	149-150	20-21
Depth (mbsf)	452.30	452.50	452.71	452.89	453.10	453.30	453.49	453.70	453.90	453.99	454.20
Micula? sp
N. frequens	.	.	.	1
P. embergeri	1	2	.	.	1	1	1	.	.	.	1
P. regularis	19	38	29	31	24	38	29	18	17	15	31
P. copulatus	1	1
P. bussoni	.	.	.	1
P. fibuliformis	5	10	7	8	22	18	9	21	21	19	28
P. sigmoides	1	1
Placozygus sp.	11	3	4	3	3	5	5	10	5	6	3
P. arkhangel'skyi
P. cretacea	64	87	68	87	83	104	70	77	62	47	82
P. spinosa	2	7	6	7	6	9	5	9	3	1	8
P. grandis	1	2
P. stoveri	3	11	6	7	12	7	7	3	9	2	8
Q. gartneri	1	.	.	1
R. aff. anthophorus
R. levis	.	.	2	.	1	1
R. angustus	.	1	.	.	1	.	2	1	.	.	.
R. reniformis	.	1	1	2	1	1	.	.	1	.	1
R. splendens	2	5	1	4	1	3	4
Rhagodiscus sp. 1
Rhagodiscus spp. indet	.	.	.	4
Scampanella spp.
S. fossilis
S. laffitei	1	.
Stephanolithion spp.	.	.	.	1	.	1	2	1	1	1	6
T. stradneri	1	.	.	.	1	.
T. ethmos
T. decorus	2	1	5	3	.	2	7	.	2	1	2
Thoracosphaera spp.	1	.	.	.	1	.	3	.	.	.	2
T. macleodae	.	1	1	.	.	1
T. phacelosus	1	.	.	1
Vagalapilla spp.	1	2	1	2	.	1	3	.	1	.	4
W. barnesae	116	80	84	99	116	110	83	94	135	125	100
W. biporta	3	2	.	2	.
Z. compactus
Z. lacunatus	1	.	.	3	.	3	.	.	2	4	.
Zygodiscus sp. 1	1	.	.	1	.
Unidentifiable	6	6	5	9	5	2	9	5	5	6	13
Sum (excl. M. staur.)	425	516	434	550	527	563	520	450	453	468	640
Micula staurophora	145	95	104	86	100	100	81	94	78	128	72
Sum of M. staur. counts	570	610	538	636	627	663	601	544	531	596	712
Fields of M. staur. counts	20.0	20.0	20.0	20.0	20.0	20.0	20.0	20.0	20.0	38.0	20.0

	55	56	57	58	59	60	61	62	63	64	65
DSDP Hole 217	217	217	217	217	217	217	217	217	217	217	217
Core-Section	20-4	20-4	20-4	20-4	20-4	20-4	21-2	21-4	22-1	22-3	23-2
cm-level	30	39-40	59-60	80-81	99-100	119-120	32-34	15-17	56-57	32-33	64-65
Depth (mbsf)	454.30	454.39	454.59	454.80	454.99	455.19	460.82	463.65	469.06	471.82	480.14
Micula? sp
N. frequens	.	1	.	1	.	1	2	1	4	.	1
P. embergeri	1
P. regularis	28	25	13	25	22	24	48	60	19	19	17
P. copulatus	.	.	2	1	P	1
P. bussoni	.	2	1	4	3	.
P. fibuliformis	11	30	5	27	17	20	11	12	18	7	31
P. sigmoides	1	1	.
Placozygus sp.	2	5	4	13	3	6	3	10	5	1	3
P. arkhangel'skyi
P. cretacea	66	89	32	64	50	67	69	125	97	82	80
P. spinosa	2	9	4	7	4	4	9	6	7	5	11
P. grandis	2	.	2	4	.	.
P. stoveri	5	8	3	7	8	9	2	11	11	7	10
Q. gartneri
R. aff. anthophorus	1	P	.
R. levis	1
R. angustus	.	.	.	2	1	1	.	4	1	2	1
R. reniformis	.	2	.	1	1	.	1	.	4	.	.
R. splendens	2	6	1	7	1	.	2	1	8	2	.
Rhagodiscus sp. 1	2	2	.
Rhagodiscus spp. indet	3	.	2	.
Scampanella spp.	1	.	.
S. fossilis	1
S. laffitei	1	.
Stephanolithion spp.	.	7	.	2	.	1	.	2	.	1	2
T. stradneri	1	.	.
T. ethmos	1
T. decorus	.	2	1	4	2	1	2	5	8	1	2
Thoracosphaera spp.	1	1	3	.	3	10	1	1	.	.	1
T. macleodae	.	.	.	2	.	1	.	2	2	1	.
T. phacelosus	.	.	1	.	1
Vagalapilla spp.	.	1	.	.	1	.	.	.	1	1	.
W. barnesae	130	114	56	93	68	79	89	101	101	113	38
W. biporta	.	2	.	1	.	.	.	1	.	.	1
Z. compactus
Z. lacunatus	1	1	.	.	.	1	1	1	2	P	1
Zygodiscus sp. 1	1	3	.	4	2	3	.	2	2	.	2
Unidentifiable	2	9	4	7	16	4	6	8	23	5	3
Sum (excl. M. staur.)	498	624	379	548	472	505	525	648	689	519	442
Micula staurophora	82	79	144	72	64	83	97	60	39	81	78
Sum of M. staur. counts	576	703	523	620	536	588	621	708	728	598	520
Fields of M. staur. counts	20.0	20.0	30.0	20.0	20.0	22.0	20.0	20.0	20.0	20.0	21.0

	66	67	68
DSDP Hole 217	217	217	217
Core-Section	23-4	24-2	24-4
cm-level	53-54	51-53	32-33
Depth (mbaf)	483.03	489.51	492.32
Age (Ma)	70.323	70.733	70.911
Sed. Rate (m/m.y.)	15.81	15.81	15.81
Carbonate (wt-%)	n.d.	n.d.	86.7
Preservation	M	M-P	M-P
Abundance	A	A	A
Fields counted	20.0	21.0	20.0
mg sediment used	20.9	21.6	21.5
A. octoradiata	10	17	9
Arkhangelskiella spp.	15	16	10
Biscutum constans	16	8	16
B. magnum	.	1	1
B. notaculum	.	2	1
Biscutum sp. 1	5	8	15
Broinsonia spp.	5	7	2
Arkhang./Broinsonia	.	.	.
C. cf aculeus	2	8	5
Chiastozygus sp. 1	.	.	.
C. completum	.	.	.
C. cf. amphipons	.	.	.
C.(?) daniae	.	.	.
C. ehrenbergii	30	24	19
C. angustiforatus	8	4	5
C. conicus	.	3	1
C. crenulatus	.	.	.
C. schizobrachiatus	.	.	.
C. surellius	.	.	.
Cretarhabdus spp. indet.	24	31	20
C. alta	.	1	.
C. reinhardii	1	.	1
C. biarcus	7	3	.
C. gallicus	.	.	.
C. serratus	1	.	.
Cylindralithus sp. 1	1	.	.
Cylindralithus spp. indet.	1	4	.
D. ignotus	41	30	47
E. eximius	.	.	.
E. parallelus	1	1	3
E. trabeculatus	2	.	2
E. turnseiffelii	10	20	32
Ericsonia sp.	2	.	1
Gartnerago spp.	.	.	2
G. feaus	7	8	12
K. magnificus	.	1	.
Lithastrinus spp.	9	5	5
L. carniolensis	3	5	7
L. grossopectinatus	.	.	.
L. kennethii	.	.	.
L. praequadratus	1	1	.
L. quadratus	.	.	.
Lithraphidites(?) sp. 1	.	.	.
L. cayeuxii	.	.	.
M. pemmatoidea	.	.	.
M. apertus	.	.	.
M. inversus	.	.	.
M. belgicus	.	.	.
M. decoratus	55	5	38
M. praemurus	.	.	.
M. murus	.	.	.
M. cf prinsii	.	.	.

	66	67	68
DSDP Hole 217	217	217	217
Core-Section	23-4	24-2	24-4
cm-level	53-54	51-53	32-33
Depth (mbaf)	483.03	489.51	492.32
Micula? sp	.	.	.
N. frequens	.	.	.
P. embergeri	.	.	.
P. regularis	18	28	28
P. copulatus	.	.	1
P. bussoni	.	.	1
P. fibuliformis	15	22	22
P. sigmoides	.	.	.
Placozygus sp.	3	3	4
P. arkhangel'skyi	.	1	.
P. cretacea	55	95	88
P. spinosa	14	8	15
P. grandis	2	3	4
P. stoveri	3	18	15
Q. gartneri	.	.	.
R. aff. anthophorus	.	.	4
R. levis	.	.	4
R. angustus	1	1	.
R. reniformis	.	1	1
R. splendens	2	2	5
Rhagodiscus sp. 1	.	.	.
Rhagodiscus spp. indet	.	.	.
Scampanella spp.	.	.	.
S. fossilis	.	.	.
S. laffitei	.	.	.
Stephanolithion spp.	.	.	.
T. stradneri	.	.	.
T. ethmos	.	.	1
T. decorus	4	1	6
Thoracosphaera spp.	.	.	.
T. macleodae	2	.	.
T. phacelosus	.	1	2
Vagalapilla spp.	3	6	1
W. barnesae	48	33	58
W. biporta	1	.	.
Z. compactus	1	3	6
Z. lacunatus	1	.	1
Zygodiscus sp. 1	.	.	2
Unidentifiable	7	7	8
<u>Sum (excl. M. staur.)</u>	<u>437</u>	<u>446</u>	<u>531</u>
Micula staurophora	66	93	100
Sum of M. staur. counts	503	539	631
Fields of M. staur. counts	20.0	21.0	20.0

	1	2	3	4	5	6	7	8	9	10	11	12	13	14	15	16	17	18	19	20	21	22
DSDP Hole 528	528	528	528	528	528	528	528	528	528	528	528	528	528	528	528	528	528	528	528	528	528	528
Core-Section	31-7	31-CC	31-CC	31-CC	32-1	32-1	32-1	32-1	32-1	32-1	32-1	32-1	32-1	32-1	32-1	32-1	32-1	32-1	32-1	32-1	32-1	32-1
cm-level	58-59	5-6	10	14	8	14	19	25	31	37	41	46-47	52-53	58-59	63-64	70-71	75-76	80-81	86-87	91-92	97-98	99-100
Depth (mbsf)	406.70	406.85	406.90	406.94	407.08	407.14	407.19	407.25	407.31	407.37	407.41	407.46	407.52	407.58	407.63	407.70	407.75	407.80	407.86	407.91	407.97	407.99
Age (Ma)	66.262	66.331	66.354	66.372	66.404	66.408	66.410	66.413	66.417	66.420	66.422	66.425	66.428	66.431	66.434	66.438	66.440	66.443	66.446	66.449	66.452	66.453
Sedimentation Rate (m/m y.)	2.17	2.17	2.17	2.17	18.53	18.53	18.53	18.53	18.53	18.53	18.53	18.53	18.53	18.53	18.53	18.53	18.53	18.53	18.53	18.53	18.53	18.53
Carbonate Content (weight-%)	62.6	70.5	72.1	47.6	67.9	63.8	60.9	59.0	64.9	72.9	74.8	75.3	68.6	59.1	56.1	50.7	57.8	70.9	79.1	82.8	83.6	77.7
Preservation	P	M-P	P	P	M	M-G	M	M	M-G	M	M	M-P	P	M-P	P	P-M	P	M-P	P	P-M	M	M
Abundance	C	C	C-R	A-C	A	A	A	A	A	A	A	A	A	A	C-A	A	A	A	A	A	A	A
Fields counted	60.0	48.4	67.8	59.0	30.0	38.0	30.0	30.0	36.0	35.0	44.0	53.9	30.0	30.0	30.0	20.0	35.0	20.0	30.0	30.0	20.0	20.0
mg sediment used	20.1	20.3	18.9	19.5	18.3	20.2	19.9	19.4	20.6	18.8	19.2	19.3	20.9	19.7	19.5	20.5	20.2	19.8	19.0	20.0	20.2	19.4
<i>Ahmullerella octoradiata</i>	?	3	.	.	.	4	.	.	1	.	.
<i>Arkhangelskiella</i> spp.	4	7	4	10	31	30	23	20	18	22	22	29	14	14	13	16	8	11	21	14	12	9
<i>Arkhangelskiella/Broinsonia</i>
<i>Biantholithus sparsus</i>
<i>Biscutum constans</i>	24	21	12	17	1	1	*	1	1	4	2	1	*	*	.	1	*	1	*	1	*	1
<i>B. notaculum</i>	1	1
<i>Biscutum</i> sp 1	1	.	4	4	.	.	4	2
<i>Braarudosphaera bigelowii</i>	1	.	1	2
<i>Broinsonia</i> spp.
<i>Calculites obscurus</i>	.	.	12
<i>Ceratolithoides kamptneri</i>	1	.	1	9	1	2	4	1	.	2	*	2	.	8	1	.	1	3	.	.	.	1
<i>Chiastozygus amphipons</i>	*	5	1
<i>Chiastozygus</i> sp. 1	2	1	*	1	*	1	*	1
<i>Corollithion completum</i>	*
<i>C. exiguum</i>	3	3	.	1	1	4	.	.	2	.	.	2	1	.	.	*	.	.
<i>Cretarhabdus angustiforatus</i>	1	3	1	3	2	7	.	1	1	4	3	3	1	1	1	2	6	5	7	7	7	1
<i>C. conicus</i>	.	.	*	.	*	4	1	2	*	1	.	1	1	*	.	*	.	1	2	.	.	.
<i>C. crenulatus</i>	1	.	*	1	.	1	4	1	2	3	1	1	*	1	.	6	3	3	5	1	.	1
<i>C. schizobrachiatus</i>	*	*	*	*	.	.	*	*	.	.	1	1	*	2	2	*
<i>C. surirellus</i>	1	*	1	2	*	4	7	7
<i>Cretarhabdus</i> spp.	2	1	.	5	.	4	5	12	6	9	11	5	5	10	3	1	14	10	9	12	10	12
<i>Cribrosphaerella(?) daniae</i>	.	.	1	1	.	2	.	.	2	*	.	1	.	*	.	*	1	*
<i>Cribrosphaerella ehrenbergii</i>	2	20	8	6	34	42	41	32	42	39	86	40	29	34	20	26	30	14	32	48	35	23
<i>Cruciplacolithus</i> spp.	?
<i>Cyclagelosphaera alta</i>
<i>Cyclagelosphaera reinhardtii</i>	22	19	32	47	4	5	2	5	1	*	2	2	2	4	7	5	6	9	16	6	7	2
<i>Cylindralithus gallicus</i>	.	1	1	5	8	11	11	8	10	9	10	10	11	8	9	10	5	6	9	17	2	8
<i>C. serratus</i>	1
<i>Discorhabdus ignotus</i>	1	1	3	.	1	3	*	2	4	8	1	*	3	3	.	2	4	2	1	4	6	11
<i>Eiffellithus parallelus</i>	1	2	1	.	3	2	3	3	1	6	5	2	2	1	.	*	1	*	1	3	2	1
<i>E. trabeculatus</i>	.	.	3	.	1	3	1	2	4	6	.	.	3	1	1	*	7	1	8	9	11	13
<i>E. turrisseiffell</i>	4	6	7	3	23	18	12	11	3	15	24	7	15	14	8	8	8	11	9	13	11	8
<i>Ericsonia</i> sp.	.	.	.	4	.	.	.	3	7	?	.	4	.	*	.	.	.	3
<i>Gartnerago</i> spp.	.	1	.	.	*	*	*	*	*	2	3	.	.	2	.	.	1	*	.	*	*	1
<i>Glaukolithus fessus</i>	2	3	2	.	8	4	3	7	5	12	6	4	12	6	5	9	13	13	13	14	10	9
<i>Hexalithus</i> spp.	3	3	1	1
<i>Kamptnerius magnificus</i>	.	1	.	.	4	*	*	1	1	2	2	1	2	1	.	.	*	1	2	1	1	.
<i>Lithastrinus</i> spp.	2	2	1	4	.	1	1	1	3	1	3	2	.	1	.	3	1	1	3	1	2	2

Sample-Depth (mbs)	406.70	406.85	406.90	406.94	407.08	407.14	407.19	407.25	407.31	407.37	407.41	407.46	407.52	407.58	407.63	407.70	407.75	407.80	407.86	407.91	407.97	407.99
Lithraphidites carniolensis	.	1	.	.	1	.	.	1	2	3	3	5	2	1	1	.	1	.	13	2	2	.
L. grossoeclinatus	.	.	1
L. praequadratus	5	5	13	20	.	16	13	16	28	28	39	39	23	17	12	19	30	22	37	25	30	22
L. quadratus	1	.	.	1	7	12	11	9	13	11	1	.	2	6	5	6	6	2	2	15	3	4
Lithraph. sp. cf. L. kennethii
Lucianorhabdus cayeuxii	.	.	1	.	.	3	7	.	2	4	5	3	3	1	1	3	.	.
Manivitella pemmatoldea
Markallus apertus	.	2
Markallus inversus	22	11	14	17	??
Microrhabdulus belgicus	.	.	1	.	1	3	3	1	1	2	1	1	2	.	1
M. decoratus	4	5	5	11	10	18	18	14	18	22	14	9	9	6	10	12	16	26	24	33	24	18
Micula murus	13	22	25	10	22	10	16	14	20	19	3	7	5	6	11	18	4	8
M. murus/prinsii	3	1	.	.	.	2	2	2	4	6	.	5	.	.	.
M. prinsii	1	.	?	4	?	?	1	3	.	3
M. swastika	1	1	.	.	1
Micula? sp	11	10	3	7	.	4	11	8	15	11	8	1	7	4	3	3	.
Neocrepidolithus spp.	10	10	1
Nephrolithus frequens	1	10	2	3	8	2	2	1	4	13	15	3	5	1	1	1	3	2	1	3	4	4
Placozygus fibuliformis	2	3	.	4	3	2	7	7	7	16	16	6	11	3	.	2	13	5	3	8	20	19
P. bussoni	2	.	.	1	.	.	.	1	.	.	.	1	1
P. sigmoides	49	18	22	17	2	1	1	?	1	.	.
Placozygus sp	.	2	1	.	1	.	.	2	1	2	.	.	2	.	5	.	.	4	2	1	2	.
Podorhabdus regularis	10	11	4	11	15	17	19	18	23	27	29	11	18	14	7	12	12	25	26	30	33	21
Prediscosphaera cretacea	15	41	16	34	64	61	82	50	62	61	132	46	88	57	35	41	70	61	91	94	51	73
P. grandis	1	.	.	2	1	1	1	.	1	.	1	.	.	1	1	.	1	.
P. spinosa	3	14	4	5	13	14	7	19	12	15	15	2	9	7	1	6	15	7	8	14	14	3
P. stoveri	6	11	8	9	18	32	40	24	33	55	49	16	26	25	12	27	46	21	19	37	36	38
Prinsius tenuiculum
Quadrum gartneri	.	1	.	2	1	1	1	.	.	.	2	1	.	.	1
Reinhardtites levis
Rhagodiscus spp.	.	1	3	.	3	3	1	.	1	4	2	.	2	1	.	.	.	1	2	4	.	2
Rhomboolithion rhombicum	.	1	1	.	1	.	.	.
Ruclinolithus hayi
Scapanella asymmetrica
Scapanella spp.
Staurolithites laffittii	1	3	1	1	.	.	3	1
Stephanolithion spp.	.	4	2	1	3	1	.	1	.	.	1	.	.	2	2	3	1
Tegumentum stradneri	1	.	1	.	.
Teichorhabdus ethmos
Tetrapodorhabdus decorus	1	3	2	1	3	2	1	2	.	2	1	2	3	2	3	3	5	5
Thoracosphaera spp.	131	79	109	106
Tranolithus macleodae	1	1	1	.	3	11	4	4	.	3	4	2	2	.	.	1	3	5	2	2	2	2
Vagalapilla spp.	1	1	2	1	3	.	1	5	2	3	4	.	2	1	1	2	1	.	.	1	2	.
Watznaueria barnesae	5	12	7	13	24	48	30	43	38	43	49	68	61	47	32	30	50	40	77	56	67	62
W. biporta	1
Zygodiscus lacunatus	1	1	2	.	1	1
Zygodiscus sp.1	1	1	1	.	.	1	2	2	1	.	5	3
Zygolithus diplogrammus
Unidentifiable	17	20	5	27	11	10	1	9	13	21	14	6	13	13	4	4	21	19	8	18	5	12
Sum (excl. M. staurophora)	363	369	316	406	325	426	398	359	401	506	607	351	427	341	220	286	421	356	486	536	448	417
M. staurophora - Fields	60	48	68	59	30	38	30	30	36	35	30	54	30	30	30	20	35	20	30	30	20	20
Micula staurophora	18	63	21	85	113	188	198	185	185	151	189	488	317	287	238	161	155	109	209	139	63	90
Sum of M. stauroph. count	381	432	337	491	438	614	596	544	586	657	593	839	744	628	458	447	576	465	695	675	511	507

	23	24	25	26	27	28	29	30	31	32	33	34	35	36	37	38	39	40	41	42	43	44
DSDP Hole 528	528	528	528	528	528	528	528	528	528	528	528	528	528	528	528	528	528	528	528	528	528	528
Core-Section	32-1	32-1	32-1	32-1	32-1	32-1	32-1	32-1	32-1	32-2	32-2	32-2	32-3	32-3	32-3	32-3	32-3	32-4	32-4	32-4	32-4	32-5
cm-level	104-105	109-110	114-115	119-120	125-126	130-131	134-135	140-141	146-147	29-30	68-69	108-109	18-19	49-50	81-82	101-102	131-132	4-5	34-35	77-78	103-104	9-10
Depth (mbsf)	408.04	408.09	408.14	408.19	408.25	408.30	408.34	408.40	408.46	408.79	409.18	409.58	410.18	410.49	410.81	411.01	411.31	411.54	411.84	412.27	412.53	413.09
Age (Ma)	66.456	66.459	66.462	66.464	66.467	66.470	66.472	66.476	66.479	66.497	66.518	66.539	66.572	66.588	66.606	66.616	66.633	66.645	66.661	66.684	66.698	66.729
Sedimentation Rate (m/m y)	18.53	18.53	18.53	18.53	18.53	18.53	18.53	18.53	18.53	18.53	18.53	18.53	18.53	18.53	18.53	18.53	18.53	18.53	18.53	18.53	18.53	18.53
Carbonate Content (weight-%)	62.1	60.4	61.8	65.1	72.6	78.6	78.3	79.7	66.4	83.1	81.8	86.9	85.9	n.d.	n.d.	n.d.	n.d.	n.d.	n.d.	n.d.	n.d.	80.8
Preservation	P	P	P	M-P	M	P-M	M	M	P-M	M-P	M	M-G	M	M	M	M	M-P	M	M	M-P	M	M
Abundance	A	A	A	A	A	A	A	A	A	A	A	A	A	A	A	A	A	A	A	A	A	A
Fields counted	30.0	30.0	40.0	30.0	20.0	30.0	20.0	20.0	30.0	40.0	20.0	20.0	20.0	20.0	20.0	20.0	20.0	20.0	20.0	20.0	20.0	20.0
mg sediment used	21.8	19.8	20.0	20.5	20.2	20.0	19.8	19.5	19.7	20.2	19.7	20.7	19.4	21.1	17.9	19.6	20.5	21.1	20.4	20.5	20.9	18.5
<i>Ahmuelerella octoradiata</i>	1	5	1
<i>Arkhangel'skiella</i> spp.	7	12	10	23	10	11	9	6	22	17	4	6	4	10	5	13	11	3	1	3	1	4
<i>Arkhangel'skiella/Broinsonia</i>	2
<i>Biantholithus sparsus</i>
<i>Biscutum constans</i>	1
<i>B. notaculum</i>	1	1
<i>Biscutum</i> sp. 1	1	1	4	.	3	1	1	4	5	2	3	1	.	1	4	1	.	
<i>Braarudosphaera bigelowii</i>
<i>Broinsonia</i> spp.	1	.	.	2	9	11	17	17
<i>Calculites obscurus</i>
<i>Ceratolithoides kemptneri</i>	2	2	6	2	1	1	.	.	.	2	3	.	3	1	1
<i>Chiastozygus amphipons</i>
<i>Chiastozygus</i> sp. 1	1	.	5	1	
<i>Corollithon completum</i>
<i>C. exiguum</i>	1
<i>Cretarhabdus angustiforatus</i>	2	4	3	5	3	4	4	1	4	3	5	9	5	4	1	.	6	5	.	.	.	
<i>C. conicus</i>	1	1	
<i>C. crenulatus</i>	.	.	1	1	.	.	.	1	.	4	.	.	.	2	2	1	3	.	.	1	.	
<i>C. schizobrachiatus</i>	1	.	.	1	.	.	.	1	.	.	.	1	2	1	.	1	.	
<i>C. surirellus</i>	1	?	1	1	2	2	2	2	.	4	2	3	10	4	3	9	3	3	1	4	1	
<i>Cretarhabdus</i> spp.	10	6	6	9	10	13	8	15	14	18	11	.	5	12	16	17	17	8	3	13	15	
<i>Cribrosphaerella(?) daniae</i>	1	.	.	2	2	.	.	.	1	
<i>Cribrosphaerella ehrenbergii</i>	45	42	16	34	15	32	23	23	35	35	21	8	18	32	34	31	25	27	24	16	25	
<i>Cruciplacolithus</i> spp.
<i>Cyclagelosphaera alta</i>	1	
<i>Cyclagelosphaera reinhardtii</i>	1	4	4	1	3	.	11	9	.	2	2	1	1	
<i>Cylindralithus gallicus</i>	9	11	8	13	7	9	2	3	4	16	7	9	2	7	8	14	13	3	11	4	6	
<i>C. serratus</i>	.	.	.	1
<i>Discorhabdus ignotus</i>	2	.	.	1	4	.	.	6	.	.	8	8	11	15	3	4	9	5	4	12	5	
<i>Eiffellithus parallelus</i>	1	.	.	2	.	2	1	2	2	1	2	2	2	2	2	2	.	1	.	.	2	
<i>E. trabeculatus</i>	3	1	1	.	5	2	6	4	.	4	1	9	10	17	7	5	7	4	2	2	5	
<i>E. turriseiffell</i>	14	6	3	19	4	18	6	12	18	21	10	6	9	16	15	10	11	15	6	12	22	
<i>Ercosonia</i> sp.	1	18	.	.	12	18	1	.
<i>Gartnerago</i> spp.	.	1	1	1
<i>Glaukolithus fessus</i>	9	7	7	9	4	11	5	6	10	12	4	9	10	10	7	12	14	7	10	10	5	
<i>Hexalithus</i> spp.
<i>Kemptnerius magnificus</i>	.	.	.	1	.	2	1	.	.	1	1	.	.	.	1	2	1	
<i>Lithastrinus</i> spp.	4	7	5	2	2	4	1	2	7	6	4	4	3	1	4	6	.	3	1	.	3	

Sample-Depth (mbsf)	408.04	408.09	408.14	408.19	408.25	408.30	408.34	408.40	408.46	408.79	409.18	409.58	410.18	410.49	410.81	411.01	411.31	411.54	411.84	412.27	412.53	413.09
Lithraphidites carnolensis	1	3	3	.	1	2	2	1	1	3	1	1	1	3	.	2	.	1	2	.	.	.
L. grossopectinatus
L. praequadratus	15	18	17	28	9	19	18	37	15	36	14	8	18	33	3	11	15	15	15	24	24	14
L. quadratus	1	5	2	1	2	14	4	7	6	13	3	1	2	8	1	1	1	3	1	5	3	3
Lithraph. sp. cf. L. kennethii
Luclanorhabdus cayeuxii	2	*	.	2	*	1	1	1	.	.	.
Maniviteila pemmatoldea	2
Markalius apertus	1	*
Markalius inversus
Microrhabdulus belgicus	*	*	1	*	.	6	2	.	2	*	1
M. decoratus	13	18	11	22	12	23	29	23	19	34	20	29	24	36	17	16	27	25	16	26	13	16
Micula murus	10	12	14	19	7	18	13	6	9	10	8	11	9	8	10	7	8	4	6	16	9	10
M. murus/prinsii	6	2	7	6	4	1	4	1	?	.	1	5	2	.	3	1	2	.	*	1	.	1
M. prinsii	.	.	2	1	.
M. swastika
Micula? sp.	.	3	8	8	8	8	4	3	10	2	7	4	2	.	5	.	1	2	2	4	.	3
Neocrepidolithus spp.
Nephrolithus frequens	2	2	2	*	*	3	2	*	*	4	4	4	3	1	*	*	2	1	1	3	.	*
Plecozygus fibuliformis	15	7	5	13	17	16	13	10	30	20	8	12	16	40	41	12	19	6	12	7	15	3
P. bussoni	*	.	.	1	1	.	.	1	*	*	2	.	*	2	*	.	*	*	1	1	.	1
P. sigmoides
Plecozygus sp.	1	3	.	*	2	3	2	1	1	1	3	2	3	4	*	*	7	1	1	3	1	1
Podorhabdus regularis	18	12	21	26	30	46	25	37	18	65	37	23	35	35	22	30	26	35	18	42	30	18
Prediscosphaera cretacea	84	63	37	75	51	71	62	71	63	93	66	81	103	78	82	72	82	68	62	69	98	82
P. grandis	*	1	.	1	.	*	2	*	1	*	3	1	*	1	1	1	2	2	1	1	2	2
P. spinosa	23	18	2	16	8	7	2	12	12	30	11	18	11	20	19	13	26	10	7	15	20	26
P. stoveri	55	15	11	29	15	31	22	26	30	51	24	14	27	33	31	31	50	30	11	18	18	52
Prinsius tenuiculum
Quadrum gartneri	1	3	3	.	*	.	1	.	1	1	*	1
Reinhardtites levis
Rhagodiscus spp.	2	*	.	2	*	3	2	2	.	2	1	6	2	2	3	1	10	2	1	3	1	6
Rhombolithion rhombicum	.	.	.	*	1
Rucinolithus hayi
Scampanella asymmetrica
Scampanella spp.	1	*	*	*	*
Staurolithites laffittel
Stephanolithion spp.	*	.	.	2	1	2	3	3	4	3	2	2	9	5	1	2	4	*	2	.	4	5
Tegumentum stradneri	*	.	.	*	.	*	1	1	.	2	.	1	*	2	.	.	*	1	.	*	.	*
Telchorhabdus ethmos	?	.	*	.	?
Tetrapodorhabdus decorus	5	1	.	1	.	1	.	2	.	8	2	1	4	4	9	7	7	4	3	3	2	.
Thoracosphaera spp.	1
Tranolithus macleodae	5	5	5	3	1	7	3	3	1	4	1	7	8	7	11	3	13	7	5	3	6	1
Vagalapilla spp.	*	1	.	2	2	1	1	1	5	5	4	3	1	2	1	3	4	*	3	1	1	4
Watznaueria barnesae	39	59	37	37	45	95	43	42	61	61	71	60	45	50	58	65	28	28	25	28	26	23
W. biporta	1	.	1	.	?	1	*	.	.	*	*	.	.	*	.	*	.	.
Zygodiscus lacunatus	*	.	.	1	1	*	.	.	*	*	*	1	*	*	*	2	*	*	.	*	.	.
Zygodiscus sp.1	2	1	2	3	.	4	*	2	1	*	3	*	4	11	3	9	14	3	3	5	3	3
Zygodiscus diplogrammus
Unidentifiable	7	6	7	5	5	9	10	8	9	10	8	6	14	12	12	12	13	15	11	13	11	10
Sum (excl. M. staurophora)	421	361	268	430	294	517	349	397	428	630	391	380	444	535	459	429	484	350	287	388	407	385
M. staurophora - Fields	30	30	40	30	20	30	20	20	30	40	20	20	20	20	20	20	20	20	20	20	20	20
Micula staurophora	236	270	380	212	165	102	99	97	148	151	79	76	68	44	71	52	48	32	87	90	73	79
Sum of M. stauroph. count	657	631	648	642	459	619	448	494	576	781	470	456	512	579	530	481	532	382	374	478	480	464

	45	46	47	48	49	50	51	52	53	54	55	56	57	58	59	60	61	62	63	64	65
DSDP Hole 528	528	528	528	528	528	528	528	528	528	528	528	528	528	528	528	528	528	528	528	528	528
Core-Section	32-5	32-5	32-5	32-5	32-CC	33-1	33-1	33-1	33-1	33-2	33-2	33-2	33-2	33-3	33-3	33-3	33-3	33-4	33-4	33-4	33-4
cm-level	49-50	86-87	108-109	132-133	9-10	12-13	58-59	91-92	124-125	23-23	59-60	112-113	143-144	1-2	55-56	80-81	132-133	10-11	41-42	101-102	141-142
Depth (mbsf)	413.49	413.86	414.08	414.32	416.50	416.62	417.08	417.41	417.74	418.23	418.59	419.12	419.43	419.51	420.05	420.30	420.82	421.10	421.41	422.01	422.41
Age (Ma)	66.751	66.773	66.786	66.801	66.930	66.938	66.965	66.985	67.004	67.033	67.055	67.086	67.105	67.110	67.142	67.157	67.188	67.204	67.223	67.258	67.282
Sedimentation Rate (m/m.y.)	16.80	16.80	16.80	16.80	16.80	16.80	16.80	16.80	16.80	16.80	16.80	16.80	16.80	16.80	16.80	16.80	16.80	16.80	16.80	16.80	16.80
Carbonate Content (weight-%)	n.d.	n.d.	n.d.	n.d.	n.d.	n.d.	n.d.	n.d.	n.d.	78.2	n.d.	n.d.	n.d.	72.2	n.d.	n.d.	n.d.	79.7	n.d.	n.d.	62.0
Preservation	M	M	M	M	M	M	M	M	M	M-G	M	M	M	M-G	M	M	M	M	M	M	M
Abundance	A	A	A	A	A	A	A	A	A	A	A	A	A	A	A	A	A	A	A	A	A
Fields counted	20.0	20.0	20.0	20.0	20.0	20.0	30.0	20.0	20.0	20.0	40.0	40.0	20.0	20.0	20.0	20.0	20.0	20.0	20.0	20.0	20.0
mg sediment used	19.8	20.5	20.8	20.2	20.4	20.9	19.0	20.2	18.8	18.2	17.6	18.5	20.4	19.6	20.1	19.8	18.9	19.9	18.9	18.7	19.9
<i>Ahmuellerella octoradiata</i>	1	.	?	.	.	5	3	.	2
<i>Arkhangelskiella</i> spp.	5	6	.	.	1	3	1	4	2	3	10	12	12	8	2	2	3
<i>Arkhangelskiella/Broinsonia</i>	3	9	9	26	11	15	3	4	6	1	4	4	15
<i>Biantholithus sparsus</i>
<i>Biscutum constans</i>	4	7	1	5	8	48	18	14	32	42	21	.	.	1	.
<i>B. notaculum</i>	1	.	2	2	.	1	.	2	1	1	1	1	.
<i>Biscutum</i> sp. 1	.	1	1	.	.	2	1	6	2	8	4	12	5	7	14	11	5	2	1	2	16
<i>Braarudosphaera bigelowii</i>
<i>Broinsonia</i> spp.	7	8	8	10	7	6	5	.	7	3	3	1	1	2
<i>Calculites obscurus</i>
<i>Ceratolithoides kamptneri</i>	2	.	.	.	1	2	20	9	2	5	11	5	4	10	13	24	9
<i>Chiastozygus amphipons</i>
<i>Chiastozygus</i> sp. 1	1	1	3
<i>Corollithion completum</i>
<i>C. exiguum</i>	2	2	.	.	1	.	1	.	1	2	1	3	2	2	.	1	1	2	.	.	.
<i>Creterhabdus angustifloratus</i>	1	.	.	5	1	1	.	1	.	.	3	.	.	1	1	.	1	3	.	.	.
<i>C. conicus</i>	.	1	1	.	1	1	1	.	.	1	1	1	1	3	1	.	.
<i>C. crenulatus</i>	.	.	.	1	1	.	.	1
<i>C. schizobrachiatus</i>	2	.	1	.	1	5	.	.	.	1	.	1	1	2	2	1	2
<i>C. surirellus</i>	4	9	5	5	1	1	2	2	4	5	2	1	1
<i>Creterhabdus</i> spp.	12	19	12	17	20	10	5	7	4	8	13	45	14	9	8	9	9	11	6	6	9
<i>Cribrosphaerella(?) daniae</i>	3	1	1	1	2	1	.	.	.	1	.	1	.	2	2	2	.	5	.	2	.
<i>Cribrosphaerella ehrenbergii</i>	13	25	30	30	19	7	22	18	19	5	19	21	15	20	23	27	36	18	14	9	16
<i>Cruciplacolithus</i> spp.
<i>Cyclagelosphaera alta</i>
<i>Cyclagelosphaera reinhardtii</i>	3	.	.	1
<i>Cylindralithus gallicus</i>	3	6	4	4	10	.	5	1	5	.	3	2	4	6	8	5	.	1	.	.	1
<i>C. serratus</i>	1
<i>Discorhabdus ignotus</i>	5	6	8	8	9	4	13	22	14	13	16	32	20	10	11	15	15	10	9	15	31
<i>Eiffellithus parallelus</i>	2	1	1	2	1	2	2	7	3	6	20	41	16	14	12	5	8	12	5	20	6
<i>E. trabeculatus</i>	1	5	2	1	3	.	1	.	6	5	2	2	.	2	3	.	3	1	2	.	3
<i>E. turriselfelli</i>	16	11	9	8	15	11	16	10	8	9	46	41	7	9	13	7	20	6	10	24	9
<i>Ericsonia</i> sp.	2	2	1
<i>Gartnerago</i> spp.	1
<i>Glaukolithus fessus</i>	3	8	20	4	17	8	7	9	5	6	10	14	1	1	2	2	6	5	.	4	5
<i>Hexalithus</i> spp.
<i>Kamptnerius magnificus</i>	1	2	2	2	2	4	3	1	1	4	2	1	.	3	2	3
<i>Lithastrinus</i> spp.	3	.	5	3	3	1	1	4	4	8	23	10	3	4	4	.	3	3	4	6	4

Sample-Depth (mbsf)	413.49	413.86	414.08	414.32	416.50	416.62	417.08	417.41	417.74	418.23	418.59	419.12	419.43	419.51	420.05	420.30	420.82	421.10	421.41	422.01	422.41
Lithraphidites carniolensis	1	4	1	1	1	3	16	3	3	1	3	2	5	5	.	5	.
L. grossopectinatus
L. praequadratus	26	19	21	28	32	17	7	17	10	11	21	32	20	25	21	29	34	15	22	22	12
L. quadratus	4	3	4	4	7	2	2	9	3	3	5	13	6	5	3	6	25	6	3	12	6
Lithraph. sp. cf L. kennethii	3
Lucianorhabdus cayeuxii	1	1
Manlivitella pemmatoldea	.	.	2	.	.	1	2	1	.	.	1
Markallus apertus
Markallus inversus	1	1	.	.	1	.	1	.	.	1
Microrhabdulus belgicus	.	.	.	1	.	.	2	2	1	1	3	3	1	.	2	.
M. decoratus	5	4	19	15	17	4	8	12	7	1	25	18	12	16	17	21	11	12	11	5	2
Micula murus	3	5	9	9	7	6	3	3	6	.	4	3	2
M. murus/prinsii	.	.	1	1	2	2	.	1	3	.	3
M. prinsii	1
M. swastika
Micula? sp	3	1	.	.	4	5	2	7	5	2	10	5	2	4	3	3	3	5	5	.	1
Neocrepidolithus spp.
Nephrolithus frequens	5	2	1	6	7	3	3	4	3	3	8	25	7	3	4	3	2	6	6	6	5
Placozygus fibuliformis	25	30	19	15	7	11	14	19	9	5	15	23	5	7	15	6	10	15	13	26	31
P. bussoni	.	.	.	1	.	1	1	2	.	1	.	1	.	.	1	.	.	.	1	.	1
P. sigmoides
Placozygus sp.	.	.	3	1	4	2	1	1	.	.	.	1	2	.	1	2	.
Podorhabdus regularis	23	22	30	28	25	20	24	17	11	7	20	34	12	21	13	18	21	20	15	14	6
Prediscosphaera cretacea	56	77	107	66	48	55	58	70	51	72	170	98	54	60	90	58	96	64	46	60	59
P. grandis	.	.	.	1	.	.	1	1	1	.	1	.	.
P. spinosa	17	15	24	6	8	16	8	12	12	5	28	20	9	25	20	20	5	17	14	10	13
P. stoveri	54	77	54	51	58	28	49	39	47	44	63	107	46	47	66	38	51	56	43	33	41
Prinsius tenuiculum
Quadrum gartneri	1
Reinhardtites levis
Rhagodiscus spp.	4	3	6	2	1	2	1	5	1	3	3	6	5	1	16	6	14	4	6	3	7
Rhombolithion rhombicum	1	.	1	.	1
Rucinolithus hayi
Scampanella asymmetrica	.	1	1
Scampanella spp.	1	.	.	1	.	1	.	1
Staurolithites laffittel	6	6	.	4	2	.	.	.	1	4	1	1	1	1	.
Stephanolithion spp.	5	8	6	.	6	.	4	1	4	3	6	15	.	10	12	4	15	10	6	7	15
Tegumentum stradneri
Teichorhabdus ethmos	.	.	1	.	.	.	1	.	.	1	5	4	2	.	1	.	.	1	1	1	.
Tetrapodorhabdus decorus	4	3	3	1	5	3	.	1	1	2	2	5	1	1	6	2	2	2	8	3	2
Thoracosphaera spp.	1
Tranolithus macleodae	.	7	12	10	7	3	2	11	3	1	1	1
Vagalapilla spp.	1	1	2	.	3	.	.	1	3	.	1	4	3	1	.	3	2	.	1	2	3
Watznaueria barnesae	18	16	20	19	20	18	22	29	34	14	76	88	39	36	18	14	22	10	22	17	22
W. biporta	1	1	.	.	1	.	1	.	1	.	.	2	.	2	1	.	.
Zygodiscus lacunatus	.	.	1	1	.	.	1	1	1	.
Zygodiscus sp.1	1	.	1	1	.	.	1	.	.	2	.	1	2	1	.	2
Zygodiscus diplogrammus
Unidentifiable	14	19	11	11	11	6	12	11	14	10	26	35	5	14	17	27	18	12	10	19	19
Sum (excl. M. staurophora)	351	423	465	376	394	277	321	388	330	301	740	876	376	416	489	414	496	351	313	369	374
M. staurophora - Fields	20	20	20	20	20	20	30	20	20	20	40	40	20	20	20	20	20	20	20	20	20
Micula staurophora	62	86	81	75	104	131	145	73	76	65	445	171	139	138	93	79	99	104	98	209	101
Sum of M. stauroph. count	413	509	546	451	498	408	466	461	406	366	1185	1047	515	554	582	493	595	455	411	578	475

Millers Ferry

Sample Number	99	96	92	91	87	83	81	78	75	71	69
cm below/above K/P boundary	-234	-225	-213	-210	-198	-186	-180	-171	-162	-150	-144
Preservation	G	M	M-P	M-G	M-G	P	G	P-M	M-G	M-G	M-G
number of fields counted	90	42	40	30	26	57	33	40	24	37	28
<i>Angulofenestrellithus snyderi</i>	1	1	.
<i>Arkhangelella</i> and <i>Bromsonia</i> spp.	66	8	39	17	14	12	47	11	10	20	13
<i>Biscutum constans</i>	.	2	3	1	.	1	1
<i>B. magnum</i>	*
<i>B. notaculum</i>	.	1	1	.	.
<i>Biscutum</i> sp. 1	8	4	2	1	1	2	3	1	2	1	1
<i>Braarudosphaera bigelowii</i>	1	.	.	1
<i>Ceratolithina kampfneri</i>	6	3
<i>Chiastozygus amphipora</i>	10	2	3	5	7	5	6	9	8	6	20
<i>C. garsonii</i>	.	.	.	4	.	3	6	2	.	.	1
<i>Chiastozygus</i> sp. 1	2	.	.	.	3	1	2	.	2	.	1
<i>Corollithion exiguum</i>	11	4	.	4	1	4	10	5	6	9	18
<i>Cretarhabdus conicus</i>	18	.	.	1	1	.	2	2	7	5	8
<i>C. crenulatus</i>	2
<i>Cretarhabdus</i> sp. 1	*
<i>Cretarhabdus</i> spp. indet.	.	3	6	3	4	3	5	5	1	6	8
<i>Cribrosphaerella? danae</i>	2
<i>C. ehrenbergii</i>	39	22	9	13	17	20	38	41	27	52	51
<i>Cyclagelosphaera</i> spp.	1	1
<i>Cylindralithus</i> spp.	1	1	2	.	1	3	3
<i>Discorhabdus ignotus</i>	63	25	7	13	11	11	10	8	6	15	22
<i>Effelithus parallelus</i>	13	4	3	4	1	1	6	6	2	3	2
<i>E. trabeculatus</i>	36	13	4	5	4	2	6	.	1	6	2
<i>E. turnseiffelii</i>	47	15	13	16	15	12	26	13	10	17	16
<i>Kampfnerius magnificus</i>	4	.	.	1
<i>Lithraphidites carniolensis</i>	11	4	4	.	.	.	1	.	.	1	1
<i>L. grossiopectinatus</i>	8	1	.	1	1	.	.	1	1	1	3
<i>L. praequadratus</i>	22	11	2	5	3	5	11	5	4	3	8
<i>L. quadratus</i>	21	4	.	.	1	.	1	1	5	3	1
<i>Lucianorhabdus cayeuxii</i>	1
<i>Manivitella</i> sp.	.	.	1	3	.	.	4
<i>Markalius inversus</i>	.	.	.	1
<i>Marthastentes inconspicuus</i>	3	2	1
<i>Microrhabdulus belgicus</i>	5	2	1	4	2	.	.	2	4	1	2
<i>M. decoratus</i>	2	2	1	1	4	6	3	6	4	4	7
<i>Micula murus</i>	.	.	.	?	.	.	?
<i>M. priusii</i>	*
<i>Nephrolithus frequens</i>	2	1	3
<i>Parhabdolithus regularis</i>	23	11	3	2	2	3	3	5	7	13	10
<i>Percivalia pontolithina</i>	4	3	.	2	.	.	1	.	.	.	3
<i>Placozygus fibuliformis</i>	33	6	3	6	2	4	5	1	2	4	4
<i>P. sigmoides</i>
<i>Placozygus</i> spp. indet.	.	5	6	5	3	5	8	.	2	.	8
<i>Prediscosphaera cretacea</i>	77	25	14	29	29	16	32	17	26	26	44
<i>P. spinosa</i>	6	1	.	1	2	3	2	1	6	4	10
<i>P. stoveni</i>	125	62	80	84	67	51	43	113	86	36	86
<i>Rhagodiscus angustus</i>	8	6	2	4	6	5	6	3	12	5	7
<i>R. asper</i>
<i>R. reniformis</i>	2	4	.	3	1	2	1	.	.	2	.
<i>R. splendens</i>	5	5	.	1	3	.	.	.	3	2	3
<i>Rhagodiscus</i> spp. indet.	.	2	.	.	1	1	1	.	.	1	.
<i>Rhombolithum rhombicum</i>	5	3	.	4	2	2	.	.	.	1	1
<i>Staurolithites laffittei</i>	9	3	3	3	6	2	2	.	3	3	3
<i>Stephanolithon</i> spp.	18	13	5	7	5	.	1	3	2	2	16
<i>Tetrapodorhabdus decorus</i>	5	2	1	.	.	.	1	2	.	.	2
<i>Thoracosphaera</i> spp.	9	4	3	5	1	.	4	.	3	8	2
<i>Tranolithus macleodae</i>	20	10	.	1	3	4	5	4	7	2	3
<i>Vagalapilla</i> spp.	34	13	1	2	4	1	8	1	3	1	3
<i>Watz. barnesae</i>	110	36	19	31	44	28	29	41	56	60	120
<i>Zygodiscus diplogrammus</i>	2
<i>Z. lacunatus</i>
Unidentifiable	11	11	10	9	15	27	10	14	2	27	7
Sum (excl. <i>M. stauropora</i>)	909	359	251	302	286	242	352	324	322	354	525
<i>Micula stauropora</i>	247	75	92	57	69	111	50	38	33	27	20
Sum (incl. <i>M. stauropora</i>)	1156	434	343	359	355	353	402	362	355	381	545

Millers Ferry

Sample Number	66	63	58	54	51	48	44	41	36	32	27
cm below/above K/P boundary	-135	-123	-111	-99	-90	-81	-69	-60	-45	-33	-26
Preservation	P-M	M-G	M-G	P	M-G	M	P	P-M	M	M	P
number of fields counted	40	18	21	55	39	45	91	64	43	36	52
<i>Angulofenestrellithus Snyder</i>	.	1	.	.	1	.	.	.	1	.	.
<i>Arkhangeskella</i> and <i>Brownsonia</i> spp.	27	18	12	25	19	9	18	17	24	21	23
<i>Biscutum constans</i>
<i>B. magnum</i>
<i>B. notaculum</i>	1	3	2	.	2	1	1
<i>Biscutum</i> sp. 1	.	3	3	3	8	5	1	6	3	1	.
<i>Braarudosphaera bigelowii</i>
<i>Ceratolithus kampfneri</i>
<i>Chiasozygus amphipons</i>	7	9	5	6	6	10	9	14	15	9	9
<i>C. garsonii</i>	.	.	1	.	.	1	.	1	.	.	.
<i>Chiasozygus</i> sp. 1	2	.	1	1	.
<i>Corollithion exiguum</i>	6	12	6	6	2	2	1	1	4	3	1
<i>Cretarhabdus conicus</i>	4	7	2	1	6	4	1	5	2	2	.
<i>C. crenulatus</i>	1	.	1	.
<i>Cretarhabdus</i> sp. 1
<i>Cretarhabdus</i> spp. indet.	4	7	8	6	1	4	4	4	6	5	6
<i>Cribrosphaerella? daniae</i>
<i>C. ehrenbergii</i>	30	46	50	52	45	33	68	77	86	99	122
<i>Cyclagelosphaera</i> spp.
<i>Cylindralithus</i> spp.	3	2	2	3	2	.	1	4	2	2	2
<i>Discorhabdus igneus</i>	6	18	22	3	20	26	4	28	36	32	2
<i>Eiffelithus parallelus</i>	3	3	7	1	5	2	2	2	1	1	.
<i>E. trabeculatus</i>	1	4	7	4	4	3	1	4	3	2	1
<i>E. tumseiffelii</i>	18	20	20	11	23	15	12	9	35	36	23
<i>Kampfnerius magnificus</i>
<i>Lithraphidites carmoliensis</i>	.	3	1	.	.	5	.	.	.	2	.
<i>L. grossopectinatus</i>	.	5	1	1	.	.	.
<i>L. praequadratus</i>	1	8	10	5	2	2	8	12	6	5	1
<i>L. quadratus</i>	1	1	.	1	3	2	2	1	.	2	2
<i>Lucianorhabdus cayeuxii</i>
<i>Manivitella</i> sp.	.	.	1
<i>Markalius inversus</i>	1
<i>Marthastertes inconspicuus</i>	.	1	1	4	1	1	1	.	1	.	.
<i>Microthabidulus belgicus</i>	2	5	3	.	3	.	2	2	1	3	.
<i>M. decoratus</i>	7	22	5	12	10	1	9	4	9	6	19
<i>Micula murus</i>
<i>M. prnsii</i>
<i>Nephrolithus frequens</i>
<i>Parhabdolithus regularis</i>	5	.	8	4	5	4	7	5	11	15	4
<i>Percivalia pontolithina</i>
<i>Pliacozygus fibuliformis</i>	3	3	6	3	9	2	1	9	13	5	6
<i>P. sigmoides</i>
<i>Pliacozygus</i> spp. indet.	2	7	5	6	.	3	2	8	5	3	.
<i>Prediscosphaera cretacea</i>	22	37	32	16	23	20	14	31	21	43	23
<i>P. spinosa</i>	5	8	4	2	1	1	.	2	.	3	.
<i>P. stoveri</i>	38	41	40	26	22	25	19	27	10	15	12
<i>Rhagodiscus angustus</i>	5	17	20	1	12	9	2	7	18	25	1
<i>R. asper</i>	.	.	1
<i>R. reniformis</i>	.	5	.	1	1	1	2
<i>R. splendens</i>	.	1	1
<i>Rhagodiscus</i> spp. indet.	1	.	.	.	1
<i>Rhombolithium rhombicum</i>	2	1	.	.	.	1	.
<i>Staurolithites laffitei</i>	1	4	4	1	6	7	.
<i>Stephanolithion</i> spp.	4	4	6	5	7	4	4	6	5	3	.
<i>Tetrapodorbabidus decorus</i>	1	1	.	1	2	3	1	2	1	1	.
<i>Thoracosphaera</i> spp.	15	4	2	20	16	22	33	44	10	16	29
<i>Tranolithus macleodae</i>	4	5	3	2	.	2	3	5	3	3	.
<i>Vagalapilla</i> spp.	3	13	2	4	3	12	6	5	.	6	5
<i>Watz. barnesae</i>	50	56	55	43	72	80	75	124	125	98	70
<i>Zygodiscus diplogrammus</i>
<i>Z. lacunatus</i>	.	1	.	1	.	1
Unidentifiable	11	4	5	4	24	19	9	22	.	1	.
Sum (excl. <i>M. staurophora</i>)	293	406	362	282	362	337	324	491	465	479	362
<i>Micula staurophora</i>	64	32	37	74	47	41	116	58	63	59	122
Sum (incl. <i>M. staurophora</i>)	357	438	399	356	409	378	440	549	528	538	484

Millers Ferry

Sample Number	22	12	3
cm below/above K/P boundary	-21	-11	-2
Preservation	M	M	G
number of fields counted	50	34	72
<i>Angulofenestrellithus snyderi</i>	.	.	.
<i>Arkhangelskiella</i> and <i>Broinsonia</i> spp.	8	7	28
<i>Biscutum constans</i>	.	.	.
<i>B. magnum</i>	.	.	.
<i>B. notaculum</i>	.	1	3
<i>Biscutum</i> sp. 1	9	5	19
<i>Braarudosphaera bigelowii</i>	.	.	1
<i>Ceratolithina kamptneri</i>	.	.	.
<i>Chiastozygus amphiporus</i>	3	8	37
<i>C. garraioni</i>	.	.	1
<i>Chiastozygus</i> sp. 1	.	.	2
<i>Corollithion exiguum</i>	1	3	15
<i>Cretarhabdus conicus</i>	2	2	25
<i>C. crenulatus</i>	2	.	.
<i>Cretarhabdus</i> sp. 1	.	.	.
<i>Cretarhabdus</i> spp. indet.	4	2	3
<i>Cribrosphaerella? danae</i>	.	.	.
<i>C. ehrenbergii</i>	89	75	283
<i>Cyclagelosphaera</i> spp.	.	.	1
<i>Cylindralithus</i> spp.	.	1	17
<i>Discoarhabdus ignotus</i>	21	24	241
<i>Eiffelithus parallelus</i>	1	1	11
<i>E. trabeculatus</i>	2	4	10
<i>E. turnseiffelii</i>	9	10	46
<i>Kamptnerus magnificus</i>	.	.	.
<i>Lithraphidites carniolensis</i>	1	1	3
<i>L. grossopectrinatus</i>	1	.	6
<i>L. praequadratus</i>	6	10	21
<i>L. quadratus</i>	2	2	11
<i>Lucianorhabdus cayeuxii</i>	.	.	.
<i>Marivitella</i> sp.	.	.	1
<i>Markalius inversus</i>	.	.	.
<i>Marthastentes inconspicuus</i>	3	.	8
<i>Microarhabdus belgicus</i>	.	3	6
<i>M. decoratus</i>	10	19	29
<i>Micula murus</i>	.	.	*
<i>M. priusii</i>	.	.	*
<i>Nephrolithus frequens</i>	.	.	.
<i>Parhabdolithus regularis</i>	9	9	29
<i>Percivalia pontolithina</i>	.	.	.
<i>Placozygus fibuliformis</i>	4	1	35
<i>P. sigmoidea</i>	.	3	.
<i>Placozygus</i> spp. indet.	2	3	.
<i>Prediscosphaera cretacea</i>	20	18	91
<i>P. spinosa</i>	7	1	28
<i>P. stoveri</i>	23	30	86
<i>Rhagodiscus angustus</i>	1	11	61
<i>R. asper</i>	.	.	.
<i>R. reniformis</i>	.	3	9
<i>R. splendens</i>	.	.	.
<i>Rhagodiscus</i> spp. indet.	.	1	.
<i>Rhombolithium rhombicum</i>	.	.	1
<i>Staurolithites laffittei</i>	1	3	11
<i>Stephanolithon</i> spp.	1	5	30
<i>Tetrapodorhabdus decorus</i>	1	1	6
<i>Thoracosphaera</i> spp.	18	17	20
<i>Tranolithus macleodae</i>	1	2	13
<i>Vagalapilla</i> spp.	1	4	15
<i>Watz. barnesae</i>	40	34	217
<i>Zygodiscus diplogrammus</i>	.	.	2
<i>Z. lacunatus</i>	.	.	.
Unidentifiable	1	.	14
Sum (excl. <i>M. staurophora</i>)	304	324	1496
<i>Micula staurophora</i>	65	68	127
Sum (incl. <i>M. staurophora</i>)	369	392	1623

Curriculum Vitae

Thomas Ehrendorfer
 Woods Hole Oceanographic Institution
 Department of Geology and Geophysics
 Woods Hole, Massachusetts 02543
 U. S. A.

after 01-March-1993:
 University College London
 Department of Geological Sciences
 Gower Street, London WC1E 6BT
 United Kingdom

EDUCATION

1982-1987: study of earth sciences at the University of Vienna, Austria; major: Geology
 since July 1987: graduate student in Woods Hole Oceanographic Institution/Massachusetts
 Institute of Technology Joint Program in Oceanography, Department of Geology and
 Geophysics; specialization in micropaleontology (calcareous nannoplankton).

PROFESSIONAL EXPERIENCE

August 1984: summer job at the Austrian Petroleum Administration (ÖMV), sedimentology
 laboratory
 summer 1985: field mapping for the Austrian Petroleum Administration (ÖMV)
 summer 1986: field mapping for the Geological Survey of Austria

HONORS AND AWARDS

1981: graduated from high school with distinction, was awarded the 'Golden Needle' for passing
 every year in high school with distinction
 1985, 1986, 1987: received a 'Stipend for the Gifted' from the University of Vienna for
 outstanding study success
 1990: AAPG Grant-in-Aid
 1991: grant from the Ocean Ventures Fund at the Woods Hole Oceanographic Institution
 1991: Research Grant-in-Aid from the Paleontological Society
 1992: Grant-in-Aid of Research from the Sigma Xi Society

PUBLICATIONS

Ehrendorfer, T., 1988. Zur Geologie der Weyerer Bögen im Gebiet von Großraming an der Enns
 (O.Ö.). Mitt. Ges. Geol. Bergbaustud. Österr. 34/35, 135-149.
 Ehrendorfer, T. W., Lea, D. W., and Boyle, E. A., 1989. Strontium/Calcium Ratios in Benthic
 Foraminifera at the Miocene/Pliocene Boundary. TERRA abstracts 1 (Abstracts of
 Third International Conference on Paleo-Oceanography), 65.
 Ehrendorfer, T., and Aubry, M.-P., 1992. Calcareous Nannoplankton Changes Across the
 Cretaceous/Paleocene Boundary in the Southern Indian Ocean (Site 750). In: Wise, S.
 W., Jr., Schlich, R., et al., 1992. Proc. ODP, Sci. Results, 120: College Station, TX
 (Ocean Drilling Program), 451-470.
 Ehrendorfer, T., 1992. Diversity changes in the calcareous nannoplankton during the
 Maestrichtian in southern high latitudes (ODP Hole 690C, Maud Rise, Weddell Sea).
 GSA Annual Meeting, Cincinnati, Abstracts w. Programs, A361.
 Ehrendorfer, T., in press. *Nephrolithus frequens* GORKA and its Morphotypes. Journal of
 Paleontology.
 Olsson, R. K., Liu, C., Aubry, M.-P., and Ehrendorfer, T., 1992. A biostratigraphically
 continuous Cretaceous/Paleocene section at Millers Ferry, Alabama: support for a bolide
 impact. GSA Annual Meeting, Cincinnati, Abstracts w. Programs, A28.